Philipps Universität Marburg

Mechanistic characterization of the late steps of mitochondrial iron-sulfur cluster protein maturation.

Dissertation

zur Erlangung des Doktorgrades
der Naturwissenschaften
(Dr. rer. nat.)

dem Fachbereich Biologie
der Philipps-Universität Marburg

vorgelegt von

M. Sc. Marta Agata Uzarska

aus Bydgoszcz, Polen

Marburg an der Lahn 2013

Vom Fachbereich Biologie der Philipps-Universität Marburg (Hochschulkennziffer 1180)

als Dissertation angenommen am: 28.10.2013

Erstgutachter: Herr Prof. Dr. Roland Lill (Fachbereich Medizin)

Zweitgutachter: Herr Prof. Dr. Uwe Maier (Fachbereich Biologie)

Tag der mündlichen Prüfung am: 1.11.2013

Erklärung

Ich versichere, dass ich die vorliegende Dissertation selbständig verfasst, keine anderen als die angegebenen Hilfsmittel verwendet und sämtliche Stellen, die im Wortlaut oder dem Sinn nach anderen Werken entnommen sind, mit Quellenangaben kenntlich gemacht habe. Die Versicherung schließt Zeichnungen und Skizzen mit ein.

Die Dissertation wurde in der jetzigen oder ähnlichen Form noch bei keiner anderen Hochschule eingereicht und hat noch keinen sonstigen Prüfungszwecken gedient. Teile dieser Arbeit sind bereits in Fachzeitschriften veröffentlicht.

_____ _____

(Ort, Datum) Marta Agata Uzarska

Parts of this work were published in following publications:

Uzarska, M. A., Dutkiewicz, R., Freibert, S.-A., Lill, R., Mühlenhoff, U. (2013) **The mitochondrial Hsp70 chaperone Ssq1 facilitates Fe/S cluster transfer from Isu1 to Grx5 by complex formation.** Mol Biol Cell. Jun;24(12):1830-41

Navarro-Sastre, A., Tort, F., Stehling, O., Uzarska, M. A., Arranz, J. A., Del Toro, M., Labayru, M. T., Landa, J., Font, A., Garcia-Villoria, J., Merinero, B., Ugarte, M., Gutierrez-Solana, L. G., Campistol, J., Garcia-Cazorla, A., Vaquerizo, J., Riudor, E., Briones, P., Elpeleg, O., Ribes, A., Lill, R. (2011) **A fatal mitochondrial disease is associated with defective NFU1 function in the maturation of a subset of mitochondrial Fe-S proteins.** Am J Hum Genet. Nov 11;89(5):656-67

During the doctoral studies following publications were published:

Lill, R., Hoffmann, B., Molik, S., Pierik, A. J., Rietzschel, N., Stehling, O., Uzarska, M. A., Webert, H., Wilbrecht, C., Mühlenhoff, U. (2012) **The role of mitochondria in cellular iron-sulfur protein biogenesis and iron metabolism.** Biochim Biophys Acta. Sep;1823(9):1491-508

Hoffmann, B., Uzarska, M. A., Berndt, C., Godoy, J. R., Haunhorst, P., Lillig, C. H., Lill, R., Mühlenhoff, U. (2011) **The multidomain thioredoxin-monothiol glutaredoxins represent a distinct functional group.** Antioxid Redox Signal. 2011 Jul 1;15(1):19-30

Mühlenhoff, U., Molik, S., Godoy, J. R., Uzarska, M. A., Richter, N., Seubert, A., Zhang, Y., Stubbe, J., Pierrel, F., Herrero, E., Lillig, C. H., Lill, R. (2010) **Cytosolic monothiol glutaredoxins function in intracellular iron sensing and trafficking via their bound iron-sulfur cluster.** Cell Metab. Oct 6;12(4):373-85

Conference contributions (choice):

Uzarska M. A. **Iron-sulphur-cluster biogenesis in yeast: an insight into the function of the monothiol-glutaredoxin Grx5.** (invited speaker talk), 6th International MST Meeting 6.07 – 7.07.2013 NanoTemper HQ, Munich, Germany

Uzarska M. A., Dutkiewicz, R., Freibert, S.-A., Roland Lill, R. Mühlenhoff, U. **The mitochondrial Hsp70 chaperone Ssq1 facilitates Fe/S cluster transfer from Isu1 to Grx5 by complex formation.** (poster), 7th International Conference on Iron-Sulfur Cluster Biogenesis and Regulation 20.05 – 24.05.2013 University of South Carolina in Columbia, South Carolina, USA.

Uzarska M. A., Dutkiewicz, R., Lill, R. Mühlenhoff, U. **Grx5 functions in Fe/S cluster biosynthesis via direct interaction with the Hsp70 chaperone Ssq1.** (poster) The FEBS/ EMBO Course on Mitochondria in life, death and disease 09.05. – 13.05.2012 Crete, Greece

Uzarska M. A., Dutkiewicz, R., Lill, R. Mühlenhoff, U. **Grx5 functions in Fe/S cluster biosynthesis via direct interaction with the Hsp70 chaperone Ssq1.** (poster) ESF-EMBO Symposium: Glutathione and Related Thiols in Living Cells 04.09 – 09.09.2011 Sant Feliu de Guixols, Spain

Uzarska M. A., Dutkiewicz, R., Lill, R. Mühlenhoff, U. **Grx5 functions in Fe/S cluster biosynthesis via direct interaction with the Hsp70 chaperone Ssq1.** (poster) 6th International Conference on Iron-Sulfur Proteins 22.08 – 25.08.2011 Cambridge, UK

CONTENS

Abbreviations

ε	Molar extinction coefficient
(v/ v)	Volume per volume
(v/ w)	Volume per weight
ADP	Adenosine-5'-diphosphate
Amp	Ampicilin
APS	Ammonium persulfate
ATP	Adenosine-5'-triphosphate
BSA	Bovine serum albumin
bp	base pairs
BPS	Bathophenanthroline disulfonic acid
CIA	Cytosolic iron sulfur protein assembly
C-terminus	Carboxyterminus
DCFDA	2',7'dichlorodihydrofluorescein diacetate
DCPIP	2,6 dichlorophenol-indophenol
DDM	Dodecylomaltozide
dH_2O	single distilled water
ddH_2O	double distilled water
D	Dextrose
DNA	Deoxyribonucleic acid
dNTPs	Deoxynucleotide Triphosphates
DMSO	Dimethylsulfoxid
DTT	Dithiothreitol
EDTA	Ethylenediamine tetraacetic acid
EPR	Electron-paramagnetic-resonance
FAD	Flavin adenine dinucleotide
Fe/S	Iron-sulfur
g	gram
Gal	Galactose
GFP	Green fluorescent protein
Glu	Glucose
Gly	Glycerol
GSH	Reduced glutathione
GSSG	Oxidized glutathione
GST	Glutathione S-transferase
HA	Hemagglutinine
His-tag	Hexahistididynyl-tag

Abbreviations

HRP	Horseradish peroxidase
IP	Immunoprecipitation
IPTG	Isopropyl-β-D-thiogalactoside
IR	Infrared
ISC	Iron-sulfur cluster
kb	Kilobase
kDa	Kilodalton
LB	Luria-Bertan (medium)
M	Molar (mol/ l)
MST	Microscale thermophoresis
Myc-tag	N-EQKLISEEDL-C protein tag derived from *c-myc* gene product
N-terminus	Aminoterminus
NADH	Nicotinamide adenine dinucleotide, reduced
NADPH	Nicotinamide adenine dinucleotide phosphate, reduced
NTA	Nitrilotriacetic acid
OD	Optical density
ORF	Open reading frame
PAGE	Polyacrylamidgel electrophorese
PBS	Phosphate-buffered-saline
PCR	Polymerase chain reaction
PEG	Polyethylenglycol
PMS	Post mitochondrial supernatant
PMSF	Phenylmethylsulfonylflouride
PVDF	Polyvinylidene fluoride
rpm	Rotations per minute
SC	Synthetic complete (minimal medium)
SDS	Sodium dodecyl sulfate
SOB	Super optimal broth
TCA	Trichloroacetic acid
TEMED	Tetramethylethylenediamine
TPP	Thiamine pyrophosphate
WT	Wild-type
UV-VIS	Ultraviolet-visible
YP	Yeast peptone (medium)

Table of standard amino acid abbreviations and their molecular mass:

amino acid	3-letter code	1-letter code	M [g/ mol]
Alanine	Ala	A	89
Arginine	Arg	R	174
Asparagine	Asn	N	132
Aspartic acid	Asp	D	133
Cysteine	Cys	C	121
Glutamic acid	Glu	E	147
Glutamine	Gln	Q	146
Glycine	Gly	G	75
Histidine	His	H	155
Isoleucine	Ile	I	131
Leucine	Leu	L	131
Lysine	Lys	K	146
Methionine	Met	M	149
Phenylalanine	Phe	F	165
Proline	Pro	P	115
Serine	Ser	S	105
Threonine	Thr	T	119
Tryptophan	Trp	W	204
Tyrosine	Tyr	Y	181
Valine	Val	V	117

Summary

Iron-sulfur (Fe/S) clusters are among the oldest protein cofactors and are essential for the function of many proteins. Fe/S cluster synthesis and insertion into apo-proteins is a complex process. In mitochondria, Fe/S protein biogenesis is performed by the ISC (iron sulfur cluster) assembly machinery and can be divided into three major steps. First, the Fe/S cluster is assembled *de novo* on the scaffold protein Isu1 from iron and sulfide which is provided by a cysteine desulfurase. In a second step, the Isu1-bound Fe/S cluster is labilized with the help of a specialized chaperone system, and third, it is transferred to target apo-proteins by specific maturation factors. Although several factors involved in Fe/S cluster transfer to target proteins have been identified, their interplay and exact functions are not resolved. This work focusses on the role of the monothiol glutaredoxin Grx5, the BolA-like proteins Aim1 and Yal044W, and Nfu1 in the late phases of Fe/S protein biogenesis.

Mutations in human Grx5 have been associated with microcytic anemia, and its deletion in zebrafish is embryonically lethal. In yeast Grx5 is not essential, yet cells lacking Grx5 display low activities of Fe/S proteins, iron accumulation in mitochondria and oxidative stress. It was shown previously that upon depletion of Grx5, Fe/S clusters accumulate on Isu1 and cannot be properly transferred to the target proteins. Here it was shown that Grx5 binds a Fe/S cluster *in vivo* and is required for maturation of all cellular Fe/S proteins, regardless of the type of bound Fe/S cofactor and subcellular localization. Grx5 and Isu1 simultaneously interact with the dedicated Hsp70 chaperone Ssq1 at non-overlapping binding sites. Grx5 does not stimulate the ATPase activity of Ssq1 and most tightly binds to the ADP form of Ssq1. The vicinity of Isu1 and Grx5 on the chaperone facilitates rapid Fe/S cluster transfer from Isu1 to Grx5. Hence, Grx5 functions as a late-acting component of the core ISC assembly machinery linking Fe/S cluster synthesis on Isu1 with Fe/S cluster targeting to dedicated apo-proteins.

BolA-like proteins have been linked to the monothiol Grxs by both bioinformatics and experimental approaches. To examine the function of mitochondrial BolA-like proteins yeast cells deleted for Aim1 and Yal044W proteins were investigated. While the role of Yal044W in Fe/S biogenesis remains unclear, a*im1Δ* cells displayed a 50 % decrease in the activities of succinate dehydrogenase and lipoate-dependent enzymes (pyruvate and α-ketoglutarate

dehydrogenases). Activities of latter enzymes depend on activity of Fe/S protein lipoate synthase Lip5. Aim1 seems to be needed for catalytic activation but not for *de novo* Fe insertion into Lip5. The phenotype of *aim1Δ* yeast cells is consistent with with the one observed in human patient cells where mutations in human Aim1 homolog BOLA3 were associated with fatal infantile encephalopathy and/ or pulmonary hypertension. Hence, the role of Aim1 protein as an auxiliary ISC assembly protein facilitating the maturation of a subset of mitochondrial [4Fe-4S] proteins is conserved throughout eukaryotes.

The human NFU1 has been associated with fatal infantile encephalopathy and/ or pulmonary hypertension, and is needed for the maturation of Fe/S clusters of respiratory complexes I and II and lipoate synthase. Previously, Nfu-like proteins were shown to bind Fe/S clusters *in vitro* and hence, a role was suggested in which Nfu1 functions as a scaffold protein alternatively to Isu1. Here, it is shown that *nfu1Δ* yeast cells display up to 5-fold decreased activities of succinate dehydrogenase and lipoate-dependent enzymes, similarly as in NFU1 patient cells. Yeast Nfu1 carrying the mutation ($Gly^{194}Cys$) corresponding to the one found in patients bound Fe/S cluster in a more stable fashion, and thus allowed for the first time the detection of Fe/S cluster association *in vivo.* Formation of the Nfu1-bound Fe/S cluster was dependent on the core ISC assembly machinery, including Isu1, ruling out the possibility of Nfu1 acting as an alternative scaffold protein. Due to the increased stability of the bound Fe/S cluster, $Gly^{194}Cys$ Nfu1 was not able to fully rescue the defects of *nfu1Δ* cells, giving an insight into disease development in the human patients.

Taken together, this study contributed to a better understanding of how Fe/S clusters are handled in mitochondria after *de novo* synthesis on the scaffold Isu1. First, the joint interaction of Isu1 and Grx5 on the specialized Hsp70 chaperone Ssq1 is important for efficient Fe/S cluster transfer from Isu1 to Grx5. Second, Grx5 is a crucial factor for maturation of all cellular Fe/S proteins. Third, an auxiliary role of yeast Nfu1 and Aim1 as dedicated maturation factors was established. These findings provide a better insight into how late-acting components of the mitochondrial ISC assembly machinery cooperate to efficiently mature Fe/S target proteins.

Zusammenfassung

Eisen-Schwefel (Fe/S) Cluster gehören zu den ältesten Co-Faktoren und sind unabdingbar für die Funktion vieler Proteine. Die Synthese von Fe/S Clustern und deren Insertion in Apoproteine sind komplexe biochemische Vorgänge. In Mitochondrien wird die Biogenese von Fe/S Proteinen durch die ISC Assemblierungsmaschinerie (Iron-Sulfur Cluster Assembly) in drei Stufen durchgeführt. Im ersten Schritt wird ein Fe/S Cluster *de novo* aus Eisenionen und Sulfid, das durch eine Cysteindesulfurase bereitgestellt wird, auf dem Gerüstprotein Isu1 assembliert. In einem zweiten Schritt wird der Isu1-gebundene Fe/S Cluster mittels eines spezifischen Chaperonsystems dissoziiert, um dann schließlich durch spezielle Reifungsfaktoren auf die verschiedenen Zielproteine übertragen zu werden. Obwohl bereits einige Faktoren identifiziert wurden, die am Transfer von Fe/S Clustern auf Zielproteine beteiligt sind, ist über deren Zusammenspiel und ihre jeweilige spezifische Funktion wenig bekannt. Diese Arbeit konzentriert sich auf die Rolle des Monothiol Glutaredoxin Grx5, der BolA-ähnlichen Proteine Aim1 und Yal044W sowie des Nfu1 in den späten Phasen der Fe/S Proteinbiogenese.

Mutationen im humanen GLRX5 wurden mit mikrozytischer Anämie in Verbindung gebracht und eine Deletion im Zebrafisch ist embryonisch letal. In der Hefe *S. cerevisiae* ist Grx5 nicht essentiell, jedoch zeigen Zellen ohne Grx5 niedrige Enzymaktivitäten von Fe/S Proteinen, eine Akkumulation von mitochondrialem Eisen und oxidativen Stress. Es wurde bereits gezeigt, dass die Depletion von Grx5 eine Akkumulation von Fe/S Clustern auf Isu1 hervorruft, und diese nicht auf Zielproteine übertragen werden können. In dieser Arbeit konnte gezeigt werden, dass Grx5 einen Fe/S Cluster *in vivo* bindet, der für die Reifung aller zellulärer Fe/S Proteine benötigt wird, unabhängig vom Typ des gebundenen Fe/S Co-Faktors und deren subzellulärer Lokalisation. Grx5 und Isu1 interagieren gleichzeitig mit dem Hsp70 Chaperon Ssq1 an unterschiedlichen Bindungsstellen. Grx5 stimuliert dabei nicht die ATPase Aktivität von Ssq1 und bindet bevorzugt an die ADP-Form von Ssq1. Die räumliche Nähe von Isu1 und Grx5 am Chaperon erleichtert den schnellen Fe/S Cluster Transfer von Isu1 auf Grx5. Somit verbindet Grx5 den Prozess der *de novo* Fe/S Clusterbiosynthese auf Isu1 mit dem Transfer des fertigen Fe/S Clusters auf entsprechende Zielproteine.

BolA-ähnliche Proteine sind mit den Monothiol Glutaredoxinen über bioinformatische und experimentelle Ansätze in Zusammenhang gebracht worden. Um die Funktion der mitochondrialen BolA-ähnlichen Proteine zu studieren, wurden Hefezellen untersucht, in denen die Gene für Aim1 und Yal044W deletiert wurden. Während die Rolle der Yal044W in der Fe/S Proteinbiogenese unklar blieb, zeigten *aim1*Δ Zellen eine 50%-ige Abnahme der Enzym-Aktivitäten der Succinatdehydrogenase und der Lipoat-abhängigen Enzyme Pyruvat- und α-Ketoglutarat-Dehydrogenase. Die Aktivitäten der letzteren Enzyme sind abhängig von der Lipoat-Synthase Lip5, einem Fe/S Protein. Aim1 scheint für die katalytische Aktivierung, aber nicht für die *de novo* Insertion von Fe/S Clustern in Lip5 benötigt zu werden. Der Phänotyp von *aim1*Δ Zellen in Hefe ist kompatibel mit dem humaner Zellen aus Patienten mit fataler infantiler Enzephalopathie und/oder pulmonaler Hypertonie. Diese Erkrankung wird u.a. durch Mutationen im humanen Aim1 Homolog BOLA3 verursacht. Offensichtlich ist die Rolle der Aim1 Proteine als spezialisierte ISC Überträger-Proteine, die bei der Reifung einer Unterklasse mitochondrialer [4Fe-4S]-Proteine benötigt werden, in Eukaryoten konserviert.

Mutationen im humanen *NFU1* wurden ebenfalls mit fataler infantiler Enzephalopathie und/ oder pulmonaler Hypertonie in Verbindung gebracht. NFU1 wird für die Reifung der Fe/S Cluster der Atmungskettenkomplexe I und II und der Lipoat-Synthase in humanen Zellen benötigt. Nfu1-ähnliche Proteine binden Fe/S Cluster *in vitro*, woraus geschlossen wurde, dass Nfu1 ein Gerüstprotein ist, dass parallel zu Isu1 arbeitet. In dieser Arbeit wurde gezeigt, dass die Deletion von *NFU1* in Hefe eine bis zu 5-fache Abnahme der Aktivitäten der Succinat-dehydrogenase und Lipoat-abhängiger Enzyme hervorruft. Dies stimmt mit den Befunden an NFU1 Patientenzellen überein. Hefe Nfu1, das eine Patienten-analoge Mutation trägt ($Gly^{194}Cys$), bindet einen Fe/S Cluster wesentlich stabiler als das Wildtyp-Protein, und erlaubte somit erstmals den Nachweis einer Fe/S Cluster Bindung auf Nfu1 *in vivo*. Die Fe/S Cluster Bindung auf Nfu1 war abhängig von der ISC Assemblierungsmaschinerie einschließlich Isu1, was ausschließt, dass Nfu1 ein zu Isu1 alternatives Gerüstprotein ist. Aufgrund der verminderten Labilität des gebundenen Fe/S Clusters in Nfu1-$Gly^{194}Cys$ konnte dieses die Defekte der *nfu1*Δ-Zellen in Hefe nur unvollständig retten, womit ein Einblick in die Krankheitsentstehung in menschlichen Patienten gegeben wurde.

Die vorliegende Arbeit trägt zu einem besseren Verständnis bei, wie Fe/S Cluster nach ihrer *de novo* Synthese auf dem Gerüstprotein Isu1 in den Mitochondrien weiter transferiert werden. Die hier gezeigte gleichzeitige Interaktion von Isu1 und Grx5 auf dem spezialisierten Hsp70 Chaperon Ssq1 ermöglicht einen effizienten Transfer der Fe/S Cluster von Isu1 zu Grx5, das wiederum als wichtiger ISC Faktor für die Reifung aller zellulärer Fe/S Proteine charakterisiert werden konnte. Weiterhin konnte eine unterstützende Funktion der Hefeproteine Nfu1 und Aim1 als spezialisierte Reifungsfaktoren nachgewiesen werden. Diese Erkenntnisse erlauben einen besseren Einblick in das mechanistische Zusammenspiel der späten Komponenten der mitochondrialen ISC Assemblierungsmaschinerie.

1 Introduction

1.1 Biochemistry of iron.

Iron belongs to the sub-family of transition elements. Its electron transfer properties are fundamental for many metabolic processes such as photosynthesis, respiration and nitrogen fixation, where it can be found as a part of many protein cofactors like iron-sulfur (Fe/S) clusters or haem. Iron is an essential nutrient for virtually all living organisms but even though it is the fourth most common element in the Earth's crust, the amount of bioavailable iron is limited. Under aerobic conditions at physiological pH iron is stable in its ferric (Fe^{3+}) form and ferrous iron (Fe^{2+}) will undergo spontaneous oxidation. In contrast to Fe^{2+}, ferric iron is extremely insoluble in water at neutral pH. This makes iron inaccessible to biologic ligands. Even though iron is essential for many biological processes, ferrous iron is also cytotoxic. Due to its ability to catalyze Fenton reactions, Fe^{2+} is a potent source of reactive oxygen species (ROS) including reactive hydroxyl radical (Kosman, 2003; Rutherford and Bird, 2004). This dual nature of iron requires biological systems efficient in iron acquisition and solubilization without accumulating iron at the toxic levels.

1.2 Iron-sulfur proteins.

1.2.1 Discovery of iron-sulfur clusters and historical perspective.

Fe/S clusters were discovered in the sixties of last century when Beinert und Sands were testing the properties of the mitochondrial membrane and of soluble iron-flavoproteins. They noticed that beef heart mitochondria produced a so far undescribed Electron Paramagnetic Resonance (EPR) spectrum with the unusual g = 1.94 signal when tested protein was reduced exogenously (Beinert, 1960). The latter studies identified this signal as non-haem iron cofactor (Shethna, 1964). Similar EPR signals were found during the next years in many biological samples coming from all kinds of organisms from bacteria to human and plants. Another line of evidence on the new iron cofactor came from a discovery of "iron protein" critical for nitrogen fixation purified in 1962 by Mortenson, Valentine, and Carnahan from the anaerobic bacterium *Clostridium pasteurianum* (Mortenson, 1962). Due to its brownish color and iron content the protein was named ferredoxin. Not much later, the existence of so called “labile sulfide” was

found in those iron containing proteins which led Beinert and coworkers to finally identify the cofactor to be a Fe/S cluster (Dervarti *et al.*, 1967; Shethna *et al.*, 1968). Today we know that the first identified Fe/S cluster proteins were complex I, II and III present in the mitochondrial membrane.

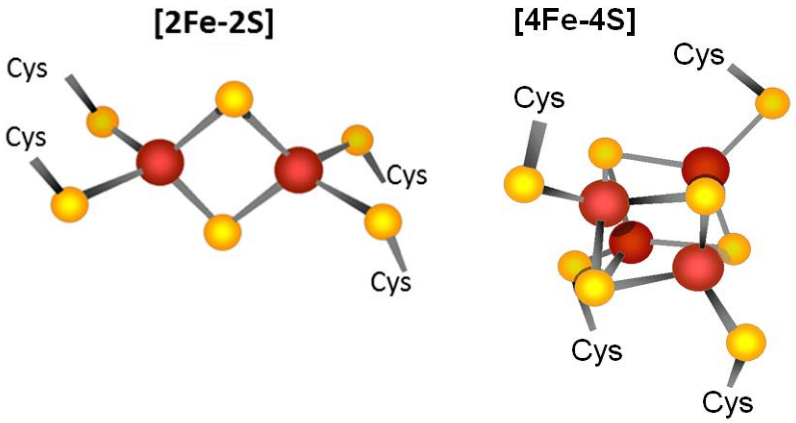

Figure 1.1 Rhombic [2Fe-2S] and cubane [4Fe-4S] clusters.

1.2.2 Types of iron-sulfur clusters and their appearance in the cell.

Fe/S clusters are believed to be one of the oldest protein cofactors in the evolution of biomolecules. They are small inorganic cofactors which consist of iron cations ($Fe^{2+/3+}$) and sulfide anions (S^{2-}). The Fe/S clusters are bound to the polypeptide chain via coordination of iron ions usually via the cysteine residues, but histidine and serine also have been shown to serve as the coordination sites. Fe/S clusters can be found in all kingdoms of life, where they are present in basically all cellular compartments. The most common and also chemically simplest Fe/S clusters are the rhombic [2Fe-2S] and cubane [4Fe-4S] types (Fig. 1.1). Rhombic clusters can be found in ferredoxins (like yeast Yah1 or human Fdx1), Rieske protein, biotin synthase or ferrochelatase. [4Fe-4S] clusters are present in aconitase, bacterial ferredoxins or complex I and II of respiratory chain. Less common are more complex or differently coordinated forms of Fe/S clusters. As examples, [3Fe-4S] cluster in bacterial ferrodoxin I or [8Fe-7S] in so called P-cluster present in nitrogenase (Chan *et al.*, 1993; Schindelin *et al.*, 1997). Even more complicated cluster types can be found in the sulfite reductase of *E. coli* where a [4Fe-4S] cluster is linked via

cysteine to the iron in a sirohaem. Some proteins or protein complexes can contain more than just one cluster. Respiratory complex II involved in electron transfer chain contains a [2Fe-2S], a [3Fe-4S] and a [4Fe-4S] cluster (Sun *et al.*, 2005). This variety of types of the Fe/S clusters present in the proteins take a part in many important biochemical processes (Fig. 1.2).

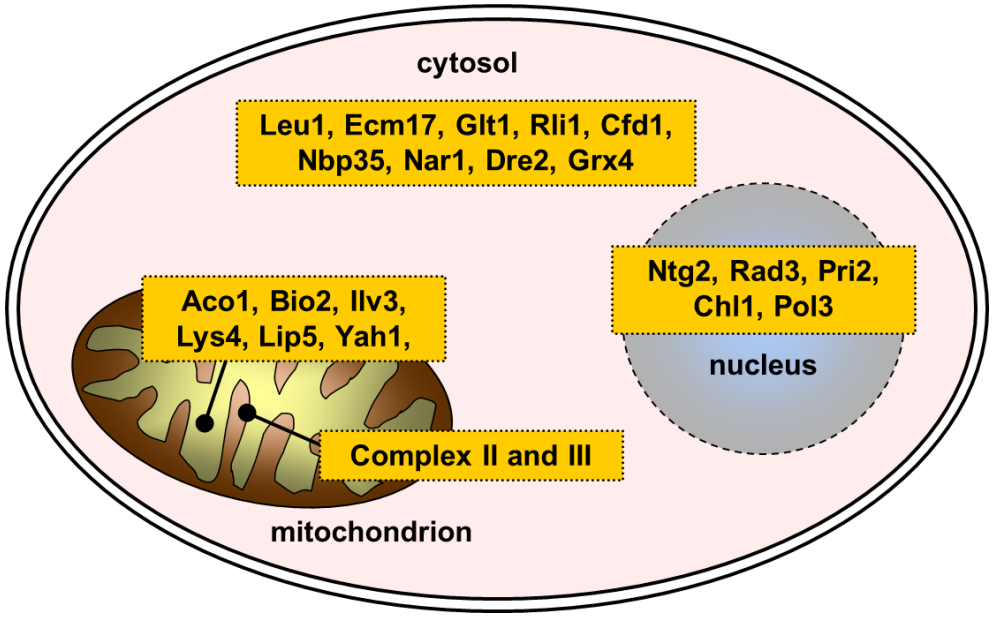

Figure 1.2: Cellular localization of Fe/S proteins in *S. cerevisiae*. In eukaryotes Fe/S proteins are localized in mitochondria, cytosol and nucleus. Representative examples of these proteins in their compartments are indicated. Names usually represent abbreviations from the model organism *Saccharomyces cerevisiae*. Examples of mitochondrial Fe/S proteins: Aco1 – aconitase; complex II and III of respiratory chain (as well as complex I in humans and other fungi); Bio2 – biotin synthase; Ilv3 – dihydroxyacid dehydratase and Lys4 – homoaconitase, both involved in aminoacids biosynthesis; Lip5 – lipoic acid synthase; Yah1 – ferredoxin involved in Fe/S clusters synthesis (Lotierzo *et al.*, 2005; Lill, 2009) Cytosolic Fe/S proteins: Leu1 – isopropylmalate isomerase; Ecm17 – sulfite-reductase; Glt1 – glutamate synthase (present both in cytosol and in mitochondria); Rli1 – ABC protein involved in ribosome biogenesis (Kispal *et al.*, 2005); Cfd1, Nbp35, Nar1 and Dre2 – components of CIA machinery (for details see chapter 1.3.1.3); Grx4 – monothiol glutaredoxin shuttling between cytosol and nucleus; Nuclear Fe/S proteins: Ntg2 – DNA repair protein N-glycosylase, Rad3 – ATP dependent 5' to 3' DNA helicase; Pri2 – subunit of DNA primase; Chl1 – DNA helicase; Pol3 – DNA polymerase (Lill, 2009; Netz *et al.*, 2012b).

1.2.3 Function of iron-sulfur clusters.

Fe/S cofactors can function as electron carriers, catalysts in chemical reactions, regulatory sensors or they can simply play a structural role. The best known function of Fe/S clusters is of

course the electron transfer. This property is based on the ability of iron to switch between ferrous (Fe^{2+}) and ferric (Fe^{3+}) oxidative states. The redox potential of Fe/S clusters, depending on the polypeptide surrounding, can vary from extreme values of −700 mV up to +400 mV (Meyer, 2008), which makes Fe/S clusters excellent donors and acceptors of electrons. Probably the best known electron transfer reactions are the ones performed by respiratory chain complexes I and II, ferredoxins and hydrogenases.

Fe/S clusters can serve as excellent active sites of catalytic enzymes. One of the classical examples is the [4Fe-4S] protein aconitase, an essential enzyme of the citric acid cycle that isomerizes citrate to isocitrate. One of the Fe atoms of this cluster is not coordinated by the protein and serves as a Lewis acid which is involved in H_2O extraction from the substrate (citrate) (Beinert, 2000). A similar mechanism can be found in the aconitase-like proteins including homoaconitase (Lys4) or isopropylmalate isomerase (Leu1).

Fe/S clusters can also function as sensors of intracellular or environmental concentrations of molecular iron, oxygen, superoxide ion or nitric oxide concentrations. For the last three the perfect examples are two bacterial transcription factors: oxygen sensing FNR (fumarate nitrate reduction) (Khoroshilova *et al.*, 1997) and SoxR (Pomposiello and Demple, 2001; Gu and Imlay, 2011) that reacts to superoxide and nitric oxide levels. Both transcription factors contain sensitive Fe/S clusters that can undergo reversible changes in response to the sensed compound and thus regulate the activity of the protein. In case of molecular iron sensing it is worth to mention yeast monothiol glutaredoxins 3 and 4 (for more details see chapter 1.4). In vertebrates regulation of cellular iron uptake and storage involves Fe/S protein IRP1 (iron regulatory protein). IRP1 regulates iron import to the cell via post-transcriptional regulation of gene expression. Under iron-replete conditions IRP1 binds a [4Fe-4S] cluster and can function as a cytosolic aconitase. Under iron-limiting conditions it loses its cluster and can bind the RNA stem-loop structures called IREs (iron responsive elements) at the 5´- or 3´- untranslated regions of specific mRNAs. When IRP1 binds to the 5´- region of mRNA its translation is inhibited which leads to lower protein synthesis of, for example, iron storage proteins H- and L-ferritin or iron export protein ferroportin. On other hand, when IRP1 attaches at the 3´- region, the mRNA is stabilized. This enhances synthesis of proteins involved in iron uptake like transferrin receptor DMT1 (Gunshin *et al.*, 2001).

Numerous bacterial and eukaryotic Fe/S cluster containing proteins are known, but in many cases the precise role of the Fe/S cluster is still not determined as they are not involved in any biochemical reactions. It is possible that in some proteins Fe/S cluster may simply play a structural role and stabilize the protein. The best examples of this function could be Fe/S clusters present in some DNA binding proteins like (ATP)-dependent DNA helicases involved in nucleotide excision repair (Rad3, XPD, FANCJ) or recently identified Fe/S clusters present in catalytic subunits of DNA polymerases (Netz *et al.*, 2012b).

1.3 Iron-sulfur clusters biogenesis.

It did not take long after the discovery of Fe/S clusters to show that it is possible to build this cofactor on the apo-proteins *in vitro* via chemical reconstitution (Malkin and Rabinowitz, 1966). Although the amounts of Fe^{2+} and S^{2-} necessary for the chemical reconstitution of Fe/S cluster are toxic to the cell, it took almost thirty years to realize that *in vivo* Fe/S biogenesis does not occur spontaneously, but is a complicated process assisted by a subset of evolutionary conserved proteins. Investigating the function of *Azotobacter vinelandii* Fe/S protein nitrogenase was within the studies that allowed the identification of the first components of Fe/S cluster assembly machinery. This then led to discovery of three different systems involved in assembly of Fe/S clusters, namely NIF (nitrogen fixation), SUF (sulfur mobilization) and ISC (iron sulfur cluster) assembly systems. Further studies revealed that *isc* operon encoded proteins (ISC assembly system) are with slight exceptions conserved through the bacterial species and as those serve as the main machinery for Fe/S clusters biosynthesis (Takahashi and Nakamura, 1999). NIF is a specialized system for nitrogenase maturation and SUF system is believed to act as alternative to oxygen sensitive ISC assembly system as it becomes activated under oxidative stress conditions (Zheng *et al.*, 1998; Outten *et al.*, 2004; Fontecave *et al.*, 2005). Most importantly, studies on bacterial Fe/S cluster assembly systems introduced a concept of a scaffold for *de novo* Fe/S cluster synthesis (Barras *et al.*, 2005).

Although discovery of Fe/S cluster biosynthesis pathway happened relatively not long ago, high conservation of ISC and SUF systems through the evolution and association of Fe/S proteins with known diseases allowed fast development of the field within the last years. Mitochondria have retained components homologous to the bacterial ISC assembly machinery (Lill and Muhlenhoff, 2006, 2008), whereas components of SUF system are found in plastids and some

parasites (Xu and Moller, 1998; Balk and Lobreaux, 2005; Py and Barras, 2010). Despite many differences, both ISC and SUF systems (in bacteria and eukaryota) share a common biosynthetic principle. The Fe/S clusters biogenesis pathway can be divided into three main steps in which Fe/S cluster is first assembled *de novo* on the scaffold protein from iron and sulfur which is provided by a cysteine desulfurase that abstracts the –SH from cysteine to form persulfide on the scaffold protein. Subsequently, Fe/S cluster is released from the scaffold and (third step) transferred to the different target apo-proteins by specific maturation factors. Each of these steps requires participation of several proteins and cofactors which perform specific biosynthetic partial reactions (Lill, 2009).

1.3.1 Biogenesis of iron-sulfur clusters in eukaryotes.

The evolutionary relationship between bacteria and mitochondria allowed the identification of mitochondrial proteins homologous to the bacterial ISC system (Fig. 1.3) (Kispal *et al.*, 1999; Schilke *et al.*, 1999). The compartmentalization of the eukaryotic cell and the fact that Fe/S proteins are not only present in the mitochondria led to the discovery of ISC export machinery and cytosolic Fe/S protein assembly machinery (CIA) (for details see following chapters). Both of them strictly rely on functional mitochondrial Fe/S biosynthesis, which makes mitochondria essential for the biogenesis of all cellular Fe/S proteins (Lill and Muhlenhoff, 2006, 2008; Lill, 2009). This fact is even more pronounced by the discovery of mitosomes, the mitochondria derived organelles that like mitochondria possess a double membrane and import their proteins from the cytosol. Function of mitosomes was heavily reduced during the evolution as they lost ability to perform haem synthesis, citric acid cycle, oxidative phosphorylation, fatty acid oxidation and mitochondrial gene expression (van der Giezen *et al.*, 2005; Hjort *et al.*, 2010; Shiflett and Johnson, 2010). The only maintained process is the Fe/S cluster biosynthesis which is likely used for the maturation extra-mitochondrial Fe/S proteins, as mitosomes do not contain any relevant Fe/S proteins themselves (Tovar *et al.*, 2003; Goldberg *et al.*, 2008).

Since this thesis was carried out mainly with the model organism *Saccharomyces cerevisiae*, I will therefore focus on summarizing the current knowledge on the biogenesis of Fe/S proteins in yeast.

1.3.1.1 Biogenesis of mitochondrial iron-sulfur proteins by the ISC assembly machinery.

The ISC assembly machinery in yeast mitochondria consists of at least 15 different proteins from which many of them are homologous to the ones present in bacterial ISC assembly machinery (Lill, 2009; Rawat and Stemmler, 2011; Lill *et al.*, 2012) (Fig. 1.3). All components are encoded in the nucleus and after their synthesis are imported into the mitochondrial matrix. For import they use specific mitochondrial targeting sequences recognized by the import machinery.

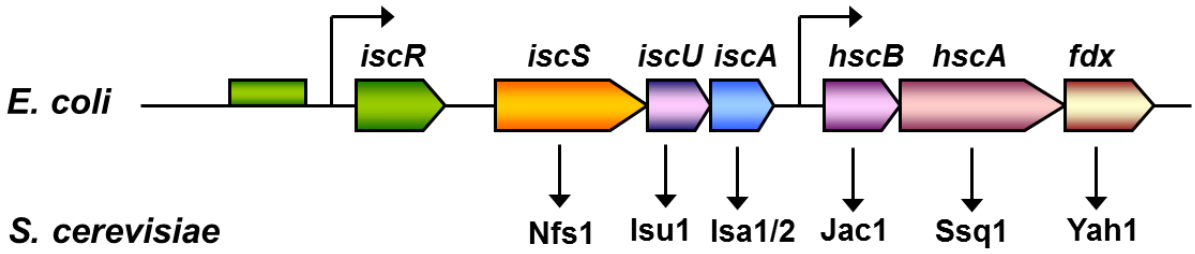

Figure 1.3: Conservation of ISC assembly system. In bacteria genes involved in the same pathways are usually organized in operons. As such, ISC operon encodes a regulatory protein (IscR), a cysteine desulfurase (IscS), a scaffold (IscU), an A-type carrier protein (IscA), a DnaJ-like co-chaperone (HscB), a DnaK-like chaperone (HscA) and a ferredoxin (Fdx). ISC assembly system reacts on changes in Fe/S clusters biosynthesis via Fe/S protein IscR, which is matured by the ISC assembly machinery. In its holo-form IscR represses expression from iscR promoter which controls *iscRSUA* genes. Little is known about how expression of *hscB, hasA* and *fdx* genes is regulated (Py and Barras, 2010). In eukaryotes mitochondria have retained components homologous to the bacterial ISC assembly machinery, namely: Nfs1 (homologous to IscS), Isu1 (IscU), Isa1/2 (IscA), Jac1 (HscB), Ssq1 (HscA) and Yah1 (Fdx).

As in bacteria, also in eukaryotes Fe/S cluster biogenesis starts with *de novo* assembly of a Fe/S cluster on the scaffold protein (Fig. 1.4). In yeast the role of scaffold is performed by the IscU homolog Isu1 and its functionally redundant homologue Isu2 that arose by gene duplication (Garland *et al.*, 1999; Muhlenhoff *et al.*, 2003a). Scaffold protein contains three conserved cysteine residues which are crucial for Fe/S cluster synthesis. Isu1 tightly interacts with cysteine desulfurase Nfs1 (IscS homolog). Nfs1 contains a conserved cysteine residue on which a persulfide is formed during conversion of cysteine to alanine. Although Nfs1 is able to perform this function alone *in vitro*, *in vivo* formation of a complex with 11 kDa protein Isd11 is necessary for sulfur transfer from Nfs1 to Isu1 (Adam *et al.*, 2006; Wiedemann *et al.*, 2006). Iron

delivery to Isu1 is still not fully understood. The iron binding protein frataxin Yfh1 has been implicated to function as an iron donor, as it is essential for Fe/S cluster assembly and it forms an iron-stimulated complex with Isu1 and Nfs1-Isd11 (Gerber *et al.*, 2003; Wang and Craig, 2008). Studies performed on the bacterial homolog of frataxin (CyaY) suggested an alternative function as an iron-dependent negative regulator of IscS (Adinolfi *et al.*, 2009; Iannuzzi *et al.*, 2011). On the other hand, recent *in vitro* work on the human frataxin suggested that it acts as an iron-dependent allosteric activator of Nfs1 that triggers sulfur delivery and Fe/S cluster assembly (Tsai and Barondeau, 2010). Due to so many contradictive data the exact function of frataxin remains

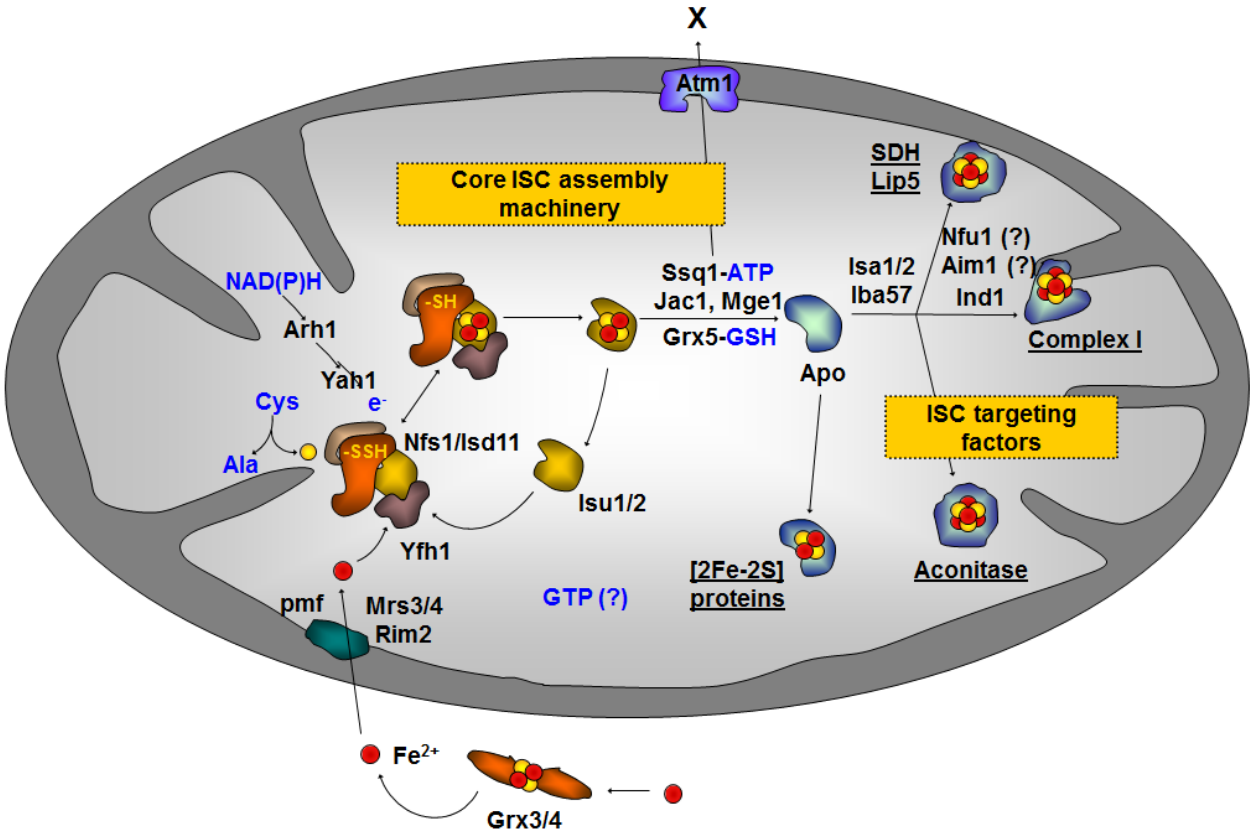

Figure 1.4: Summary of mitochondrial Fe/S cluster assembly machinery. Mitochondria import iron (red circle) from the cytosol in a process involving monothiol glutaredoxins (Grx3/4) as iron donors and the inner membrane carriers Mrs3–Mrs4 which use the proton motive force (pmf) as a driving force for membrane transport. The biogenesis of mitochondrial Fe/S proteins is accomplished by the ISC assembly machinery in three major steps. First, the [2Fe–2S] cluster is synthesized on the scaffold protein Isu1, a step which requires the cysteine desulfurase complex Nfs1–Isd11 as a sulfur (yellow circle) donor releasing sulfur from cysteine via persulfide intermediates (− SSH). This step further requires frataxin (yeast Yfh1) that undergoes an iron-dependent interaction with Isu1 and

may serve as an iron donor and/or an allosteric regulator of the desulfurase enzyme. An electron transfer chain consisting of NAD(P)H, ferredoxin reductase (Arh1) and ferredoxin (Yah1) is needed for Fe/S cluster assembly on Isu1. In the second step, the Isu1-bound Fe/S cluster is labilized by functional involvement of a dedicated chaperone system comprising the ATP-dependent Hsp70 chaperone Ssq1, its co-chaperone Jac1, and the nucleotide exchange factor Mge1. Monothiol glutaredoxin Grx5 also seems to be involved in this step. The mentioned proteins are involved in the biogenesis of all mitochondrial Fe/S proteins, and are thus termed the core ISC assembly components. In a third step, specialized ISC targeting factors catalyze the generation of [4Fe–4S] clusters by involving Isa1–Isa2–Iba57 proteins, and they assist the insertion of Fe/S clusters into specific apoproteins. Additionally, Nfu1 seems to have a role in efficient assembly of lipoate synthase and respiratory complex II (SDH), while Ind1 is specific for complex I. The role of the BolA-like protein Aim1 is still hypothetical. For details please see main text. Figure modified after (Lill *et al.*, 2012)

elusive. However, an excellent *in vitro* work by Bridwell-Rabb and coworkers shows that whether frataxin acts as the activator or repressor of cysteine desulfurase activity strictly depends on origin (bacterial or eukaryotic) of latter one (Bridwell-Rabb *et al.*, 2012). Additionally, experiments performed in the yeast system show that point mutation localized close to the one of conserved cysteine residues of Isu1 is able to rescue the Fe/S defect of *yfhΔ* cells (Yoon *et al.*, 2012). Taken together, those findings strongly point into direction of frataxin being an allosteric regulator of cysteine desulfurases. Another, not yet completely understood point considering Fe/S cluster assembly is the fact that this process strongly depends on electron transfer from the [2Fe-2S] cluster containing ferredoxin Yah1, which in turn receives electrons from the ferredoxin reductase Arh1 and NAD(P)H (Fig. 1.4) (Lange *et al.*, 2000; Li *et al.*, 2001a; Muhlenhoff *et al.*, 2003a; Sheftel *et al.*, 2010; Shi *et al.*, 2012). It is not exactly known for what this electron flow is used. One possibility is the need for reduction of the sulfan sulfur (S^0) present in the cysteine to the sulfide (S^{2-}) present in the Fe/S cluster (Lill, 2009). It was also suggested to be needed for fusion of two [2Fe-2S] clusters into one [4Fe-4S] by reductive coupling (Chandramouli *et al.*, 2007; Unciuleac *et al.*, 2007). Interestingly, Yah1 which is also necessary for haem A and coenzyme Q biosynthesis (Barros *et al.*, 2002; Pierrel *et al.*, 2010), is the only essential Fe/S protein of yeast mitochondria (beside the scaffold protein Isu1) and requires the core ISC assembly machinery for its own maturation (Muhlenhoff *et al.*, 2011).

After its synthesis the Fe/S cluster has to be released from the scaffold and delivered to target proteins. This step is more complicated than initially thought and can be divided into two

major steps. First, the Fe/S cluster is released from Isu1 and then transiently bound by intermediate proteins, which specifically insert the Fe/S cluster into target proteins (Lill *et al.*, 2012). Fe/S cluster release from Isu1 is facilitated by the dedicated chaperone system consisting of Hsp70 protein Ssq1, its co-chaperone J-type protein Jac1 and nucleotide exchange factor Mge1. All this components belong to so called „core ISC assembly machinery“, since they are required for the maturation of all cellular Fe/S proteins (Lill *et al.*, 2012). Studies performed on bacterial functional homologs of Ssq1 (HscA) and Jac1 (HscB) (Hoff *et al.*, 2000; Silberg *et al.*, 2004; Vickery and Cupp-Vickery, 2007), as well as numerous studies on the related function of Hsp70 chaperones in protein folding (Bukau and Horwich, 1998; Kampinga and Craig, 2010), gave an insight how the chaperones work within the ISC assembly pathway. According to the current model (Fig. 1.5), Ssq1 recruits the holo-form of Isu1 in its relaxed (open) ATP-state. The process requires Jac1 as a co-chaperone which binds Isu1 and targets it to Ssq1 (Knieszner *et al.*, 2005; Ciesielski *et al.*, 2012). Both proteins stimulate the ATPase activity of Ssq1 thus inducing a conformational change of Ssq1 to its tense (closed) ADP state. This conformational change stabilizes the interaction between Ssq1 and the LPPVK motif of Isu1 (Hoff *et al.*, 2002; Hoff *et al.*, 2003; Dutkiewicz *et al.*, 2004), while Jac1 leaves the complex. Nucleotide exchange factor Mge1 joins the complex and nucleotide exchange from ADP to ATP occurs (Dutkiewicz *et al.*, 2003). This not only induces the conformational change of Ssq1 back to the relaxed state which then leads to disassembly of the whole protein complex, but also a conformational change of Isu1. The altered conformation is thought to bind the Fe/S cluster in a more labile fashion and thus accelerate the Fe/S cluster release from the scaffold protein (Bonomi *et al.*, 2008, 2011) (Fig. 1.5). Another protein most likely acting at this stage of Fe/S protein maturation is monothiol glutaredoxin Grx5. Depletion of this protein in yeast causes severe oxidative stress which is known to damage Fe/S clusters of, for example, aconitase. However, iron overload of mitochondria and Fe/S clusters accumulation on Isu1 were also observed (Rodriguez-Manzaneque *et al.*, 2002; Muhlenhoff *et al.*, 2003a) similar as in the case of Jac1- or Ssq1-depleted cells. These data pointed to the involvement of Grx5 in Fe/S cluster transfer from Isu1. *In vitro* experiments on monothiol glutaredoxins from different organisms showed their ability to transiently bind a glutathione-coordinated [2Fe-2S] cluster (Rada *et al.*, 2009; Johansson *et al.*, 2011). The exact function of Grx5 and its bond cluster is not fully understood (Bandyopadhyay *et al.*, 2008; Iwema *et al.*, 2009) and will be investigated within this work. A need for GTP was also

proposed for the common step of the Fe/S cluster biogenesis although the mechanism is not understood (Amutha *et al.*, 2008).

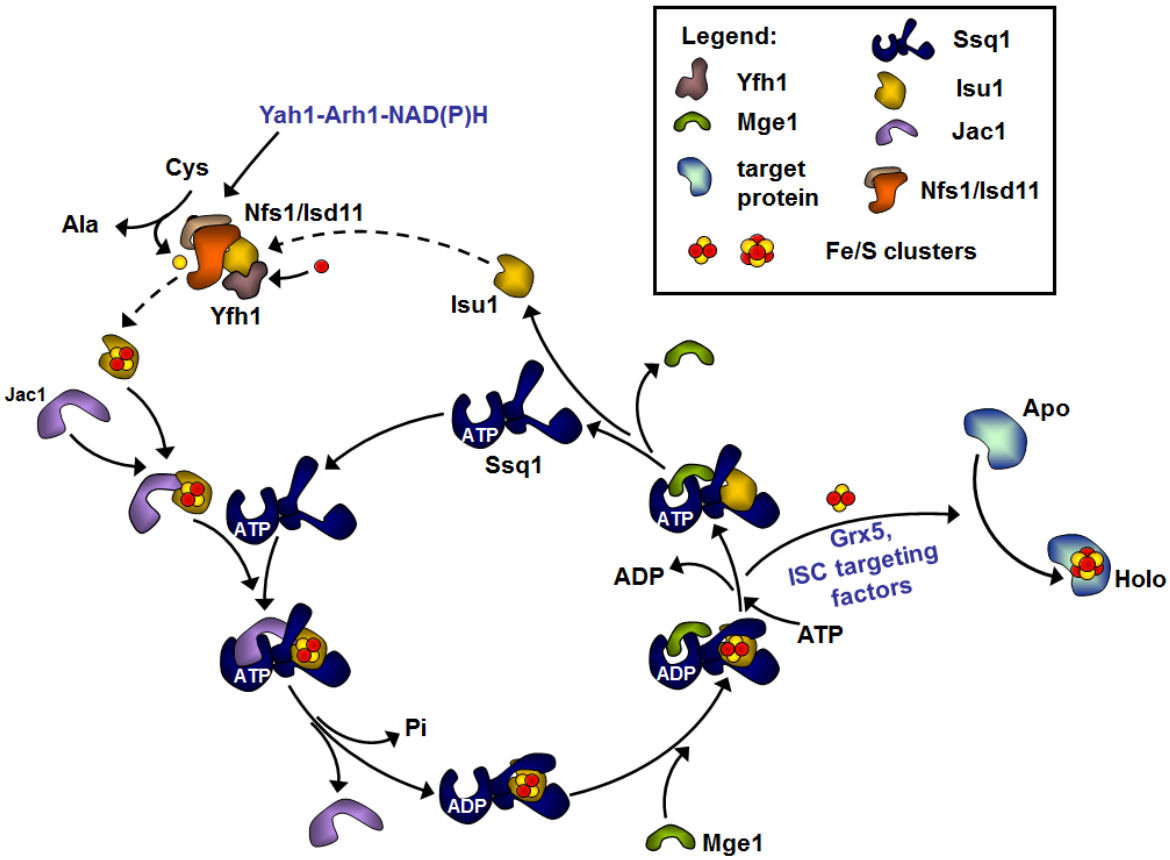

Figure 1.5: The working cycle of the dedicated chaperone system of mitochondrial Fe/S protein biogenesis. The working cycle of ISC chaperone system is similar to that of Hsp70 chaperones in protein folding (Kampinga and Craig, 2010). After synthesis of the [2Fe–2S] cluster on the scaffold protein Isu1 (Fig. 5) the co-chaperone Jac1 recruits holo-Isu1 and delivers it to the ATP-bound form of the Hsp70 chaperone Ssq1. ATP hydrolysis triggers a conformational change of the peptide binding domain of Ssq1 thus creating a tight binding interaction with the LPPVK motif of Isu1. In turn, this is believed to induce a conformational change on the scaffold and may weaken the binding of the Fe/S cluster to Isu1. Eventually, this results in Fe/S cluster transfer from Isu1 to Grx5, and late acting ISC targeting factors (Fig. 1.4). Concomitantly, ADP is exchanged for ATP by the exchange factor Mge1 which triggers a conformational change of the peptide binding domain of Ssq1 from the closed to an open state thus leading to disassembly of the Ssq1–Isu1 complex. The reaction cycle can then resume with the binding of a new holo-Isu1–Jac1 complex to Ssq1–ATP. (Lill *et al.*, 2012)

After the Fe/S cluster is released from Isu1 it is bound by the specific ISC targeting factors and delivered to the different subsets of target apo-proteins. Proteins involved in this step are not needed for the maturation of [2Fe-2S] containing proteins, suggesting that core ISC assembly machinery is sufficient for that process (Lill *et al.*, 2012). The formation of [4Fe-4S] clusters, in both yeast and human cells, strongly depends on the IscA homologs Isa1 and Isa2, as well as Isa-interacting protein Iba57 (Muhlenhoff *et al.*, 2007; Gelling *et al.*, 2008; Muhlenhoff *et al.*, 2011; Sheftel *et al.*, 2012). Their deletion in *S. cereviasie* leads to respiratory deficiency, loss of mitochondrial DNA and a growth deficiency on non-fermentable carbon sources (Jensen and Culotta, 2000; Kaut *et al.*, 2000; Pelzer *et al.*, 2000). Recently the Isa proteins were shown to bind iron which accumulates when the major [4Fe-4S] containing protein of mitochondria – aconitase, or Iba57 are not present (Muhlenhoff *et al.*, 2011). The precise role of Iba57 and Isa proteins is still not fully understood. Isa1 and Isa2 are known to form a hetero-oligomer and cannot functionally replace each other. The *ISA1* deletion phenotype can be rescued by other A-type proteins like IscA or SufA which is not the case for *ISA2* deletion (Muhlenhoff *et al.*, 2011). Additionally, Isa proteins were shown to interact with Grx5 (Kim *et al.*, 2010), which is believed to be an Fe/S cluster transfer protein (Bandyopadhyay *et al.*, 2008). It may be that Iba57 is involved in the displacement of the iron from the Isa proteins, which could be then used for the synthesis of [4Fe-4S] cluster on the target proteins (Muhlenhoff *et al.*, 2011). Another late-acting factor is P-loop NTPase Ind1, which binds [4Fe-4S] cluster at two conserved cysteines present on its C-terminus. Studies performed on *Yarrowia lipolytica* and human cells showed that deficiency of Ind1 (human NUBPL1) affects the assembly of respiratory complex I (Bych *et al.*, 2008; Sheftel *et al.*, 2009). Since the Fe/S cluster present on Ind1 is dependent on functional core ISC assembly machinery (Bych *et al.*, 2008) it was proposed that Ind1 may serve as a specific Fe/S cluster assembly factor for the matrix-exposed electron transfer arm of complex I (Lill *et al.*, 2012), but the molecular basis for that process needs to be elucidated.

1.3.1.2 ISC export machinery.

Biogenesis of extra-mitochondrial Fe/S proteins strictly depends on the mitochondrial ISC assembly machinery (Kispal *et al.*, 1999; Lill *et al.*, 1999; Gerber *et al.*, 2004) (Fig. 1.6). It was shown that depletion of core components of ISC assembly machinery results in strong defects of cytosolic and nuclear Fe/S protein maturation (Lill *et al.*, 1999; Kaut *et al.*, 2000; Lange *et al.*,

2000; Li *et al.*, 2001a). The expression of Nfs1 and Isu1 in the cytosol did not rescue the Fe/S cluster assembly defects in that compartment (Kispal *et al.*, 1999; Gerber *et al.*, 2004; Muhlenhoff *et al.*, 2004), which led to the conclusion that mitochondria export a component that is utilized for cytosolic and nuclear Fe/S cluster biogenesis. The nature of this component, named "X", is not presently known, although the dependence of the cytosolic Fe/S protein assembly machinery on mitochondrial Nfs1 points into the direction of a sulfur-containing molecule. To date, three members of ISC export machinery have been identified: the ABC transporter Atm1, the FAD-dependent sulfhydryl oxidase Erv1 and glutathione (GSH) (Fig. 1.6). Depletion of the mitochondrial inner membrane ABC transporter Atm1 causes cytosolic Fe/S proteins defects and an accumulation of iron in the mitochondria (Kispal *et al.*, 1997; Kispal *et al.*, 1999). Hence, it was proposed that Atm1 is responsible for export of compound "X". *In vitro* studies on purified Atm1 reconstituted into proteoliposomes showed that its ATPase activity can be stimulated by components containing free sulfhydryl (SH) groups (Kuhnke *et al.*, 2006), further suggesting that it is indeed a sulfur compound which is exported from mitochondria. The second component necessary for cytosolic Fe/S protein maturation is intermembrane space protein Erv1. It is known to be involved in introducing disulfide bridges into the target proteins during their Mia40-dependent import to the intermembrane space (Mesecke *et al.*, 2005) but the Erv1 function during export of component "X" is not clear. Interestingly, also the tripeptide GSH was shown to play an important role in this process (Sipos *et al.*, 2002), as its depletion leads to the same defects in the cytosol as a deficiency of Atm1 and Erv1. Hence, GSH is believed to be the third component of ISC export machinery.

1.3.1.3 Biogenesis of extra-mitochondrial iron sulfur proteins requires the CIA machinery

Biosynthesis of extra-mitochondrial Fe/S proteins is assisted by the cytosolic Fe/S protein assembly machinery (CIA) (Fig. 1.6). CIA components do not show any sequence similarity to the ISC assembly machinery components and their depletion does not cause any defects in the mitochondrial Fe/S clusters assembly, but they seem to follow the same basic biosynthetic concept as ISC assembly machinery (Lill *et al.*, 2012). The hetero-tetramer of the P-loop NTPases Cfd1 and Nbp35 (Roy *et al.*, 2003; Hausmann *et al.*, 2005) is believed to act as a scaffold on which synthesis of Fe/S cluster occurs (Netz *et al.*, 2007; Netz *et al.*, 2012a). The cluster formation on Cfd1 and Nbp35 strictly depends on the core components of ISC assembly

machinery and ISC export machinery, which most likely provide the sulfur component necessary for Fe/S clusters biosynthesis (Lill *et al.*, 1999; Kaut *et al.*, 2000; Lange *et al.*, 2000; Li *et al.*, 2001a). Additionally, an electron transfer chain consisting of NADPH, the diflavin reductase Tah18 and Fe/S cluster-containing protein Dre2 are required (Netz *et al.*, 2010). Dre2 and Tah18 form a complex which can transfer the electrons from NADPH via the FAD- and FMN-containing Tah18 to the Fe/S clusters of Dre2 (Netz *et al.*, 2010). Interestingly, in contrast to the target proteins, Fe/S cluster assembly on the Cfd1 scaffold protein and Dre2 does not require the electron transfer chain, which suggests a need for reduction in the generation of stably inserted Fe/S clusters in Nbp35 and target Fe/S proteins (Netz *et al.*, 2010).

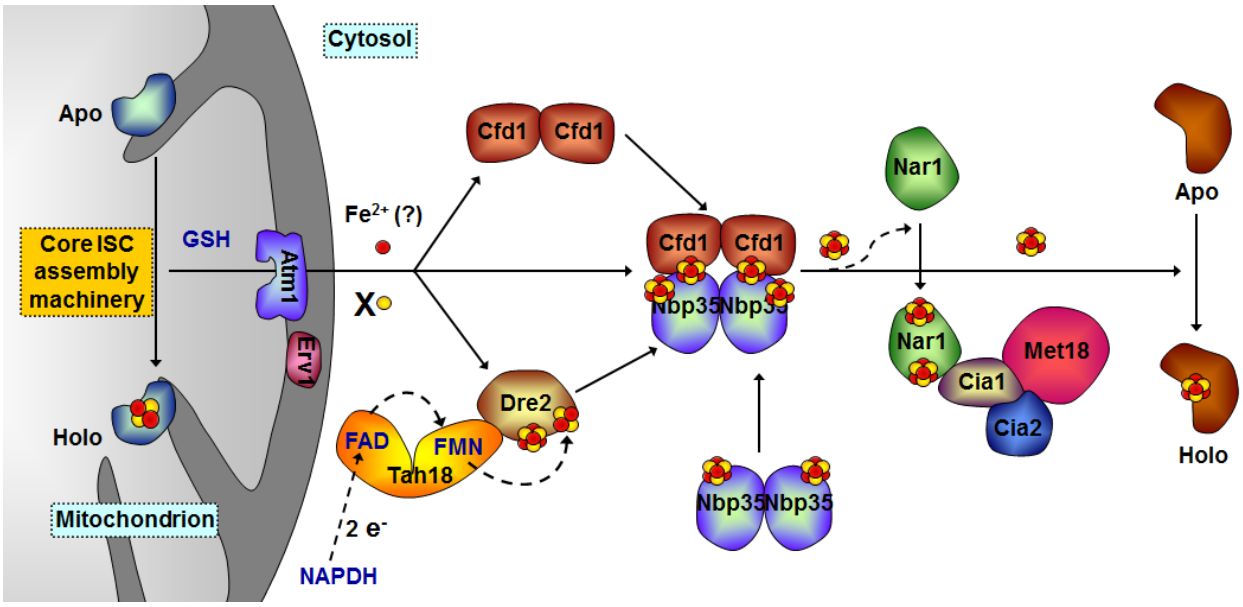

Figure 1.6: The function of the ISC export and CIA machineries in the biogenesis of cytosolic and nuclear Fe/S proteins. Both cytosolic and nuclear Fe/S protein biogenesis requires functional ISC assembly machinery. The ABC transporter Atm1 of the mitochondrial inner membrane, the intermembrane space sulfhydryl oxidase Erv1 and glutathione (GSH) are involved in the export of yet unidentified sulfur-containing compound "X" from the mitochondria. In the cytosol, Fe/S cluster assembly is assisted by CIA machinery. First Fe/S clusters are assembled on P-loop NTPases complex Cfd1-Nbp35. Sulfur is most likely provided by the component "X". The source of iron remains to be identified. Fe/S clusters assembly on Cfd1-Nbp35 requires electron transfer chain provided by NADPH, diflavin reductase Tah18 and Fe/S protein Dre2. Fe/S clusters assembled on Cfd1-Nbp35 are labile. By assistance of hydrogenase-like protein Nar1, WD40-repeat protein Cia1, Cia2 and Met18 (named also Mms19) the Fe/S clusters can be delivered to the target apo-proteins.

The exact mechanism and molecular role of electron transfer chain, as well as the source of Fe/S cluster on Dre2 and Cfd1, are still unclear. It is known that the Fe/S cluster of Dre2, but not of Cfd1, depends on the monothiol glutaredoxins Grx3 and Grx4 (Daili A. Netz personal communication). This is not surprising as Grx3/4 function as general iron donors for the whole cell and their depletion affects basically all iron-containing proteins (Muhlenhoff *et al.*, 2010). Once Fe/S clusters are assembled on Cfd1-Nbp35 they are transferred to the recipient apo-proteins in a reaction requiring Nar1 (Balk *et al.*, 2004), Cia1 (Balk *et al.*, 2005), Cia2 and Met18 (Gari *et al.*, 2012; Stehling *et al.*, 2012) proteins. Cia1 is a WD40 repeat protein which seems to act as the scaffold protein for the interaction of late CIA components (Balk *et al.*, 2005; Srinivasan *et al.*, 2007). It interacts with hydrogenase-like protein Nar1. Nar1 contains two [4Fe-4S] clusters, most likely received from Cfd1-Nbp35 complex (Urzica *et al.*, 2009). The C-terminal Fe/S cluster is stably buried within the protein, whereas the N-terminal one is exposed at the protein surface and hence is more labile (Urzica *et al.*, 2009). Cia1 also interacts with the Cia2, yet the function of this protein is unknown. Additionally, the recently identified protein Met18 (also known as Mms19 in humans), was shown to interact with both Cia1 and Cia2 proteins in yeast and with their homologs in human cells (Gari *et al.*, 2012; Stehling *et al.*, 2012). In yeast, depletion of Met18 causes profound defects in cytosolic and nuclear Fe/S protein assembly. It was proposed, that Met18 can act as a platform or an adapter protein facilitating Fe/S cluster insertion into the target proteins (Gari *et al.*, 2012; Stehling *et al.*, 2012).

1.4 Iron homeostasis and trafficking in yeast.

Once iron enters the cell it is believed to bind to diverse low molecular mass compounds and forms so called “labile iron pool” (Kakhlon and Cabantchik, 2002) (Fig. 1.7). It is necessary to distribute iron within the cell in order to avoid its accumulation resulting in toxicity. In contrast to bacteria, plants and animals – yeast (and most other fungi) do not produce the iron storage protein ferritin. Instead, excess of iron is stored in the vacuoles, most likely associated with polyphosphates (Raguzzi *et al.*, 1988; Haas *et al.*, 2008). Cycling of iron between cytosol and vacuoles can occur via two vacuolar membrane proteins Ccc1 (cross-complements Ca^{2+} phenotype of csg1) and Smf3 (suppressor of mitochondria import function). Both proteins function as divalent metal ion transporters and have been associated with calcium, manganese, and iron homeostasis in yeast (Li *et al.*, 2001b). Both transporters are thought to support vectorial

iron flux with Ccc1 acting as vacuolar iron importer (Li *et al.*, 2001b) and Smf3 as exporter of iron from the vacuolar lumen (Portnoy *et al.*, 2000) (Fig. 1.7). Additionally, Fth1 (iron (Fe) transporter homologue) protein was shown to play a role in vacuolar iron flux (Urbanowski and Piper, 1999). Vacuolar iron can be mobilized under iron-limiting conditions and utilized in the cytosol or mitochondria (Blaiseau *et al.*, 2011). Iron import to the mitochondria is conducted via carrier proteins Mrs3 and Mrs4 (mitoferrin 1 and 2 in vertebrates) (Muhlenhoff *et al.*, 2003b). Recent study of Yoon and coworkers identified an additional unique function of pyrimidine nucleotide exchanger Rim2 in promoting mitochondrial iron utilization (Yoon *et al.*, 2011) (Fig. 1.7). The triple deletion of *MRS3/4* and *RIM2* is still viable (Yoon *et al.*, 2011; Froschauer *et al.*, 2013), suggesting that there have to be other, yet unidentified carriers able to maintain the iron supply of yeast mitochondria.

Mitochondrial ISC assembly and export machineries are very tightly linked to cellular iron homeostasis. Since iron is a substrate for Fe/S cluster biogenesis, mutants of core ISC assembly and export machineries display increase of cellular iron acquisition which results in significant iron accumulation in mitochondria (Lill, 2009). These cells undergo strong transcriptional remodeling of iron-dependent cellular pathways, which resembles the transcriptional response observed under iron deprivation (Lill *et al.*, 2012). Expression of iron uptake and storage genes is tightly regulated by two iron-responsive transcription factors, Aft1 and Aft2 (Activator of Ferrous Transport) (Yamaguchi-Iwai *et al.*, 1995; Yamaguchi-Iwai *et al.*, 1996; Puig *et al.*, 2005). Aft1/2 proteins are constitutively expressed and shuttle between cytosol and nucleus in the iron-dependent manner. Under iron-deplete conditions Aft1/2 translocate from cytosol to the nucleus where they bind to consensus sequences in the upstream regions of target genes (so called “iron regulon”), and subsequently activate their transcription (Yamaguchi-Iwai *et al.*, 2002). Iron regulon includes all genes encoding components involved in high-affinity reductase-dependent and -independent iron uptake, vacuolar reductive iron export pathway, degradation of haem and post-transcriptional regulation of iron metabolism (Blaiseau *et al.*, 2011). The latter is provided by Cth1 and Cth2, two members of a conserved family of tandem zinc finger containing mRNA binding proteins, that in low iron conditions promote degradation of mRNAs encoding proteins involved in iron-dependent pathways (Puig *et al.*, 2005; Puig *et al.*,

2008; Vergara and Thiele, 2008). Cth1 and Cth2 can bind to the specific AU-rich regions (AREs) within the 3' untranslated region (UTR) of those mRNAs and recruit Dhh1 RNA helicase that

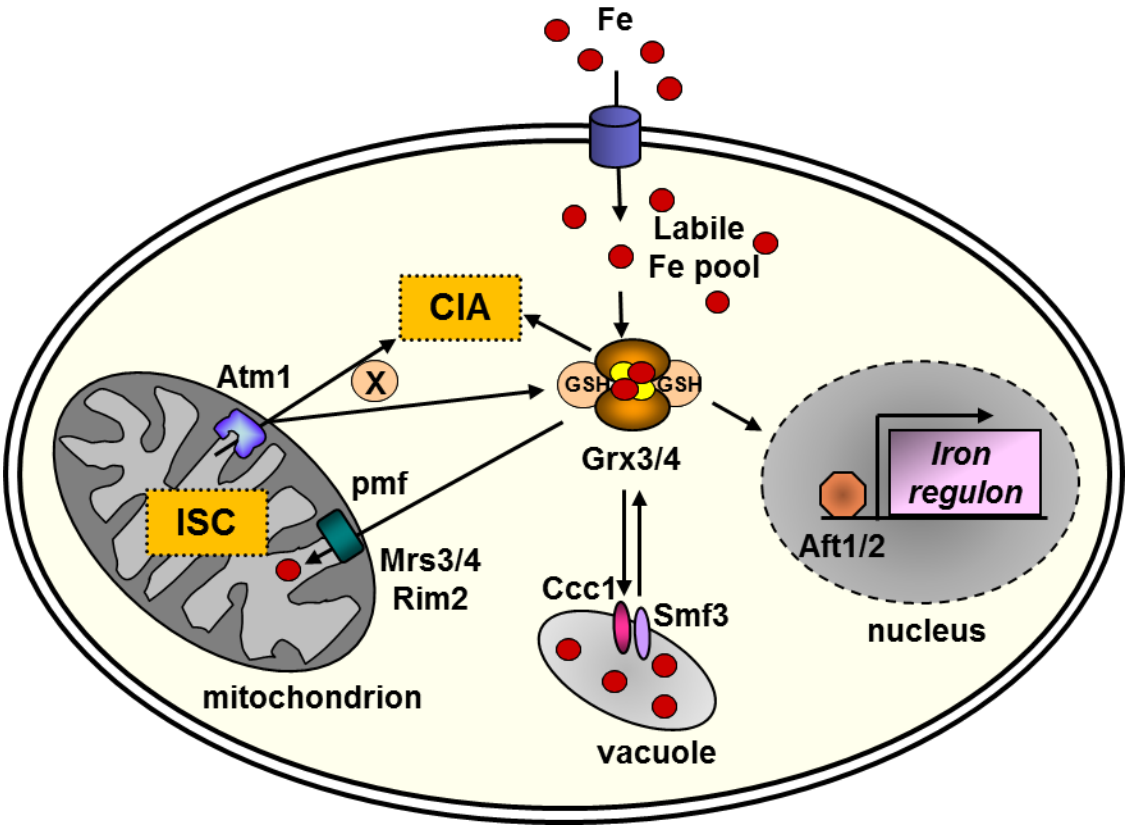

Figure 1.7: Iron trafficking and distribution in *S. cerevisiae*. Acquired iron (red dots) enters the cytosol, where it binds to diverse low molecular mass compounds. From this "labile iron pool" the iron is removed by multi-domain monothiol glutaredoxins 3 and 4 (Grx3/4) which bind a bridging, GSH-coordinated [2Fe–2S] cluster (red and yellow dots). Grx3/4 distribute iron within different cellular compartments facilitating cytosolic (CIA) and mitochondrial (ISC) Fe/S cluster assembly as well as maturation of other iron-containing proteins. Mitochondria import iron in a proton motive force (pmf) dependent fashion via the carrier proteins Mrs3, Mrs4 (Mrs3/4) and Rim2. Imported iron is utilized for maturation of Fe/S and di-iron proteins and for haem synthesis. Mitochondria export so called component "X" that is utilized by CIA machinery. Vacuoles serve as a storage and detoxification compartment that import iron via Ccc1 and export it via Smf3. In the absence of Grx3/4, or its bound Fe/S cluster, iron accumulates in the cytosol but is not biologically available. The Grx-bound Fe/S cluster functions as a sensor for the iron-responsive transcription factor Aft1 (and possibly Aft2) signaling the status of the cytosolic iron pool. In addition, Aft1 responds to the levels of a mitochondria-supplied molecule "X" that transmits the information about iron status of mitochondria. Aft1 constitutively activates transcription of multiple genes involved in cellular iron uptake, the so called iron regulon. For details see text. Figure modified after (Lill *et al.*, 2012).

through direct interaction with several members of general mRNA degradation machinery promotes 5'-to-3' decay of target mRNAs in the cytosolic P bodies (Pedro-Segura *et al.*, 2008). Post-transcriptional regulation assures efficient response to the environmental conditions and allows the cell to "save" the iron for the processes essential for the cell viability. Both Aft1 and Aft2 transcription factors have overlapping functions, but Aft1 preferentially controls the expression of iron uptake genes, whereas Aft2 is rather involved in the expression of genes responsible for intracellular iron distribution as it can, in contrast to Aft1, activate *MRS4* (involved in mitochondrial iron import) and *SMF3* (involved in vacuolar iron export) genes (Courel *et al.*, 2005). Sensing of intracellular iron by Aft1 additionally requires the regulatory proteins Fra1 and Fra2, and the multi-domain monothiol glutaredoxins Grx3 and Grx4 (Ojeda *et al.*, 2006; Pujol-Carrion *et al.*, 2006; Kumanovics *et al.*, 2008). Grx3/4 remove the iron from the "labile pool" by binding a bridging, GSH-coordinated [2Fe-2S] cluster. This Grx-bound cluster serves as an iron sensor for Aft1 (and possibly also Aft2) as those proteins physically interact with each other (Hoffmann *et al.*, 2011) (Fig. 1.7). Iron sensing by Aft1 most likely requires cysteine at position 291, as its mutations cause retaining Aft1 in nucleus and constitutive activation of target genes (Yamaguchi-Iwai *et al.*, 1995). Cells lacking Grx3/4 accumulate iron but they are not able to utilize it, which suggests that additionally to the role in iron sensing, Grx3/4 can facilitate the delivery of iron to cytosolic iron-dependent enzymes, iron binding proteins and to various intracellular compartments. Aft1/2 do not only respond to iron but also to the so called "X" factor, yet unidentified, probably low molecular weight sulfur containing component produced by the mitochondrial ISC assembly machinery and exported to the cytosol via the ABC transporter Atm1. "X" is also required for the maturation of cytosolic and nuclear Fe/S proteins by the cytosolic iron sulfur cluster assembly (CIA) machinery (Fig. 1.7). In presence of "X" or Fe/S clusters on Grx3/4 (excess of iron), Aft1/2 undergo a conformational change and are exported back to the cytosol (Chen *et al.*, 2004; Rutherford *et al.*, 2005).

1.5 Late-acting ISC assembly machinery components.

This work was focused mainly on the late-acting ISC assembly machinery components, namely Grx5, Nfu1 and BolA-like proteins. Therefore, the following chapters will give the introduction into each of these proteins.

1.5.1 The mitochondrial monothiol glutaredoxin – Grx5.

Two major redox systems are known which fight the cellular thiol-disulfide redox imbalance in the cell. Those systems are the thioredoxin system consisting of thioredoxin (Trx), NADPH and thioredoxin reductase (TrxR), and the glutaredoxin system composed of glutaredoxin (Grx), NADPH, GSH and glutathione reductase. Their main function is to reduce disulfide bridges formed in the target proteins (Meyer *et al.*, 2009). Both thioredoxins and glutaredoxins share similar structure, so called thioredoxin-fold, comprising of a four to five-stranded β-sheets surrounded by three or more α-helices (Berndt *et al.*, 2008). Grxs were identified in 1976 when Arne Holmgren found that the growth of an *E. coli* mutant lacking thioredoxin (Trx1) can be rescued by Grx protein. Grxs were then described as GSH-dependent reductases of the disulfide formed in ribonucleotide reductase during its catalytic cycle (Holmgren, 1976). Trxs and Grxs share a number of functions but with time it became clear that glutaredoxins are more versatile when it comes to the mode of action and substrate specificity. These low molecular mass thiol-disulfide oxidoreductases are strongly conserved throughout the evolution and contain three highly conserved areas within their structure: (i) an easily accessible active-site motif with one or two cysteine residues (ii) a GSH binding site and (iii) a hydrophobic surface area responsible for substrate binding (Xia *et al.*, 1992). The initial classification of Grxs was based on the nature of their active-site which was used to divide them into two major groups: dithiol Grxs with a CXXC motif in the active-site and monothiol Grx with CGFS motif. As the Grxs protein family grew, the comparative genomic analyses revealed that the initial classification is not sufficient due to diverse active-site sequences, differences in GSH binding and the presence of multidomain fusion proteins built from different Grx, Trx and other domains (Rouhier *et al.*, 2010). Hence, new classification was suggested consisting of six groups. Of those classes I and II are highly conserved in evolution and with few exceptions found in basically all living organisms (Rouhier *et al.*, 2010) (for details see Table 1).

Class	domain composition	active-site	examples
I	single Grx domain	monothiol or dithiol with **C**PY[**C**/S], **C**GY**C**, **C**PF**C** or **C**SY[**C**/S] motif	human GLRX1 and GLRX2, ScGrx1, ScGrx2 and EcGrx1-3

II	single or multiple Grx domain often fused with Trx or other domains	**C**GFS motif in the active site	single: human GLRX5, ScGrx5, EcGrxD and plant GrxS14 and GrxS16 multidomain: human PICOT (GLRX3), ScGrx3/4
III	single Grx domain	**CC**XX motif	unique for higher plants
IV	Grx domain fused to the two domains of unknown function	**C**XX[**C**/S] motif	present in photosynthetic organisms and non-mammalian animals
V	Grx domain fused to the domain of unknown function	**C**PWG motif	found only in cyanobacteria and few other bacterial species
VI	Grx domain fused to the domain of unknown function	**C**PW[**C**/S] motif	found only in cyanobacteria and few other bacterial species

Table 1: Current classification of the glutaredoxins. Sc – *S. cerevisiae*, Ec – *E. coli* (Rouhier *et al.*, 2010)

Since this work deals with the function of glutaredoxin Grx5, the rest of this chapter will be mainly focused on this protein. Grx5 is a mitochondrial matrix protein that belongs to the Class II Grxs. This class possesses only one cysteine in the active-site and thus it is unlikely that it can substitute dithiol glutaredoxins or thioredoxins as disulphide reductases as it requires dithiol mechanism (Fig. 1.8) (Bushweller *et al.*, 1992). It was proposed that the function of the monothiol Grxs can be the reduction of protein-mixed disulfides, which are formed during exposure to oxidative agents, a reaction that is conducted via monothiol mechanism (Fig. 1.8) (Bushweller *et al.*, 1992; Rodriguez-Manzaneque *et al.*, 2002; Shenton *et al.*, 2002). This theory was in agreement with elevated oxidative stress and increased total protein carbonyl content prevailing in *GRX5* deletion mutant and the fact that yeast mitochondrial Grx5 protein seemed to be required for efficient dethiolation of the Tdh3 GAPDH isoenzyme (Shenton *et al.*, 2002).

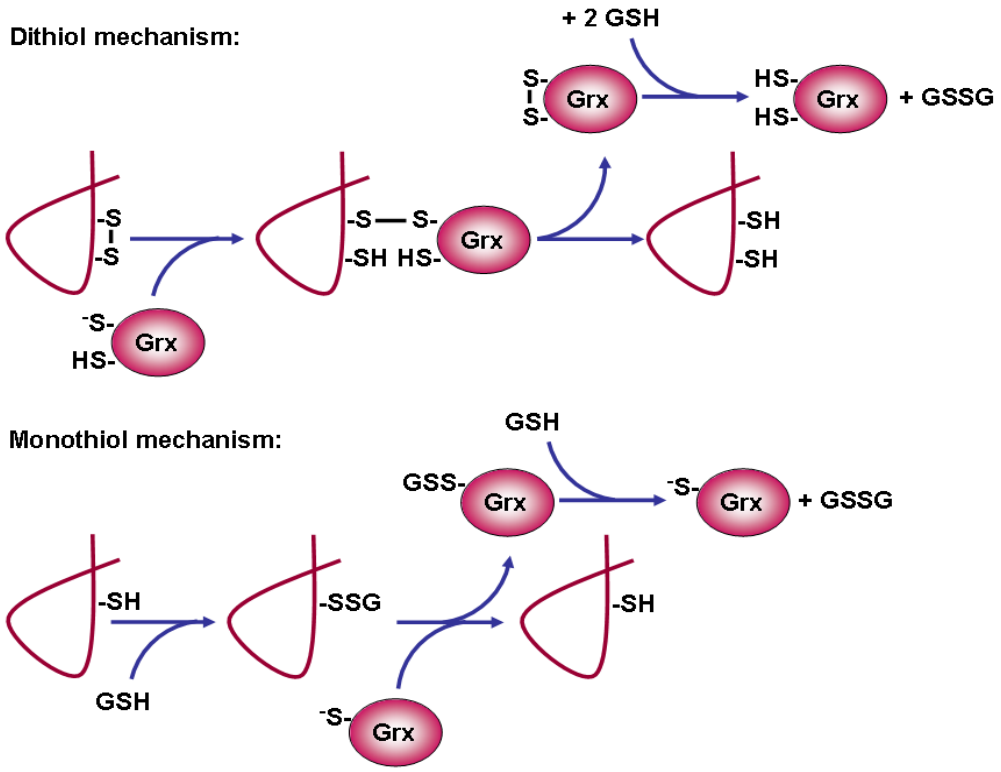

Figure 1.8: Mechanism of glutaredoxin action in the reduction of dithiol groups: dithiol vs monothiol. Glutaredoxins (Grx) can reduce both disulfide bridges and protein-glutathione adducts. The first process requires dithiol mechanism where two thiol groups of Grx are needed to reduce disulfide bond of target protein. Afterwards, intramolecular disulfide bond between Grx's active-site cysteines is formed that is then reduced by reduced glutathione (GSH). In the monothiol mechanism involved in deglutathionylation reactions, only one active-site cysteine is used to reduce mixed disulfide between the target protein and GSH. Glutathionylated Grx is regenerated by another GSH molecule. Active-site cysteine residues are shown as SH or S^- depending on the redox state. GSSG – glutathione disulfide (Herrero and de la Torre-Ruiz, 2007; Rouhier *et al.*, 2008).

However, enzymatic characterization showed that although Grx5 has the potential to form a GSH-mixed disulfide with its active site cysteine, and further to reduce glutathionylated carbonic anhydrase, this activity was twenty times less efficient than the one determined for dithiol Grxs, indicating that Grx5 is not specific for GSH-mixed disulfides (Tamarit *et al.*, 2003). A different point of view came from studies performed on *S. cerevisiae GRX5* deletion mutant showing that Grx5 is involved in the Fe/S cluster biogenesis as these yeast cells displayed inactivation of enzymes requiring Fe/S clusters for their activity. In addition, an iron accumulation in the cell was observed, a condition which in turn could promote oxidative damage (Rodriguez-

Manzaneque *et al.*, 2002). A similar phenotype, together with an impaired haem synthesis, was also shown for zebrafish and human cells (Wingert *et al.*, 2005; Ye *et al.*, 2010). Also bacterial class II monothiol glutaredoxin, *E. coli* GrxD, was demonstrated to be involved in Fe/S cluster protein biogenesis as *grxD* mutant showed strong synthetic lethality when combined with mutations in *isc* operon (Butland *et al.*, 2008). ^{55}Fe-radiolabeling experiments in *S. cerevisiae* showed that in absence of Grx5, Fe/S clusters accumulate on the scaffold protein Isu1 suggesting that Grx5 most likely facilitates Fe/S cluster transfer from this U-type scaffold to the acceptor proteins (Muhlenhoff *et al.*, 2003a). This view is supported by the fact that the *GRX5* deletion phenotype could be suppressed by overexpression of the specialized Hsp70 protein Ssq1, which is itself involved in the Fe/S cluster release from the scaffold (Rodriguez-Manzaneque *et al.*, 2002), and by the direct interaction of Grx5 with late-acting Isa proteins involved in the formation of [4Fe-4S] type of clusters (Kim *et al.*, 2010). The function of Grx5 seems to be conserved throughout evolution as *GRX5* deletion can be complemented by most monothiol glutaredoxins from both prokaryotic and eukaryotic species (Molina-Navarro *et al.*, 2006; Bandyopadhyay *et al.*, 2008). A series of recent papers indicates that class II glutaredoxins, including recombinant versions of bacterial, human, plant and the mitosome-containing parasitic protist *Gardia intestinalis* Grx5 orthologues are able to incorporate labile Fe/S cluster (Picciocchi *et al.*, 2007; Bandyopadhyay *et al.*, 2008; Rada *et al.*, 2009). *In vitro* kinetic studies indicated that it is possible to perform cysteine desulfurase-mediated assembly of [2Fe-2S] cluster in plant apo-GrxS14 and that this cluster is rapidly and quantitatively transferred to the chloroplast apo-ferredoxin (Bandyopadhyay *et al.*, 2008). These data suggested that chloroplast CGFS Grxs have the potential to function as the scaffold proteins for *de novo* Fe/S cluster synthesis and further transfer to the recipient target proteins.

Fe/S cluster assembly on Grx requires GSH. Cysteine mutagenesis studies and recently determined structure of *E. coli* Grx4 homodimer allowed to determine that Grx-bound [2Fe-2S] cluster is coordinated by two GSH molecules and active-site cysteines of two Grx monomers (Rouhier *et al.*, 2007; Bandyopadhyay *et al.*, 2008; Iwema *et al.*, 2009). The presence and possible role of Grx5-bound cluster *in vivo* remain to be determined. It is known that the active-site cysteine residue is necessary for Grx5 *in vivo* function as its substitution results in the same phenotype as that seen for the null mutant (Belli *et al.*, 2002). It was shown that other member of

class II glutaredoxins, the yeast Grx3/4 are able to carry a Fe/S cluster *in vivo.* This cluster is essential for Grx3/4 function in iron sensing and trafficking (Muhlenhoff *et al.*, 2010) (for details see chapter 1.4).

1.5.2 BolA-like proteins.

The bacterial gene *bolA* was first discovered in late 80's during the investigation of the role of D-alanine carboxypeptidases (CPases) in controlling cell shape of *E. coli.* Cell shape is maintained by the murine layer of the cell envelope. In a proposed model, the activity of some CPases could switch between cylindrical and hemispheral murine synthesis (Markiewicz *et al.*, 1982). However, the deletion of two main CPases of *E. coli*, PBP5 and PBP6, did not affect the cell division (Spratt, 1980; Broome-Smith and Spratt, 1982). This stimulated Aldea and coworkers to search for another factor involved in this process. They identified a gene whose product caused round morphology when overexpressed and named it *bolA* (from Spanish word „bola", meaning ball or sphere) (Aldea *et al.*, 1989). They proposed that the product of the *bolA* gene could be involved in the switching between cell elongation and septation systems during the cell division cycle (Aldea *et al.*, 1989). However, despite a considerable amount of research the molecular function of the BolA protein is still unknown.

BolA-like proteins are highly conserved through the evolution and with few exceptions are present in all living organisms. Yeast, as well as humans, possess three BolA-like proteins, two in the mitochondria, namely Yal044W/ BOLA1 (yeast/ human) and Aim1/ BOLA3 and one in the cytosol termed Fra2/ BOLA2. In comparison to their bacterial homologs, even less is known about the function of BolA-like proteins in eukaryotes. Studies performed on the *S. pombe* BOLA1 homolog Uvi31 showed that it is localized in the cytosol and nucleus. Similarly to the bacterial BolA protein, Uvi31 possesses a putative DNA binding domain and possible "gearbox" element in the promoter region. Moreover, the mRNA levels of the *uvi31* gene are increased when cells reach the diauxic shift phase just before stationary phase during cellular growth and after UV radiation that causes DNA damage and cell arrest in G2 phase (Kim *et al.*, 1997). These results suggested that the Uvi31 is involved in the progression of defective cell cycle after DNA replication checkpoint arrest caused by UV-light induced DNA damage (Kim *et al.*, 1997). The molecular basis of this suggested function remains to be determined. Deletion of both *YAL044W* and *AIM1* (altered inheritance of mitochondria) in *S. cerevisiae* does not cause any obvious

phenotype, although it was indicated that Aim1 protein may be involved in mitochondrial function or organization and that the *aim1* null mutant displayed elevated frequency of mitochondrial genome loss (Hess *et al.*, 2009).

A first clue about potential interaction partners of BolA proteins came from bioinformatics study combining genome sequences, physical interaction data and 3D structures (Huynen *et al.*, 2005). The work showed that BolA is homologous to the peroxide reductase OsmC and related to other class II KH-fold proteins (K protein homology). OsmC can detoxify hydroperoxides by reducing them into alcohols and has two conserved cysteines in the active-site which are missing in BolA-like proteins and thus cannot be used as reducing equivalents. Phylogenic analysis of BolA-like proteins showed that they have strong genomic association with the monothiol glutaredoxins. The fact that an interaction between Fra2 and Grx3 proteins was previously detected in yeast by two-hybrid and FLAG-tag experiments (Ito *et al.*, 2000; Bhan *et al.*, 2002) made likely that BolA-like proteins may cooperate with Grxs as reductases to potentially reduce and/ or deglutathionylate substrates (Huynen *et al.*, 2005). A few years later the group of Jerry Kaplan identified Fra2 as a protein involved in regulating the yeast iron regulon in response to decreased Fe/S cluster synthesis (Kumanovics *et al.*, 2008), a signaling pathway that also requires Grx3/4 in yeast. They found that mutations in *FRA2* gene led to an increase in transcription of the iron regulon, as the iron-sensing transcription factor Aft1 was transferred to the nucleus where it occupied the promoter of *FET3* gene encoding multicopper oxidase involved in iron import to the cell (Kumanovics *et al.*, 2008). Further *in vitro* studies showed that Grx3/4 and Fra2 can form a heterodimeric complex bridged by a [2Fe-2S] cluster. This cluster is coordinated by the active-site cysteine of Grx3/4, GSH, and a histidine residue of Fra2. This complex was suggested to act as a signal to control the iron regulon in response to the cellular iron status in yeast (Li *et al.*, 2009). Furthermore, a similar complex formation was shown for the human proteins GLRX3 and the Fra2 homolog BOLA2 (Ren *et al.*, 2012), implying that Grx-BolA interaction is conserved in higher eukaryotes. More recently, the interaction between mitochondrial human proteins BOLA1 and GLRX5 was reported (Willems *et al.*, 2013). In the same study the potential role of BOLA1 was investigated. Overexpression of BOLA1 in mitochondria attenuates the effect of GSH depletion on the mitochondrial thiol redox potential and prevents changes in mitochondrial morphology under these conditions (Willems *et*

al., 2013). These results are in agreement with the previously suggested role of BolA proteins as reductases working together with monothiol glutaredoxins (Huynen *et al.*, 2005). The physiological role of BOLA1 protein as well as the biochemical meaning of BOLA1-GLRX5 complex formation is still not understood.

Partial characterization of the possible function of BOLA3 protein came from the discovery of a frame shift mutation introducing premature stop codon in the Canadian patients. The individuals died at the age of few months. Patients' cells displayed severe defects in the lipoic acid-containing proteins pyruvate dehydrogenase and α-ketoglutarate dehydrogenase as well as in respiratory complexes I and II but had normal mitochondrial Fe/S protein aconitase activities (Cameron *et al.*, 2011). More or less at the same time patients with a BOLA3 mutation were discovered in Germany. Individuals displayed the same phenotype with additional complex III deficiency (Haack *et al.*, 2013). Results of clinical and biochemical studies performed on all of these patients suggested that the BOLA3 protein plays an essential role in the production of Fe/S clusters necessary for the normal maturation of lipoic acid synthase and for the assembly of the respiratory chain complexes (Cameron *et al.*, 2011; Haack *et al.*, 2013). Similar to other BolA-like proteins, BOLA3 could also cooperate with GLRX5 (Cameron *et al.*, 2011) but the confirmation of this view is missing. It is not unlikely though, as involved in Fe/S cluster biogenesis in *E.coli* GrxD was shown to form a heterodimeric complex with BolA protein. This heterodimeric complex was bridged by a [2Fe-2S] cluster which could be transfered to the apo-ferredoxin *in vitro* (Yeung *et al.*, 2011). Taken together, although BolA-like proteins were linked to the Fe/S cluster maturation and iron metabolism, little is known about their biochemical function in the cell.

1.5.3 Nfu-like proteins.

Proteins containing the 70 amino acid long C-terminal part of *A. vinelandii* NifU protein are termed as Nfu-like proteins. Although this conserved segment possesses a CXXC motif and is able to transiently bind a [4Fe-4S] cluster, its function was not clear for a long time. Especially, the bacterial *nfuA* gene is located outside the *isc* operon (Frazzon and Dean, 2003). Initial evidence that the Nfu-like proteins are involved in Fe/S cluster biosynthesis was obtained through a synthetic lethal screen study in yeast where the *nfu1Δ* deletion mutant was synthetic lethal together with deletion of *SSQ1* (Schilke *et al.*, 1999). In this study, Nfu1 was shown to be a

nonessential, mitochondrial protein. Deletion of *NFU1* caused some sensitivity to oxidative stress, yet no other severe defects in the cell metabolism. *nfu1Δ* mutant cells grow slower than wild-type cells on non-fermentable carbon sources and tested Fe/S cluster containing enzymes activities are only slightly affected. When *NFU1* deletion was combined with *ISU1* deletion, cells developed problems with respiration, a decrease in Fe/S cluster containing enzymes activity as well as iron accumulation in mitochondria. As this phenotype is typical for cells deficient in Fe/S cluster biosynthesis and Nfu1 protein is highly conserved through the evolution, it was concluded that it may be a part of mitochondrial ISC assembly machinery (Schilke *et al.*, 1999).

The *Arabidopsis thaliana* genome encodes five Nfu-like proteins. AtNfu1-3 are localized in plastids and AtNfu4-5 in the mitochondria. The latter have a structural organization similar to yeast Nfu1 but AtNfu1-3 possess a duplicated Nfu-like domains from which one has lost the CXXC motif. AtNfu1-2 and AtNfu4-5 were able to rescue *nfu1Δisu1Δ* phenotype when targeted to yeast mitochondria and AtNfu2 was shown to carry labile [2Fe-2S] cluster *in vitro* (Leon *et al.*, 2003). In plants Nfu-like proteins are not essential but plants lacking, for example, the *NFU2* gene show a dwarf and pale green leaf phenotype and they have largely affected photosynthetic growth. *NFU2* mutant plants were also shown to have impaired assembly of [4Fe-4S] and [2Fe-2S] ferredoxin clusters and reduced electron flow coming from the photosynthetic apparatus, but Rieske and [3Fe-4S] glutamate synthase clusters were not affected (Touraine *et al.*, 2004). It was suggested that AtNfu2 can act as an alternative scaffold for Fe/S cluster assembly for a subset of target proteins (Touraine *et al.*, 2004; Yabe *et al.*, 2004).

Deletion of *E. coli* and *A. vinelandii nfuA* genes led to the increased mortality under various stress conditions, such as iron starvation or oxidative stress (Yabe *et al.*, 2004; Angelini *et al.*, 2008). NfuA was shown to assemble a Fe/S cluster *in vitro* and this [4Fe-4S] cluster could be then transferred to apo-aconitase (Angelini *et al.*, 2008). Interestingly, additionally to the Nfu-like domain, NfuA possesses degenerated ATC* (A-type carrier) domain which is typical for the Fe/S carrier proteins. As it is very difficult to distinguish between a scaffold and a carrier protein based just on *in vitro* experiments, group of Frederic Barras continued with *in vitro*, *in vivo* and *in silico* approaches to determine the actual role of the NfuA protein. They were able to show that NfuA is a novel carrier protein that interacts with target proteins via its ATC* domain and receives Fe/S cluster from $SufBC_2D$ scaffold complex via Nfu-domain. However, NfuA was not

able to transfer the Fe/S cluster back to the $SufBC_2D$ scaffold complex. It was suggested that Fe/S cluster transfer to the apo-proteins could possibly happen within shielded transfer space of NfuA-target complex. This shielding could protect the Fe/S cluster from the potentially destructive environment, which is especially important for oxygen species sensitive targets AcnB and IspH (Py *et al.*, 2012). Similarly as in case of *A. thaliana nfu2Δ* mutant, no effect of *nfuA* mutation was seen on glutamate synthase, which possess stable Fe/S cluster regardless on growth conditions, further supporting the view that NfuA acts as a carrier protein especially required under the stress conditions (Py *et al.*, 2012).

In 2003 the group of Tracy A. Rouault showed that human NFU1 is able to assemble a labile [4Fe-4S] cluster coordinated by two NFU1 monomers. In agreement with the plant and bacterial data available at the time, it was suggested that NFU1 could act as the alternative scaffold for the Fe/S clusters biogenesis (Tong *et al.*, 2003). In 2011 two groups reported on patients carrying the mutations in the *NFU1* gene (Cameron *et al.*, 2011; Navarro-Sastre *et al.*, 2011). In the first case a non-sense mutation resulting in abnormal mRNA splicing and complete loss of the protein (Cameron *et al.*, 2011), while in the second, a G→C point mutation led to glycine to the cysteine exchange just next to the active-site (CXXC) of NFU1 (Navarro-Sastre *et al.*, 2011). Affected individuals were born on time with no evident symptoms, but fast developed severe developmental retardation, brain abnormalities and pulmonary hypertension, eventually leading to death between about 3 months (Cameron *et al.*, 2011) and one year (Navarro-Sastre *et al.*, 2011) after birth. The biochemical analyses of these patients showed a phenotype similar to the one observed in BOLA3 patients, in example normal activities of aconitase (Cameron *et al.*, 2011; Navarro-Sastre *et al.*, 2011) but massive decrease in complexes I (Cameron *et al.*, 2011) and II activities (Cameron *et al.*, 2011; Navarro-Sastre *et al.*, 2011). Additionally strong defects in lipoic acid-containing proteins, pyruvate dehydrogenase (PDH) and α-ketoglutarate dehydrogenase (KGDH), together with hyperglycinemia and an increase in organic ketoacids were detected (Cameron *et al.*, 2011; Navarro-Sastre *et al.*, 2011). This phenotype was explained by a defect of the Fe/S cluster-containing protein lipoate synthase (Hiltunen *et al.*, 2010). Lipoate synthase was not routinely tested during Fe/S protein biogenesis studies explaining why this phenotype was missed during previous studies. RNAi-depletion of NFU1 in human cell culture gave the same phenotype as observed in patients (Navarro-Sastre *et al.*, 2011), pointing to a role

of NFU1 in the assembly of complex Fe/S proteins (respiratory complexes I and II and lipoate synthase containing eight, three or two Fe/S clusters, respectively) (Cameron *et al.*, 2011; Navarro-Sastre *et al.*, 2011; Lill *et al.*, 2012). Despite the progress made with the analyses of human patients, still little is known about exact role of Nfu1 protein in Fe/S cluster biogenesis and possibly other processes in the cell.

1.6 Aim of the work

During the last years substantial progress has been achieved in the characterization and understanding of Fe/S protein biogenesis in both prokaryotes and eukaryotes. It is now well known that this process is essential for cell viability and well conserved through the evolution. Several components of mitochondrial Fe/S cluster assembly machinery are disease relevant. Examples include the iron transporter mitoferrin (Mrs3/4) which is associated with erythropoietic protoporphyria (Shaw *et al.*, 2006), the human Isu1 homolog ISCU which is associated with myopathy with exercise intolerance (Mochel *et al.*, 2008; Olsson *et al.*, 2008), frataxin causative of Friedreich's ataxia (Campuzano *et al.*, 1997), and ABCB7 (yeast Atm1) with X-linked sideroblastic anaemia and cerebellar ataxia (Bekri *et al.*, 2000). Also, some Fe/S target proteins are disease relevant like XPD which is mutated in Xeroderma pigmentosum or FANCJ associated with Fanconi anemia (Lill, 2009). The detailed understanding of the mechanisms of Fe/S protein assembly is therefore not only of basic scientific interest, but also of medical importance with the potential treat related diseases.

Previous work by many groups allows us to divide the maturation pathway of mitochondrial Fe/S proteins into three distinct major steps. The general function of many ISC assembly machinery components involved in those steps is quite well described in the literature. However, we still do not completely understand the mechanistic details of many of the partial reactions of Fe/S clusters assembly at the molecular level (Lill *et al.*, 2012). Hence, the aims of my work are focused on a better understanding of the fate of the Fe/S cluster after its synthesis on the scaffold protein Isu1 and before Fe/S cluster insertion into target apo-proteins.

In the first part of my work, I address the role of the mitochondrial monothiol glutaredoxin Grx5 in Fe/S cluster release and/ or transfer from the Isu1 scaffold protein. It was previously shown that upon depletion of Grx5 Fe/S clusters accumulate on Isu1 and cannot be

properly transferred to the target proteins (Muhlenhoff *et al.*, 2003a). Human GLRX5 has been associated with microcytic anemia (Wingert *et al.*, 2005) and its deletion in zebrafish is embryonically lethal (Camaschella *et al.*, 2007). In yeast, Grx5 is not essential although cells lacking Grx5 suffer from a severe phenotype including loss of activities of Fe/S cluster proteins, iron accumulation in mitochondria and oxidative stress (Rodriguez-Manzaneque *et al.*, 2002). The latter phenotype raised the question if the Fe/S protein deficiency is the result or the cause of the oxidative stress? I therefore focused my work on testing whether Grx5 is specifically involved in the Fe/S cluster biosynthesis pathway. A further important goal was to better describe its mechanistic role in Fe/S cluster release from the scaffold protein.

In the second and third part of my work, my goal was to define the molecular function of Nfu1, the yeast homologue of human NFU1, and of Aim1, the homologue of human BOLA3. Both proteins have recently been linked with fatal infantile encephalopathy and/ or pulmonary hypertension (Cameron *et al.*, 2011; Navarro-Sastre *et al.*, 2011). Despite this disease-relevant function and the description of the patient phenotypes little is known about the molecular function of those two proteins, besides the fact that they are important for the maturation of Fe/S clusters of respiratory complexes I and II and of lipoate synthase (Cameron *et al.*, 2011; Navarro-Sastre *et al.*, 2011). Nfu1-like proteins were previously associated with Fe/S cluster biosynthesis as they are similar to the C-terminal part of *A. vinelandii* NifU protein, a member of the bacterial NIF Fe/S cluster assembly system which is crucial for the maturation of the complex Fe/S protein nitrogenase (Frazzon and Dean, 2003). As many Nfu1-like proteins are able to bind an Fe/S cluster *in vitro* (Frazzon and Dean, 2003; Tong *et al.*, 2003), a role of Nfu1 as an alternative scaffold protein working in parallel to the well-characterized Isu1 was suggested (Touraine *et al.*, 2004; Yabe *et al.*, 2004). However, a recent investigation of the phenotypes observed in human patients and NFU1-deficient cell culture suggests that both NFU1 and BOLA3 proteins may not function as general Fe/S maturation factors but rather as dedicated targeting proteins. To biochemically resolve this problem I therefore investigated the molecular role of Nfu1 and Aim1, as well as another mitochondrial BolA-like protein termed Yal044W.

The elucidation of the molecular role of Grx5, Nfu1 and BolA-like proteins will contribute to the better understanding of how Fe/S clusters are handled within the mitochondrial matrix after their synthesis on the scaffold protein Isu1, and how the target apo-proteins received

their Fe/S cluster. Results from such work will potentially answer some of the important questions concerning the molecular mechanism of mitochondrial Fe/S protein biosynthesis. Additionally, as all proteins investigated in this study are disease relevant, it is important to understand how their functional loss contributes to the development of the disease phenotypes and the progression of the pathological state.

2 Materials and methods

2.1 Devices

device	manufacturer
Advanced primus 25 PCR machine	*peqlab*
Accublock™ digital dry bath	*Labnet*
Autoclave Systec V-150	*Systec*
Centrifuge Biofuge pico	*Heraeus*
Centrifuge 3K30	*Sigma*
Centrifuge Avanti J20 XP	*Beckmann*
Chemostar professional chemiluminescence documentation system	*Intras*
Electrophoresis Power Supply EPS 600	*Amersham Pharmacia Biotech*
Electrophoresis Power Supply EC 105	*E-C Apparatus Corporation*
Electrophoresis system for agarose gels Model B1A	*Owl Separations Systems*
Electrophoresis system for SDS-PAGE: Minigel-Twin	*Biometra*
Emulsifier EmulsiFlex® C3	*Avestin*
Fluorescence spectrometer FP-6300	*Jasco*
Gel Documentation System for agarose gels (GDS)	*Intras*
LS 6500 Multi-Purpose Scintilation Counter	*Beckmann*
Multitron flasks shaker	*INFORS HT*
pH-Meter UB-10	*Denver Instruments*
Pipettes (with range of 0 - 2 µl; 2 - 10 µ; 2 - 20 µl; 20 - 200 µl and 200 - 1000 µl)	*Gilson*
Plate reader Infinite® M200	*Tecan*
Scale PT 1500	*Sartorius*
Scale SBC22	*Saltec*
Semi-dry Blotter Sedec™ M	*Sedec*
Steri-Cult Incubator	*Forma Scientific*
UV/VIS spectrometer U-550	*Jasco*
Thermomixer Comfort	*Eppendorf*

2.2 Chemicals

All chemicals and reagents used in this work were at least 99 % pure or at highest available purity and quality. They were purchased from *Sigma-Aldrich*, *Roth*, *Merck KGaA*, *Serva*, *Difco Laboratories* or *AppliChem*.

2.3 Enzymes

All restriction enzymes used in this work were purchased from *Fermentas* or *New England Biolabs*. Enzymes listed below were purchased from: Phusion® DNA Polymerase (*Finnzymes*), T4 DNA Ligase (*New England Biolabs*), Alkaline Phosphatase (*Fermentas*), Zymolyase 100T (*Seikagaku*), Hexokinase (*Sigma-Aldrich*), Glucose-6-phosphate dehydrogenase (*Sigma-Aldrich*).

2.4 Antibodies

Primary antibodies used in this study were raised in rabbits against recombinant proteins. Antibodies against C-Myc or HA were obtained from *Santa-Cruz* and antibody against GST from *GE Healthcare*. Secondary antibodies, Goat Anti-Rabbit IgG (H+L) HRP Conjugate and Goat Anti-Mouse IgG (H+L) HRP Conjugate were obtained from *BioRad*.

2.5 Molecular weight standards

Molecular weight standards used in this work were:

- for DNA electrophoresis: „GeneRuler™ 1 kb Plus DNA Ladder“ (*Fermentas*)
- for SDS-PAGE: „PageRuler™ Prestained Protein Ladder“ (*Fermentas*)

2.6 Oligonucleotides

All oligonucleotides used in this work were purchased from *Metabion* and they are listed below.

name	sequence (5'→3')	application
For_GRX5_60CGFS_SGFS	AAG TCT GGA TTT TCA AGA GCA ACC ATT GG	Mutagenesis of Cys 60 to Ser in *S. cerevisiae* Grx5
Rev_GRX5_60CGFS_SGFS	TCC AGA CTT GGG AAA TTC AGG AGT ACC TT	Mutagenesis of Cys 60 to Ser in *S. cerevisiae* Grx5
For_HsGrx5_EcoRI(mtScTarg)	GTA GAA TTC ATG TTT CTC CCA AAA TTC AAT CCC ATA AGG TCA TTT TCC CCC ATC CTC CGG GCT AAG ACT GCG GGC TCG GGC GCG GGC	Cloning of *Homo sapiens* GLRX5 into p424-TDH3 vector. Mitochondrial targeting sequence exchanged to the *S. cerevisiae* one.
Rev_HsGrx5_HA_XhoI	GTA CCT CGA GTC AAG CGT AAT CTG GAA CAT CGT ATG GGT ACT TGG AGT CTT GGT CTT T	Cloning of *Homo sapiens* GLRX5 into p424-TDH3 vector with additional C-terminal HA-tag.

For_SpGRX5_C51S	ATG TCT GGT TTT TCT TTG AAA GCT ATT CAA	Mutagenesis of Cys 51 to Ser in *S. pombe* Grx5
Rev_SpGRX5_C51S	ACC AGA CAT TGG TCT AGT TGG AGT ACC TTT	Mutagenesis of Cys 51 to Ser in *S. pombe* Grx5
For_NFU1_G194C	CAA TGT GCA TGT ACC TCA TGC TCT TCT AGT	Mutagenesis of Gly 194 to Cys in *S. cerevisiae* Nfu1
Rev_NFU1_G194C	TGC ACA TTG TAA TCT TAA ATA AAC GGT TCC	Mutagenesis of Gly 194 to Cys in *S. cerevisiae* Nfu1
For_NFU1_C196S_C199S	GCA TCT ACC TCA TCC TCT TCT AGT GAA GTG	Mutagenesis of Cys 196 to Ser and Cys 199 to Ser in *S. cerevisiae* Nfu1
Rev_NFU1_C196S_C199S	AGA GGA TGA GGT AGA TGC ACC TTG TAA TCT	Mutagenesis of Cys 196 to Ser and Cys 199 to Ser in *S. cerevisiae* Nfu1
For_SpUVI31_BamHI	ATC GGA TCC ATG ATT AGA AGA TTT TTT CAC	Cloning of *S. pombe* UVI31 into p424-TDH3 vector with already cloned in C-terminal Myc-tag.
Rev_SpUVI31_EcoRI	ATC GAA TTC CGA AAC TTC ATC AGG AGT CTT	Cloning of *S. pombe* UVI31 into p424-TDH3 vector with already cloned in C-terminal Myc-tag.
For_SpCC4B311C_BamHI	ATC GGA TCC ATG AAG TTA GCC ATC GGT AGG	Cloning of *S. pombe* CC4B311.C into p424-TDH3 vector with already cloned in C-terminal Myc-tag.
Rev_SpCC4B311C_EcoRI	ATC GAA TTC TGA ACT TGT AGT CGA TCC GCC	Cloning of *S. pombe* CC4B311.C into p424-TDH3 vector with already cloned in C-terminal Myc-tag.

2.7 Purchased genes

DNA fragment containing codon optimized (for *S. cerevisiae* expression) *S. pombe GRX5* gene together with C-terminal short linker and 3x Myc-tag was purchased from *GeneScript*.

Sequence (5'→3'):

GGATCCATGAACTCTATGTTTAGATTTTGGATTCCAAAAACTTCTATTTCTATGCAACTAAGAATGTTGT
CTACTCAAACTAGACAAGCTCTCGAGCAAGCTGTTAAAGAAGATCCAATTGTTTTGTTTATGAAAGGTA
CTCCAACTAGACCAATGTGTGGTTTTTCTTTGAAAGCTATTCAAATTTTGTCTTTGGAAAATGTTGCTT
CTGATAAATTGGTTACTTATAATGTTTTGTCTAATGATGAATTGAGAGAAGGTATTAAAGAATTTTCTGA
TTGGCCAACTATTCCACAATTGTATATTAATGGTGAATTTGTTGGTGGTTCTGATATTTTGGCTTCTAT

GCATAAATCTGGTGAATTGCATAAAATTTTGAAAGAAATTAATGCTTTGGCTCCAGAACAACCAAAAGA
TTCTGAAGAAGAAACTACTAAAAAAGATGAATTCCTGCAGGTGGACTCCGGTTCCGCTGCTAGTGGT
GAACAGAAGTTGATTTCTGAAGAAGATCTGAACGGTGAGCAAAAGCTAATCTCCGAGGAAGACTTGA
ATGGTGAACAGAAATTAATATCAGAAGAGGACCTCAACGGATAAGTCGAC

Annotations:

1 – 6: BamHI site

7 – 444: Sp*GRX5*

445 – 483: linker

484 – 591: 3x Myc-tag

592 – 594: stop codon

595 – 600: HincII; SalI site

2.8 Plasmids

plasmid	ORF	backbone	source/ reference
p416-*SSQ1-GST*	*SSQ1,* C-terminal GST	p416-*Met25* (Funk *et al.*, 2002)	(Gerber *et al.*, 2003)
p424-*SSQ1*	*SSQ1*	p424-*TDH3* (Funk *et al.*, 2002)	U. Mühlenhoff
pYES2-*SSQ1*-His	*SSQ1*; C-terminal His-tag	pYES2	(Dutkiewicz *et al.*, 2003)
p424-*GRX5*	*GRX5*	p424-*TDH3*	U. Mühlenhoff
p424-*GRX5C^{60}S*	*GRX5* site directed mutant	p424-*TDH3*	this work.
p424-*SpGRX5-Myc*	*GRX5 (Schizosaccharomyces pombe;)* C-terminal Myc	p424-*TDH3*	this work.
p424-*SpGRX5C^{51}S-Myc*	*GRX5* site directed mutant *(Schizosaccharomyces pombe;)* C-terminal Myc	p424-*TDH3*	this work.
p424-*HsGRX5-HA*	*GRX5 (Homo Sapiens);* C-terminal HA	p424-*TDH3*	this work.
pET15b-His-*GRX5*	*GRX5* (truncated to M28)*;* N-terminal His-Tag	pET15b	U. Mühlenhoff
p426-*HIPIP-Myc*	Pre-F1*β*(1-40)-[4Fe/4S]-*HIPIP*; (*C. vinosum);* C-terminal Myc	p426-*TDH3* (Funk *et al.*, 2002)	(Muhlenhoff *et al.*, 2011)
p426-*BFD-Myc*	Pre-F1*β*(1-40)- [2Fe-2S]-*Bfd; (E. coli*)*;* C-terminal Myc	p426-*TDH3*	U. Mühlenhoff
p426-*ISU1*	*ISU1*	p426-*TDH3*	(Muhlenhoff *et al.*, 2003a)
pCM189-*ISU1D^{71}A*	*ISU1* site directed mutant	pCM189	U. Mühlenhoff

p426-*LIP5-HA*	*LIP5;* C-terminal HA	p426-*TDH3*	(Gelling *et al.*, 2008)
p424-*DNAK*	*DNAK (E. coli)*	p426-*TDH3*	U. Mühlenhoff
p426-*BIO2*	*BIO2*	p426-*TDH3*	U. Mühlenhoff
p424-*FET3-GFP*	*GFP*	p424-*TDH3*	(Hausmann *et al.*, 2008)
p426-*HsGRX2-Myc*	*GRX2 (H. sapiens);* C-terminal Myc	p426-*TDH3*	U. Mühlenhoff
p426-*HsFDX1-HA*	*FDX1 (H. sapiens);* C-terminal HA	p426-*TDH3*	U. Mühlenhoff
p426-*GRX4-HA*	*GRX4*	p426-*TDH3*	U. Mühlenhoff
p426-*mtGRX4-HA*	*GRX4* (with mitochondrial targeting sequence of *GRX5* (length 81 bp))*;* C-terminal HA	p426-*TDH3*	U. Mühlenhoff
p416-*AIM1-Myc*	*AIM1;* C-terminal Myc	p416-*TDH3*	U. Mühlenhoff
p424-*AIM1-HA*	*AIM1;* C-terminal HA	p424-*TDH3*	U. Mühlenhoff
p416-*YAL044W-Myc*	*YAL044W;* C-terminal Myc	p416-*TDH3*	U. Mühlenhoff
p424-*SpUVI31-Myc*	*UVI31 (S. pombe);* C-terminal Myc	p424-*TDH3*	this work.
p424-*SpCC4B3.11C-Myc*	*CC4B3.11C (S. pombe);* C-terminal Myc	p424-*TDH3*	this work.
p426-*NFU1-Myc*	*NFU1;* C-terminal Myc	p426-*TDH3*	J. Gerber
p426-*NFU1G^{194}C-Myc*	*NFU1* site directed mutant*;* C-terminal Myc	p426-*TDH3*	this work.
p426-*NFU1C^{196}S/C^{199}S-Myc*	*NFU1* site directed mutant*;* C-terminal Myc	p426-*TDH3*	this work.

2.9 Bacterial and yeast strains

2.9.1 *Escherichia coli* strains used in this study

strain	genotype	source/ reference
E. coli DH5α	*F*$^-$ φ80d*lac*ZΔM15 Δ(*lac*ZYA-*arg*F)U169 *rec*A1 *end*A1 *hsd*R17(rk$^-$mk$^+$) *pho*A *sup*E44 *thi*-1 g*yr*A96 *rel*A1 λ$^-$	*Invitrogen*
E. coli BL21(DE3)-Gold	*F*$^-$ *ompT, hsdSB (rB*$^-$ *mB*$^-$*), dcm*$^+$ *Tet*^{R} *gal*λ *(DE3) endA Hte*	*Invitrogen*

2.9.2 *Saccharomyces cerevisiae* strains used in this study

strain	genotype	method of generation	source/ reference
W303-1A	*MATa; ura3-1; ade2-1; trp1-1; his3-11,15; leu2-3,112*	Obtained from Euroscarf	
BY4742	his3-1; leu2-0; ura3-0, met15-0	Obtained from Euroscarf	
BY4742 (trp1Δ)	BL4742 *his3Δ1, leu2 Δ0, met15 Δ0 ura3Δ0 YDR007w(TRP1)::kanMX4*	PCR fragment (pFA6a-KanMX4)	Nadine Richter
Gal-*NFS1*	W303-1A, *pNFS1::GAL1-10-HIS3*	PCR fragment (pFA6a-HIS3-Gal)	(Gerber *et al.*, 2003)
Gal-*SSQ1*	W303-1A, *pSSQ1::GAL1-10-LEU2*	PCR fragment (pTL26)	(Gerber *et al.*, 2003)
Gal-*ISU1/ isu2Δ*	W303-1A, *pISU1::GAL1-10-HIS3, isu2::LEU2*	PCR fragment (pFA6a-HIS3-Gal, pUG73)	(Gerber *et al.*, 2004)
Gal-*JAC1*	W303-1A, *pJAC1::GAL1-10-HIS3*	PCR fragment (pFA6a-HIS3-Gal)	(Gerber *et al.*, 2003)
Gal-*GRX5*	W303-1A, *pGRX5::GAL1-10-HIS3*	PCR fragment (pFA6a-HIS3-Gal)	(Gerber *et al.*, 2003)
Gal-*GRX4/ grx3 Δ*	W303-1A, *pGRX4:: GAL-L-natNT2; grx3::LEU2*	W303 grx3; PCR fragment (pYM-N27) (Janke et al., 2004)	Muhlenhoff, 2011
aim1Δ	BY4742, *pAIM1::KanMX4 YDR007w(TRP1)::CloneNAT*	PCR fragments (pFA6a-KanMX4, pFA6a-CloneNat) Obtained from Euroscarf	
bio2Δ	W303-1A, *bio2::KanMX4*	PCR fragment (pFA6a-KanMX4)	Nadine Richter
grx5Δ	W303-1A, *grx5::KanMX4*	PCR fragment (pFA6a-KanMX4)	(Rodriguez-Manzaneque *et al.*, 1999)
sod2Δ	BY4742, *pSOD2::KanMX4*	Obtained from Euroscarf	
isa1/2Δ	W303-1A, *pISA1::KanMX4, isa2::HIS3*	PCR fragments (pFA6a-HIS3MX6; pFA6a-KanMX4)	(Pelzer *et al.*, 2000)
nfu1Δ	W303-1A, *pNFU1::HIS3MX6*	PCR fragments (pFA6a-HIS3MX6)	This study
yfh1Δ	W303-1A, *yfh1::KanMX4*	PCR fragment (pFA6a-KanMX4)	Nadine Richter
yal044wΔ	BY4742, *pYAL044W::KanMX4 YDR007w(TRP1)::CloneNAT*	PCR fragments (pFA6a-KanMX4, pFA6a-CloneNat) Obtained from Euroscarf	
aim1Δ/ yal044wΔ	W303-1A, *pAIM1/pYAL044W::LEU2*	PCR fragments (pFA6a-LEU2MX6)	This study

2.10 Growth conditions

2.10.1 *E. coli*: culture and media

E. coli cells were grown in LB medium (Sambrook and Russel, 2001). Depending on selection marker requirements medium was supplemented with Ampicillin in end concentration 100 μg/ ml.

LB medium	
Tryptone	10 g/ l
Yeast extract	5 g/ l
NaCl	10 g/ l

For preparation of *E. coli* competent cells, SOB medium was used instead of LB medium.

SOB medium (pH 7,0)	
Tryptone	20 g/ l
Yeast extract	5 g/ l
NaCl	10 mM
KCl	2,5 mM
$MgCl_2$	10 mM
$MgSO_4$	10 mM

After dissolving in dH_2O medium was autoclaved for 20 min (121°C, 1,5 bar). *E. coli* liquid cultures were incubated under aerobic conditions at 28ºC or 37ºC with shaking (250 rpm). For preparation of LB agar plates 20 g/ l of agar was added. After plating, *E. coli* was incubated in 37ºC over-night.

2.10.2 *S. cerevisiae* culture and media

Yeast cells were grown in 30°C in rich medium (YP) or synthetic minimal medium (SC). Depending on growth conditions needed medium was supplemented with different carbon source, amino acids and other supplements.

YP medium	
Casein peptone	20 g/ l
Yeast extract	10 g/ l
Adenine sulfate	80 mg/ l

Through addition of carbon source listed media were obtained:

medium	carbon source
YPD medium	20 g/ l Glucose
YPGal medium	20 g/ l Galactose
YPGly medium	30 g/ l Glycerol

SC medium:

SD medium	
Yeast Nitrogen Base without Amino Acids & Ammonium Sulphate (*Formedium LTD*)	1,9 g/ l
Ammonium Sulfate	5 g/ l

Through addition of carbon source listed media were obtained:

medium	carbon source
SD medium	20 g/ l Glucose
SGal medium	20 g/ l Galactose

S. cerevisiae strains used in our laboratory are auxotrophic and require Adenine, Uracil, Leucine, Tryptophan and Histidine for normal growth. Those amino acids are essential for cell growth and were added to the SC medium depending on the cells' requirements as mentioned in the text in the following concentrations:

amino acid	concentration
Adenine sulfate	80 mg/ l
L-Histidine	20 mg/ l
L-Leucine	60 mg/ l
L-Tryptophan	40 mg/ l
Uracil	20 mg/ l

Some of the regulatable or deletion strains used in this work develop additional auxotrophies and in those cases used medium was additionally supplemented with 25 ml/ l of amino acid mix containing:

amino acid	concentration
L-Arginine	4 g/ l
L-Methionine	1 g/ l
L-Tyrosine	1,5 g/ l
L-Isoleucine	1,5 g/ l
L-Lysine	1,5 g/ l
L-Phenyloalanine	2,5 g/ l
L-Glutamate	20 g/ l
L-Aspartate	5 g/ l
L-Valine	0,6 g/ l
L-Threonine	10 g/ l
L-Serine	20 g/ l
L-Asparagine	0,5 g/ l

In case of determination of *de novo* Fe/S cluster biogenesis by ^{55}Fe radiolabelling experiments „iron-poor“ SC medium was used. In this medium “Yeast Nitrogen Base without Amino Acids & Ammonium Sulphate & Iron” (*Formedium LTD*) was used instead of “Yeast Nitrogen Base without Amino Acids & Ammonium Sulphate”.

After dissolving in dH_2O medium was autoclaved for 20 min (121°C, 1,5 bar). *S. cerevisiae* liquid cultures were incubated under aerobic (with shaking 150 rpm) or anaerobic conditions at 30ºC.

For preparation of SC agar plates 20 g/ l of agar was added. After plating yeast cells were incubated under aerobic or anaerobic conditions at 30ºC for 2 - 3 days.

2.11 Molecular biological methods

2.11.1 Preparation of genomic DNA from *S. cerevisiae*

For isolation of yeast genomic DNA 10 ml of *S. cerevisiae* YPD over-night culture was used. Cells were harvested by centrifugation (3000 rpm, 5 min) and then resuspended in 0,9 ml of

Solution I. To break down the cell wall of the yeast cells 100 µl Zymolyase (2 mg/ ml) and 1 µl 2-Mercaptoethanol were added and the cell suspension was incubated at 37°C. After 30 min cells were harvested by centrifugation (1 min, 4000 rpm.) Pellet was then resuspended in 0,4 ml of TE buffer. In order to break formed spheroplasts 30 µl of TES buffer was added and followed with 30 min incubation at 60°C. After addition of 80 µl of 5 M potassium acetate and 60 min incubation on ice solution was centrifuged (10 min, 14000 rpm, 4°C) and supernatant was transferred into a fresh tube. Precipitation of DNA was performed with 1 ml of ethanol (60 min on ice). After centrifugation, DNA pellet was washed with 70 % ethanol and when dry, resuspended in 300 µl of TE buffer.

Solution I	TE buffer	TES buffer
10 mM potassium phosphate pH 7,4	10 mM Tris-HCl pH 8,0	0,2 M Tris-HCl pH 8,0
0,9 M Sorbitol	1 mM EDTA	0,3 M EDTA
0,1 M EDTA		2 % (w/ v) SDS

2.11.2 Isolation of plasmid-DNA from *E. coli*

The isolation of Plasmid-DNA from *E. coli* was performed by alkyline lysis (Birnboim and Doly, 1979). Thanks to its superhelical form, plasmid DNA in contrast to chromosomal DNA, is stabile under basic conditions. This feature allows isolating it from the mixture of chromosomal DNA, RNA, proteins and membranes during centrifugation. After neutralization plasmid DNA stays in solution and can be precipitated by isopropanol treatment. DNA pellet can be then further cleaned with ethanol and after drying resuspended in water. In case of DNA sequencing, the plasmid-DNA was isolated using the NucleoSpin Plasmid-Kit from *Macherey-Nagel* following the manufacturer´s protocol.

2.11.3 DNA agarose gel electrophoresis (Sambrook and Russel, 2001)

1 % to 2 % agarose gels were routinely used to separate plasmid or linear DNA fragments. The appropriate amount of agarose was dissolved in 1x TAE buffer. DNA samples were mixed with 1 / 10 volumes of 10x DNA loading buffer containing GelRed™ Nucleic Acid Gel Stain (*Biotium).* Electrophoresis was conducted in TAE buffer by applying a voltage of 80-120 V. As size standard GeneRuler™ 1 kb Plus DNA Ladder (*Fermentas*) was used. After

completion of electrophoresis the gel was examined on a 302 nm UV transilluminator and documented using a thermoprinter.

1x TAE buffer	10x DNA loading buffer
40 mM Tris-HCl pH 8,0	0,25 % (w/ v) Bromophenolblue sodium salt
1 mM EDTA	0,25 % (w/ v) Xylencyanol FF
0,01 % (v/ v) acetic acid	30 % (v/ v) glycerol

2.11.4 Extraction of DNA from agarose gels

To extract and purify DNA from agarose gels the NucleoSpin Extract II Kit was used following the instruction of the supplier *Macherey-Nagel*. Purification of DNA is based on binding of DNA to the silicate membrane in chaotropic environment (Vogelstein and Gillespie, 1979). Elution of DNA is performed with 15 to 50 µl of 10 mM Tris-HCl pH 8,5.

2.11.5 Polymerase chain reaction (PCR)

Polymerase Chain Reaction (PCR) allows amplification of particular DNA fragment *in vitro* (Mullis and Faloona, 1987). PCR relies on thermal cycling consisting of repeated heating and cooling of the reaction. Each cycle usually consists of three steps:

1) denaturation step (95 - 98ºC) in which high temperature causes melting of template DNA
2) annealing step (50 - 60ºC) in which allows annealing of the primers (short DNA fragments) to the single-stranded template DNA
3) elongation step (70 - 80ºC) in which DNA polymerase synthesizes a new DNA strand complementary to the template DNA

All PCR reactions were performed in a 50 µl of reaction volume. Genomic *S. cerevisiae* or plasmid DNA was used as a template. Phusion® DNA Polymerase (*Finnzymes*) was used as polymerizing enzyme due to its proof reading activity. Conditions of each PCR reaction (buffer used, addition of DMSO, length of elongation step or number of cycles) were adjusted according to product size and GC base pairs content.

Standard PCR reaction:	volume (50 µl total)
template DNA (1 – 500 ng)	1 µl
5x HF or GC buffer	5 µl
dNTP mix (each 10 mM)	1 µl
primer 1	2,5 µl
primer 2	2,5 µl
Phusion polymerase (2 U/ µl)	0,5 µl
ddH_2O	37,5 µl

2.11.6 Digestion of DNA with restriction endonucleases

Restriction endonucleases allow cleaving DNA at specific site by catalyzing the hydrolysis of DNA phosphodiester bonds. For DNA cleavage Type II restriction enzymes cutting double-stranded DNA from *Fermentas* or *New England Biolabs* were used. Generally, restriction digests were performed in 10 µl (analytical purposes) or 50 µl (preparative purposes) final volume with 2 - 3 Units of enzyme pro 1 µg DNA. Reaction conditions (buffer, incubation time and temperature) were chosen according to the instruction of the supplier.

2.11.7 Ligation of DNA fragments

For ligation of DNA fragments the T4 DNA Ligase (*New England Biolabs*) was used. T4 DNA Ligase catalyzes the formation of a phosphodiester bond between juxtaposed 5' phosphate and 3' hydroxyl termini of adjacent nucleotides in either a cohesive-ended or blunt-ended configuration. The ligation reactions were performed in a 10 µl of total volume with 0,5 µl T4 DNA Ligase and 1 µl of 10x Ligase buffer. Vector to insert ratio was 1 : 4. The ligation reactions were incubated over night at 16ºC.

2.11.8 Determination of DNA concentration

To determine the DNA concentration 1 - 2 µl of DNA samples were loaded on an agarose gel. For comparison GeneRuler™ 1 kb Plus DNA Ladder (*Fermentas*) (1 µg/ µl) was used. After agarose gel electrophoresis the fluorescence intensity from GelRed™ Nucleic Acid Gel Stain (*Biotium*) bound to DNA samples was visually compared to that of bound to DNA marker.

2.11.9 Preparation of competent *E. coli* cells

Preparation of „super“ competent cells (RbCl method, *Sinclair* laboratory). For preparation of competent cells for transformation, a single colony of the appropriate *E. coli* strain was inoculated into 5 ml of SOB medium and grown over night at 30ºC. Then, 1 ml of over-night culture was inoculated in 100 ml SOB medium in 1 liter flask to maximize aeration. After addition of 7,2 ml of 5 M NaCl cells were grown in 30ºC until they reached OD_{600} = 0,5. Cells were harvested by centrifugation (4000 rpm, 5 min) and then resuspended in 10 ml of cold TFB buffer. After 10 min incubation of ice 350 µl of DMSO was added and cells were incubated on ice for another 10 min. Competent cells were aliquoted and stored at -80ºC.

TFB buffer
10 mM MES-KOH pH 6,2
100 mM RbCl
45 mM $MnCl_2$
10 mM $CaCl_2$*$2H_2O$
3 mM hexamine cobalt chloride

2.11.10 Transformation of *E. coli* competent cells

The competent cells (50 µl per transformation) were incubated on ice for 30 min with 50 - 100 ng of plasmid DNA or with 10 - 20 µl of ligation mixture. Incubation was followed by a „heat shock“ (90 s, at 42ºC) and incubation on ice for 2 min. Then the cells were resuspended in 1 ml LB medium and incubated for 60 min at 37ºC under moderate shaking conditions. The transformed cells were harvested by centrifugation and plated on LB-medium plates supplemented with the appropriate selection marker. The plates were incubated over-night at 37ºC.

2.11.11 QuikChange® site-directed mutagenesis

The procedure (with minor changes from the original protocol: www.stratagene.com) utilizes a supercoiled double-stranded DNA vector with an insert of interest and two synthetic oligonucleotide primers containing the desired mutation. The oligonucleotide primers, each complementary to opposite strands of the vector, are extended during a PCR reaction (see chapter 2.11.5) by Pwo DNA polymerase (*Peqlab*). Incorporation of the oligonucleotide primers into

DNA strands generates a mutated plasmid containing staggered nicks. The generated plasmid is then treated with DpnI endonuclease. DpnI is specific for methylated and hemimethylated DNA which allows to digest the parental DNA template and to select for mutation-containing synthesized DNA. DNA isolated from almost all *E. coli* strains is Dam methylated and therefore susceptible to DpnI digestion. The nicked vector DNA containing the desired mutations is then transformed (see chapter 2.11.10) into the *E. coli DH5α* competent cells.

2.11.12 Transformation of yeast cells with recombinant DNA

The *S. cerevisiae* cells were transformed using the lithium acetate method (Ito *et al.*, 1983). By this method the yeast cells were transformed with plasmid-DNA or with linear DNA-fragments used for genomic homologous recombination. The corresponding yeast strain was grown over-night and diluted the next morning in 50 ml YPD medium to an OD_{600} of 0,2. The cells were further grown until they reached an OD_{600} = 0,6 - 1 and harvested by centrifugation (5 min, 3000 rpm). After washing with 20 ml of autoclaved ddH_2O, the cells were pelleted under the same conditions and resuspended in 1 ml lithium-acetate solution. For each transformation 100 µl suspension of cells was mixed with 5 µl denaturated salmon sperm DNA and 5 - 10 µg of DNA to be transformed. The mix was incubated for 15 min, at 30°C, with moderate shaking followed by addition of 700 µl of PEG solution and a heat shock for 30 min, at 42°C. Afterwards cells were harvested, resuspended in 1 ml of YPD medium and incubated for 60 min at 30°C. After harvesting, the cells were washed with autoclaved ddH_2O and spread on selective solid SC plates. The plates were incubated for 2 - 5 days at 30°C to recover transformants.

PEG solution	LiAc solution
40 % Polyethylenglycol 4000	100 mM Lithiumacetate
100 mM Lithiumacetate	10 mM Tris-HCl pH 7,5
10 mM Tris-HCl pH 7,5	1 mM EDTA pH 8,0
1 mM EDTA pH 8,0	

2.11.13 Preparation of long storage cultures of *S. cerevisiae*

For long storage of yeast strains glycerol cultures were prepared. For this purpose 1200 µl of over-night full medium culture were mixed with 280 µl of glycerol, shock-frozen in liquid nitrogen and stored in -80ºC.

2.12 Cell biological and biochemical methods

2.12.1 Isolation of mitochondria from *S. cerevisiae.*

To isolate mitochondria from *S. cerevisiae* the cell wall of the yeast cells are first enzymaticaly degraded by Zymolyase treatment. Resultant spheroplasts are then broken mechanically by douncing and mitochondria can be isolated by differential centrifugation.

Yeast cells were cultivated either in reach or minimal medium at 30°C to OD_{600} of 1 - 1,5 and harvested by centrifugation (5 min, 3000 rpm). The cells were washed once with ddH_2O and the wet weight of cells was measured. The following procedure describes treatment of 10 g of wet cells. For weights different than 10 g volumes of buffers used were calculated accordingly. After washing with water cells were washed in 30 ml of Tris-SO_4 buffer and afterwards in Sorbitol buffer. After washing the cells were resuspended in 40 ml of the same buffer and Zymolyase T100 (0,7 mg/ g cells) was added to the cell suspension which was then incubated for 30 - 45 min at 30°C with shaking (150 rpm). To test the cell wall digestion (spheroplast formation), 25 µl cell suspension was diluted with 1 ml dH_2O. The solution of spheroplasts in H_2O becomes clear because spheroplasts burst under these conditions. All subsequent steps were performed at 4°C. The spheroplasts were isolated by centrifugation (5 min, 3000 rpm, 4°C) and washed twice in 40 ml of Sorbitol-buffer. The spheroplasts were then resuspended in 30 ml of 2x BB buffer and volume was filled up to 60 ml with ice-cold water. After homogenization by 15 strokes in a glass-glass homogenizer, the cell remnants and unopened cells were sedimented by double centrifugation (5 min, 4000 rpm, 4°C). The containing mitochondria supernatant was centrifuged (12 min, 10000 rpm, 4°C). The supernatant containing soluble cytosolic proteins and other organelles was used for further experiments as post-mitochondrial supernatant (PMS). Pelleted mitochondria were washed once in 25 ml of 1x BB buffer to remove the remaining PMS and finally resuspended in a small volume of 1x BB buffer. Mitochondria and PMS were aliquoted, shock-frozen in liquid nitrogen and stored at -80°C.

Tris-SO_4 buffer	Sorbitol buffer	2x BB buffer	1x BB buffer
10 mM Dithiothreitol (DTT)	1,2 M Sorbitol	1,2 M Sorbitol	0,6 M Sorbitol
100 mM Tris-SO_4 pH 9,4	20 mM potassium phosphate buffer pH 7,4	40 mM Hepes-KOH pH 7,4	20 mM Hepes-KOH pH 7,4
		1 mM PMSF	

2.12.2 Preparation of mitochondrial extracts.

Purified mitochondria (1 µg of mitochondria for 1 µl of buffer) were resuspended in the cold TNETG buffer with addition of PMSF (10 mM end concentration) for 10 min on ice to allow mitochondria swelling and breaking. The samples were then centrifuged (10 min, 12000 rpm, 4°C) to remove rests of the mitochondrial membranes. Supernatant was transferred to the fresh tube and used for further experiments.

TNETG buffer
20 mM Tris-HCl pH 7,4
150 mM NaCl
2,5 mM EDTA
10 % (v/ v) glycerol
0,5 % (v/ v) Triton-X-100

2.12.3 Preparation of yeast cell extract by alkaline lysis

For analysis of yeast proteins from the whole cell extract by SDS-PAGE, 1 ml of yeast cell liquid culture at OD_{600} = 1 was transferred to a 1,5 ml Eppendorf tube and centrifuged (3 min, 13000 rpm, 4°C). The pellet was washed once with 0,5 ml TE buffer and after centrifugation resuspended in 0,5 ml ice-cold ddH_2O. After addition of 75 µl lysis buffer cell suspension was vortexed and incubated for 10 min on ice. After incubation, 575 µl 50 % cold TCA were added, followed by a short vortexing and incubation on ice for 10 min. The samples were centrifuged (10 min, 12000 rpm, 4°C), supernatant removed, pellet washed twice with 1 ml cold acetone. The pellet was air-dried and resuspended in 100 µl 1x Laemmli buffer and 25 µl were loaded on SDS polyacrylamide gel.

TE buffer	lysis buffer	1x Laemmli buffer
10 mM Tris-HCl	1,85 M NaOH	50 mM Tris-HCl pH 8,0
1 mM EDTA pH 8,0	7,4 % (v/ v) 2-Mercaptoethanol	5 % (w/ v) glycerol
	10 mM PMSF	2 % (w/ v) SDS
		0,05 mg/ ml Bromphenolblue
		2,5 % (v/ v) 2-Mercaptoethanol

2.12.4 Preparation of yeast cell extract with glass beads

To prepare big amounts of yeast cell extract, for example to measure enzyme activities or co-immunoprecipitation experiments, cells were lysed mechanically by robust vortexing with glass beads. For this purpose 0,5 g of yeast cells (wet weight) were washed with 10 ml dH_2O and then resuspended in 0,5 ml cold TNETG buffer with addition of PMSF (10 mM end concentration). After addition of a half volume of glass beads (diameter: 0,75 - 1 mm) cells were vigoursly vortexed three times for 1 min with cooling on ice in between. After centrifugation (5 min, 4000 rpm, 4 °C), supernatant was transferred to a 1,5 ml Eppendorf tube and centrifuged again (3 min, 13000 rpm, 4°C). Yeast cell extract was obtained as supernatant from the last centrifugation and was used for further experiments.

TNETG buffer
20 mM Tris-HCl pH 7,4
150 mM NaCl
2,5 mM EDTA
10 % (v/ v) glycerol
0,5 % (v/ v) Triton-X-100

2.12.5 Measurements of enzymes activities from *S. cerevisiae*

Enzymes are biological molecules that catalyze chemical reaction without being consumed by the reaction that they catalyze. To measure enzyme activity the conversion of the substrate to product is usually followed. In spectrophotometric assays (used in this study), one can follow the course of the reaction by measuring a change in light absorption during the reaction. The wavelength is chosen in the way that only measured species (product, substrate or

cosubstrate) absorb the light at that particular wavelength. Sometimes, enzyme reaction does not result in a change in the light absorbance. In those situations coupled assays are used, in which product of one reaction is used as a substrate of another, which product can be then easily detected. To make sure that measured light absorption is specific for reaction of interest and does not come from other reactions that can take place for example in the cell lysate, the reference measurements are performed. Beer–Lambert law allows to calculate enzyme activity (E_{Act}) from absorption over time ($\Delta E/ \Delta t$). In this work specific enzyme activity (E_{SpAct}) was calculated which takes into account total protein amount (m) used for the measurement. Calculation follows the equation:

$$E_{SpAct} = \frac{E_{Act}}{m} = \frac{\Delta E}{\Delta t * m} = \frac{\Delta E}{\Delta t * d * \varepsilon * m}$$

Where (d) path length was equal 1 cm and (ε) extinction coefficient was chosen according to measured species.

2.12.5.1 Enzyme activities of mitochondrial proteins

2.12.5.1.1 Aconitase (ACO)

Aconitase (Aco1) is a mitochondrial enzyme that possess [4Fe-4S] cluster. It catalyzes the reversible isomerization of citrate to isocitrate via *cis*-aconitate in the tricarboxylic acid cycle. In contrast with the majority of Fe/S proteins that function as electron carriers, the Fe/S cluster of aconitase reacts directly with an enzyme substrate.

To measure aconitase activity two methods were used. In the first one, isocitrate was added to the sample and formation of *cis*-aconitate was followed by measuring its double bond absorbance at 235 nm (ε_{235nm} = 4950 M^{-1} cm^{-1}). This method was used to measure aconitase activity in purified mitochondria which were lysed just before the measurement by incubation with 0,0024 % (w/ v) dodecylomaltoside (DDM).

$$citrate \underset{+H_2O}{\overset{-H_2O}{\leftrightarrow}} cis-aconitate \underset{+H_2O}{\overset{-H_2O}{\leftrightarrow}} isocitrate$$

buffer	substrate	sample	assay
50 mM Tris-HCl pH 8,0	200 mM isocitrate in buffer (IC)	lysed mitochondria: 0,4 µg/ µl in buffer with 0,0024 % DDM	850 µl buffer
50 mM NaCl			100 µl IC
			50 µl sample

Second method was used to measure aconitase activity in the cell lysates. In this case coupled assay was used in which *cis*-aconitate was used as a substrate. *Cis*-aconitate was first converted to isocitrate by aconitase and then to α-ketoglutarate via oxalosuccinate by the isocitrate dehydrogenase (IDH). IDH is $NADP^+$ dependent and reduces it to NADPH during isocitrate conversion to oxalosuccinate. NADPH absorbs UV light (ε_{340nm} = 6220 M^{-1} cm^{-1}) in its reduced form, but does not in its oxidized form and can be used to indirect estimate aconitase activity.

$$cis-aconitate \underset{+H_2O}{\overset{-H_2O}{\leftrightarrow}} isocitratre \underset{-NADP^+}{\overset{+NADP^+}{\underset{+NADPH+H^+}{\overset{-NADPH-H^+}{\leftrightarrow}}}} oxalsuccinate \overset{-CO_2}{\leftrightarrow} \alpha-ketoglutarate$$

buffer	substrate	sample	assay	reference
50 mM Triethanolamine pH 8,0	20 mM cis-aconitate	yeast cell extract	950 µl buffer	950 µl buffer
50 mM NaCl	40 mU/ µl IDH		12 µl cis-aconitate	
1,5 mM $MgCl_2$	100 mM $NADP^+$		10 µl IDH	
			12 µl $NADP^+$	12 µl $NADP^+$
			50 - 100 µg sample	50 - 100 µg sample

2.12.5.1.2 Succinate dehydrogenase (SDH, complex II)

Respiratory complex II is an enzyme complex, bound to the inner mitochondrial membrane (IM). It participates in both the citric acid cycle and the electron transport chain. The whole complex consists of four subunits: two hydrophilic and two hydrophobic. Hydrophobic,

namely SdhC and SdhD are IM anchored proteins and they contain haem as prosthetic group. Hydrophilic are SdhA and SdhB (also known as Sdh2). SdhA contains a covalently attached flavin adenine dinucleotide (FAD) cofactor and the succinate binding site. SdhB contains three Fe/S clusters: [2Fe-2S], [4Fe-4S] and [3Fe-4S]. To estimate SDH activity purified mitochondria were used. Electron transfer from succinate to the artificial electron acceptor dichlorophenol indophenol (DCPIP) at 600 nm (ε_{600nm} = 21000 M^{-1} cm^{-1}) was measured with phenazine methosulfate (PMS) as electron transporter. Measurement with malonate (complex II inhibitor) was performed as reference.

buffer	substrate/ cosubstrate/ inhibitor	sample	assay	reference
50 mM Tris-HCl pH 8,0	20 % (w/ v) succinate	purified mitochondria	950 µl buffer	950 µl buffer
50 mM NaCl	20 % (w/ v) malonate		12 µl succinate	12 µl succinate
1 mM KCN	10 mM DCPIP			12 µl malonate
0,1 % Triton-X-100	20 mg/ ml PMS		12 µl DCPIP	12 µl DCPIP
			12 µl PMS	12 µl PMS
			25 µg sample	25 µg sample

2.12.5.1.3 Malat dehydrogenase (MDH)

Malate dehydrogenase catalyzes the reversible oxidation of malate to oxaloacetate, utilizing the NAD/ NADH cofactor system. This reaction is part of many metabolic pathways, including the citric acid cycle. To estimate activity of mitochondrial MDH, oxidation of NADH was measured at 340 nm (ε_{340nm} = 6220 M^{-1} cm^{-1}).

$$malate + NAD^+ \leftrightarrow oxalacetat\,e + NADH + H^+$$

buffer	substrate/ cosubstrate	sample	measurement
50 mM Tris-HCl pH 8,0	10 mg/ ml NADH	cell lysate or lysed mitochondria: 0,4 µg/ µl in buffer with 0,0024 % DDM	930 µl buffer
50 mM NaCl	5 mg/ ml oxalacetate		10 µl NADH
			10 µl oxalacetate
			20 µg sample

2.12.5.1.4 Pyruvate dehydrogenase complex

Pyruvate dehydrogenase complex (PDH) is located in the mitochondria and consists of three enzymes, namely: pyruvate dehydrogenase (E1) with thiamine pyrophosphate (TPP) as a cofactor, dihydrolipoyl transacetylase (E2) with lipoate and Coenzyme A as cofactors, and dihydrolipoyl dehydrogenase (E3) with FAD and NAD^+ as cofactors. Joined work of those three enzymes results in transformation of pyruvate into acetyl-CoA by a process called pyruvate decarboxylation. Acetyl-CoA is then utilized in the citric acid cycle. To estimate activity of PDH, reduction of NAD^+ was measured at 340 nm (ε_{340nm} = 6220 M^{-1} cm^{-1}).

$$puryvate + CoA - SH + NAD^+ \rightarrow Acetyl - CoA + NADH + H^+ + CO_2$$

buffer	substrate/ cosubstrate	sample	measurement	reference
100 mM MOPS pH 7,4	100 mM cysteine	lysted mitochondria: 0,4 µg/ µl in buffer with 0,0024 % DDM	550 µl buffer	550 µl buffer
1 mM $CaCl_2$	18 mM TPP		40 µl cysteine	40 µl cysteine
1 mM $MgCl_2$	100 mM NAD^+		25 µl TPP	25 µl TPP
	0,72 mM Coenzyme A		30 µl NAD^+	30 µl NAD^+
	100 mM pyruvate		250 µl Coenzyme A	250 µl Coenzyme A
			50 µg sample	50 µg sample
			75 µl pyruvate	

2.12.5.1.5 α-Ketoglutarate dehydrogenase complex

α-Ketoglutarate dehydrogenase complex (KGDH) is located in mitochondria and consists of three enzymes, namely: α-ketoglutarate dehydrogenase (E1) with thiamine pyrophosphate (TPP) as a cofactor, dihydrolipoyl succinyltransferase (E2) with lipoate as a cofactor, and dihydrolipoyl dehydrogenase (E3) with FAD as a cofactor. Joined work of those three enzymes results in transformation of α-ketoglutarate into succinyl-CoA by a process called pyruvate decarboxylation. Succinyl-CoA is then utilized in the citric acid cycle. To estimate activity of KGDH, reduction of NAD^+ was measured at 340 nm (ε_{340nm} = 6220 M^{-1} cm^{-1}).

$$\alpha - ketoglutarate + CoA - SH + NAD^{+} \rightarrow succinyl - CoA + NADH + CO_2$$

buffer	substrate/ cosubstrate	sample	measurement	reference
100 mM MOPS pH 7,4	100 mM cysteine	lysted mitochondria: 0,4 µg/ µl in buffer with 0,0024 % DDM	550 µl buffer	550 µl buffer
1 mM $CaCl_2$	18 mM TPP		40 µl cysteine	40 µl cysteine
1 mM $MgCl_2$	100 mM NAD^+		25 µl TPP	25 µl TPP
	0,72 mM Coenzyme A		30 µl NAD^+	30 µl NAD^+
	100 mM α-ketoglutarate		250 µl Coenzyme A	250 µl Coenzyme A
			50 µg sample	50 µg sample
			75 µl α-ketoglutarate	

2.12.5.2 Enzyme activities of cytosolic proteins

2.12.5.2.1 Isopropylmalate isomerase (Leu1)

Cytosolic isopropylmalate isomerase (Leu1) possesses one [4Fe-4S] cluster as cofactor. It catalyzes the second step in the leucine biosynthesis pathway where it catalyzes the reversible reaction of isomerization between 2-isopropylmalate and 3-isopropylmalate, via the formation of dimethylcitraconate. To estimate the activity of Leu1 the increase in absorption of the double bond of the intermediate product dimethylcitraconate was measured at 235 nm (ε_{235nm} = 4950 M^{-1} cm^{-1}).

$$2 - isopropylmalate \underset{+H_2O}{\overset{-H_2O}{\leftrightarrow}} dimethylcitraconate \underset{+H_2O}{\overset{-H_2O}{\leftrightarrow}} 3 - isopopylmalate$$

buffer	substrate/ cosubstrate	sample	measurement
50 mM Tris-HCl, pH 8,0	10 mM isopropylmalate (IPM)	whole cell extract	970 µl buffer
50 mM NaCl			20 µl IPM
			50 - 100 µg sample

2.12.6 Stimulation of Ssq1 ATPase activity by purified proteins in equilibrium conditions

Release of radioactive phosphorus from [γ^{32}P]ATP was conducted according to modified method of Viitanen et al (Viitanen *et al.*, 1990). Reaction mixture containing Ssq1 and other proteins in buffer A. Reaction was initiated by addition of [γ^{32}P]ATP (2 µCi, DuPont NEG-003H, 3000Ci/ mM) to concentration of 118 µM. Whole mixture was incubated at 25°C. At different time points 10 µl samples were taken from the reaction mixture and transferred to an 1,5 ml Eppendorf tube containing 100 µl of stop buffer. Samples were stored on ice. When all samples were collected, 400 µl of 20 mM amonium molybdate and 400 µl of isopropyl octane were added to each sample. After robust vortexing, phases were separated by centrifugation (1 min, 12000 rpm, 4°C). 150 µl of organic phase containing radioactive complex of phosphorus and molybdate was added to 1 ml of scintillation cocktail (EcoLite^{TM}(+), *ICN*), vortexed and then directly subjected to a scintillation counter (Beckman LS6000). For all experiments control reactions were performed to correct effects of slight spontaneous [γ^{32}P]ATP hydrolysis taking place during performing the experiment.

buffer A	stop buffer
40 mM Hepes-KOH pH 7,5	1 M perchloric acid
100 mM KCl	1 mM trisodium phosphate
10 % (v/ v) glycerol	
1 mM DTT	
10 mM $MgCl_2$	

2.12.7 Determination of *de novo* Fe/S cluster biogenesis by ^{55}Fe radiolabelling

To estimate *de novo* Fe/S cluster biogenesis in *S. cerevisiae* iron-starved yeast cells are incubated with ^{55}Fe and incorporation of this radioactive isotope into protein of interest is determined by immunoprecipitation and following scintillation counting (Kispal et al, 1999).

Yeast cells were grown over-night in 50 ml SC medium containing the required carbon source and harvested by centrifugation (5 min, 3000 rpm). After washing with autoclaved ddH_2O cells were inoculated in 100 ml of „iron-poor“ SC medium (containing glucose or galactose as the carbon source) to an OD_{600} of 0,2 and incubated over-night at 30°C. Cells were harvested (5 min, 3000rpm) and washed once in 10 ml ddH_2O. 0,5 g cells (wet weight) were resuspended in 10 ml „iron-poor“ SC medium and after 10 min of incubation in 30°C, 10 µCi of $^{55}FeCl_3$ (*Perkin*

Elmer) in 100 mM ascorbate was added to the cells and the labeling reaction was incubated for 2 h at 30°C with shaking. Radioactively labeled cells were then transferred into a 15 ml tube and pelleted by centrifugation (5 min, 3000 rpm). Cell pellet was washed in 10 ml citrate buffer and then in 3 ml 20 mM Hepes-KOH pH 7,4. After washing yeast cell extract was prepared with glass beads method (see chapter 2.12.4). 5 µl of the radioactive cell lysate were mixed with 1 ml of scintillation cocktail to quantify the iron uptake into the cells. 25 µl were taken for the TCA protein precipitation (see chapter 2.12.17) and subsequent protein level visualization by SDS-PAGE and Western Blot. The remaining supernatant was used also to quantify *de novo* Fe/S cluster biogenesis. For this purpose, 250 µl cell lysate were used for immunoprecipitation of protein of interest (see chapter 2.12.13). Finally, 50 µl of ddH_2O and 1 ml scintillation cocktail were added to the washed beads and the amount of ^{55}Fe associated with the beads was counted in a scintillation counter (Beckman LS6000).

citrate buffer
50 mM citrate
1 mM EDTA pH 8,0

2.12.8 Determination of protein concentration (Bradford)

Protein concentration was determined according to Bradford (Bradford, 1976). This assay is based upon ability of Coomassie-Brilliant Blue G-250 dye to bind alkaline side chains of proteins. The absorbance maximum for an acidic solution of Coomassie Brilliant Blue G-250 shifts from 465 nm to 595 nm when binding to protein occurs which allows determination of protein concentration. Bradford solution (*Bio-Rad*) was diluted 1 : 5 with ddH_2O and 1 ml of this dilution was added to the measured samples and to the standard (bovine serum albumine (BSA) in concentrations from 0 to 100 µg). Afterwards, samples were gently mixed to avoid foam formation and after 10 min of incubation the measurement was carried out at 595 nm.

2.12.9 Determination of mitochondrial iron content (modified after Li et al 1999)

To determine mitochondrial iron content (not haem- or Fe/S bound iron) 0,2 mg mitochondria were lysed with 0,6 % SDS in 100 mM Tris-HCl buffer pH 7,4. Iron was reduced by addition of dithionite (20 mM end concentration) and the indicator bathophenanthroline disulfonic acid (BPS) was added at 10 mM final concentration. The colored ferrous iron-BPS

complex was measured by determining the absorption at 540 nm. ε_{540} = 23.5 M^{-1} cm^{-1} and mitochondrial iron content was calculated from the difference between absorption at 540 nm and 700 nm.

2.12.10 Measurement of ROS production by 2',7' dichlorodihydrofluorescein diacetate (DCFDA)

Over-night cultures of yeast cells were diluted to an OD_{600} of 0,3 in 15 ml SD medium with addition of 15 µM DCFDA. After 2 hours of incubation cells were collected by centrifugation (5 min, 3000 rpm, 4°C) and washed with cold water and then two times with cold phosphate-buffered-saline (PBS). After washing cells were resuspended in 200 µl of 0,1 mM Tris-HCl pH 8,0 and lysed by glass beads. After clarifying centrifugation (3 min, 13000 rpm, 4°C) cell extracts were analyzed for the fluorescence in a spectrometer (λ_{ex}504 – λ_{em}524). Results were normalized to protein concentration.

2.12.11 GFP-Reporter assay

To estimate activation of yeast iron regulon the plasmids containing *GFP* (Green Fluorescent Protein) gene under the control of *FET3* promoter were used. Fet3 is a multicopper oxidase involved in reductase-dependent iron import to the cells. Promoter of *FET3* gene is a target of Aft1 transcription factor and *FET3* gene expression becomes up-regulated under iron-deplete conditions. Yeast cells carrying plasmids p415-FET3-GFP or p416-FET3-GFP were grown in minimal medium supplemented with 200 µM ferric ammonium citrate. Over-night cultures were diluted to an OD_{600} = 0,2 and incubated further until the OD_{600} reached 0,5. The cells were collected by centrifugation (5 min, 3000 rpm) and resuspended in 3 ml of dH_2O to get a final OD_{600} of 1. The fluorescence emission of the cell suspension was measured at 513 nm (excitation 480 nm) using a fluorescence spectrophotometer.

2.12.12 Coupling of antibodies to Protein A Sepharose

Protein A is a 56 kDa surface protein isolated from bacterium *Staphylococcum aureus*. Its ability to stable bind F_C region of antibodies is used to create Protein A beads which after coupling to specific antibody can be used for purification of proteins or protein complexes.

50 mg of Protein-A-Sepharose® (*GE Healthcare*) were resuspended in cold 500 µl TNETG buffer and incubated at the 10 °C with the smooth rotation for 2 h for > 30 min to allow

swelling of the beads. After swelling beads were pelleted (5 min, 3000 rpm, 4 °C), mixed with 500 µl of antibody serum and incubated at the 10 °C with the smooth rotation for 2 h. Coupled beads were pelleted (5 min, 3000 rpm, 4 °C) and washed 5 times in 500 µl cold TNETG. Finally, the beads were resuspended in 500 µl TNETG and stored at 4°C.

TNETG buffer
20 mM Tris-HCl pH 7,4
150 mM NaCl
2,5 mM EDTA
10 % (v/ v) glycerol
0,5 % (v/ v) Triton-X-100

2.12.13 (Co)Immunoprecipitation (Co-IP)

Immunoprecipitation (IP) is a method which allows purification and later detection of the protein of interest from the protein mixture (like for example cell or mitochondrial extract). Specific antibody coupled with the beads recognizes the protein of interest and forms a complex with it. The antibody-protein complex can be then purified, released from the beads (by for example denaturation) and detected by SDS-PAGE followed by Coomassie staining or Western blot. This method can be also used for detection of protein-protein interactions (Coimmunoprecipitation (Co-IP)), where together with the protein recognized by the antibody coupled to the beads, also its binding partners are purified as a complex. These protein complexes can be then analyzed to identify new binding partners (Berggard et al, 2007).

For *in vitro* Co-IP experiments, purified proteins (4 µM each) were incubated in buffer B for 15 in 25 °C before addition of 40 µl of immunobeads. Protein mixture with immunobeads was incubated at the 10 °C with the smooth rotation for 2 h. After incubation immunobeads were pelleted (5 min, 3000 rpm, 4 °C) and washed 3 times with 0,5 ml cold buffer B. Purified immunobeads were resuspended in the 1x Laemmli buffer and boiled for 10 min at 95°C before loading onto polyacrylamide gel.

For *in vivo* IP and Co-IP experiments, cell or mitochondrial extracts were incubated with the 10 – 40 µl specific immunobeads at the 10 °C with the smooth rotation for 2 h. After incubation immunobeads were pelleted (5 min, 3000 rpm, 4 °C) and washed 3 times with 0,5 ml

cold TENTG buffer. Purified immunobeads were resuspended in the 1x Laemmli buffer and boiled for 10 min at 95°C before loading onto polyacrylamide gel.

buffer B	1x Laemmli buffer	TNETG buffer
40 µM Hepes-KOH pH 7,5	50 mM Tris-HCl pH 8,0	20 mM Tris-HCl pH 7,4
5 % (v/ v) glycerol	5 % (w/ v) glycerol	150 mM NaCl
100 mM KCl	2 % (w/ v) SDS	2,5 mM EDTA
2 mM DTT	0,05 mg/ ml Bromphenolblau	10 % (v/ v) glycerol
20 mM $MgCl_2$	2,5 % (v/ v) 2-Mercaptoethanol	0,5 % (v/v) Triton-X-100
2mM ADP		

2.12.14 Glutathione affinity purification (pull down experiments)

To purify Glutathione S-transferase (GST) tagged proteins glutathione affinity purification was conducted. GST-fusion proteins can be purified via their strong and specific binding to the tripeptide ligand glutathione, which is stably immobilized on the bead support. This method allows specific purification and later detection of the protein of interest (or protein complexes) from the protein mixture.

For *in vivo* affinity purification experiments, cell or mitochondrial extracts were incubated with the 40 µl of Glutathione Sepharose^{TM} 4B (*GE Healcare*) at the 10 °C with the smooth rotation for 2 h. After incubation, beads were pelleted (5 min, 3000 rpm, 4 °C) and washed 3 times with 0,5 ml cold TENTG buffer. Purified beads were resuspended in the 1x Laemmli buffer and boiled for 10 min at 95°C before loading onto polyacrylamide gel.

buffer B	1x Laemmli buffer	TNETG buffer
40 µM Hepes-KOH pH 7,5	50 mM Tris-HCl pH 8,0	20 mM Tris-HCl pH 7,4
5 % (v/ v) glycerol	5 % (w/ v) glycerol	150 mM NaCl
100 mM KCl	2 % (w/ v) SDS	2,5 mM EDTA
2 mM DTT	0,05 mg/ ml Bromphenolblau	10 % (v/ v) glycerol
20 mM $MgCl_2$	2,5 % (v/ v) 2-Mercaptoethanol	0,5 % (v/ v) Triton-X-100
2mM ADP		

2.12.15 Microscale thermophoresis (MST) experiments

Microscale thermophoresis (MST) is a relatively novel technique for the analysis of biomolecules, developed by the NanoTemper Technologies GmbH, a German high tech company with headquarters in Munich. MST is defined as the directed movement of the molecules in a microscopic temperature gradient. This thermophoretic effect is not yet fully understood on the microscopic level but allows very sensitive detection of biomolecules interactions. Any change in size, conformation, charge or the hydration shell result in the change of movement along the temperature gradient and can be used to determine binding affinities, binding kinetics and activity kinetics. MST has very low sample consumption and is an immobilization-free technology, which means that measurements can be performed in the buffer of choice or directly in the cell extract without the need of attaching one of the binding partners to the surface (Jerabek-Willemsen *et al.*, 2011). The temperature gradient is generated by the IR laser focused into the glass capillary containing the reaction mixture and is strongly absorbed by water. For easy MST detection one of the tested molecules is fluorescently labeled and kept at fixed concentration in all reactions. Labeled molecule is titrated by the non-labeled possible binding partner. Polarized light is used to excite the fluorescent dye. The non-bound fluorescently labeled partner diffuses fast and the emitted light is almost not polarized. When binding event occurs fluorescently labeled molecule is usually slowed down and higher fraction of the emitted light remains polarized. The differences in the emitted fluorescence are detected by the same optical element through which the capillary is excited (Fig 2.1 A). The obtained signal consists of several subsequent processes (Fig 2.1 B): "Initial Fluorescence" (fluorescence of sample at ambient temperature before the laser heating), ''MST T-Jump'' (fluorescence change induced by sample heating before the thermophoretic molecule transport sets in), ''thermophoresis'' (fluorescence change induced by thermophoretic motion), ''inverse T-Jump'' (induced by sample cooling after turning of IR-Laser), and ''Back diffusion'' (fluorescence recovery triggered by pure mass diffusion of molecules after heating laser is turned off). Each phase of the thermophoretic analysis contains information about the affinity and mechanism of binding. The set of data coming from the set of sixteen different concentrations of the dilution series allows obtaining a sigmoidal binding curve, which can be then directly fitted with the nonlinear solution of the law of mass action, with the dissociation constant K_d as a result (Jerabek-Willemsen *et al.*, 2011).

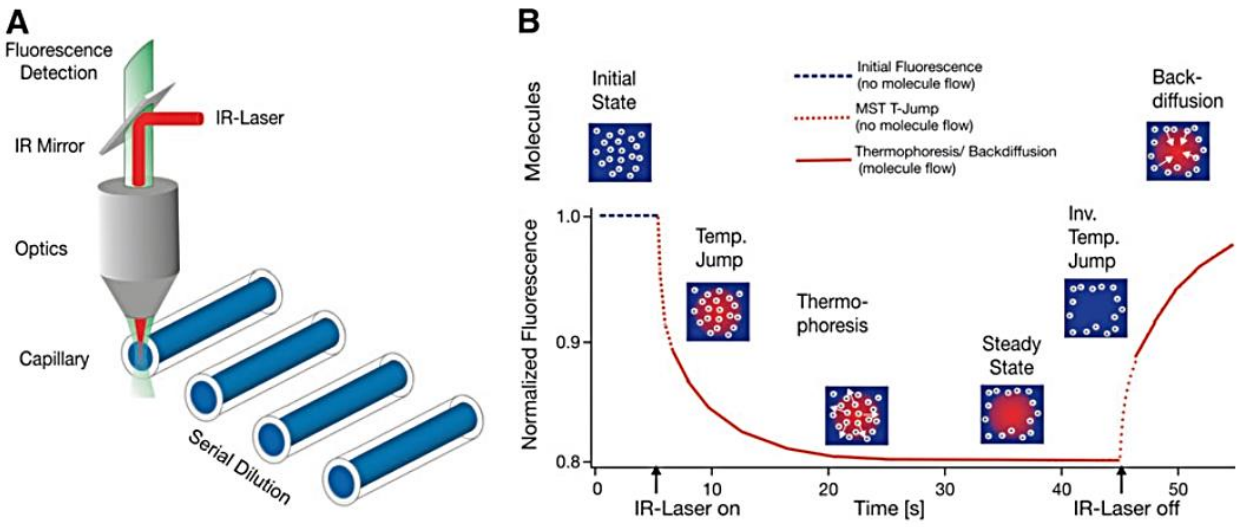

Fig. 2.1 Microscale thermophoresis. (**A**) Experimental setup of the MST experiment. MST is measured in the small glass capillary containing the minimal sample volume of 4 µl. The fluorescence within the capillary is induced and measured by the same optical element. An IR-laser is used to locally heat up the sample and create the temperature gradient. Change of temperature can be observed immediately by the change in fluorescence. (**B**) A typical MST signal obtained for a single capillary. As soon as IR-laser is on, a T-Jump and the following thermophoretic molecule movement can be observed. The fluorescence decrease is measured for about 30 seconds. After turning off the IR-laser, an inverse T-Jump is observed followed by the backdiffusion of molecules. Backdiffusion is purely driven by mass diffusion and gives the information about the molecule size. Figure taken from (Jerabek-Willemsen *et al.*, 2011).

For MST experiments the bait proteins (Grx5 or Cia1) were labeled using the Monolith NT^{TM} Protein Labeling Kit RED (NanoTemper Technologies, Munich, Germany) with NT-647 dye as recommended by the manufacturer. Labeled bait proteins were titrated with the serial dilutions of Cia2, Ssq1 or Isu1 peptide AKELSLPPVKLHC (LPPVK) alone or in the combinations in the buffer T. Binding assays were performed using Monolith NT.015 (NanoTemper Technologies, Munich, Germany) at 21°C (LED power – 100 %, IR laser power – 75 %). Three independent experiments were recorded at 680 nm and data were processed by Nano Temper Analysis 1.2.009 and Origin 8G software to estimate K_d values.

buffer T
50 mM KPi pH 7,4
150 mM NaCl
1 mM $MgCl_2$
1 mM GSH

2.12.16 ATP depletion in mitochondrial lysates

To deplete ATP present in mitochondrial lysates samples were incubated for 15 min on ice with solution A containing hexokinase and glucose-6-phosphate dehydrogenase. Hexokinase phosphorylates glucose to glucose-6-phosphate in a reaction consuming a molecule of ATP. Since glucose-6-phosphate is known to have an inhibitory effect on hexokinase, glucose-6-phosphate dehydrogenase was added to prevent inhibition of ATP depletion. Glucose-6-phosphate dehydrogenase removes glucose-6-phosphate by its conversion to 6-phosphoglucono-δ-lactone in NADP dependent reaction.

solution A (end concentrations in the reaction mixture)
2 mM $MgCl_2$
0,5 mM glucose
0,15 mM NADP
1,4 U/ ml hexokinase
3 U/ ml glucose-6-phosphate dehydrogenase

2.12.17 TCA protein precipitation

To concentrate protein samples or to remove contaminations (for example lipids) proteins or protein mixtures (for example yeast cell extract) were precipitated by TCA. To do so, samples were mixed with an equal volume of 25 % TCA and incubated for 15 min on ice. After incubation samples were centrifuged (15 min, 13000 rpm, 4 °C) and the supernatant was carefully removed by needle leaving the protein pellet intact. Pellet was then washed twice with 1 ml cold acetone and dried at room temperature. The samples were resuspended in 1x Laemmli buffer and boiled for 10 min at 95°C before loading onto polyacrylamide gel. If the sample color turned yellow (acidic pH) few µl of 1 M Tris-HCl pH 8,0 were added until the sample color turned back to blue.

1x Laemmli buffer
50 mM Tris-HCl pH 8,0
5 % (w/ v) glycerol
2 % (w/ v) SDS
0,05 mg/ ml Bromphenolblau
2,5 % (v/ v) 2-Mercaptoethanol

2.12.18 SDS-polyacrylamide gel electrophoresis (SDS-PAGE)

The denatured polypeptides bind SDS and become negatively charged. Because the amount of SDS bound is usually proportional to the molecular mass of the polypeptide and is independent of its sequence, the mobility of protein-SDS complexes in polyacrylamide gels is inverse proportional to the size of the protein. By using markers of known size it is therefore possible to estimate the molecular mass of a protein.

SDS-PAGE was performed in vertical apparatus designed after Laemmli (Laemmli, 1970). For most purposes a 5 % stacking gel and 10 to 15 % resolving gel were prepared. Polymerization of the gel was obtained by addition of 0,001 % (v/ v) TEMED und 0,05 % (w/ v) Ammoniumperoxodisulfate (APS). Samples loaded on the gel were boiled in advance for 5 min at 95 ºC. Power applied pro gel (7 cm x 10 cm) was around 35 mA. Separated proteins were afterwards were stained with Coomassie Brilliant-Blue or transferred onto nitrocellulose membrane.

5 % stacking gel	10 - 15 % resolving gel	electrophoresis buffer
125 mM Tris-HCl pH 6,8	375 mM Tris-HCl pH 8,8	25 mM Tris
0,1 % (w/ v) SDS	0,1 % (w/ v) SDS	0,1 % (w/ v) SDS
5 % (w/ v) Acrylamid (Acrylamid: Bisacrylamid = 37,5 : 1	10 - 15 % (w/ v) Acrylamid (Acrylamid: Bisacrylamid = 37,5 : 1	192 mM glycin

2.12.19 Protein staining with Coomassie Brilliant-Blue

Method of Coomassie staining of SDS-PAGE gels allows to visualize proteins in the gel according to their concentration (Bennett and Scott, 1971). After electrophoresis, SDS gels were incubated in staining solution for 30 – 60 min. After staining, gel was washed once with water and put into hot destaining solution for 30 minutes. Background staining was removed by 2 h incubation in water. For documentation of stained gels GDS system from *Intras* was used.

Coomassie staining solution	destaining solution
0,25 % (v/ v) Coomassie Brilliant-Blue R-250	30 % (v/ v) ethanol
50 % (v/ v) ethanol	10 % (v/ v) acetic acid
10 % (v/ v) acetic acid	

2.12.20 Transfer of proteins to nitrocellulose membrane (Western-Blot) and Ponceau staining

Western blot method allows transferring the proteins from the SDS- or native gels to a membrane (nitrocellulose or PVDF), where they can later be detected using specific antibodies.

Proteins separated via SDS-PAGE were transferred onto nitrocellulose membrane using the semi-dry blotting method (Kyhse-Andersen, 1984). The gel, membrane, and four sheets of Whatman filter paper were incubated in transfer buffer. Two sheets of filter paper were placed on the anode electrode followed by the membrane and the gel. Those were covered with another two filter papers and with the cathode electrode. The proteins move from within the gel onto the membrane maintaining the same organization they had within the gel. The transfer was performed at 2 mA/ cm^2 for 45 to 90 min. To verify transfer efficiency, the nitrocellulose membranes were reversibly stained with Ponceau S solution.

transfer buffer	Ponceau S solution
25 mM Tris	0,2 % (w/ v) Ponceau S
200 mM glycine	3 % (w/ v) TCA
20 % (v/ v) methanol	
0,02 % (w/ v) SDS	

2.12.21 Protein detection by immunostaining

Protein bands immobilized on the nitrocellulose or PVDF membranes can be visualized via staining with specific antibodies. Combination of two antibodies is used, the primary antibodies, which recognize an epitope on the protein of interest, and the secondary antibodies which recognize the primary antibody. Secondary antibodies are linked to a reporter enzyme, horseradish peroxidase (HRP), which when exposed to H_2O_2 can oxidize a chemiluminescent agent and the reaction product produces luminescence in proportion to the amount of detected protein.

To avoid non-specific antibody binding to the membrane, the "protein-free" sites of the membrane were blocked by incubation with 5 % (w/ v) skim milk or 1 % (w/ v) BSA in TBST buffer at RT for 1 h or overnight at 4 °C. Membrane was then incubated with specific primary antibody (1 : 500 – 1 : 2000 in TBST buffer 5 % (w /v) skim milk or 1 % (w /v) BSA) for 1 h at RT. After washing 3 times with TBST buffer, the membrane was incubated (1 h at RT) with the HRP coupled secondary antibody (anti-rabbit-IgG or anti-mouse-IgG diluted 1 : 10.000 in 5 % (w/ v) skim milk or 1 % (w/ v) BSA in TBST buffer). The membrane was washed again 3 times with TBST buffer and treated with ECL detection solution (*GE Healthcare*). After incubating for 1 min, excess of detection reagent was drained off and detected proteins were visualized by Chemostar professional system (*Intras*).

TBST buffer
10 mM Tris-HCl pH 7,4
150 mM NaCl
0,1 % (v/ v) Tween 20

2.12.22 Quantification of protein levels after immunostaining

After immunostaining levels of detected proteins were quantified using LabImage 1D software (*Kapelan*). The values obtained for each protein band (from independent experiments) were taken and the average was calculated.

2.12.23 Protein purification

2.12.23.1 Purification of Grx5 from *E. coli*

E. coli strain BL21(DE3)-Gold harboring *S. cerevisiae* Grx5 overexpressing plasmid pET16bGRX5$_{His}$ was inoculated in 100 ml of LB medium supplemented with ampicillin (100 µg/ ml) and incubated with shaking for 18 h. The over-night culture was then diluted in 6 liters of LB medium with ampicillin to OD_{575} of 0,1 and grown at 37 °C until OD_{575} reached 0,6. Medium was then supplemented with 50 µM ferric ammonium citrate and cells were induced with 1 mM IPTG for 5 h at 30 °C. After induction cells were harvested by centrifugation (5 min, 7000 rpm), washed once with water, shock frozen in liquid nitrogen and stored in -80 °C.

After thawing cells were resuspended in cold Ni buffer and opened by applying a pressure of 1,0 x 10^8 Nm^{-2} using an high pressure homogenisator EmulsiFlex® C3 (*Avestin*). To reduce amount of DNA pinch of DNAse I was added and lysate was incubated on ice for 10 min. The unopened cells and cell debris were removed by centrifugation (90 min, 20000 rpm, 4 °C). All following purification steps were performed at 10 °C.

Because recombinant Grx5 contained hexa-histidine tag (His-tag) on its N-terminus, lysate was then applied on column containing 2 ml Ni-NTA Superflow agarose (*QIAGEN*) previously equilibrated with 40 ml of Ni buffer. Immobilized metal ion affinity chromatography (IMAC) is based on the specific coordinate covalent bond of amino acids, particularly histidine, to the metals. Immobilized nickel ions (Ni^{2+}) interact with His-tag of the proteins and allow their purification. Bound protein can be then eluted with imidazole which competes with His-tag for Ni^{2+} binding at high concentrations.

After binding, Ni-NTA column was washed with 100 ml of Ni buffer, then with 30 ml of ATP buffer and again with 30 ml Ni buffer. After washing Grx5$_{His}$ was eluted with buffer E. 0,5 ml fractions were collected and analyzed by SDS-PAGE followed by Coomassie staining to evaluate their purity. Fractions containing Grx5$_{His}$ were pulled together and desalted on PD10 columns (*GE Healthcare*). After desalting, protein was aliquoted, shock frozen in liquid nitrogen and stored in -80 °C. Protein concentration was estimated with Bradford solution as 5 µg/ µl.

Ni buffer	ATP buffer	buffer E
20 mM Tris-HCl pH 8,0	20 mM Tris-HCl pH 8,0	20 mM Tris-HCl pH 8,0
10 % (v/ v) glycerol	10 % (v/ v) glycerol	10 % (v/ v) glycerol
0,5 M NaCl	1 M NaCl	0,5 M NaCl
30 mM imidazole pH 8,0	30 mM imidazole pH 8,0	300 mM imidazole pH 8,0
1 mM PMSF	1 mM PMSF	1 mM PMSF
	1 mM ATP	
	2 mM $MgCl_2$	

2.12.23.2 Purification of Ssq1 from *S. cerevisiae*

Yeast cells *S. cerevisiae* strain WY11 (defective in proteinase A) harboring the Ssq1 overexpression vector pYES2*SSQ1*$_{His}$ were grown in 500 ml SD medium without uracil until they reached stationary phase. This culture was then diluted 30-fold in 10 liters of SGal medium without uracil to induce overexpression of Ssq1. When OD_{600} reached 2,5 cells were harvested by centrifugation (10 min, 4000 rpm, 4 °C). Cells pellet was washed once with water, shock frozen in liquid nitrogen and stored in -80 °C.

After thawing cells were resuspended in cell wall digesting buffer and incubated for 30 - 45 min at 30°C with shaking (150 rpm). To test the cell wall digestion (spheroplast formation), 25 µl cell suspension was diluted with 1 ml H_2O. Formed spheroplasts were then harvested by centrifugation (5 min, 4500 rpm, 4 °C), resuspended in 120 ml of cold lysis buffer and lysed by French Press at 16000 psi.

After clarifying centrifugation (90 min, 35000 rpm, 4 °C) supernatant was loaded over-night on column containing 2,5 ml Ni-NTA Superflow agarose (*QIAGEN*) previously equilibrated with 40 ml of lysis buffer. After binding Ni-NTA column was washed with 100 ml of buffer A1, then with 30 ml of buffer A2 and again with 15 ml buffer A1. After washing, Ssq1$_{His}$ was eluted with linear gradient of imidazole (20 to 350 mM) in buffer A1. Fractions of 1,2 ml were collected.

Fractions containing Ssq1$_{His}$ were pooled together and dialyzed over-night against buffer B and applied on column containing 2,5 ml hydroxyapatite agarose (*BioRad*) equilibrated previously with 30 ml of buffer B. Hydroxyapatite possess several functional groups consisting of positively charged pairs of crystal calcium ions (C-sites) and the six negatively charged oxygen atoms associated with triplets of crystal phosphates (P-sites). C-sites, P-sites, and

hydroxyl groups are distributed in a fixed topogeographic pattern on the crystal surface. This combination of active groups supports retention by at least three distinct mechanisms: cation exchange with P-sites, anion exchange and calcium coordination with C-sites. Depending on buffer pH, composition and the surface properties of the applied protein, different mechanism or combination of mechanisms will dominate in a given application (Gangon, 1998).

After loading, hydroxyapatite column was washed over-night with 30 ml of buffer B and afterwards $Ssq1_{His}$ was eluted with 50 ml of linear potassium phosphate buffer pH 6,8 gradient (20 to 220 mM) in buffer B. Fractions of 1,2 ml were collected. Fractions containing pure $Ssq1_{His}$ protein were pooled together and applied directly on a column containing 0,25 ml of Ni-NTA equilibrated previously with 4 ml of buffer B. After loading, column was washed with 4 ml buffer B. Afterwards protein was eluted with buffer B containing 350 mM imidazole and 350 µl fractions were collected. Fractions containing pure $Ssq1_{His}$ were pooled together and dialyzed for 4 h against end buffer. Protein concentration was estimated with Bradford solution as 1,2 µg/ µl.

lysis bufer	buffer A1	buffer A2	buffer B	end buffer
20 mM Tris-HCl pH 8,0	20 mM Tris-HCl pH 8,0	20 mM Tris-HCl pH 8,0	20 mM potassium phosphate buffer pH 6,8	20 mM Tris-HCl pH 8,0
10 % (v/ v) glycerol	10 % (v/ v) glycerol	10 % (v/ v) glycerol	0,15 M NaCl	10 % (v/ v) glycerol
1 mM PMSF	1 mM PMSF	1 mM PMSF	10 % (v/ v) glycerol	5 mM 2-merkaptoethanol
0,5 % (v/ v) Triton-X-100	0,05 % (v/ v) Triton-X-100	0,05 % (v/ v) Triton-X-100	5 mM 2-mercaptoethanol	0,05 % (v/ v) Triton-X-100
0,5 M NaCl	0,5 M NaCl	1 M NaCl	0,05 % (v/ v) Triton-X-100	200 mM KCl
20 mM imidazole pH 8,0	20 mM imidazole pH 8,0	20 mM imidazole pH 8,0		
		1 mM ATP		
		2 mM $MgCl_2$		

2.12.23.3 Purification of Isu1, Jac1 and Mge1 from *E. coli*

His-tagged versions of *S. cerevisiae* Isu1, Jac1 and Mge1 proteins were purified as described in (Dutkiewicz *et al.*, 2003) and were receivead as generous gift from Dr. Rafal Dutkiewicz from Laboratory of Evolutionary Biochemistry at Intercollegiate Faculty of Biotechnology, Gdansk, Poland.

2.12.23.4 Purification of Cia1 and Cia2 from *E. coli*

His-tagged versions of *S. cerevisiae* Cia1 and Cia2 proteins were purified from *E. coli* strain BL21(DE3)-Gold harboring overexpressing plasmid pET15bCIA1$_{His}$ or pET15bCIA2$_{His}$ as described in (Srinivasan *et al.*, 2007) by Sven-Andreas Feibert.

3 Results

3.1 Role of Grx5 in mitochondrial iron-sulfur cluster assembly.

3.1.1 Oxidative stress in *grx5Δ* cells is caused in part by the role of Grx5 in ISC assembly.

Cells deleted for Grx5 (*grx5Δ* cells) display an inactivation of Fe/S enzymes (Fig. 3.1 A), *FET3* promoter induction (Fig. 3.1 B), the accumulation of iron within the cell (Fig. 3.1 C) and massive oxidative stress (Rodriguez-Manzaneque et al., 1999; Rodriguez-Manzaneque et al., 2002). This phenotype suggests that the monothiol Grx5 performs an important role in mitochondrial oxidative stress protection. Oxidative stress may, in turn, indirectly impair mitochondrial Fe/S protein maturation, questioning the identification of Grx5 as a *bona fide* component of the mitochondrial ISC assembly system. In yeast, severe oxidative stress in mitochondria induces auxotrophies for glutamate and lysine (Liu et al., 1992; Wallace et al., 2004). These amino acids require aconitase-type Fe/S proteins for their biogenesis that are especially susceptible to oxidative damage which may explain the glutamate and lysine auxotrophies of *grx5Δ* cells (Rodriguez-Manzaneque et al., 1999; Rodriguez-Manzaneque et al., 2002; Djaman et al., 2004). Consistent with this conclusion, the growth defects of *grx5Δ* cells on minimal SD medium lacking lysine and glutamate disappeared under anaerobic conditions (Fig. 3.2). This was not the case for *isa1/2Δ* cells that lack Isa1 and Isa2, a further indication that Grx5 is not part of the specialized ISC assembly system that is dedicated to the maturation of [4Fe-4S] proteins (Fig. 3.2), (Muhlenhoff et al., 2011). In order to further investigate the idea that the defects in the maturation of cellular Fe/S proteins in *grx5Δ* cells may be caused by oxidative stress alone, the aconitase activities were compared in *grx5Δ* and *sod2Δ* cells. The latter strain displays a similar glutamate auxotrophy as *grx5Δ* cells due to increased mitochondrial oxidative stress in the absence of functional mitochondrial superoxide dismutase (Yang et al., 2006). Indeed, aconitase activities that were reduced to 18 % of wild-type levels in *grx5Δ* and to 25 % in *sod2Δ* under aerobic conditions, recovered in both strains under anaerobic conditions to 60 % of wild-type levels (Fig. 3.3).

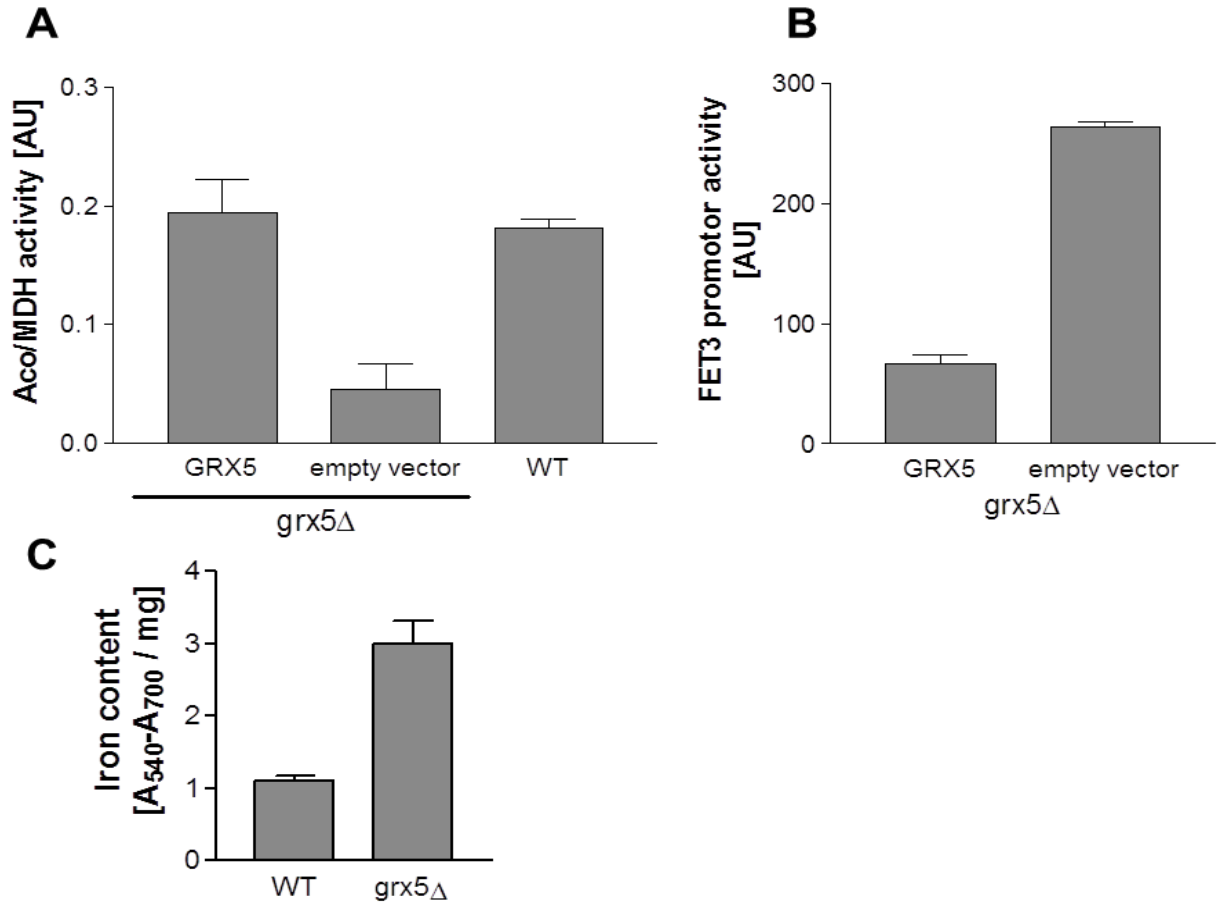

Figure 3.1 Phenotype of *grx5Δ* cells. (**A**) Whole cell extracts from wild-type (WT) or *grx5Δ* cells containing empty pRS424 or Grx5 overexpressing vector were grown over-night in SD medium without tryptophan. Cells were collected and cell lysates were assayed for activity of aconitase (Aco) and malate dehydrogenase (MDH). Bars represent aconitase activity normalized to MDH. (**B**) The *grx5Δ* cells with or without overexpressed Grx5, harboring reporter plasmid pFET3-GFP were cultivated in iron replete conditions. *FET3* promoter activities were determined by measuring the GFP-specific fluorescence emission of logarithmically grown cells. (**C**) Iron levels were measured for mitochondria isolated from *grx5Δ* cells containing empty or Grx5 overexpressing vector grown on SD medium without tryptophan. Error bars indicate the SEM (n > 4).

A central indication for an involvement of Grx5 in Fe/S cluster assembly was the accumulation of iron on the scaffold protein Isu1 in cells with low levels of Grx5 (Muhlenhoff et al., 2003a). In order to investigate whether this iron accumulation was the result of oxidative stress, iron binding to overproduced Isu1 was followed by ^{55}Fe radiolabeling and

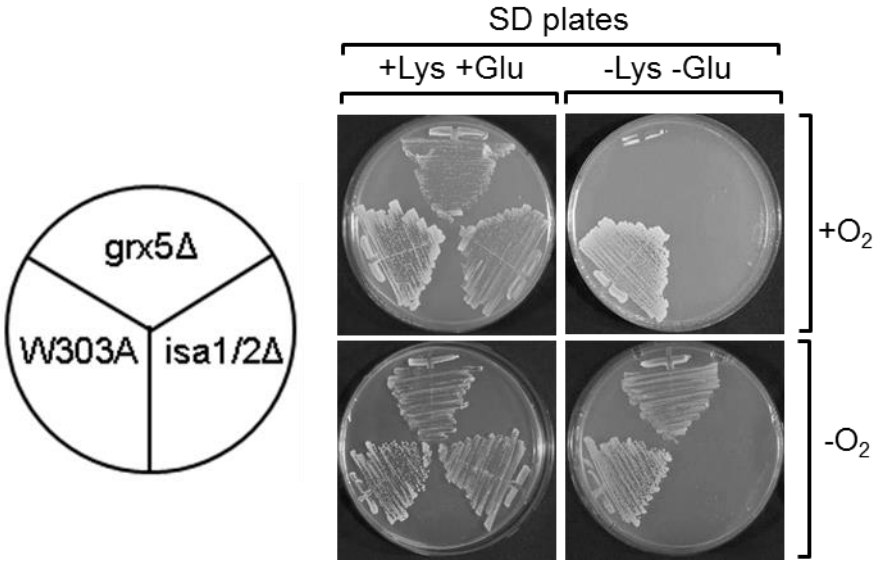

Figure 3.2 Auxotrophies of *grx5Δ* cells are not observed under anaerobic conditions. The yeast strains W303A (WT), *isa1/2Δ* and *grx5Δ* were streaked on SD plates containing or lacking both lysine (Lys) and glutamate (Glu), and incubated at 30ºC for two days under aerobic or anaerobic conditions

immunoprecipitation of wild-type, *grx5Δ* and *sod2Δ* cells (Fig. 3.3 B). In *sod2Δ* cells, the amount of iron bound to Isu1 *in vivo* was slightly lower than in wild-type cells under both aerobic and anaerobic conditions. In *grx5Δ* cells, however, a 7-fold increase in iron binding to Isu1 was observed under aerobic conditions and this was only moderately reduced to 4,5-fold the levels found in wild type under anaerobic conditions (Fig. 3.3 B). These data show that the accumulation of iron on Isu1 is a specific phenotype of *grx5Δ* cells. It is not caused by oxidative stress, as it is only marginally cured upon removal of oxygen.

In order to explore the differences between the oxidative stress mutant *sod2Δ* and *grx5Δ* cells further, the activity of lipoic acid synthase was analyzed by determining the attachment of lipoic acid to the E2 subunits of the mitochondrial PDH (Lat1) and KGDH (Kgd2) and the H-subunit of GCS (Gcv3). Lipoic acid content can be determined by Western blot analysis of mitochondrial extracts using anti-lipoic acid antibodies (Gelling *et al.*, 2008). In *grx5Δ* mitochondria, strongly diminished lipoylation of Lat1, Kgd2 and Gcv3 was detected (Fig. 3.3 C). However, in *sod2Δ* all proteins were lipoylated at wild-type levels, with the exception of Gcv3.

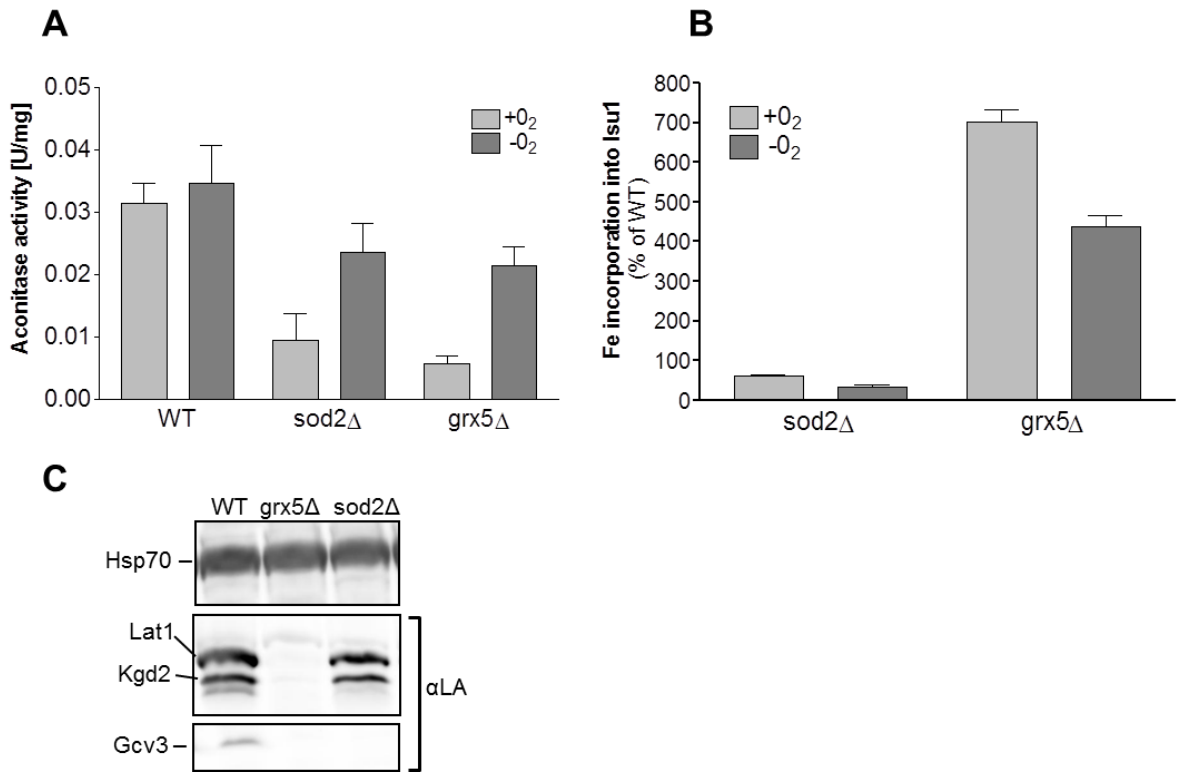

Figure 3.3 Iron accumulation on Isu1 occurring in *grx5Δ* cells cannot be rescued under anaerobic conditions. (**A**) Whole cell extracts from the WT, *sod2Δ* and *grx5Δ* cells grown over-night in full medium containing glucose (YPD) in aerobic or anaerobic conditions were assayed for activity of aconitase. (**B**) WT, *sod2Δ* and *grx5Δ* cells overproducing Isu1 were grown over-night in iron-poor SD medium and then radiolabeled with 10 µCi ^{55}Fe for 2 h in aerobic or anaerobic conditions. The overproduced Isu1 was immunoprecipitated from cell extracts with specific antibodies and the amount of co-precipitated ^{55}Fe was quantified by scintillation counting. (**C**) Mitochondrial extracts were prepared from the indicated strains grown on lipoic acid-free SD medium and probed with antibodies against Hsp70 and lipoic acid (Onder *et al.*, 2006). The latter recognizes the lipoylated forms of the E2 subunits of PDH (Lat1) and KDH (Kgd2) and the H-subunit of glycine cleavage system – GCS (Gcv3p) (Schonauer *et al.*, 2009). Error bars indicate the SEM (n > 4).

These data indicate that lipoic acid synthase is active in *sod2Δ*, likely because it is much more oxygen-resistant than aconitase-type Fe/S proteins that are known to be easily converted to an inactive [3Fe-4S] form upon oxidative stress (Djaman *et al.*, 2004; Wallace *et al.*, 2004). In *grx5Δ* cells, however, lipoic acid synthase was inactive, most likely because the maturation of mitochondrial Fe/S proteins is impaired in the absence of Grx5 (Fig. 3.3 C). Taken together, the

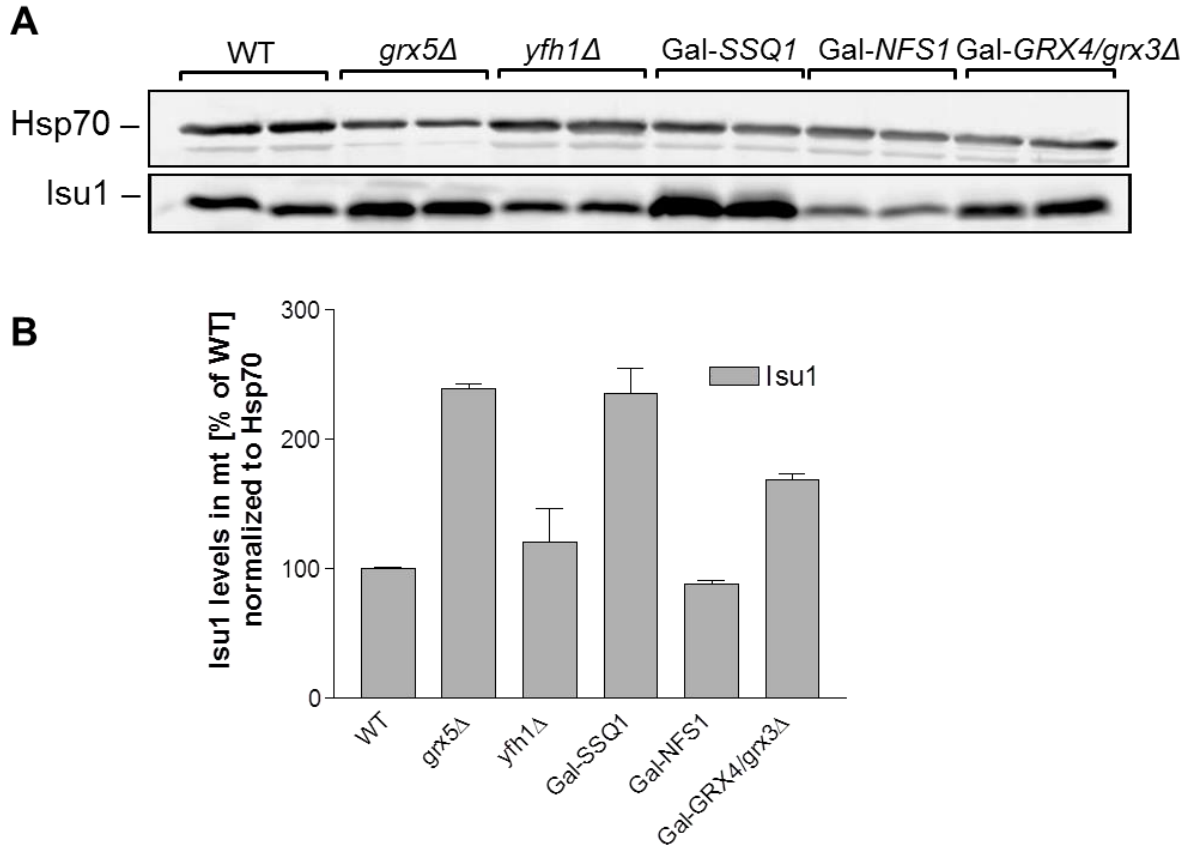

Figure 3.4 Isu1 levels in mitochondria isolated from various yeast cells. (A) Mitochondrial lysates (50 µg of protein each) from wild-type (WT), *grx5Δ*, *yfh1Δ*, Gal-*SSQ1*, Gal-*NFS1*, and Gal-*GRX4/grx3Δ* cells grown on full medium with glucose (YPD) were subjected to SDS-PAGE followed by immunostaining with antibodies against Isu1 and Hsp70. Gal-ISC strains were depleted to the critical levels prior to experiment. Each sample was analyzed in duplicate. **(B)** Isu1 levels were quantified by densitrometry and normalized to the Hsp70 protein levels.

sum of these data suggests that the oxidative stress that prevails in cells with low levels of Grx5 is not alone responsible for the defects in the *de novo* synthesis of Fe/S proteins. Rather, the recovery of aconitase activities in *grx5Δ* cells under anaerobic conditions is most likely caused by the combination of an increased stability of aconitase, a reduced demand for Fe/S proteins involved in respiration, a reduction in mitochondrial iron overload (Miao *et al.*, 2008), and a moderate general improvement of cellular ISC assembly in the absence of oxygen.

It was shown previously that changes in mitochondrial iron levels such as those seen in *grx5Δ* cells may result in the inactivation of Mn-Sod2 due to a mis-incorporation of iron into the protein, resulting in loss of superoxide protection of mitochondria (Naranuntarat *et al.*, 2009). The degree of Sod2 inactivation appeared to be correlated with mitochondrial Isu1 levels. Since

Isu1 is heavily overproduced in *GRX5* deletion mutant ((Andrew et al., 2008) and Fig. 3.4) and it is not able to efficiently transfer its Fe/S cluster to target proteins in the absence of Grx5, I reasoned that the Fe/S-cluster accumulation on Isu1 may be responsible for the oxidative stress phenotype of *grx5Δ* cells. In order to follow this idea, a vector expressing Isu1 in which aspartate 71 was exchanged for alanine was constructed.

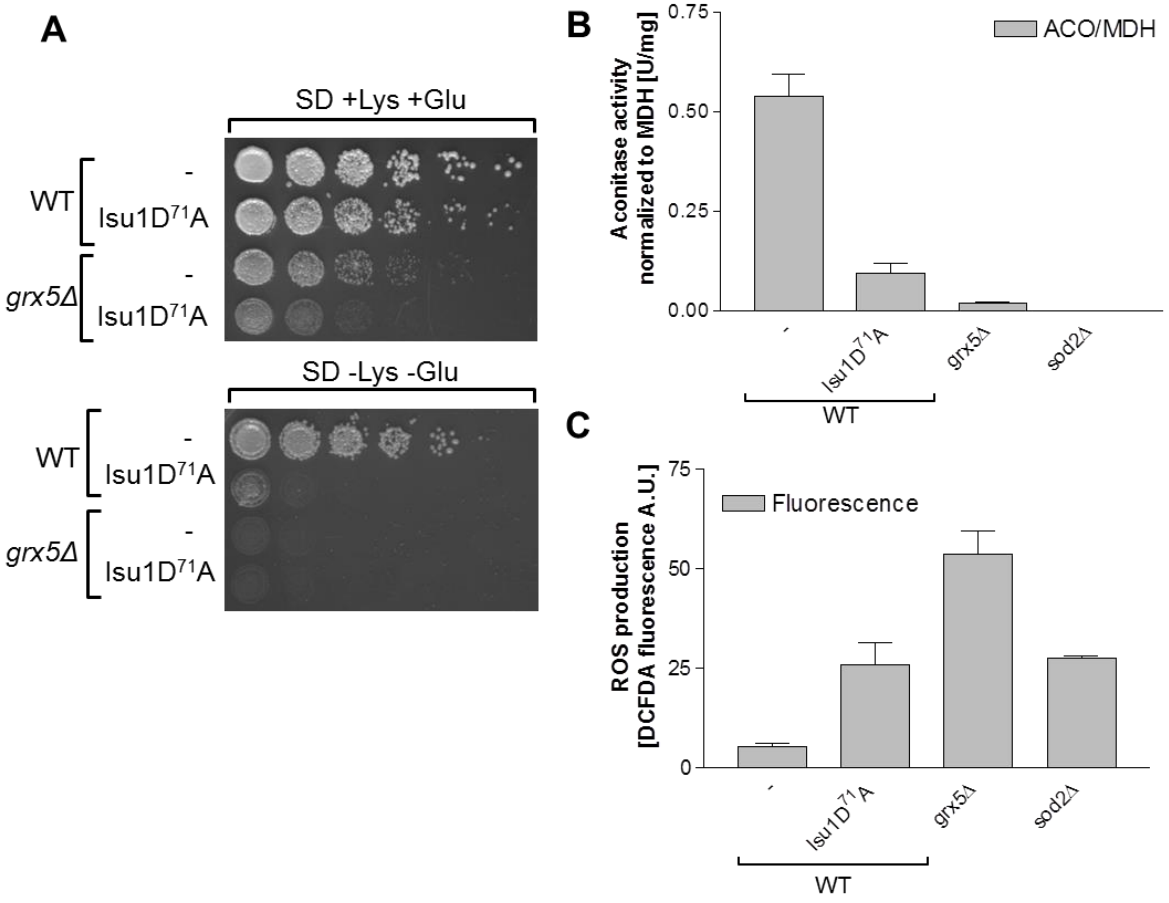

Figure 3.5 Impaired Fe/S cluster biogenesis is the primary cause of the oxidative stress in *grx5Δ* cells. (**A**) Over-night cultures of WT and *grx5Δ* cells carrying the empty pRS416 vector or pCM189-*ISU1D71A* vector overproducing the site-directed mutant Isu1D^{71}A were spotted onto SD plates without uracil in presence or absence of both lysine and glutamate. Plates were incubated at 30ºC for two days. (**B, C**) WT, *grx5Δ* and *sod2Δ* cells containing empty pRS416 vector and WT cells overproducing Isu1D^{71}A protein were grown over-night in SD medium lacking uracil. (**B**) Cell extracts were assayed for aconitase activities and normalized to those of malate dehydrogenase. (**C**) Cells were diluted to OD_{600} = 0,3 in SD medium supplemented with 15 µM 2',7' dichlorodihydrofluorescein diacetate (DCFDA). After 2 hours, cell extracts were analyzed for the fluorescence emission at 524 nm (excitation 504 nm). Results were normalized to protein concentration. Error bars indicate the SEM (n > 4).

This mutation is known to stabilize the Fe/S co-factor on bacterial IscU, thus mimicking the situation for Isu1 in *grxΔ* cells (Raulfs et al., 2008). Indeed, the over-expression of Isu1D^{71}A induced a lysine and glutamate auxotrophy in wild-type cells, a phenotype characteristic for *grx5Δ* (Fig. 3.5 A). When expressed in *grx5Δ* cells, cell growth was further reduced, even on medium containing both amino acids. In addition, the overproduction of Isu1D^{71}A in wild-type cells caused a strong 5-fold decrease in aconitase activities (Fig. 3.5 B). Next, it was analyzed whether the Isu1D^{71}A mutant may induce oxidative stress. For this, wild-type cells expressing Isu1D^{71}A, *grx5Δ* and *sod2Δ* cells were probed with the fluorescence dye 2',7' dichlorodihydrofluorescein diacetate (DCFDA) (Fig. 3.5 C). DCFDA is non-fluorescent when chemically reduced, but becomes fluorescent after cellular oxidation by reactive oxygen species (ROS) (Jakubowski and Bartosz, 1997). As expected, *grx5Δ* cells exhibit massive oxidative stress when compared to the wild type. ROS production in wild-type cells expressing Isu1D^{71}A reached 50 % of those of *grx5Δ* cells and was similar to that of *sod2Δ* cells. Taken together these data suggest that the oxidative stress observed in cells lacking Grx5 is, at least in part, caused by the impaired Fe/S cluster transfer from Isu1 to target proteins in the absence of Grx5.

3.1.2 Grx5 specifically interacts with the dedicated Hsp70 chaperone Ssq1.

Yeast *SSQ1* and *GRX5* genetically interact (Rodriguez-Manzaneque et al., 2002) (Rodriguez-Manzaneque *et al.*, 2002). A depletion of both gene products caused accumulation of Fe/S clusters on Isu1, they were suggested to participate in the same step of Fe/S protein biogenesis (Muhlenhoff *et al.*, 2003a). Additionally, both strains could be rescued by addition of BPS to the medium (Fig. 3.6 and (Andrew *et al.*, 2008)), and *grx5Δ* cells could be partially rescued by overexpression of Ssq1 protein but not by overexpression of the other Hsp70 family member DnaK (Fig. 3.7). All these connections and similarities prompted me to analyze a potential physical interaction between the two proteins. A yeast expression vector encoding a Ssq1-GST (glutathione-S-transferase) fusion protein (Gerber *et al.*, 2003) was co-transformed with a vector overproducing Grx5 into wild-type and *grx5Δ* yeast cells. Mitochondria were purified, lysed in detergent-containing buffer, and extracts were subjected to GST-affinity purification (Fig. 3.8 A) or immunoprecipitation of Grx5 with specific antibodies (Fig. 3.8 B)

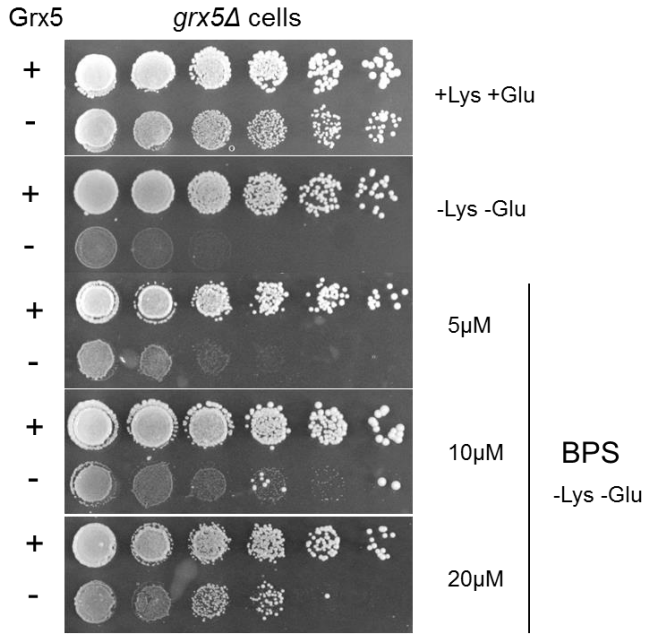

Figure 3.6 Addition of BPS to the medium rescues auxotrophies of *grx5Δ* cells. Over-night cultures of *grx5Δ* cells carrying Grx5 overproducing or the empty pRS424 vector were spotted onto SD plates without tryptophane in presence or absence of both lysine (Lys) and glutamate (Glu), and 5 to 20 μM bathophenanthroline (BPS) as indicated. Plates were incubated at 30ºC for two days.

(Gerber *et al.*, 2003). In both cases, Grx5 and Ssq1-GST were co-isolated as identified by immunostaining and quantitative densitometry (Fig. 3.8 A - B, lanes 2 - 3). This interaction was specific, because no Grx5-specific signal was detected in wild-type mitochondria that overproduced Grx5 but lacked Ssq1-GST (Fig. 3.8 A - B, lane 1), or in mitochondria isolated from *grx5Δ* cells that expressed only Ssq1-GST (lane 4). Furthermore, the amount of co-purified Grx5 increased 2-fold upon overproduction of Grx5, indicating a dosage specific interaction with Ssq1-GST (Fig. 3.8 A - B, lanes 2 - 3). No Ssq1-GST-specific signal was observed in an anti-Grx5 immunoprecipitation using mitochondria from cells that did not express Ssq1-GST or that did not contain Grx5 (Fig. 3.8 B, lanes 1, 2 and 4). It was riveting whether the observed Grx5-Ssq1 interaction is specific or related to a general Hsp70 chaperone function of Ssq1. Previously, it was found that Ssq1 does not cooperate with the co-chaperone Mdj1 and thus should not be involved in protein folding in yeast mitochondria (Dutkiewicz *et al.*, 2003). On the other hand, purified Ssq1 has been shown to be capable of protecting denatured rhodanese from aggregation

in vitro (Dutkiewicz *et al.*, 2006). A similar situation is observed in *E. coli* where HscA, an ISC-specialized Hsp70 protein, is not able to promote protein folding, but can prevent protein aggregation *in vitro* (Silberg *et al.*, 1998). Hence, it was important to analyze the relative Grx5

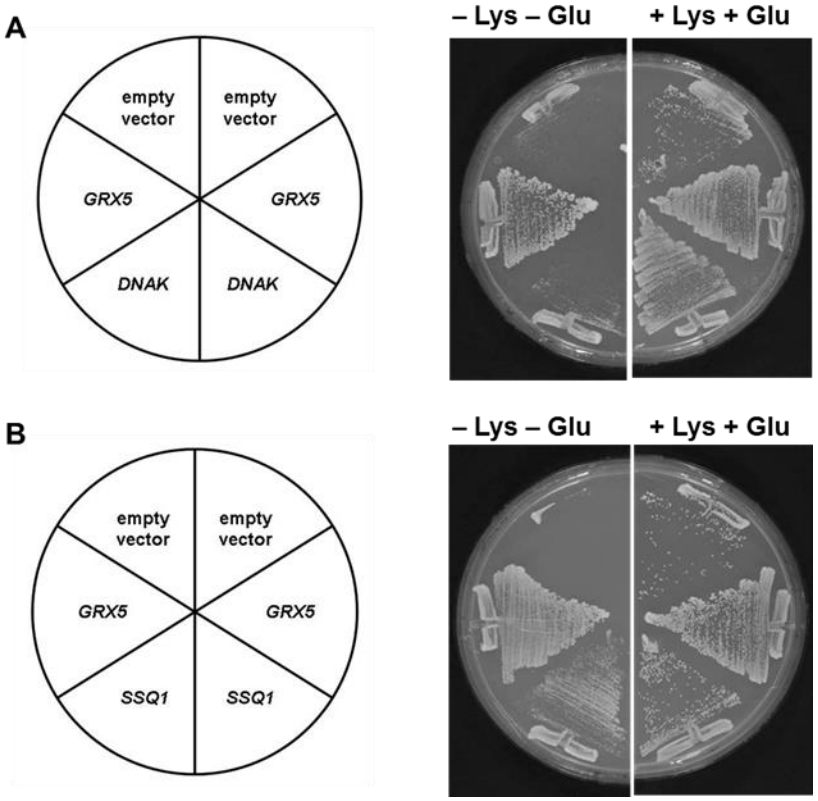

Figure 3.7 Ssq1 but not DnaK can rescue the growth of *grx5Δ* cells (**A,B**) Yeast *grx5Δ* cells were transformed with vector overproducing Grx5, (**A**) Ssq1 or (**B**) DnaK, or empty pRS424. Obtained cells were streaked as indicated on SD plates containing or lacking both lysine (Lys) and glutamate (Glu), and incubated at 30ºC for two days

binding efficiencies of Ssq1 and Ssc1. Extracts from wild-type mitochondria containing overproduced Ssq1-GST and Grx5 were subjected to GST-affinity purification or anti-Grx5 immunoprecipitation, and bound Ssq1-GST or Ssc1 were analyzed by immunostaining and quantified (Fig. 3.8 C). As expected for a protein folding chaperone, both GSH- and anti-Grx5 beads co-purified a small amount of Ssc1 (Fig. 3.8 C, lanes 3 - 4). However, the amount of Ssq1-GST binding to anti-Grx5 immunobeads was at least 4-times higher than that of Ssc1 (lanes 1 - 3)

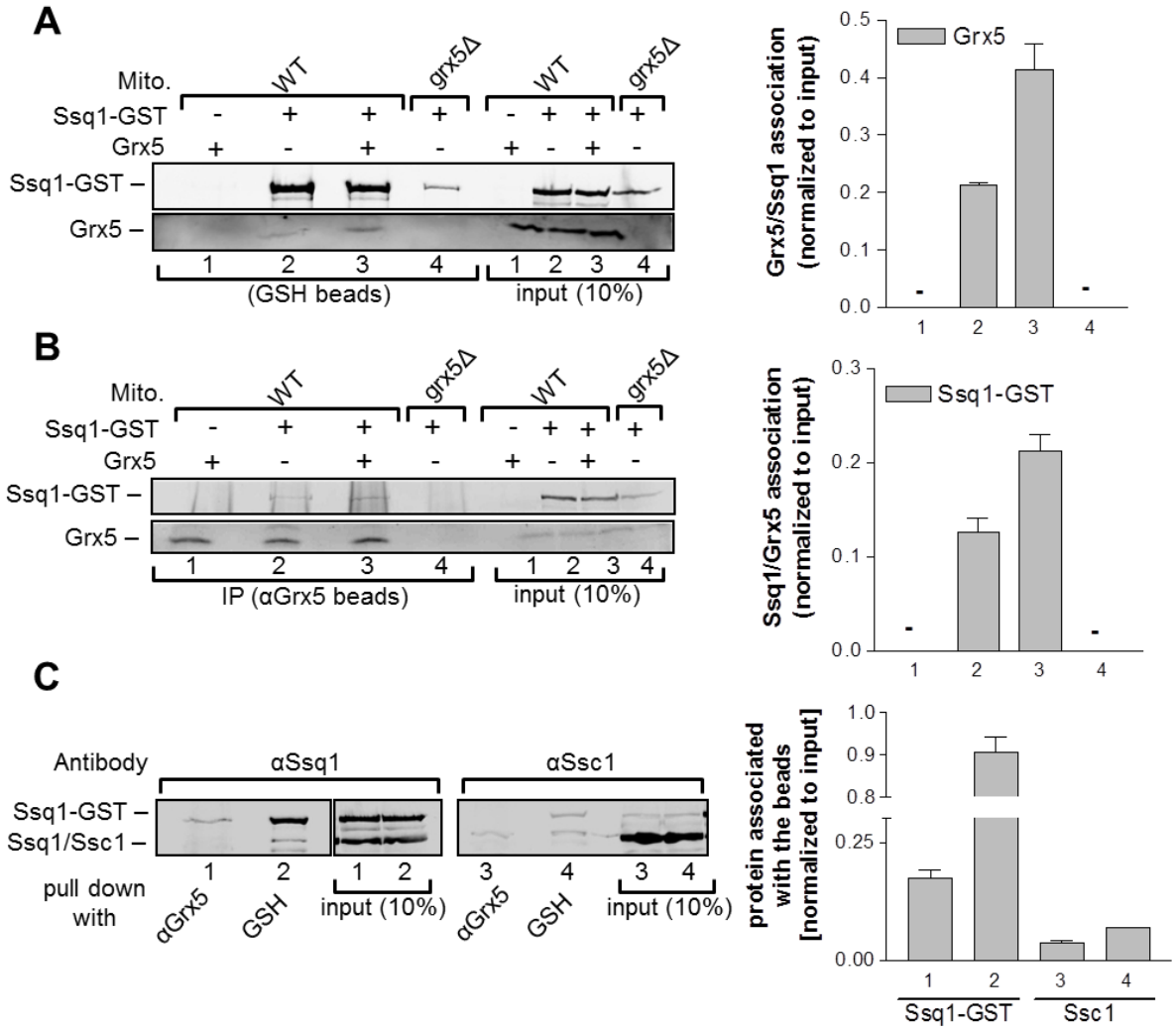

Figure 3.8 Grx5 specifically interacts with the dedicated Hsp70 chaperone Ssq1 *in vivo*. (**A, B**) Mitochondria (Mito) from wild-type (WT) and *grx5Δ* yeast cells overproducing either Ssq1-GST, Grx5, or both were lysed by detergent (0,5 % Triton X-100) in buffer A, and subjected to affinity purification with (**A**) glutathione (GSH) sepharose or (**B**) antibodies against Grx5 bound to Protein A sepharose. The purified proteins Ssq1-GST and Grx5 were analyzed by SDS-PAGE and immunostaining (left side, by αSsq1 and αGrx5 antibodies), and quantified by densitometry (right). Data were normalized to the protein levels in the respective extracts. Numbers on the right correspond to lane numbers of the immunoblots. (+) represents presence and (-) represents absence of the indicated protein. (**C**) Mitochondrial lysates from WT cells with overproduced Ssq1-GST and Grx5 were subjected to immunoprecipitations with GSH-sepharose or antibodies against Grx5. Analysis for the presence of Ssq1 or Ssc1 was as described above. The immunoblots for the two proteins were performed on the same gel in parallel. The αSsq1 and αSsc1 antibodies show slight cross reactivity due to similarities between Ssq1 and Ssc1 proteins. Error bars indicate the SEM (n = 3).

documenting the preferential interaction of Grx5 with Ssq1 rather than Ssc1. This result is even more significant, since Ssc1 is at least 500-times more abundant than Ssq1 in yeast mitochondria (Schilke *et al.*, 1996; Voisine *et al.*, 2000). Hence, if the Grx5-Ssq1 interaction would be due to a general Hsp70 chaperone function, Grx5 is expected to bind almost exclusively to Ssc1. Collectively, *in vivo* co-precipitation results suggest a specific interaction between Ssq1 and Grx5. Notably, no significant interaction of Ssq1 with canonical Fe/S proteins was detectable, neither in the holo- nor in the apo-form (Fig. 3.9 for aconitase, and data not shown).

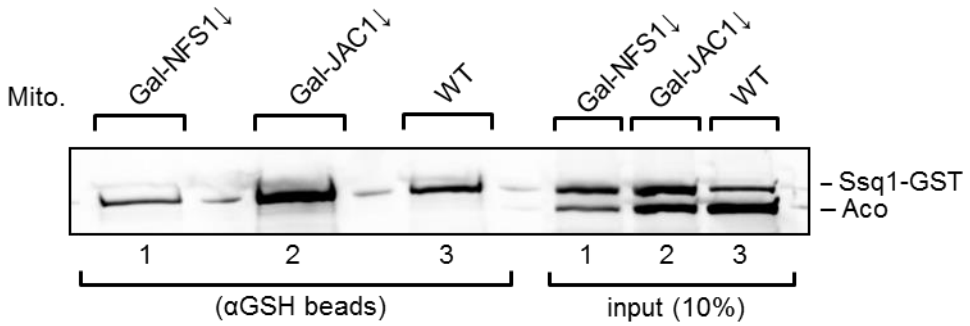

Figure 3.9 Ssq1 does not interact with recipient protein aconitase. Mitochondrial detergent lysates (Mito.) from Gal-*NFS1*, Gal-*JAC1* and wild-type (WT) cells (grown on SD medium) with overproduced Ssq1-GST and Grx5 were subjected to affinity purification with glutathione (GSH) sepharose. Beads were analyzed for the presence of Ssq1-GST and aconitase (Aco) by SDS-PAGE and immunostaining.

3.1.3 ISC components and ATP modulate the interaction of Grx5 and Ssq1.

Next, it was examined which parameters influence the Grx5-Ssq1 association. First, the possibility was investigated that this interaction is modulated by the availability of other ISC assembly components. Regulatable GAL1-10 promoter-exchange strains of ISC components overproducing both Ssq1-GST and Grx5 were grown to critical levels under depletion conditions in minimal medium containing glucose. Mitochondrial extracts were subjected to immunoprecipitation with anti-Grx5 antibodies and the amount of co-immunoprecipitated Ssq1-GST was quantified by densitometry. When compared to the wild-type situation, mitochondria from Gal-*NFS1* cells showed a 4-fold increase in Ssq1-GST association with Grx5 (Fig. 3.10

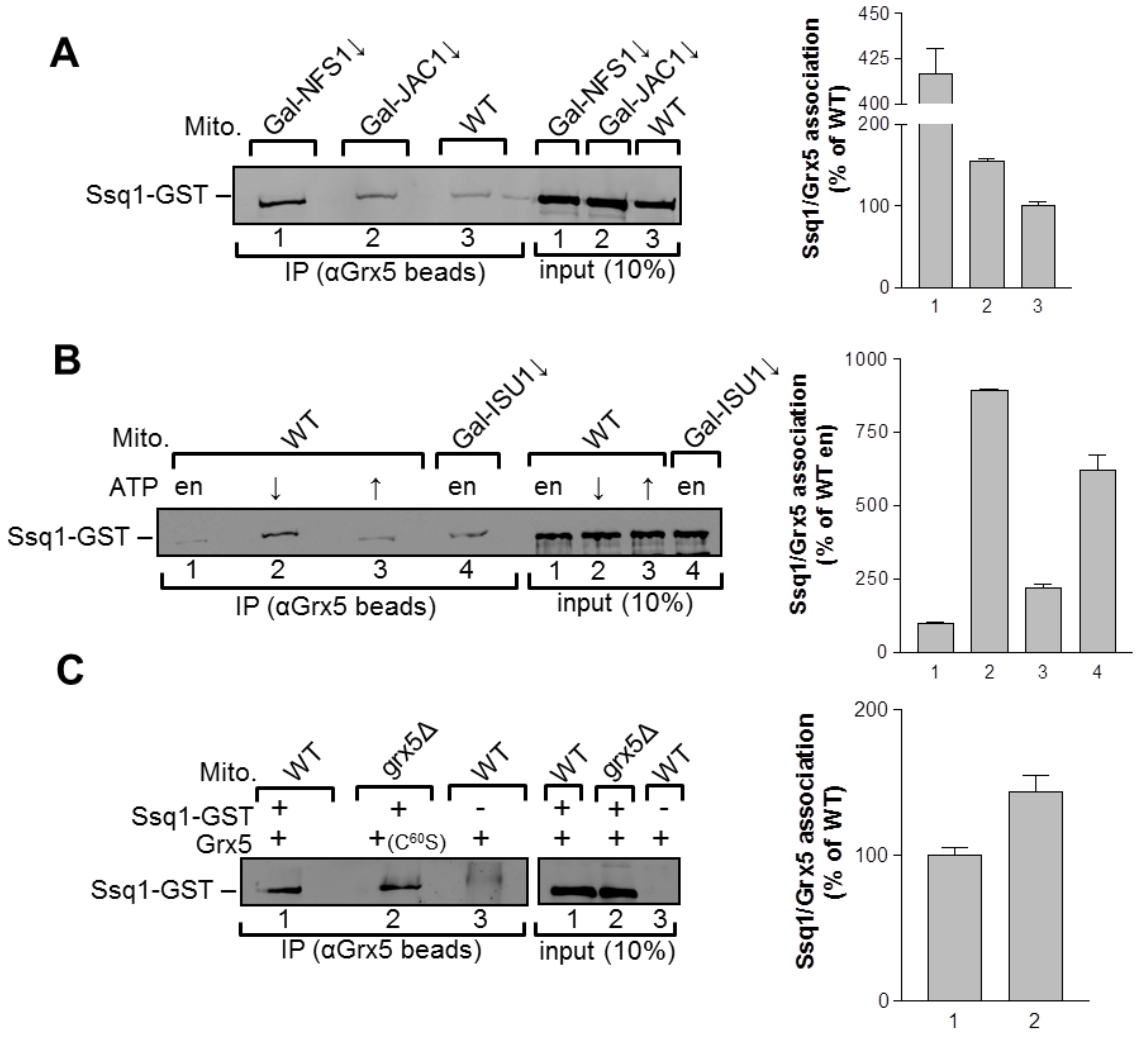

Figure 3.10 ISC components and ATP/ ADP levels modulate the interaction of Grx5 and Ssq1. (**A**) Mitochondrial detergent lysates (Mito) from Gal-*NFS1*, Gal-*JAC1* and wild-type (WT) cells (grown on SD medium) with overproduced Ssq1-GST and Grx5 were subjected to immunoprecipitations (IP) with antibodies against Grx5. Immunobeads were analyzed for the presence of Ssq1-GST by SDS-PAGE, immunostaining (left), and quantitation by densitometry (right) as in Fig. 3.8. (**B**) Mitochondrial lysates from WT or Gal-*ISU1/isu2Δ* cells (grown on SD medium) overproducing Ssq1-GST and Grx5 were subjected to immunoprecipitations with antibodies against Grx5 in buffer A without ATP supplementation (endogenous (en)) or with 1 mM ATP (↑). Another sample was first depleted for ATP in the presence of hexokinase and glucose-6-phosphate (↓). The amount of coimmunopurified Ssq1-GST was determined by immunostaining and densitometry as in Fig. 3.8. (**C**) Mitochondrial lysates from WT and *grx5Δ* cells with overproduced Ssq1-GST, Grx5 or the site-directed mutant protein Grx5C^{60}S as indicated were subjected to immunoprecipitations with antibodies against Grx5. (+) represents presence and (-) represents absence of the indicated protein. The amount of coimmunopurified Ssq1-GST was determined by immunostaining and densitometry as in Fig. 3.8. Error bars indicate the SEM (n = 3).

Since no Fe/S clusters are formed on the scaffold protein Isu1 in the absence of the cysteine desulfurase Nfs1, this increase indicated that Grx5 can efficiently associate with Ssq1 before the chaperone binds Fe/S cluster-loaded Isu1. A 1,5-fold increase in Grx5-Ssq1 association was observed in mitochondria depleted for Jac1, the J-type protein known to deliver Isu1 to Ssq1 (Fig. 3.10 A). The relatively low increase in Grx5-Ssq1 complex formation was likely due to the less efficient depletion of this ISC protein. Mitochondria from Isu1-depleted Gal-*ISU1/isu2Δ* cells showed a 5-fold increase in Ssq1-GST association with Grx5 (Fig. 3.10 B). These data strongly suggest that Grx5 binding to Ssq1 occurs independently of both Fe/S cluster formation on Isu1 and the complex formation between Ssq1 and holo-Isu1.

Since Ssq1 is an ATP-dependent Hsp70 chaperone, the nucleotide status of Ssq1 may influence the Grx5-Ssq1 interaction. To test this hypothesis, wild-type mitochondria with overproduced Ssq1-GST and Grx5 were incubated in buffer without and with 1 mM ATP. In addition, ATP was depleted in the organelles by treatment with hexokinase and glucose-6-phosphate. Mitochondrial extracts were subjected to immunoprecipitation with antibodies against Grx5. Under conditions of ATP supplementation, a 2-fold increase in Ssq1-GST association with Grx5 was observed compared to endogenous ATP levels (Fig. 3.10 B, lanes 1 and 3). This increase suggests that Grx5 is able to bind to Ssq1 in its ATP-bound state. The result consistent with a Grx5 interacting with Ssq1 before the recruitment of holo-Isu1. Strikingly, under ATP-depleting conditions, an 8-fold increase in Ssq1-Grx5 association was observed (Fig. 3.10 B, lane 2). This indicates that Grx5 binding to Ssq1 is not restricted to one of the nucleotide binding states, yet is most stably bound to Ssq1-ADP. Consistent with this conclusion, we found a similar efficiency of Grx5-Ssq1-GST co-immunoprecipitation in the presence of the non-hydrolysable ATP analogue AMP-PNP as with endogenous ATP levels (Fig. 3.11). Taken together, these data indicate that the Ssq1 shows the highest affinity to Grx5 in its ADP-bound state. Grx5 may be rleased to some extent after the exchange of ADP to ATP by the nucleotide exchange factor Mge1.

Previous studies have shown that the active-site cysteine residue of monothiol glutaredoxin Grx5 is essential for protein function *in vivo* (Belli *et al.*, 2002; Lillig *et al.*, 2008). To test if binding of Grx5 to Ssq1 was dependent on this active-site residue, a point mutation was created in which Cys60 of Grx5 was exchanged for serine. The resulting Grx5C^{60}S protein was overproduced together with Ssq1-GST in *grx5Δ* cells. Mitochondrial extracts were subjected to

immunoprecipitation with antibodies against Grx5, and the Ssq1-GST association with Grx5C^{60}S was determined. Ssq1-GST bound to wild-type and mutant Grx5 with similar efficiency (Fig. 3.10 C). The independence of the Grx5-Ssq1 interaction on the active-site cysteine of Grx5 suggests that the Grx5-Ssq1 complex formation does not directly involve the thiol-related function of Grx5. The active-site cysteine residue therefore may play a role in either the stimulation of Ssq1 ATPase activity, Fe/S cluster binding, and/ or Fe/S cluster delivery from Isu1 to client apo-proteins, as previously suggested (Bandyopadhyay *et al.*, 2008).

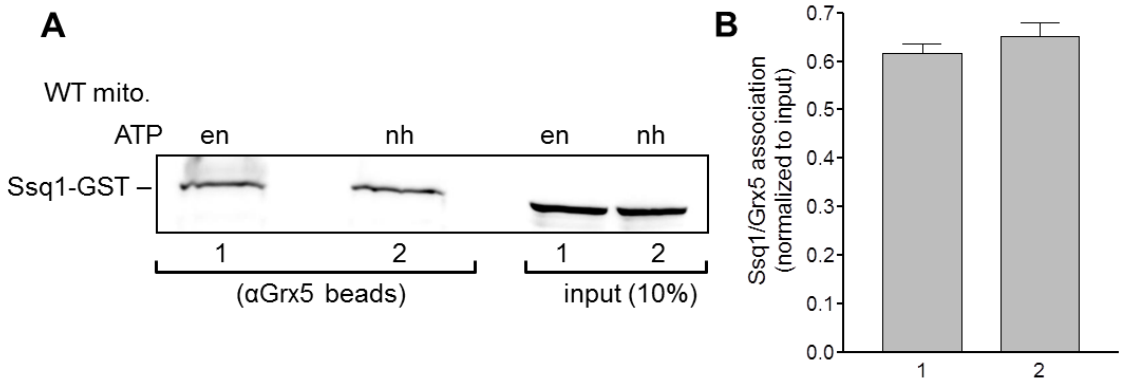

Figure 3.11 Grx5-Ssq1-GST co-immunoprecipitation in the presence of the non-hydrolysable ATP analogue AMP-PNP. Mitochondrial detergent lysates (Mito) from wild-type (WT) cells (grown on SD medium) with overproduced Ssq1-GST and Grx5 were subjected to immunoprecipitations (IP) with antibodies against Grx5 in buffer A without ATP supplementation (endogenous (en)) or with 1 mM non-hydrolysable AMP-PNP analogue (nh). Immunobeads were analyzed for the presence of Ssq1-GST by SDS-PAGE, immunostaining (A), and quantitation by densitometry (B) as in Fig. 3.8.

3.1.4 Grx5 does not stimulate the ATPase activity of Ssq1 distinguishing it from Isu1.

Client proteins interacting with the peptide binding domain of Hsp70 chaperones stimulate their ATPase activity (Mayer and Bukau, 2005; Craig and Marszalek, 2011). The increased ATPase activity of Hsp70 is considered to be a hallmark of productive interaction with partner proteins. The effect of Grx5 on the Ssq1 ATPase activity was tested *in vitro* using purified proteins, and the results were compared to those for added Jac1 and Isu1 (Dutkiewicz *et al.*, 2003). The Ssq1 ATPase activity was measured in presence of Mge1 and either Isu1 (Fig. 3.12 A) or Jac1 (Fig. 3.12 B) under steady-state conditions. Under these conditions, the overall rate of ADP formation depends on the rates of three sub-reactions: ATP binding, ATP hydrolysis,

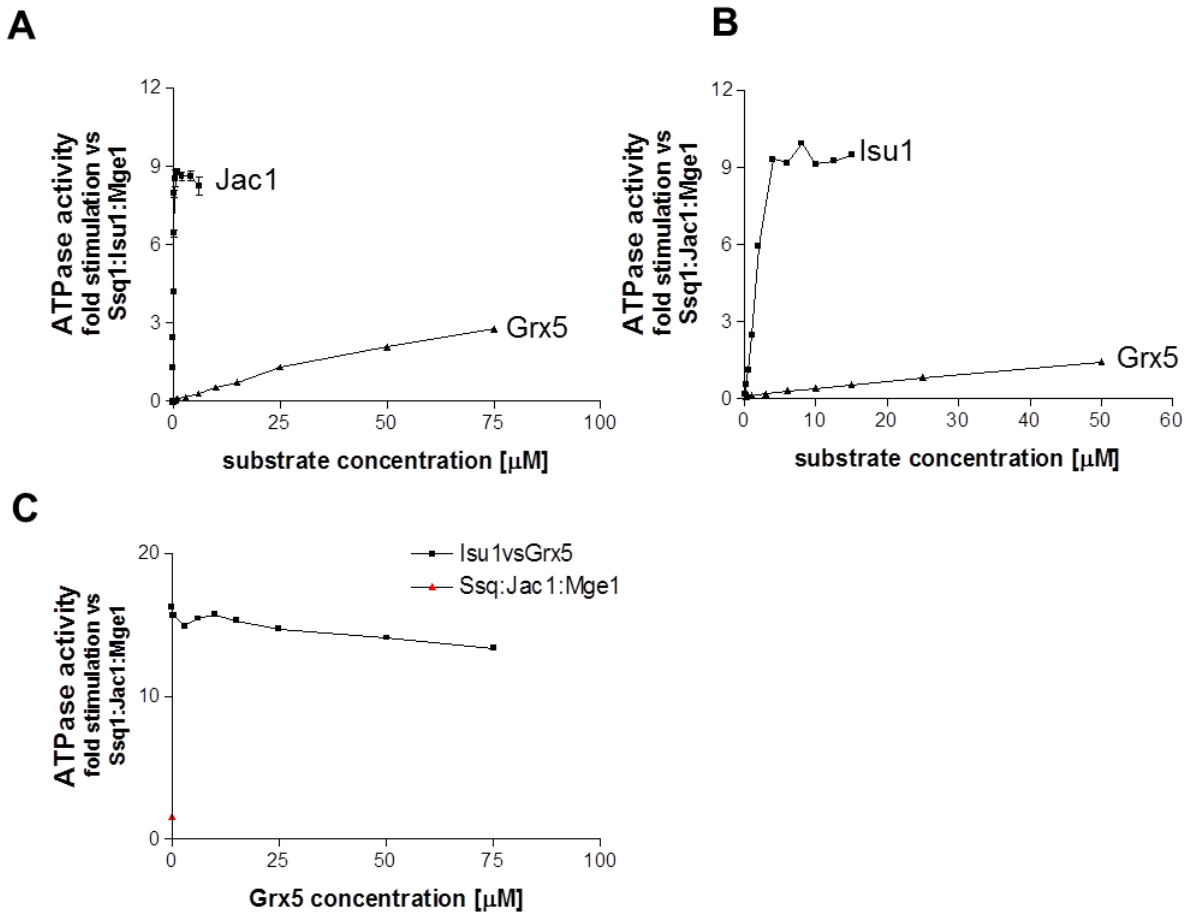

Figure 3.12 Grx5 does not stimulate ATPase activity of Ssq1. (**A, B, C**) The ATPase activity of Ssq1 (0,5 µM) was measured in the presence of varying amounts of Grx5 as a potential substrate. Samples contained (**A**) 0,5 µM Mge1 and 10 µM Isu1, or (**B**) Mge1 and Jac1 (0,5 µM each). The ATPase stimulation by increasing amounts of (**A**) Jac1 or (**B**) Isu1 as a substrate is included for comparison. The ATPase activity in the absence of titrated proteins was set to zero. (**C**) The sample in which competition between Isu1 and Grx5 was determined contained 0,5 µM Mge1, 0,5 µM Jac1 and as a substrate 4 µM Isu1. The ATPase activity in the absence of titrated proteins was set to 1. (**A, B, C**) Reactions (15 µl) were started by the addition of [γ^{32}P]-ATP (1 µCi) to a final concentration of 120 µM. Incubation was carried out at 25°C, and the reaction was terminated after 15 min by the addition of 100 µl of 1 M perchloric acid and 1 mM sodium phosphate. The release of radioactive inorganic phosphate from [γ^{32}P]-ATP was measured as described (Dutkiewicz *et al.*, 2003).

and dissociation of the reaction products: ADP and phosphate. Hardly any stimulation of the ATPase activity of Ssq1 was detected upon addition of up to 10 µM Grx5 in the presence of Mge1 and Isu1 (Fig. 3.12 A) or Jac1 (Fig. 3.12 B), while increasing levels of Jac1 and Isu1, respectively, were highly effective.The slight increase in ATP hydrolysis at higher concentrations of Grx5 may be due to residual contaminants present in the protein samples. Taken together, these data suggest that Grx5 differs from Isu1 and Jac1, the previously identified specific interaction partners of Ssq1, in that Grx5 is not able to stimulate the ATPase activity of Ssq1. Additionally, when Grx5 was added in increasing concentrations to the reaction containing Ssq1, Jac1, Mge1 and Isu1 as a substrate, it did not affect the ATPase activity stimulation showing that there is no c ompetition between Isu1 and Grx5 proteins (Fig. 3.12 C). It is thus unlikely that Grx5 interacts at the canonical peptide binding site of Ssq1 (see below).

In order to investigate whether the physical interaction between Grx5 and Ssq1 can be observed with the isolated proteins, an *in vitro* association study by microscale thermophoresis (MST) was performed. MST is the directed movement of particles in a microscopic temperature gradient. Changes in the structure/ conformation and hydration shell of biomolecules result in a relative change of their thermophoretic behavior and can be employed to determine binding affinities, binding kinetics and activity kinetics (Wienken *et al.*, 2010; Zillner *et al.*, 2012). In order to observe the interaction between Grx5 and Ssq1, fluorescently-labeled Grx5 was subjected to microscale thermophoresis in the presence of increasing amounts of Ssq1. Indeed, the presence of Ssq1 changed the thermophoretic behaviour of Grx5 indicating a binary association. From a fit of the obtained data, a binding constant of K_a = 0,44 (± 0.1) μM^{-1} was calculated (Fig. 3.13). This interaction was specific as virtually no binding of Grx5 to the unrelated protein Cia2 was observed under the same experimental setup (Fig 3.13 A, lane 1). Remarkably, this interaction did not increase upon addition of ATP (Fig. 3.13 A, lane 3), indicating that either Grx5 binds outside of the substrate binding site of Ssq1, or Ssq1 does not function as a canonical Hsp70 under these conditions. The latter was unlikely, as Ssq1 has been shown previously to engage in protein folding *in vitro* (Dutkiewicz *et al.*, 2006). Using this assay it was next determined whether Grx5 and Isu1 bind to the same position of Ssq1. The latter specifically recognizes the short conserved peptide motive LPPVK of Isu1 (Hoff *et al.*, 2003; Dutkiewicz *et al.*, 2004; Vickery and Cupp-Vickery, 2007). MST experiments were carried out in the presence of a LPPVK-containing peptide which was shown previously to efficiently bind to

Ssq1 and stimulate its ATPase activity (Hoff *et al.*, 2003; Knieszner *et al.*, 2005; Andrew *et al.*, 2006). The peptide was thus expected to compete with Grx5 for Ssq1 binding in case Isu1 and Grx5 would use overlapping substrate binding sites. In contrast, the Grx5-Ssq1 interaction increased 2-fold in the presence of the LPPVK-containing peptide at 1,4-fold excess over Ssq1 (Fig. 3.13 A, lane 4). A similar increase in Grx5-Ssq1 interaction was induced by the LPPVK-containing peptide in the presence of ADP (Fig. 3.13 C, lanes 5 and 6). Since no direct interaction of Grx5 to the peptide was detected (Fig. 3.13 A, lane 7), these observations indicate that the binding site of Grx5 does not overlap with the Isu1 substrate binding site on Ssq1. This is consistent with the observation above that Grx5 is not a regular client protein of Ssq1, as it failed

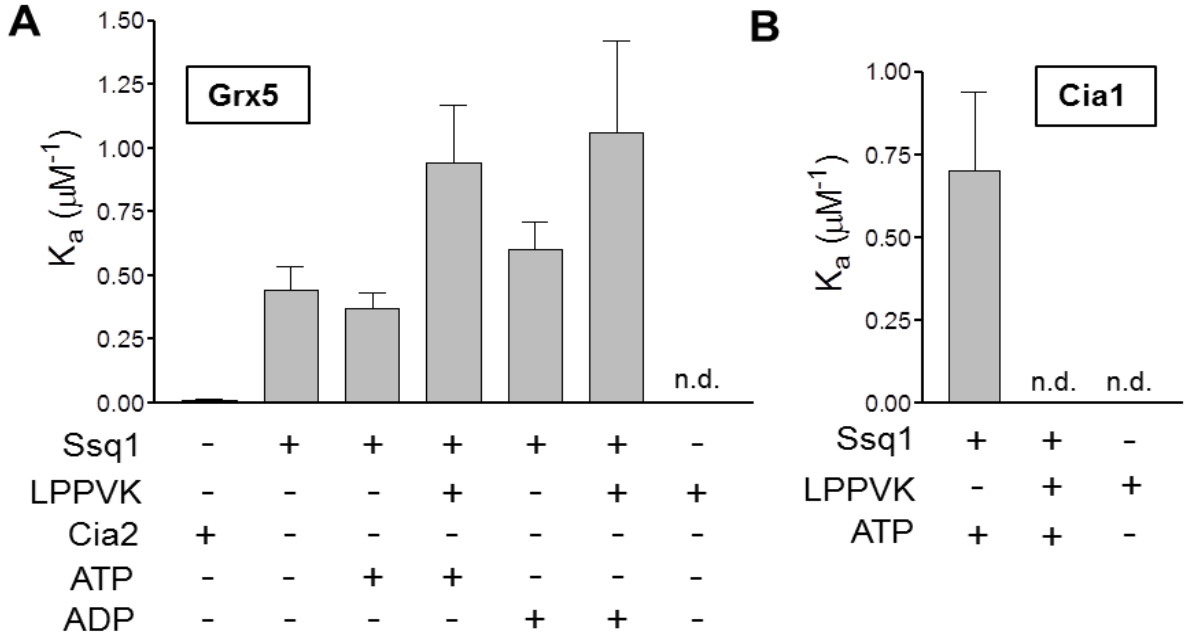

Figure 3.13 Grx5 interacts with Ssq1 *in vitro*. Fluorescently-labeled Grx5 (**A**) or Cia1 (**B**) at 200 nM each were titrated with serial (1 : 2) dilutions of Cia2 (ranging from 116 µM to 3,5 nM), Ssq1 (87 µM to 2,65 nM) or Isu1 peptide AKELSLPPVKLHC (LPPVK) (130 µM to 3,9 nM) alone, or in the indicated combinations in the buffer T (50 mM KPi pH 7,4; 150 mM NaCl; 1 mM $MgCl_2$; 1 mM GSH) containing 1 mM ATP or 1 mM ADP as indicated. The MST binding reactions were measured using Monolith NT.015 at 21°C and binding constants (K_a) were calculated from fits of the obtained data (See below for the original data Fig. 3.13 C (for panel A) and D (for panel B)). Error bars indicate the SD (n = 3). (n.d.: not determinable; in the absence of observable protein interactions, MST data cannot be fitted satisfactorily and K_a values cannot be determined.)

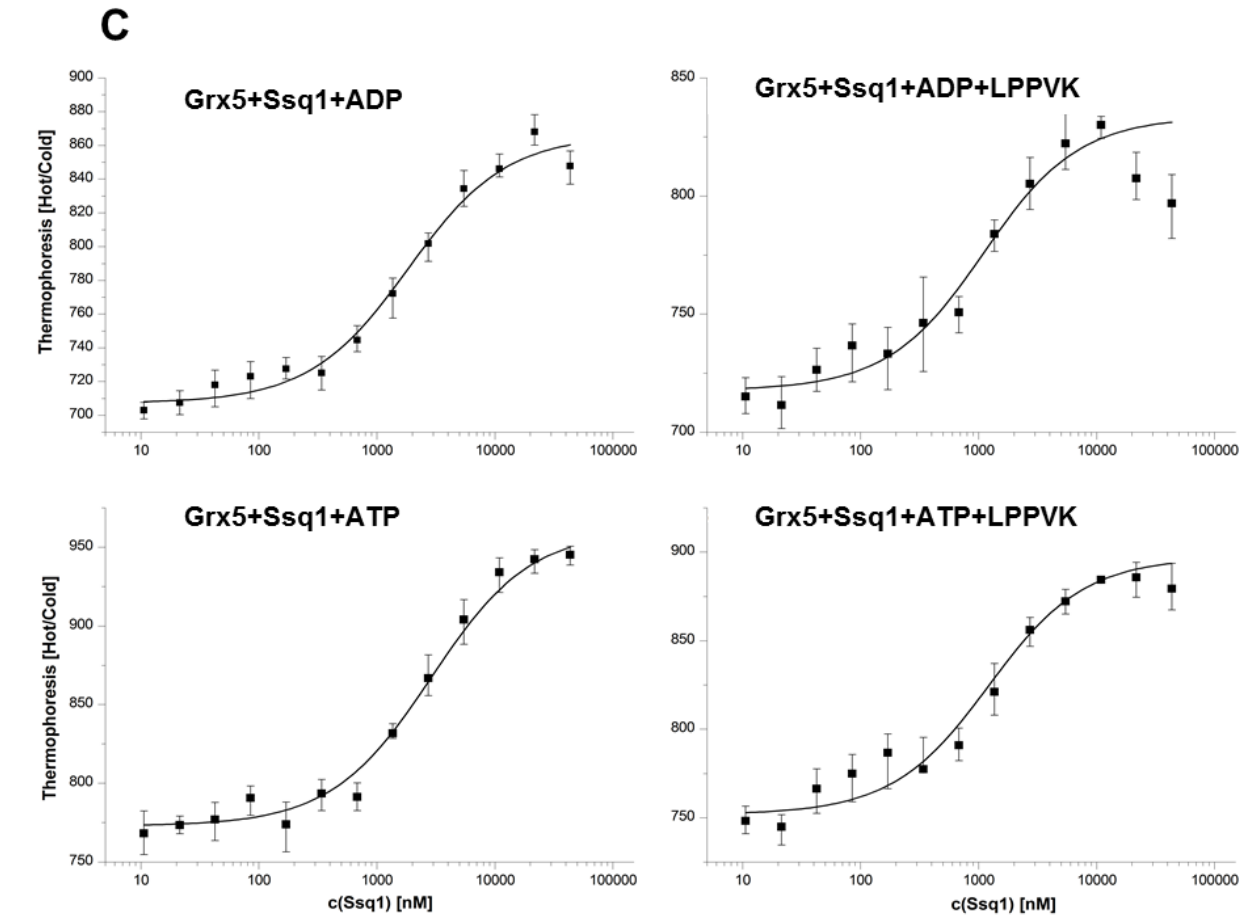
C
Grx5+Ssq1+ADP
Grx5+Ssq1+ADP+LPPVK
Grx5+Ssq1+ATP
Grx5+Ssq1+ATP+LPPVK
Thermophoresis [Hot/Cold]
c(Ssq1) [nM]

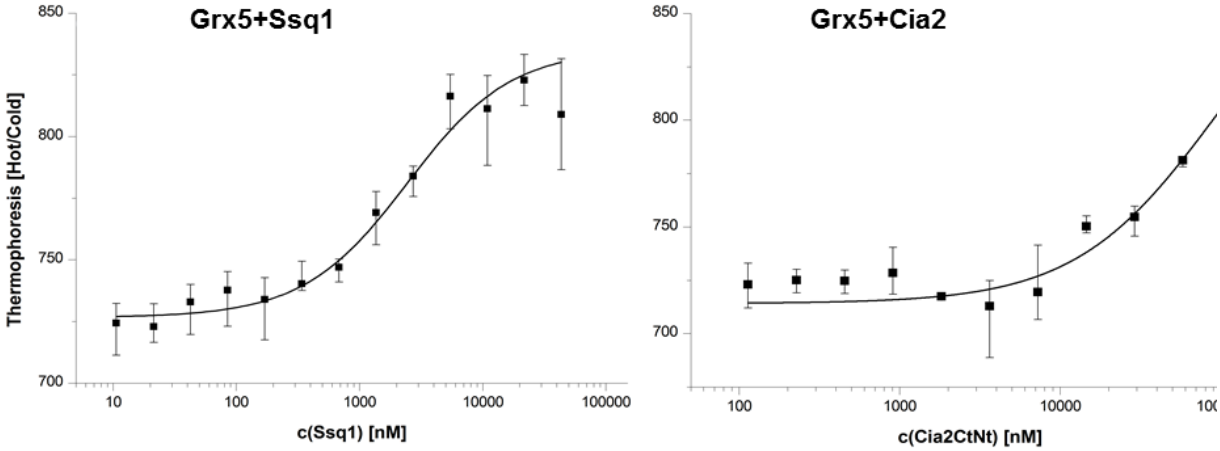
Grx5+Ssq1
Grx5+Cia2
Thermophoresis [Hot/Cold]
c(Ssq1) [nM]
c(Cia2CtNt) [nM]

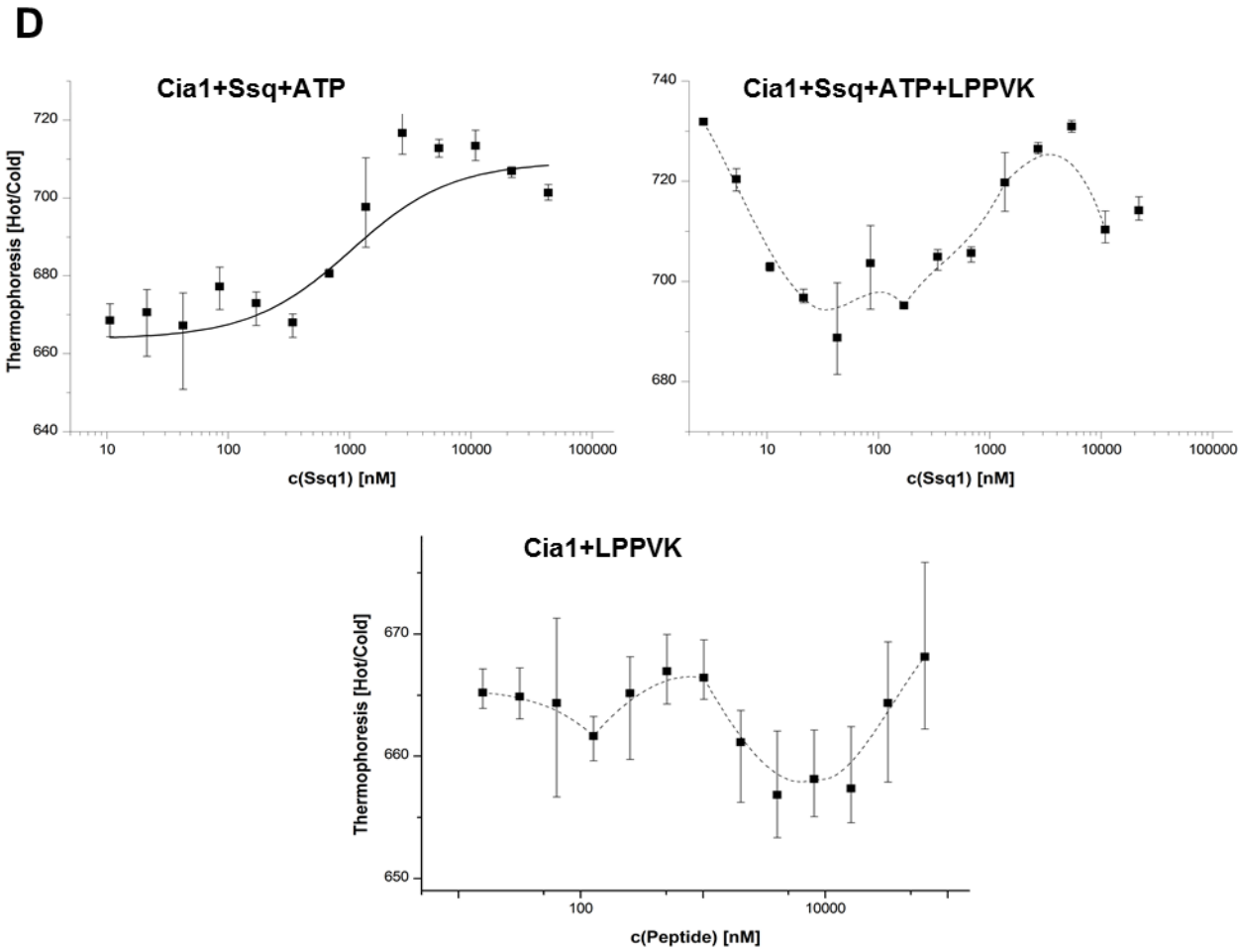

to stimulate the chaperone ATPase activity of Ssq1. Furthermore, the interaction between Grx5 and Ssq1 was strongest in the presence of ADP and the LPPVK-containing peptide (Fig. 3.13 A, lane 6), which was qualitatively reminiscent of the interaction characteristic seen *in vivo* (Fig. 3.10 B).

In order to directly demonstrate that the LPPVK-containing peptide binds to the substrate binding site of Ssq1 under *in vitro* conditions, the interaction of Ssq1 with Cia1, a cytosolic protein unlikely to engage with Ssq1 in Fe/S cluster assembly was analyzed (Lill *et al.*, 2012). Indeed, in the presence of ATP and Ssq1, changes in the thermophoretic behavior of fluorescent-labeled Cia1 were observed that indicate the binding of Cia1 to the Hsp70 chaperone (Fig. 3.13B, lane 1). Upon addition of 1,4-fold excess over Ssq1 of the LPPVK-containing peptide the interaction between Cia1 and Ssq1 disappeared (lane 2). Since Cia1 did not interact with the

peptide (lane 3), this observation indicates that Cia1 and the LPPVK-containing peptide bind to the same binding site on Ssq1, indicating that Cia1 is treated as a Hsp70 client protein of the Ssq1 chaperone. The completely opposite binding behavior of Cia1 (Fig. 3.13 B) and Grx5 (Fig. 3.13 A) in the presence of the LPPVK-containing peptide strongly indicates that Grx5 binds outside the substrate binding site of Ssq1.

The Grx5-Ssq1 interaction was further characterized by *in vitro* binding studies using protein A sepharose coupled with antibodies against Grx5. When Ssq1 was incubated alone with anti-Grx5 beads, only weak binding to the beads was observed (Fig. 3.14 A, lane 2). In the presence of Grx5, this binding was considerably increased, verifying the Grx5-Ssq1 interaction under *in vitro* conditions (Fig. 3.14 lane 3). When binding experiments were carried out in the presence of the LPPVK-containing peptide the Grx5-Ssq1 interaction remained unchanged, even in the presence of a 100-fold excess of the peptide (Fig. 3.14 A, lanes 4 - 5). Taken together, the data of these different interaction studies indicate that the Grx5 and Isu1 substrate binding sites on Ssq1 do not overlap.

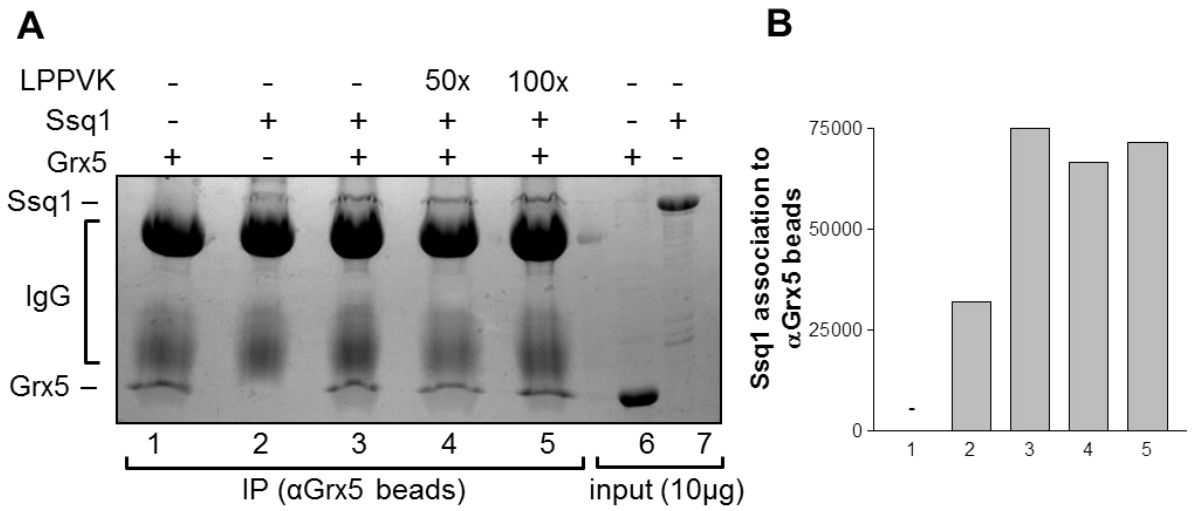

Figure 3.14 Grx5 interacts with Ssq1 *in vitro*. Purified Grx5 and/ or Ssq1 proteins (4 µM each) were incubated in buffer H containing 2 mM ADP and, where indicated, the Isu1 peptide (LPPVK) at 200 µM (50x) or 400 µM (100x) concentration. Immunoprecipitations were carried out with antibodies against Grx5. The presence of (co-)immunoprecipitated Grx5 and/ or Ssq1 was analyzed by SDS-PAGE and Coomassie staining (**A**), and Ssq1 was quantified by densitometry (**B).**

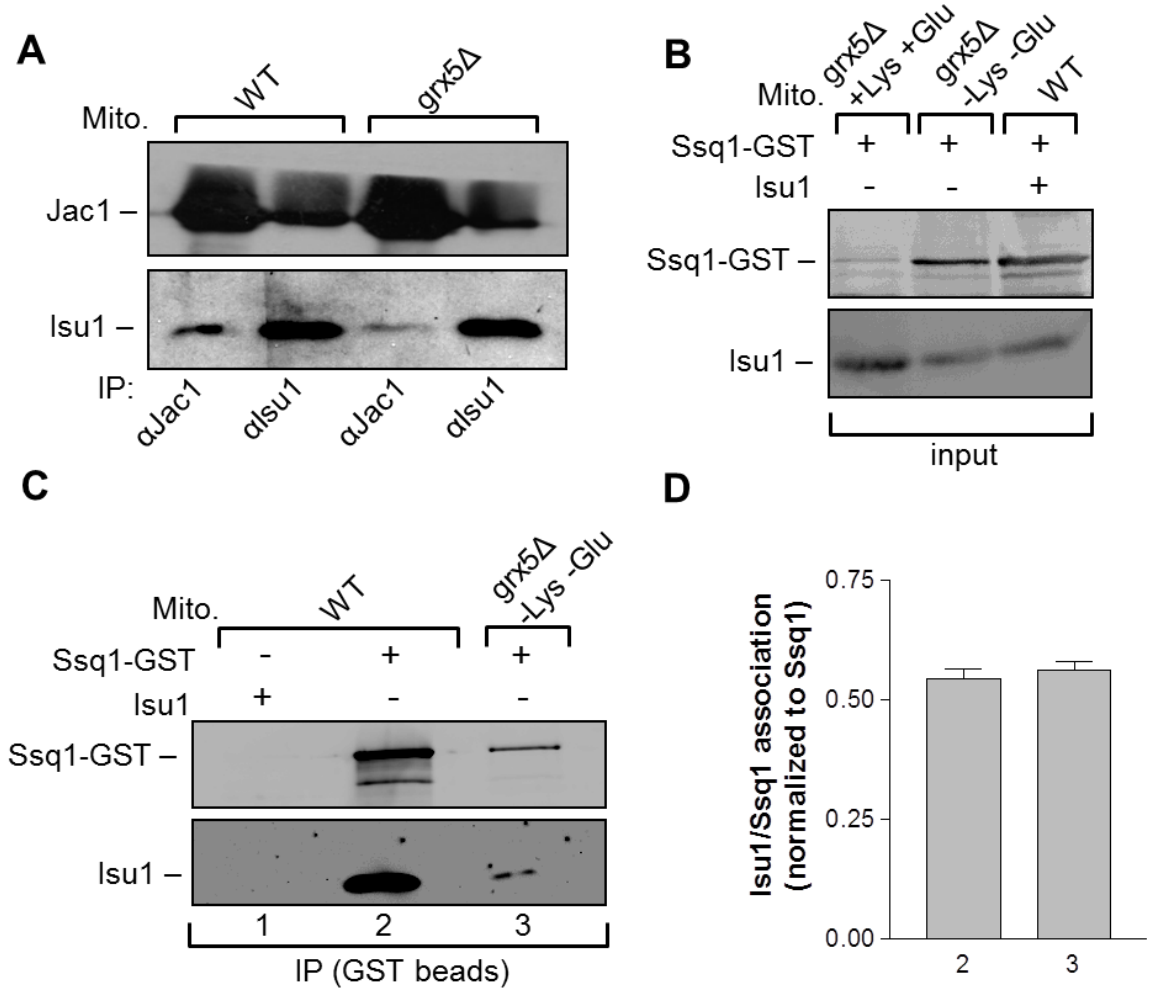

Figure 3.15 Grx5 is not required for complex formation of Isu1 with Jac1 and Ssq1. (A) Mitochondria from wild-type (WT) and *grx5Δ* cells overproducing Jac1 and Isu1 were lysed by detergent, and extracts were subjected to immunoprecipitation with antibodies against Jac1 or Isu1. The purified immunobeads were stained with antibodies against Jac1 and Isu1. **(B)** Levels of Ssq1-GST and Isu1 in WT and *grx5Δ* cells cultivated in minimal medium with or without lysine (Lys) and glutamate (Glu) supplementation. **(C)** Mitochondrial lysates from WT and *grx5*Δ cells overproducing Ssq1-GST or Isu1 were subjected to affinity purification with glutathione sepharose. Beads were analyzed for the presence of Ssq1-GST and Isu1 by immunostaining. **(D)** Association between Isu1 and Ssq1-GST in part C was quantified by densitometry and normalized to the amount of precipitated Ssq1-GST. (**B, C**)

Finally, it was investigated whether Grx5 modulated the known interactions of Isu1 with Jac1 and Ssq1. Purified mitochondria from wild-type and *grx5Δ* cells overproducing both Isu1 and Jac1 were subjected to co-immunoprecipitation experiments with specific anti-Isu1 and anti-Jac1 immunobeads. No significant difference in the binding of Isu1 to Jac1 was observed

between wild-type and *grx5Δ* cells (Fig. 3.15 A). For studying the Isu1-Ssq1 association, mitochondrial extracts from wild-type and *grx5Δ* cells overproducing Ssq1-GST were subjected to affinity purification with glutathione-sepharose. In both cells, Isu1 was bound to glutathione-sepharose (Fig. 3.15 B). However, in *grx5Δ* cells the overproduction of Ssq1-GST was inefficient and could be achieved only by omitting lysine and glutamate from the medium (Fig. 3.15 C). As a consequence, the amount of co-purified Isu1 during Ssq1-GST affinity purification was low. When the amount of co-purified Isu1 per Ssq1-GST was quantified by densitometry, no difference in relative binding was detectable between wild-type and *grx5Δ* cells (Fig. 3.15 D).

3.1.5 Grx5 transiently binds a [2Fe-2S] cluster and is involved in maturation of both [2Fe-2S] and [4Fe-4S] proteins.

Monothiol glutaredoxins have been shown *in vitro* to bind a labile, GSH-coordinated Fe/S co-factor that can be transferred to recipient apo-proteins, suggesting a role as an Fe/S scaffold or transfer protein (Bandyopadhyay *et al.*, 2008; Iwema *et al.*, 2009; Rouhier, 2010). When Grx5 from *S. cerevis*iae was synthesized and purified from *E. coli*, the protein carried a [2Fe-2S] cluster as judged by UV-Vis spectroscopy (Fig. 3.16). However, the physiological relevance of Fe/S cluster binding to mitochondrial Grx5 has not been confirmed by *in vivo* approaches. We therefore investigated this problem in yeast. Cells overproducing *S. cerevisiae* Grx5 were radiolabeled with ^{55}Fe, Grx5 was immunoprecipitated with specific antibodies and the amount of co-immunoprecipitated ^{55}Fe was quantified by scintillation counting. The amount of ^{55}Fe specifically co-immunoprecipitated with Grx5 was low, yet the signal was significantly above

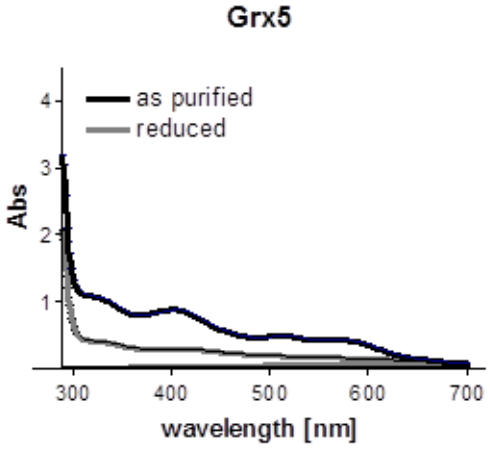

Figure 3.16 Grx5 binds an Fe/S cluster *in vitro*. UV-visible spectra of recombinant Grx5 from *S. cerevisiae* were recorded for 1 mg of protein, as purified or after reduction by 2 mM sodium dithionite. The inset shows a Coomassie staining of the purified protein analyzed by SDS-PAGE

background (Fig. 3.17 A). Previous studies showed that *Schizosaccharomyces pombe* cytosolic monothiol glutaredoxins Grx3 and Grx4 had largely increased Fe/S cluster binding compared to the *S. cerevisiae* Grx3/4 when expressed in budding yeast (Hoffmann *et al.*, 2011). To overcome problem of low Fe/S cluster binding to Grx5, it was analyzed whether Grx5 homologues from other species would bind Fe/S cluster more efficiently. A Myc-tagged Grx5 from *S. pombe* (SpGrx5) and a HA-tagged version of human Grx5 (HsGrx5) were used. Both foreign Grx5 proteins were targeted to mitochondria and were functional, as they rescued the growth defects of *grx5Δ* cells (Fig. 3.18). Remarkably, using the ^{55}Fe radiolabeling assay both SpGrx5 and HsGrx5 bound much higher levels of ^{55}Fe than *S. cerevisiae* Grx5 (Fig. 3.17 A). Subsequent ^{55}Fe binding studies were therefore performed with SpGrx5.

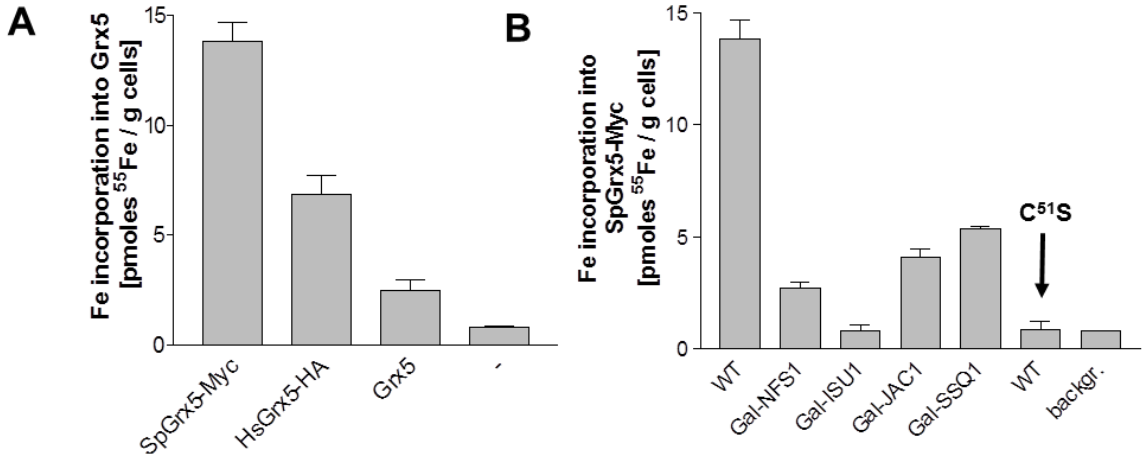

Figure 3.17 Grx5 binds a Fe/S cluster *in vivo*. (**A**) Wild-type cells overproducing Grx5 from *S. pombe* (SpGrx5-Myc), *H. sapiens* (HsGrx5-HA) or *S. cerevisiae* (Grx5), or harboring the empty vector p424-TDH3 (-) were grown over-night in iron-poor SD medium and then radiolabeled with 10 µCi ^{55}Fe for 2 h. The overproduced proteins were immunoprecipitated from cell extracts with antibodies against Myc (SpGrx5-Myc), HA (HsGrx5-HA) or Grx5 and the amount of co-precipitated ^{55}Fe was quantified by scintillation counting. (**B**) The indicated yeast strains overproducing SpGrx5-Myc and wild-type (WT) cells overproducing SpGrx5C^{51}S-Myc (Cys 51/ Ser) were grown in iron-poor SD medium. ^{55}Fe binding to the SpGrx5-Myc proteins was determined by radiolabeling and immunoprecipitation as described above. The indicated Gal-ISC strains were depleted to critical levels. Error bars indicate the SEM (n > 4).

First, it was determined whether ^{55}Fe is coordinated by the active-site cysteine residue of SpGrx5. When this amino acid was exchanged to serine (mutant C^{51}S), ^{55}Fe binding to SpGrx5

was completely abolished indicating the specificity of ^{55}Fe binding (Fig. 3.17 B). To analyze whether the bound iron is part of a Fe/S cluster, we determined the dependence of ^{55}Fe binding on components of the mitochondrial ISC assembly machinery such as the cysteine desulfurase Nfs1, the scaffold protein Isu1, and the chaperones Jac1 and Ssq1. The ISC proteins were depleted to critical levels by cultivation of the corresponding GAL-promoter regulated strains in

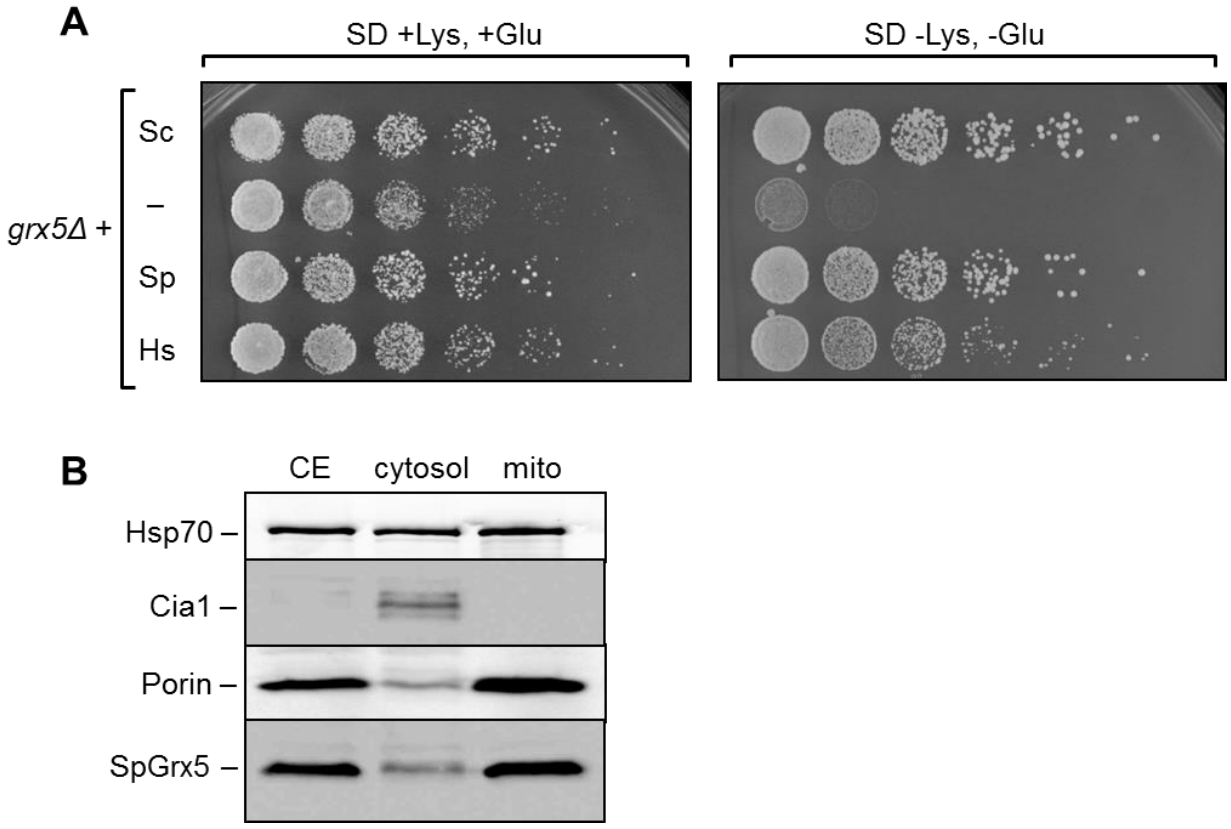

Figure 3.18 *S. pombe* Grx5 targeted to mitochondria of *S. cerevisiae* rescues the growth defect of *grx5Δ* cells. (**A**) 10-fold serial dilutions of over-night cultures of *grx5Δ* cells overproducing *S. cerevisiae* (Sc), *S. pombe* (Sp) or *H. sapiens* (Hs) Grx5 were cultivated on SD plates without uracil in presence or absence of both lysine (Lys) and glutamate (Glu) at 30ºC for two days. *grx5Δ* cells carrying the empty pRS424 vector (−) were used as a control. (**B**) Whole cell extracts (CE), cytosol or isolated mitochondria (mito) from *grx5Δ* cells overproducing SpGrx5 grown in SD medium were subjected to SDS-PAGE. The indicated proteins were immunostained with specific antibodies: Hsp70, present in mitochondria, cytosol and ER; Cia1, a member of the CIA machinery; porin, mitochondrial outer membrane pore.

presence of glucose, and ^{55}Fe binding was measured by the radiolabeling-immunoprecipitation assay described above. Upon depletion of the four ISC proteins the amounts of ^{55}Fe co-immunoprecipitated with SpGrx5 were severely decreased (Fig. 3.17 B). These results suggest that Grx5 binds a Fe/S cluster under physiological conditions. The dependence on the active-site cysteine supports the physiological relevance of the [2Fe-2S] cluster assembled on Grx5 under *in*

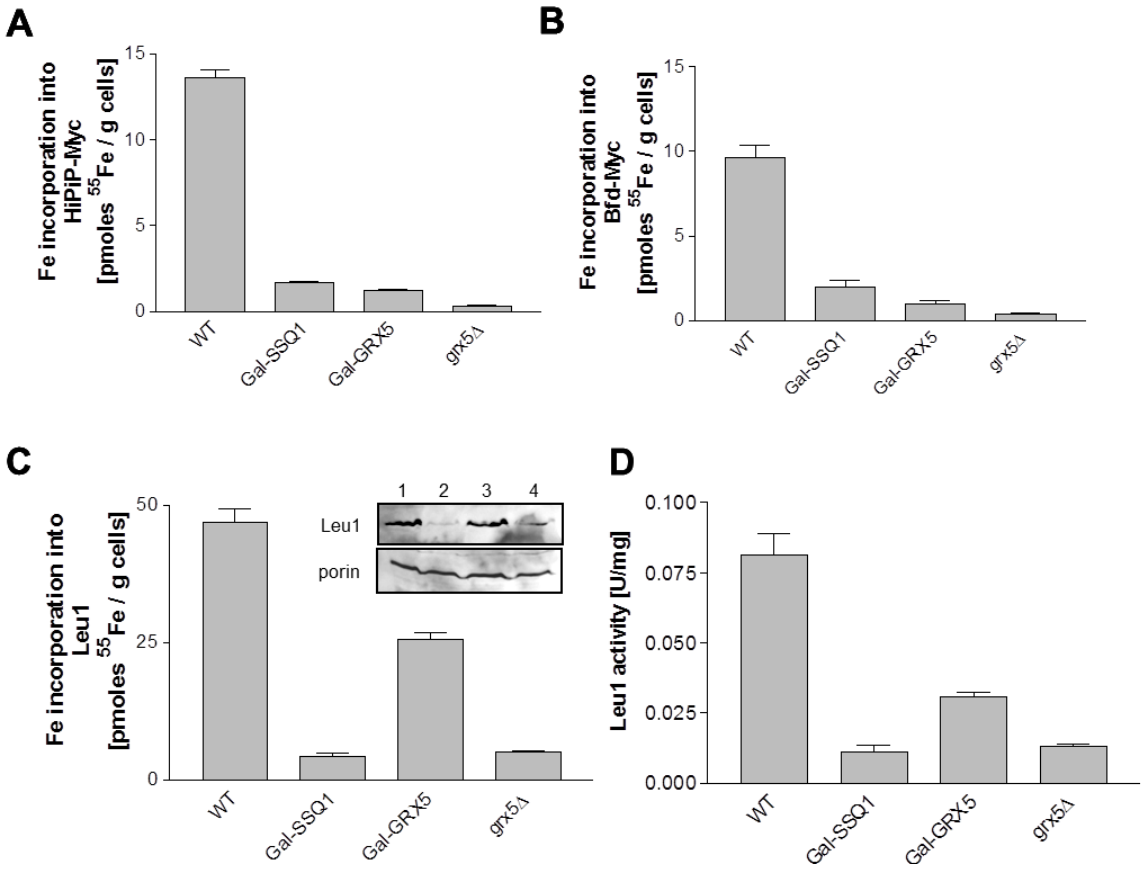

Figure 3.19 Grx5 is required for both mitochondrial and cytosolic Fe/S protein maturation. Wild-type (WT), Gal-*SSQ1*, Gal-*GRX5* and *grx5Δ* cells (grown on SD medium, for Gal-ISC strains 64h depletion prior to experiments) overproducing mitochondria-targeted (**A**) [4Fe-4S] HiPiP or (**B**) [2Fe-2S] Bfd bacterial proteins were grown in iron-poor SD medium over-night and then radiolabeled with 10 µCi ^{55}Fe for 2 h. Protein-bound radioactivity was determined by immunoprecipitation as described in Fig. 3.17. (**C**) ^{55}Fe binding to endogenous Leu1 was determined by radiolabeling and immunoprecipitation as described in Fig. 3.17. The inset shows Leu1 protein levels in analyzed samples. (**D**) Leu1 enzyme activities were determined in whole cell extracts from the indicated strains cultivated in YPD. Gal-strains were depleted to critical levels by cultivation in SD medium for 64 h prior to experiments Error bars indicate the SEM (n > 4).

vitro conditions (Picciocchi *et al.*, 2007) (Fig. 3.16). Importantly, the fact that ^{55}Fe binding to Grx5 was dependent on Isu1 made a scaffold function of Grx5 in the *de novo* synthesis of Fe/S clusters unlikely. Rather, the findings indicated that Grx5 receives its Fe/S cluster from Isu1 and hence might function subsequently to Isu1. This scenario fits perfectly to the previous *in vivo* observation that depletion of Grx5 leads to the accumulation of Fe/S clusters on Isu1 (Muhlenhoff *et al.*, 2003a). Taken together, these data suggest a role of Grx5 in mediating the transfer of Fe/S clusters from Isu1 to target apo-proteins, possibly by acting as a Fe/S cluster transfer protein as recently proposed (Rouhier *et al.*, 2010).

Next fascinating question was whether Grx5 is required for the maturation of both [2Fe-2S] and [4Fe-4S] cluster-containing proteins or whether its function is specific for one type of Fe/S cluster as this has been found, e.g., for the Isa1-Isa2 or Iba57 proteins which specifically assist the maturation of mitochondrial [4Fe-4S] proteins but are dispensable for [2Fe-2S] protein maturation (Gelling *et al.*, 2008; Muhlenhoff *et al.*, 2011; Sheftel *et al.*, 2012). The previously observed genetic interaction of *GRX5* and *ISA2* and the fact that *grx5Δ* cells display a glutamate auxotrophy, similar to ISA- and IBA57-defective cells, may suggest a specificity for [4Fe-4S] proteins (Rodriguez-Manzaneque *et al.*, 2002; Kim *et al.*, 2010). In order to clarify the Fe/S cluster specificity of Grx5, we used the ^{55}Fe radiolabeling assay to study the maturation of two bacterial reporter Fe/S proteins, the HiPiP ferredoxin which harbors a [4Fe-4S] cluster, and the small [2Fe-2S] protein Bfd from *E. coli* (Garg *et al.*, 1996; Muhlenhoff *et al.*, 2011). For both proteins, the amount of ^{55}Fe binding declined to background levels in *grx5Δ* cells and strongly decreased in Grx5-depleted Gal-*GRX5* cells to levels exceeding those found in cells depleted of Ssq1 (Fig. 3.19 A and B). This observation clearly distinguishes Grx5 from the Isa and Iba57 proteins which do not affect [2Fe-2S] protein maturation (Gelling *et al.*, 2008; Muhlenhoff *et al.*, 2011; Sheftel *et al.*, 2012). In a similar fashion, the maturation and the enzyme activity of the cytosolic Fe/S protein Leu1 were strongly diminished in *grx5Δ* and depleted Gal-*GRX5* cells, similar to cells depleted of Ssq1 (Fig. 3.19 C and D). Thus, Grx5 is also required for cytosolic Fe/S protein biogenesis, unlike the Isa and Iba57 proteins (Gelling *et al.*, 2008; Muhlenhoff *et al.*, 2011). Consistent with this observation, depletion of yeast Grx5 showed a strong activation of the iron regulon (Gelling *et al.*, 2008). This phenotype is observed in cells with defects in core members of the mitochondrial ISC assembly machinery, but not in cells lacking late-acting ISC proteins such as the Isa or Iba57 proteins. Taken together, these data strongly suggest that Grx5

belongs to the core part of the mitochondrial ISC assembly system that is involved in the maturation of all cellular Fe/S proteins and participates in cellular iron regulation.

3.1.6 The human mitochondrial Grx2 does not rescue *grx5Δ* cells.

The simultaneous deletion of *GRX5* and *GRX2* in yeast is synthetic lethal suggesting some overlapping functions between those glutaredoxins (Rodriguez-Manzaneque *et al.*, 1999). However, when overexpressed in mitochondria Grx2 failed to rescue the *grx5Δ* phenotype (Molina *et al.*, 2004), refuting this simple idea. Yeast Grx2 is a classical class I dithol glutaredoxin with CPYC motif in the active-site that is involved in oxidative stress protection. There is some indication that Grx2 might be expressed in both the cytosol and the mitochondria (Pedrajas *et al.*, 2002; Porras *et al.*, 2006). Its possible involvement in regulating iron metabolism has been suggested (McDonagh *et al.*, 2011), but the functional relevance of these findings remains not clear. More is known about the human dithiol glutaredoxin GLRX2 (with CSYC motif in the active site; protein further referred to as HsGrx2) for which a dual cytosolic and mitochondrial localization has been shown (Gladyshev *et al.*, 2001; Lundberg *et al.*, 2001). The mitochondrial version of HsGrx2 was shown to be crucial in protection against hydrogen peroxide-induced apoptosis and was able to physically interact with complex I and protect it from the damage under oxidative stress conditions (Wu *et al.*, 2011). Previous studies demonstrated that HsGrx2, like many other glutaredoxins, is able to carry an Fe/S cluster *in vitro* (Lillig *et al.*, 2005; Johansson *et al.*, 2007) and this result was confirmed by *in vivo* experiments in mammalian cells using the split Venus protein approach (Hoff *et al.*, 2009). It was interesting to analyze whether mitochondrial HsGrx2, similarly to Grx5, can also have a role in Fe/S cluster biogenesis, as proposed by Qi and Cowan (Qi and Cowan, 2011). First, it was determined if HsGrx2 is able to carry a Fe/S cluster *in vivo* in the yeast cells. To this end, a vector containing a C-terminal Myc-tagged version of HsGrx2 was constructed and the mitochondrial localization of the protein was confirmed by Western blotting (Fig 3.20 D). Wild-type, Gal-*NFS1* and *isa1/2Δ* cells overproducing HsGrx2 were radiolabeled with ^{55}Fe. HsGrx2 was immunoprecipitated with specific antibodies and the amount of co-immunoprecipitated ^{55}Fe was quantified by scintillation counting. The amount of ^{55}Fe specifically co-immunoprecipitated with HsGrx2 in the WT cells

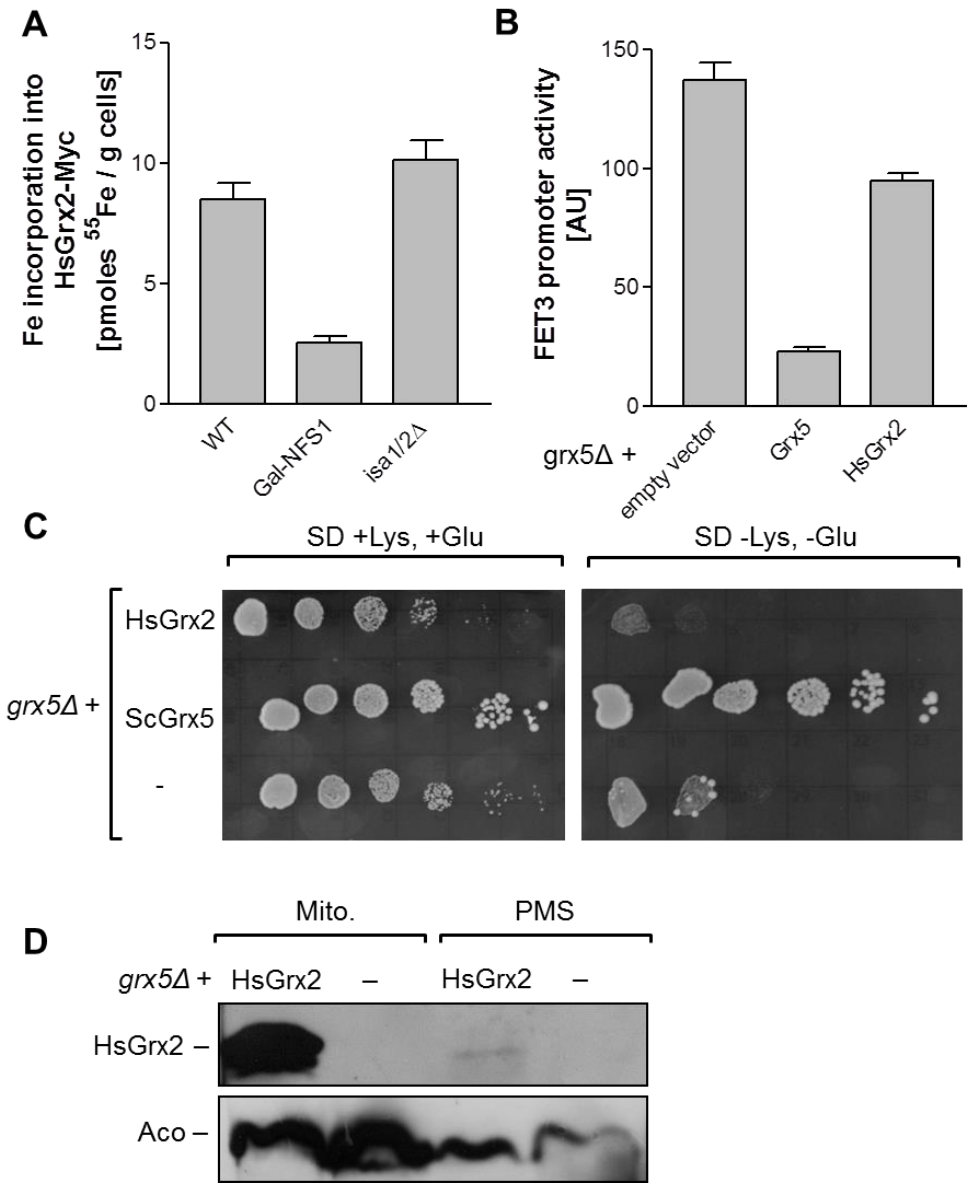

Figure 3.20 Mitochondria targeted HsGrx2 binds a Fe/S cluster *in vivo* but does not rescue *grx5Δ* cells. (**A**) Wild-type, *isa1/2Δ* or Gal-*NFS1* cells overproducing Myc-tagged version of HsGrx2 were grown over-night in iron-poor SD medium and then radiolabeled with 10 µCi ^{55}Fe for 2 h. The overproduced protein was immunoprecipitated from cell extracts with antibodies against Myc and the amount of co-precipitated ^{55}Fe was quantified by scintillation counting. Gal-*NFS1* strain was depleted to critical levels prior to experiments. (**B**) The *grx5Δ* cells carrying the overproducing *Sc*Grx5 or HsGrx2, or empty pRS424 vector, harboring reporter plasmid pFET3-GFP were cultivated in iron-replete conditions. *FET3* promoter activities were determined by measuring the GFP-specific fluorescence emission of logarithmically grown cells. (**A, B**) Error bars indicate the SEM (n > 4). (**C**) Tenfold serial dilutions of over-night cultures of *grx5Δ* cells overproducing *S. cerevisiae* (Sc) Grx5 or *H. sapiens* (Hs) Grx2 were cultivated on SD plates without uracil in presence or absence of both lysine (Lys) and glutamate (Glu) at 30ºC for two days. *grx5Δ*

cells carrying the empty pRS424 vector (−) were used as a control. (**D**) Isolated mitochondria (Mito) or post mitochondrial supernatant (PMS) from *grx5Δ* cells overproducing HsGrx2 grown in SD medium were subjected to SDS-PAGE. The indicated proteins were immunostained with specific antibodies against mitochondrial protein aconitase and against the Myc tag of HsGrx2.

was significantly above the background (Fig. 3.20 A). To analyze whether the bound iron is part of a Fe/S cluster, the dependence of ^{55}Fe binding on components of the mitochondrial ISC assembly machinery such as the cysteine desulfurase Nfs1 and the Isa1/2 proteins was determined. The Nfs1 protein was depleted to critical level by cultivation under depletion conditions in minimal medium containing glucose, and ^{55}Fe binding was measured by the radiolabeling-immunoprecipitation assay described above. Upon depletion of Nfs1 protein, the amount of ^{55}Fe co-immunoprecipitated with HsGrx2 was severely decreased (Fig. 3.20 A). This was not the case in cells lacking Isa1/2 proteins (Fig. 3.20 A), which were shown to be specifically involved in [4Fe-4S] cluster biogenesis in mitochondria (Muhlenhoff *et al.*, 2011). These results indicated that most likely HsGrx2, similarly to Grx5 protein, binds a [2Fe-2S] cluster *in vivo* when expressed in *S. cerevisiae*. Even though both HsGrx2 and Grx5 are able to carry the Fe/S cluster, HsGrx2 failed to rescue the growth on medium lacking lysine and glutamate (Fig. 3.20 C), and to decrease the activation of iron regulon (represented by the *FET3* promoter activity) (Fig 3.20 B) when overexpressed in *grx5Δ* cells.

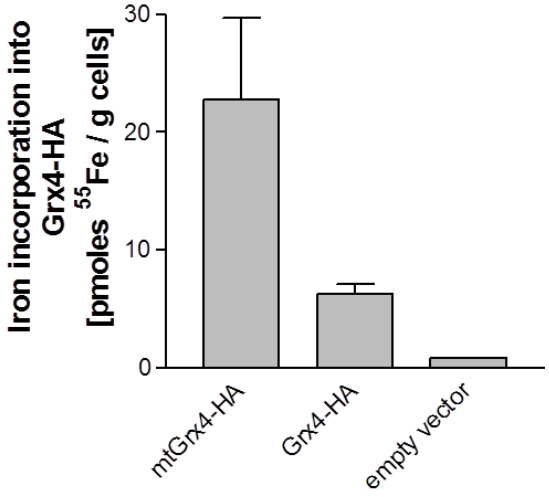

Figure 3.21 Grx4 binds a Fe/S cluster *in vivo* both in the cytosol and in mitochondria. Wild-type cells overproducing the cytosolic (Grx4-HA) and mitochondrial (mtGrx4-HA) HA-tagged versions of Grx4 or empty vector p424-TDH3 (-) were grown over-night in iron-poor SD medium and then radiolabeled with 10 µCi ^{55}Fe for 2 h. The overproduced proteins were immunoprecipitated from cell extracts with antibodies against HA and the amount of co-precipitated ^{55}Fe was quantified by scintillation counting. Error bars indicate the SEM (n > 4).

Yeast cytosolic CGFS active-site glutaredoxin Grx4, similary to HsGrx2, also was able to bind the iron when expressed in mitochondria, even with higher efficiency compared to expression in its native environment, the cytosol (Fig 3.21). In contrast to HsGrx2, Grx4 was able to partially rescue *GRX5* deletion (Molina *et al.*, 2004), similarly to many other CGFS active-site glutaredoxins from both prokaryotic and eukaryotic species (Molina-Navarro *et al.*, 2006; Bandyopadhyay *et al.*, 2008). It seems that only monothiol glutaredoxins can functionally replace Grx5 in the ISC assembly machinery. To test this hypothesis mutagenesis of Grx5 active-site into CSYC of HsGrx2 and subsequent analysis of Fe/S cluster binding and *grx5Δ* complementation would be necessary. If the function of the protein is indeed determined by the active-site thiols, then mutated version of Grx5 should not be able to rescue *GRX5* deletion.

3.2 Role of BolA-like proteins in mitochondrial Fe/S cluster assembly.

Until recently, little was known about role of BolA-like proteins in the mitochondria. After BolA-like proteins were associated with monothiol glutaredoxins, by both bioinformatics (Huynen *et al.*, 2005) and experimental approaches (Ito *et al.*, 2000; Bhan *et al.*, 2002), the potential involvement of yeast mitochondrial BolA-like proteins Yal044W and Aim1 in Fe/S clusters biogenesis was investigated. Yeast cells deleted for Aim1 (*aim1Δ*) display an elevated frequency of mitochondrial genome loss (Hess *et al.*, 2009). However, in our hands deletion of both *YAL044W* and *AIM1* showed virtually no phenotype when iron regulon activation and activities of aconitase were tested. The interest in BolA-like proteins increased when Cameron and coworkers described mitochondrial BOLA3-associated fatal disease with multiple respiratory chain and 2-oxoacid dehydrogenase (Cameron *et al.*, 2011). The patient studies inspired me to revisit the mitochondrial BolA-like proteins in *S. cerevisiae*. Single deletions of *YAL044W* and *AIM1* were analyzed in the BY4742 strain background and the double deletion in the W303A background. As observed previously, deletions of *YAL044W* and/ or *AIM1* did not affect aconitase activity (Fig. 3.22 A). Deletion cells grew normally on medium containing non-fermentable carbon source (data not shown) and did not show an activation of iron regulon (Fig. 3.22 B). The latter effect is the hallmark of all cells with defects in the core ISC assembly machinery, excluding that mitochondrial BolA-like proteins are members of the core ISC system. Since human BOLA3 was shown to be essential for maturation of lipoate containing 2-oxoacid dehydrogenases, the activities of PDH and KGDH were tested. Both enzymes showed a significant drop in the activities in *aim1Δ* but not in *yal044WΔ* cells (Fig. 3.22 C and D). Additionally, a 50 % drop in SDH activity was observed for *aim1Δ* and a 30 % drop for *yal044WΔ* cells (Fig. 3.22 E). In order to check, if loss of the enzyme activities was specific, Aim1 or Yal044W were reintroduced into the deletion strains by overproducing vectors. Both proteins were able to efficiently rescue the drop in SDH, PDH and KGDH activities to wild-type or even higher levels (Fig. 3.22 C, D and E). Additionally, Aim1 overexpression rescued slight drop in SDH activity observed in *yal044WΔ* cells. This is most likely due to the similarity of the two proteins.

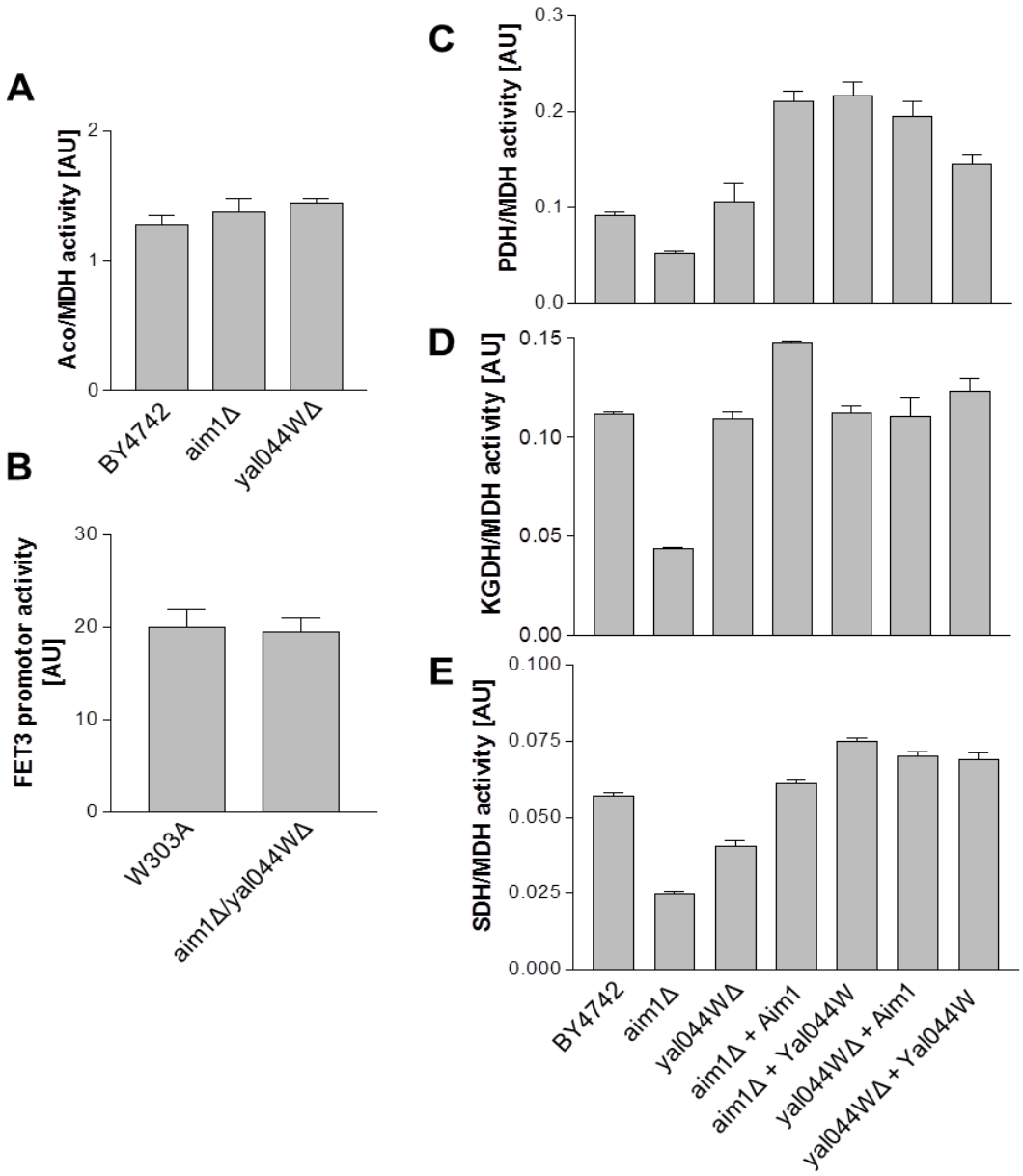

Figure 3.22 Deletion of *AIM1* affects activities of PDH, KGDH and SDH and can be rescued by overexpression of both Aim1 and Yal044W. (**A, B, C and E**) BY4742, *aim1Δ* or *yal044WΔ* cells were transformed with empty pRS416 or vector overexpressing Aim1 or Yal044W. Cells were grown in SD medium without uracil and used for mitochondria preparation. Mitochondrial extracts were assayed for activities of (**A**) Aconitase (Aco), (**C**) pyruvate dehydrogenase (PDH), (**D**) α-ketoglutarate dehydrogenase (KGDH) and (**E**) succinate dehydrogenase (SDH) and normalized to malate dehydrogenase (MDH) activites. (**B**) The WT and *aim1Δ/yal044WΔ* cells harboring reporter plasmid pFET3-GFP were cultivated in iron-replete conditions. *FET3* promoter activities were determined by measuring the GFP-specific fluorescence emission of logarithmically grown cells. Error bars indicate the SEM (n > 4).

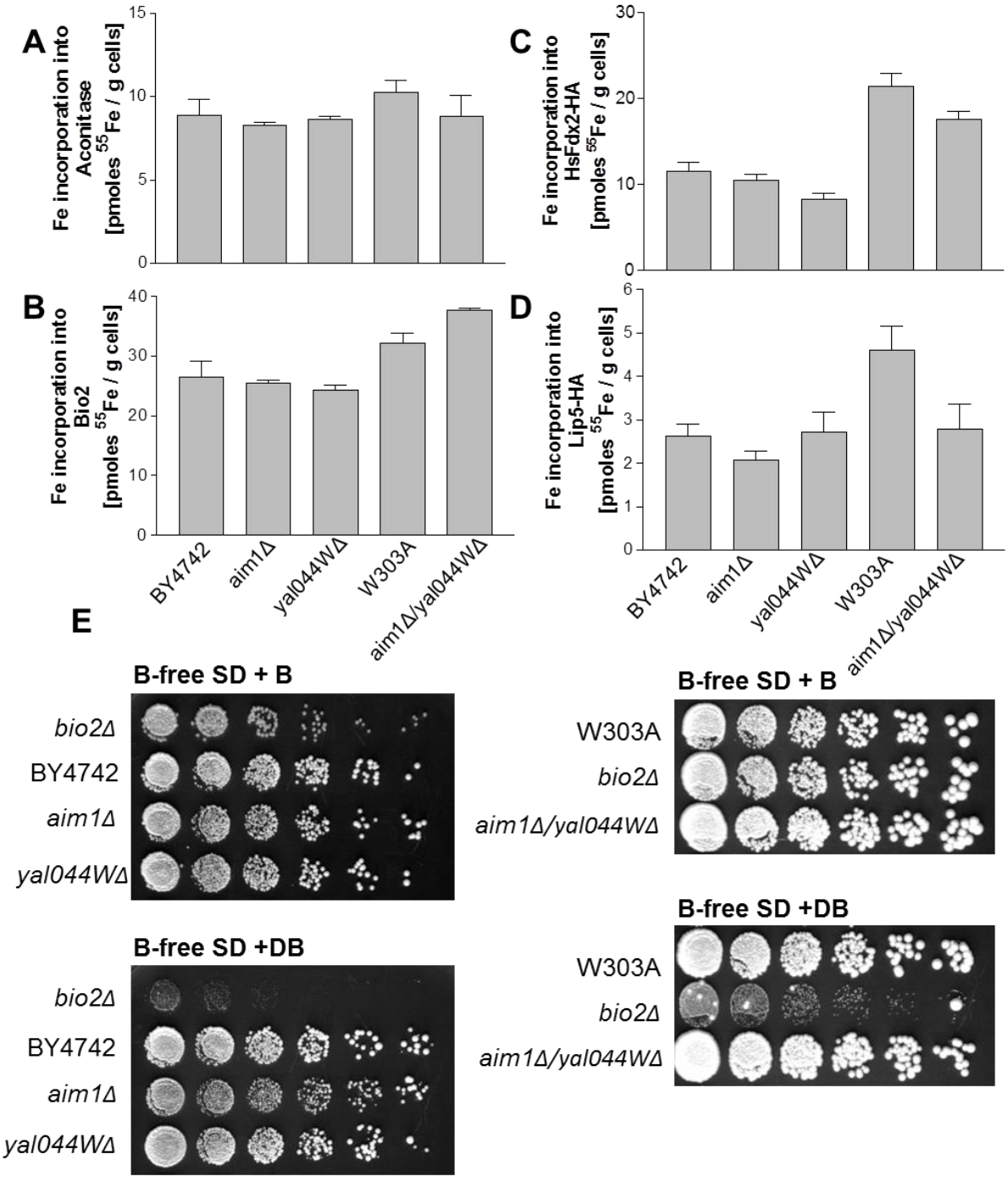

Figure 3.23 Analysis of iron binding to potential target proteins of Aim1 and Yal044W. Wild-type BY4742 and W303A cells and *aim1Δ*, *yal044WΔ* and *aim1Δ/yal044WΔ* cells were grown over-night in iron-poor SD medium and then were radiolabeled with 10 µCi ^{55}Fe for 2 h. (**A**) Endogenously expressed aconitase (Aco) or (**B**) biotin synthase (Bio2) and mitochondria targeted (**C**) human ferredoxin (HsFdx-HA) or (**D**) lipoic acid synthase (Lip5-HA) were

immunoprecipitated from cell extracts with specific antibodies against aconitase, Bio2 or HA-tag (in case of HsFdx-HA and Lip5-HA) and the amount of co-precipitated ^{55}Fe was quantified by scintillation counting. Error bars indicate the SEM (n > 4). (**E**) Serial dilutions of the *bio2Δ*, BY4742, *aim1Δ* and *yal044WΔ* cells were spotted on biotin-free minimal medium (B-free SD) containing 0,2 µg liter^{-1} of either biotin (indicated as B) or desthiobiotin (DB), and growth was recorded after 3 days at 30°C.

To further characterize involvement of BolA-like proteins in Fe/S protein maturation, several target proteins were tested with the ^{55}Fe radiolabeling and immunoprecipitation assay. There was no effect of deletions of *YAL044W* and/ or *AIM1* on ^{55}Fe binding to aconitase (Fig. 3.23 A), consistent with enzyme activity data. Likewise, radical SAM Fe/S protein Bio2 (containing [2Fe-2S] and [4Fe-4S] clusters) (Fig. 3.23 B) was similar to wild-type cells. The latter result is consistent with the normal growth of *AIM1* and *YAL044W* deletion strains on biotin-free medium (Fig. 3.23 E). Similarly to Bio2 and aconitase, hardly any change in ^{55}Fe binding was observed for overproduced [2Fe-2S] human ferredoxin HsFdx (Fig. 3.23 C) indicating that BolA-like proteins are not involved in the maturation of [2Fe-2S] proteins. In the case of overproduced, lipoate synthase Lip5 containing two [4Fe-4S] clusters, only a slight decrease in ^{55}Fe binding was seen for *aim1Δ* cells. The effect was more pronounced (40 %) when both mitochondrial BolA-like proteins were deleted (Fig. 3.23 D). Loss of Lip5 activity without decrease in ^{55}Fe binding to the protein resembles situation observed for Lip5 in cells lacking Isa1/2 proteins (Muhlenhoff *et al.*, 2007). It is likely, that similarly to Isa proteins, Aim1 plays a role in catalytic activation rather than *de novo* synthesis of Lip5 Fe/S clusters. Taken together, these data indicate that Aim1 is a specialized factor facilitating the maturation of Sdh2, Lip5 and indirectly also lipoic acid-containing proteins. The phenotype prevailing in yeast *aim1Δ* cells is in agreement with the observations made for the human patients with BOLA3 deficiency (Cameron *et al.*, 2011; Haack *et al.*, 2013). Precise role of Yal044W could not be determined within this work, although the fact that overexpression of Yal044W could rescue *aim1Δ* cells suggests that Aim1 and Yal044W might have some overlapping functions.

3.2.1 Do mitochondrial BolA-like proteins interact with monothiol glutaredoxin Grx5?

BolA-like proteins have been shown to have a genetic association with the monothiol glutaredoxins and to physically interact with them (Ito *et al.*, 2000; Bhan *et al.*, 2002). As example, interaction between yeast BolA-like protein Fra2 and Grx3/4 is conserved throughout the evolution and found also between their human homologs BOLA2 and GLRX3. It is likely that

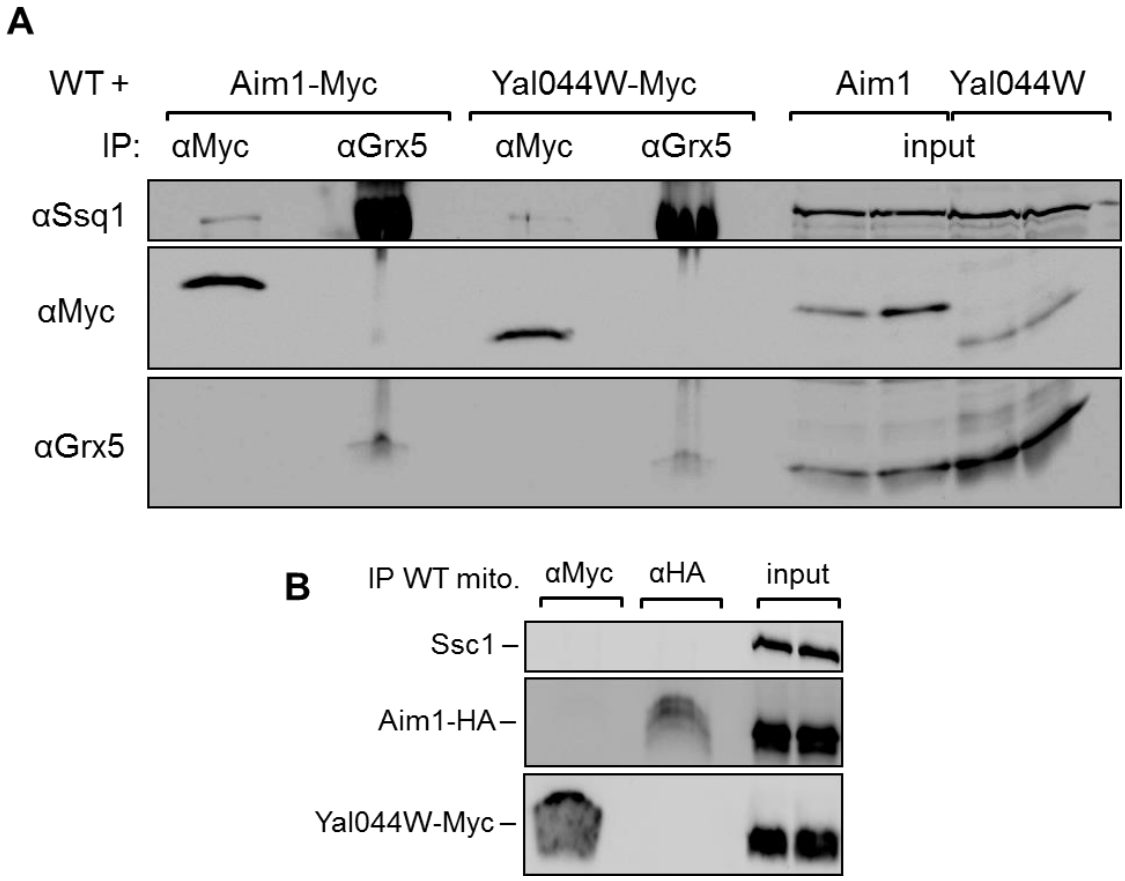

Figure 3.24 Mitochondrial BolA-like proteins do not interact with Grx5 and with each other *in vivo*. (**A**) Mitochondria from wild-type yeast cells overproducing Grx5 and either Aim1-Myc or Yal044W-Myc proteins were lysed by detergent (0,5 % Triton X-100) in buffer A, and subjected to affinity purification with antibodies against Myc-tag or against Grx5 bound to Protein A sepharose as indicated. The purified proteins Grx5, Aim1 and Yal044W were analyzed by SDS-PAGE and immunostaining by αGrx5 and αMyc antibodies. (**B**) Mitochondria from wild-type yeast cells overproducing Aim1-HA and Yal044W-Myc proteins were lysed by detergent (0,5 % Triton X-100) in buffer A, and subjected to affinity purification with antibodies against Myc-tag or against HA-tag bound to Protein A sepharose as indicated. The purified proteins Aim1 and Yal044W were analyzed by SDS-PAGE and immunostaining by αHA and αMyc antibodies.

the interaction between Grx5 and mitochondrial BolA-like proteins is also conserved throughout evolution, especially the interaction between mitochondrial human proteins BOLA1 and GLRX5 was recently reported (Willems *et al.*, 2013). Moreover, Cameron et al proposed that BOLA3 cooperates with GLRX5 to assist Fe/S cluster transfer to the target proteins (Cameron *et al.*, 2011). *In vitro* both Aim1 and Yal044W can form a heterodimeric complex with Grx5 bridged by [2Fe-2S] cluster (Bo Zhang, personal communication), similarly to Fra2 and Grx4. To check if those proteins can also interact with each other *in vivo*, vectors expressing Myc-tagged versions of Aim1 or Yal044W were introduced into the WT cells together with vector expressing Grx5 protein. Mitochondria were purified, lysed in detergent-containing buffer, and extracts were subjected to the immunoprecipitation with specific antibodies against Grx5 or Myc-tag (Fig. 3.24 A) (Gerber *et al.*, 2003). In all cases, Grx5 and BolA-like proteins were isolated by specific antibody and identified by immunostaining. No interaction between the proteins was detectable

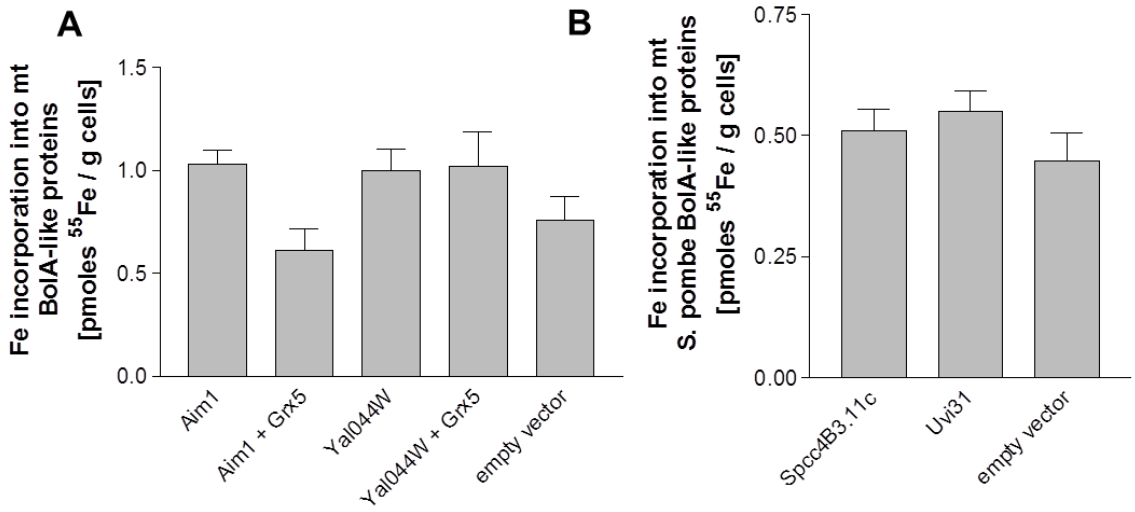

Figure 3.25 Analysis of iron binding by the mitochondrial BolA-like proteins. (**A**) Wild-type (W303A) cells were transformed with vectors overexpressing Grx5 and/ or mitochondria-targeted, Myc-tagged versions of Aim1 and Yal044W, as indicated. Obtained cells were grown over-night in iron-poor SD medium and then radiolabeled with 10 µCi ^{55}Fe for 2 h. The overproduced BolA-like proteins were immunoprecipitated from the cell extracts with the antibodies against Myc and the amount of co-precipitated ^{55}Fe was quantified by scintillation counting. (**B**) Wild-type (W303A) cells were transformed with vectors overexpressing mitochondria-targeted, Myc-tagged versions of *S. pombe* Cc4B3.11c and Uvi31. Cells were treated as described above and the proteins were immunoprecipitated from the cell extracts with antibodies against Myc. The amount of co-precipitated ^{55}Fe was quantified by scintillation counting. Error bars indicate the SEM (n > 4).

(Fig. 3.24 A). It seems that either the interaction is not taking place in yeast mitochondria or it is too transient to be visualized by co-immunoprecipitation, a non-equilibrium method. Perhaps more sensitive methods or the use of cross-linking agents is needed to verify this complex formation. Additionally, the potential interaction of mitochondrial BolA-like proteins with each other was tested. To this end, wild-type yeast cells were transformed with vectors containing a Myc-tagged version of Yal044W protein and a HA-tagged version of Aim1. Mitochondria were purified, lysed in detergent-containing buffer, and extracts were subjected to immunoprecipitation with specific antibodies against Myc- or HA-tag (Fig. 3.24 B) (Gerber *et al.*, 2003). Proteins were isolated by the specific antibodies, but no interaction between them was detectable as visualized by immunostaining (Fig. 3.24 B).

Studies performed on *E. coli*, yeast and human BolA-like proteins suggested a link to the cellular iron metabolism (Kumanovics *et al.*, 2008; Cameron *et al.*, 2011; Yeung *et al.*, 2011). Additionally, purified *E. coli* BolA, yeast Fra2 and human BOLA2 were shown to form a heterodimeric, Fe/S cluster-containing complex with monothiol glutaredoxins GrxD, Grx3/4 and GLRX3, respectively (Li and Outten, 2012). As Fe/S cluster binding by Fra2 was recently validated by *in vivo* ^{55}Fe radiolabelling and immunoprecipitation (Ulrich Mühlenhoff unpublished data), the assay was used to test if Fe/S cluster binding can be observed for Aim1 or Yal044W *in vivo*. Myc-tagged versions of both mitochondrial BolA-like proteins showed no ^{55}Fe binding, also when Grx5 was additionally overexpressed in the cells to allow possible complex formation (Fig 3.25 A). Since previously an increase in ^{55}Fe binding was observed when Grx3/4 or Grx5 from other species were used ((Hoffmann *et al.*, 2011), and see results chapter 3.1.5), constructs containing Myc-tagged versions of *S. pombe* homologes of Aim1 (Spcc4B3.11c) and Yal044W (Uvi31) were introduced into WT cells and analyzed by ^{55}Fe radiolabelling and immunoprecipitation. Also in this case, no ^{55}Fe binding was seen (Fig. 3.25 B), possibly because the native binding partner, SpGrx5, was missing. It would be interesting to repeat ^{55}Fe radiolabelling and immunoprecipitation experiments in conditions where, additionally to SpCc4B3.11c or Uvi31, also SpGrx5 is present.

3.3 Role of Nfu1 in mitochondrial iron-sulfur protein biogenesis.

Evidence that the Nfu-like proteins are involved in Fe/S cluster biosynthesis came from a synthetic lethal screen in yeast, where the deletion of *NFU1* mutant was found to be synthetic lethal with that of *SSQ1* (Schilke et al., 1999). In this study, Nfu1 was shown to be a nonessential, mitochondrial protein whose depletion does not cause any severe defects in cell metabolism. Only when *NFU1* deletion was combined with the one of *ISU1*, cells developed problems typical for cells deficient in Fe/S cluster biosynthesis (Schilke et al., 1999). Based on the weak effects of

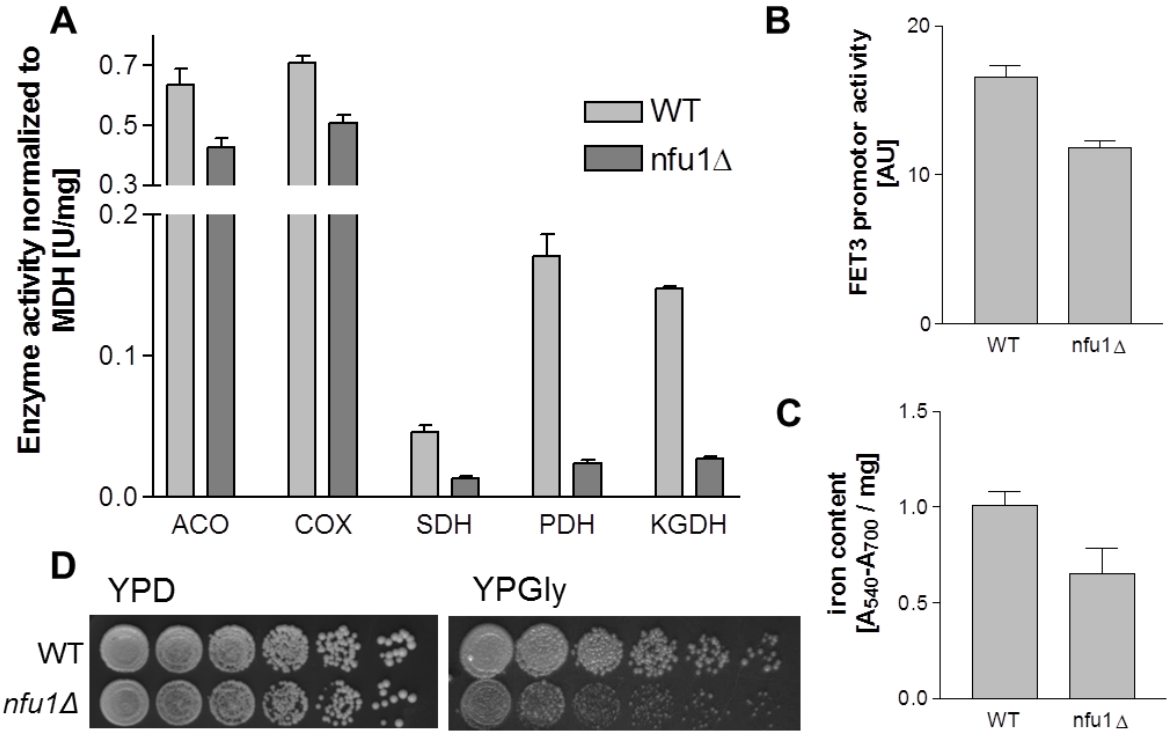

Figure 3.26 *nfu1Δ* cells display drop in SDH, PDH and KGDH activities. (**A**) Wild-type (WT) and *nfu1Δ* cells cultivated over-night in YPD medium and mitochondria were isolated. Mitochondrial extracts were assayed for activities of aconitase (ACO), cytochrome C oxidase (COX), succinate dehydrogenase (SDH), pyruvate dehydrogenase (PDH) and α-ketoglutarate dehydrogenase (KGDH) and normalized to the activities of malate dehydrogenase (MDH). (**B**) Wild-type and *nfu1Δ* cells were transformed with reporter plasmid pFET3-GFP. Obtained cells were cultivated in iron-replete conditions and *FET3* promoter activities were determined by measuring the GFP-specific fluorescence emission of logarithmically grown cells. (**C**) Iron levels were measured for mitochondria isolated from WT, *nfu1Δ* or *grx5Δ* cells grown on YPD medium. (**D**) Over-night cultures of WT and *nfu1Δ* cells were spotted onto full medium plates with glucose (YPD) or glycerol (YPGly) as carbon source. Plates were incubated at 30ºC for two days. Error bars indicate the SEM (n > 4).

NFU1 deletion it was impossible to define the function of Nfu1 protein. Studies on human patient cells showed that NFU1 is involved in the maturation of complex I and II, and lipoate synthase (LAS) (Cameron *et al.*, 2011; Navarro-Sastre *et al.*, 2011). The observed phenotype pointed into the direction of NFU1 protein being, similarly to BOLA3, a dedicated maturation factor, although Cameron et al. suggested a role as an alternative scaffold protein (Cameron *et al.*, 2011).

To determine the actual function of the yeast Nfu1 protein a strain in which the *NFU1* gene was deleted was prepared and analyzed. *nfu1Δ* cells showed no activation of iron regulon (Fig. 3.26 B), no iron accumulation in mitochondria (Fig. 3.26 C) and only slightly reduced growth on the non-fermentable carbon source glycerol (Fig. 3.26 D), as expected from the previous studies (Schilke *et al.*, 1999). Slight decrease in aconitase and COX activities was observed (1,3-fold) and substantial (> 4-fold) decrease in SDH and lipoate-dependent enzymes (PDH and KGDH) were observed (Fig. 3.26 A). This phenotype was in striking similarity to the affected individuals' phenotype (Navarro-Sastre *et al.*, 2011). To get a closer insight into the target specificity of Nfu1, ^{55}Fe radiolabeling and immunoprecipitation of several mitochondrial Fe/S proteins was performed in wild-type and *nfu1Δ* cells. As expected from the enzyme measurements, ^{55}Fe binding to aconitase (Fig. 3.27 A), as well as to [2Fe-2S] human ferredoxin (HsFdx) (Fig. 3.27 B) was not affected upon *NFU1* deletion, showing that Nfu1 is not involved in the maturation of these proteins. No change in iron binding was observed in case of Bio2 (Fig. 3.27 C), consistent with the unaltered activity of this protein in *nfu1Δ* cells (Fig. 3.27 E). Lipoate-dependent enzymes are inactive in *nfu1Δ* cells. As their maturation strongly depends on Fe/S protein lipoate synthase Lip5, the ^{55}Fe binding to Lip5 was tested (Fig. 3.27 D). No significant drop in ^{55}Fe binding was observed in comparison to the wild type. This result shows that Nfu1, similarly to Aim1, seems to have a role in catalytic activation of Lip5 protein. Taken together, these data suggest that Nfu1 is a late-acting rather than general maturation factor of mitochondrial Fe/S proteins.

To address the functionality of the mutated NFU1 protein found in patients (Navarro-Sastre *et al.*, 2011), a corresponding p.Gly^{194}Cys mutation was introduced into yeast *NFU1*. Additionally, a vector in which both active site cysteines (Cys^{196} and Cys^{199}) were mutated to serine was constructed in order to determine if the bound Fe/S cluster is necessary for Nfu1 function (Frazzon and Dean, 2003; Leon *et al.*, 2003; Angelini *et al.*, 2008). Plasmids encoding

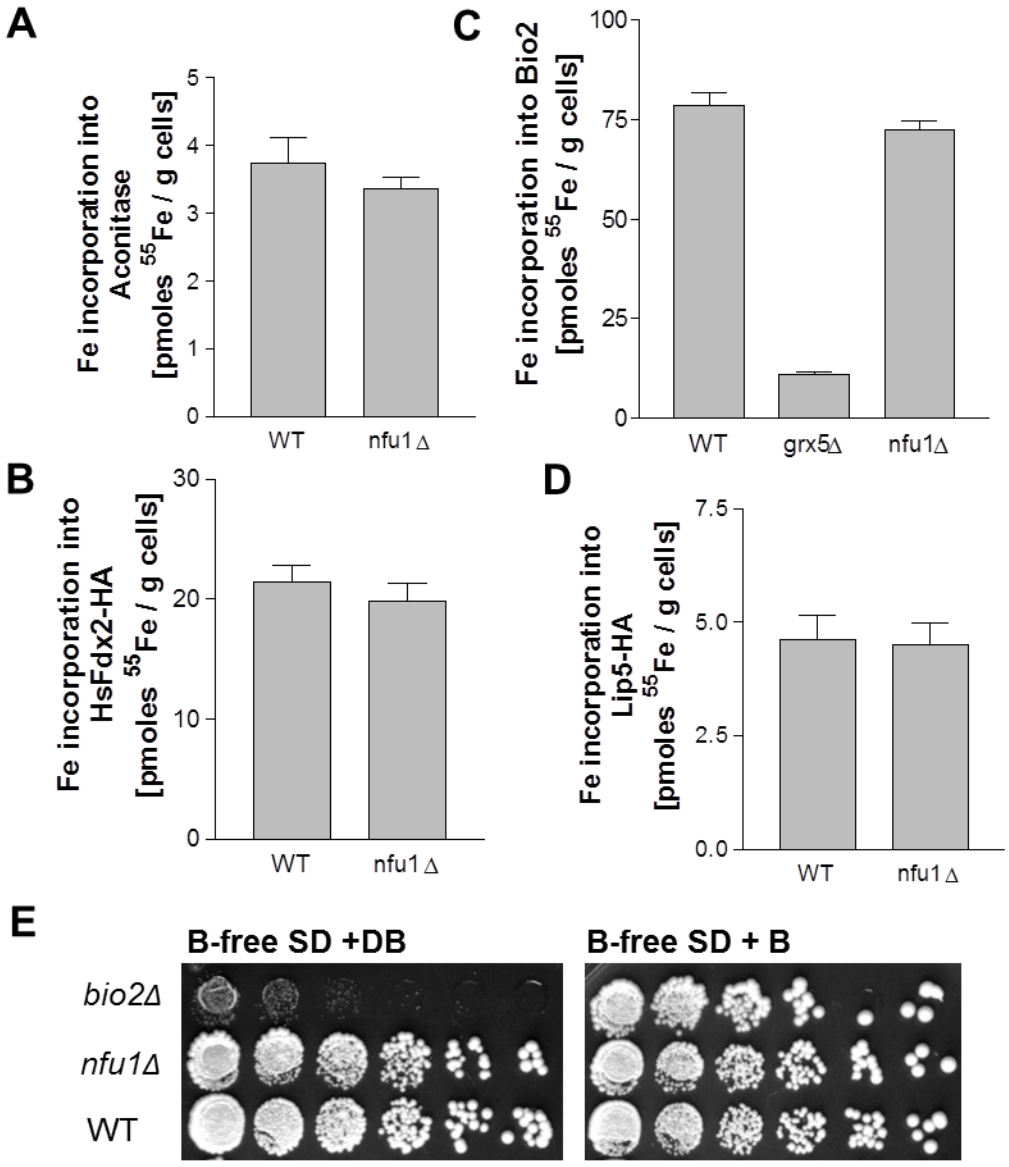

Figure 3.27 Analysis of ^{55}Fe binding to potential target proteins of Nfu1. Wild-type (WT) and *nfu1Δ* cells were transformed with vectors overexpressing mitochondria-targeted biotin synthase (Bio2), human ferredoxin (HsFdx) and lipoate synthase (Lip5). Obtained cells were grown over-night in iron-poor SD medium and then were radiolabeled with 10 µCi ^{55}Fe for 2 h. (**A**) Endogenously expressed aconitase and mitochondria targeted overexpressed (**B**) human ferredoxin (HsFdx-HA), (**C**) biotin synthase (Bio2), or (**D**) lipoic acid synthase (Lip5-HA) were immunoprecipitated from cell extracts with specific antibodies against aconitase, Bio2 or HA-tag (in case of HsFdx-HA and Lip5-HA) and the amount of co-precipitated ^{55}Fe was quantified by scintillation counting. Error bars indicate the SEM (n > 4). (**E**) Serial dilutions of the *bio2Δ*, *nfu1Δ* and WT cells were spotted on biotin-free minimal medium (B-free SD) containing 0,2 µg liter^{-1} of either biotin (indicated as B) or desthiobiotin (DB), and growth was recorded after 3 days incubation at 30°C,

wild-type and mutated yeast Nfu1 were transformed into *nfu1Δ* cells, and enzyme activities were recorded. Wild-type Nfu1 was able to restore the severe enzyme defects of SDH, PDH and KGDH to normal levels (Fig. 3.28 A, B and C). In contrast, Nfu1 Gly^{194}Cys conferred only a minor improvement of these activities, demonstrating that this protein is functionally impaired.

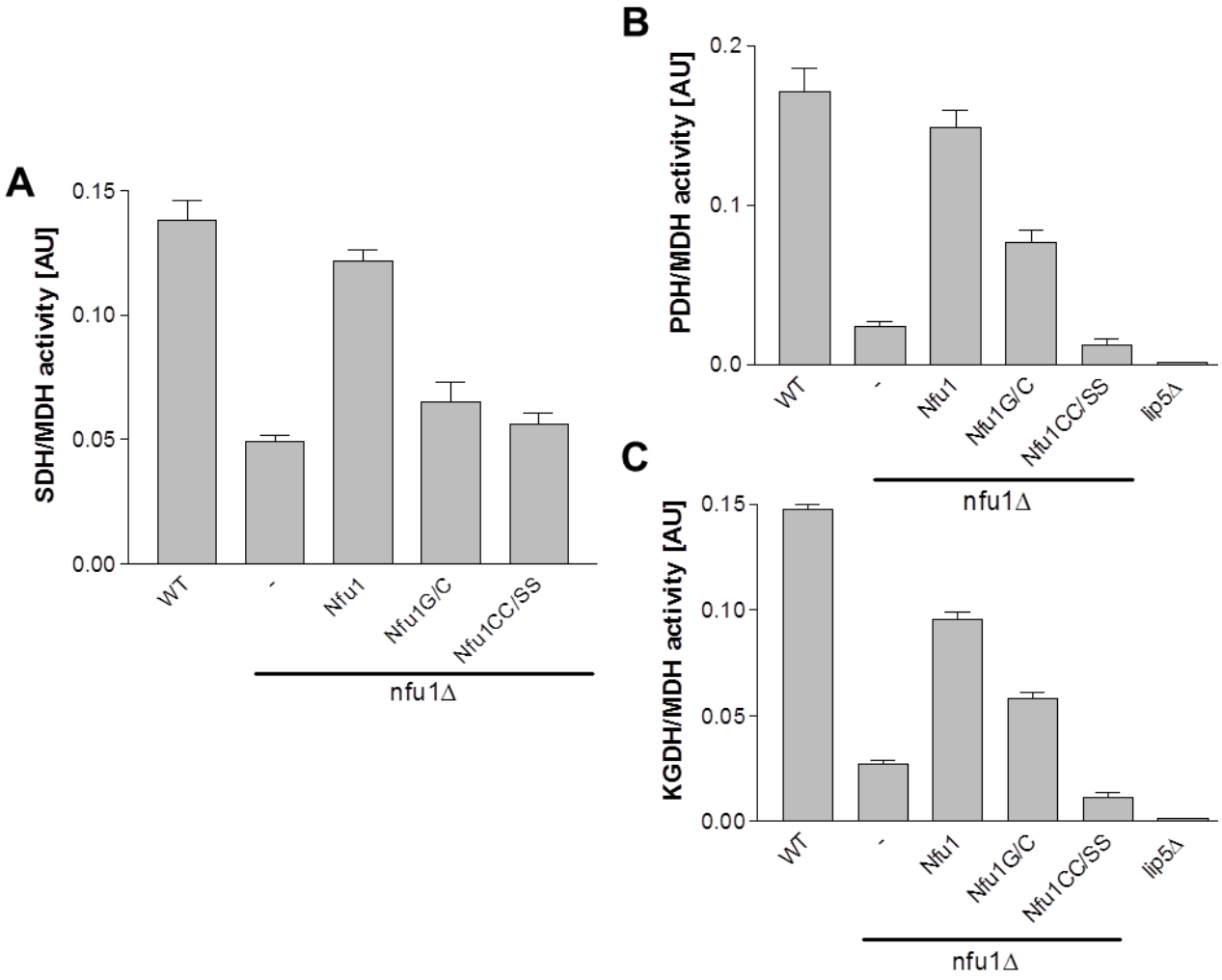

Figure 3.28 Nfu1 active-site cysteines are necessary for the protein function. (**A, B, C**) *nfu1Δ* cells were transformed with vectors overproducing wild-type or mutated G^{194}C (Nfu1 G/C) or C^{196}S C^{199}S (Nfu1CC/SS)) versions of Nfu1. Additionally, *nfu1Δ* and WT cells were transformed with empty vector. Obtained cells were grown on minimal SD medium without tryptophan and mitochondria were isolated. Enzyme activities of (**A**) succinate dehydrogenase (SDH), (**B**) puryvate dehydrogenase (PDH) and (**C**) α-ketoglutarate dehydrogenase (KGDH) were determined in mitochondrial extracts and normalized to malate dehydrogenase (MDH) activities. (**B, C**) Enzyme activities of mitochondrial extracts from *lip5Δ* cells were included as control. Error bars indicate the SEM (n > 4).

What might be the mechanistic basis of the functional impairment of Nfu1 Gly^{194}Cys? The fact that purified Nfu1 can bind an Fe/S cluster (Frazzon and Dean, 2003; Leon *et al.*, 2003; Angelini *et al.*, 2008) and active-site Nfu1 mutant (Cys^{196}Ser and Cys^{199}Ser) was not able to rescue SDH, PDH and KGDH enzyme activities when introduced into the *nfu1Δ* cells (Fig. 3.28 A, B and C), indicates a possible involvement of the active-site cysteines in Fe/S cluster binding and transfer. Yet, *in vivo* no such binding was detectable by ^{55}Fe radiolabeling and immunoprecipitation of Nfu1, even upon overproduction (Pierik *et al.*, 2009) (Fig. 3.29), most likely due to unstable or transient binding of the Fe/S cluster to Nfu1 protein. It has been reported

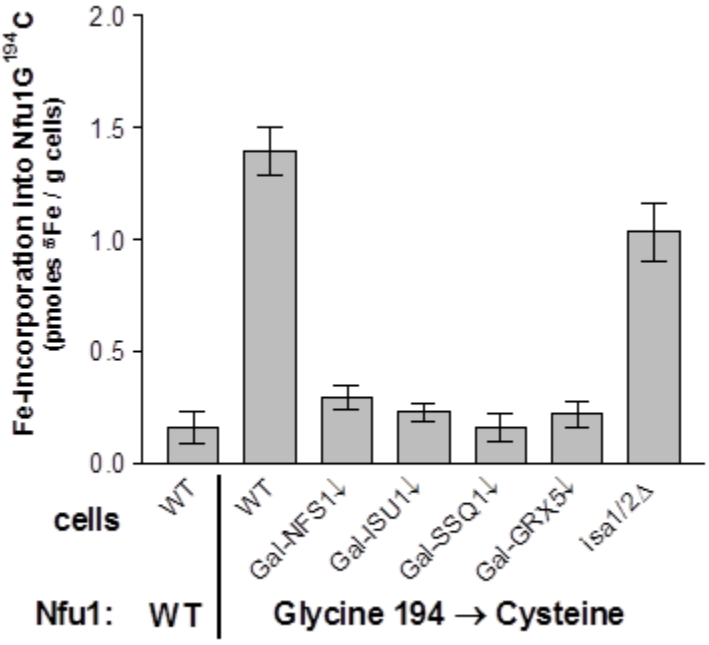

Figure 3.29 Nfu1 binds a Fe/S cluster *in vivo*. The indicated yeast strains overproducing wild-type or mutated (G^{194}C), Myc-tagged versions of Nfu1 protein were grown in iron-poor SD medium and then radiolabeled with 10 µCi ^{55}Fe for 2 h. Nfu1 proteins were immunoprecipitated from cell extracts with specific antibodies against Myc-tag. The amount of co-precipitated ^{55}Fe was quantified by scintillation counting. Gal-ISC strains were depleted to critical levels by cultivation in SD medium for 64h prior to experiments Error bars indicate the SEM (n > 4).

for ferredoxins or the bacterial Fe/S scaffold protein IscU that mutations might stabilize the association of bound Fe/S clusters (Yeh *et al.*, 2000; Unciuleac *et al.*, 2007). To check if patient Gly to Cys mutation has a similar effect on Fe/S cluster binding to mutated Nfu1, ^{55}Fe binding to Nfu1 Gly^{194}Cys was measured by the radiolabeling and immunoprecipitation assay. Significant amounts of radioactive ^{55}Fe were found to bind to Nfu1 Gly^{194}Cys *in vivo* (Fig. 3.29). Iron binding was dependent on several core members of the ISC assembly machinery (Nfs1, Isu1, Ssq1, and Grx5) (Lill *et al.*, 2012). The deletion of late-acting Isa1/2 proteins that are specifically involved in the maturation of [4Fe-4S] clusters did not affect iron binding to Nfu1 Gly^{194}Cys (Muhlenhoff *et al.*, 2011). This striking result suggests that the Nfu1 Gly^{194}Cys-bound iron is part of a [2Fe-2S] cluster whose synthesis is dependent on both the major scaffold protein Isu1 and factors releasing the Fe/S cluster from Isu1 (Ssq1, Grx5). Hence, Nfu1 appears to receive its cluster from Isu1 and act late in Fe/S protein maturation as a specific Fe/S cluster transfer protein (Fig. 3.29), a conclusion which nicely fits to the observations made in HeLa cells where NFU1 depletion, in contrast to ISU1 depletion, impaired only of small subset of mitochondrial proteins (Navarro-Sastre *et al.*, 2011). Together, these results make it rather unlikely that Nfu1 plays a role as an alternative Fe/S scaffold protein in parallel to Isu1. Rather, Nfu1 acts late in Fe/S cluster biogenesis as a specialized maturation factor for a small subset of mitochondrial Fe/S proteins, possibly in cooperation with the Isa1/2 and Iba57 proteins, which were shown previously to be required for [4Fe-4S] clusters maturation in mitochondria (Gelling *et al.*, 2008; Muhlenhoff *et al.*, 2011). This newly defined role of Nfu1 in the Fe/S protein biogenesis pathway is similar to the assumed function of the mitochondrial P loop NTPase Ind1, which also transiently binds an Fe/S cluster and is specifically required for assembly of respiratory complex I, but not for assembly of other mitochondrial Fe/S proteins (Bych *et al.*, 2008).

4 Discussion

Fe/S cluster biogenesis in mitochondria is complex processes that requires several proteins working together, in order to synthetyze Fe/S clusters and deliver them to recipient apo-proteins. Although most of the components of ISC assembly machinery have been identified, the specific function of many of them is not yet completely understood. Most prominently, little is known about the mechanism underlying the delivery of the preassembled Fe/S cluster to target proteins. To answer some of the open questions considering this part of Fe/S cluster biogenesis, the role of proteins expected to act after Fe/S cluster synthesis on the scaffold protein Isu1 was investigated in this work. First, a functional characterization of monothiol glutaredoxin Grx5 was performed to clarify if and how it may be involved in Fe/S cluster release from the scaffold. Second, proposed function of Grx5 as Fe/S cluster transfer protein was validated *in vivo*. In the following parts, the roles of the highly conserved Nfu1 and BolA-like proteins were investigated in *S. cerevisiae* in order to explore if, similarly to their human homologs, they may be involved in Fe/S protein maturation as specific targeting factors.

4.1 Grx5 – a member of ISC assembly machinery or a protein protecting mitochondria from oxidative stress?

Grx5 is a mitochondrial class II monothiol glutaredoxin. In *S. cerevisiae*, its deletion causes oxidative stress, accumulation of iron in mitochondria, inactivation of Fe/S cluster-containing proteins and the constitutive activation of iron regulon. This phenotype on the one hand suggests an involvement of Grx5 in mitochondrial Fe/S cluster biogenesis, but on the other hand could also be explained by oxidative damage prevailing in *grx5Δ* cells. Consistent with role of Grx5 in oxidative stress protection, glutamate and lysine auxotrophies, as well as aconitase activities were recovered under oxygen free conditions up to 60% of WT cells (Fig 3.2 and 3.3). This recovery was similar to cells lacking manganese superoxide dismutase (Sod2), which is one of the main components in mitochondrial oxidative stress protection. The glutaredoxin system is well studied in the context of its role in reducing disulfide bridges formed in target proteins, by for example ROS (reactive oxygen species) (Meyer *et al.*, 2009). Disulfide bridges reduction is an important step in protecting the cell against oxidative stress. Mitochondria lacking Grx5 could be deprived of this protection, resulting in damage of Fe/S cluster containing proteins which in turn could

cause the induction of yeast cellular iron uptake systems and subsequent mitochondrial iron accumulation. This scenario seemed likely as the double deletion of *GRX5* and classic dithiol glutaredoxin *GRX2* is synthetic lethal suggesting some overlapping functions (Rodriguez-Manzaneque *et al.*, 1999). Dithiol glutaredoxins play an important role in oxidative stress protection. However, the enzymatic characterization of Grx5 showed that its activity in reducing GSH-mixed disulfides is twenty times lower than the one of dithiol glutaredoxins (Tamarit *et al.*, 2003). Consistent with this, overexpression of the dithiol Grx2 from yeast and human did not rescue *GRX5* deletion phenotype. Furthermore, *grx5Δ* cells display an accumulation of Fe/S clusters on the scaffold protein Isu1 ((Muhlenhoff *et al.*, 2003a) and Fig. 3.3), and a strong activation of the iron regulon, two characteristic features that are not found in cells lacking proteins involved in oxidative stress protection, like for example Sod2. Moreover, in this work it was shown that Fe/S cluster accumulation on Isu1 remains in Grx5 depleted cells even under anaerobic conditions (Fig. 3.3), indicating that Grx5 is directly involved in the Fe/S cluster transfer step from Isu1 to the target proteins. Hence, the oxidative stress prevailing in *grx5Δ* cells is either a secondary effect of impaired ISC machinery, or Grx5 is involved in both Fe/S cluster biosynthesis and oxidative stress protection. If the first explanation would be true, what could be the source of oxidative stress in *grx5Δ* cells? Studies of the Culotta group showed that in cells with impaired iron homeostasis, such as *grx5Δ*, Sod2 protein becomes inactivated due to the mis-incorporation of iron into its active site instead of its usual cofactor manganese, resulting in the loss of enzyme activity and superoxide protection of mitochondria (Naranuntarat *et al.*, 2009). The elevated levels of iron alone were not sufficient to inactivate Sod2 protein. Mis-incorporation of iron into Sod2 strongly correlated with the levels of Fe/S cluster scaffold protein Isu1. Levels of Isu1 are elevated in several mutants of ISC assembly machinery, including *ssq1Δ* and *grx5Δ* cells, most likely in order to suppress inefficient Fe/S cluster flow to the target proteins (Fig. 3.4 and (Andrew *et al.*, 2008)). Cells lacking Grx5 have strongly elevated Isu1 levels and problem with Fe/S cluster transfer from Isu1 to the target proteins. When the Isu1 mutant (Isu1D^{71}A) which is unable to efficiently release the Fe/S clusters was overexpressed in the WT cells, mimicking the situation observed in *grx5Δ*, ROS production was induced at levels similar to those observed in *sod2Δ* cells (Fig. 3.5). Thus, it seems likely that defects in Fe/S cluster biogenesis are potent source of ROS and that the oxidative stress observed in cells lacking Grx5

is, at least in part, caused by the impaired Fe/S cluster transfer from Isu1 to the target proteins in the absence of Grx5. Taken together, these results suggest that Grx5 is an ISC assembly component and that oxidative stress prevailing in *grx5Δ* cells is not a primary cause of defects in Fe/S cluster biosynthesis.

4.2 Role of Grx5 in iron-sulfur cluster transfer from the scaffold protein Isu1 to the target apo-proteins.

How is Grx5 involved in Fe/S cluster release from Isu1? In this work several key observations were made that allow a better definition of the function of the monothiol glutaredoxin Grx5 in the mitochondrial ISC assembly pathway. First, Grx5 is a Fe/S protein *in vivo* that receives its Fe/S cluster from the Isu1 scaffold. This makes it unlikely that Grx5 *per se* functions as a scaffold protein as previously suggested (Bandyopadhyay *et al.*, 2008; Rouhier, 2010). Second, a so far unknown protein interaction between Grx5 and the dedicated Hsp70 chaperone Ssq1 was identified. This specific complex formation was verified by several independent *in vivo* and *in vitro* approaches, and appears to be crucial for the transfer of the Fe/S cluster synthesized on the scaffold protein Isu1 to target Fe/S apoproteins. Third, formation of the Ssq1-Grx5 complex was increased when Fe/S cluster synthesis was impaired. This, together with the fact that the absence of Grx5 active-site cysteine did not affect the complex formation, indicates that already the apoform of Grx5 may bind to Ssq1. Since Fe/S cluster binding to Grx5 was dependent on the Ssq1-Jac1 chaperone system, it seems likely that apo-Grx5 binds to Ssq1 and is matured to its holo-form in this bound state. Fourth, the Isu1 peptide LPPVK and Grx5 were shown to bind simultaneously to the Ssq1 chaperone using independent binding sites. Most efficient Ssq1-Grx5 interaction was observed in the ADP-state of Ssq1, i.e. the conformation which tightly binds Isu1 (Dutkiewicz *et al.*, 2003; Silberg *et al.*, 2004; Vickery and Cupp-Vickery, 2007; Craig and Marszalek, 2011). In the bacterial ISC assembly system, the conformational change of the U-type scaffold protein upon binding to the Ssq1 orthologue HscA weakens Fe/S cluster association to IscU (Bonomi *et al.*, 2011). Thus, the simultaneous binding of the holo-U-type scaffold protein and the monothiol Grx5 on the dedicated Hsp70 chaperones Ssq1 or HscA likely facilitates the efficient Fe/S cluster transfer from the U-type scaffold to Grx5 in both bacteria and eukaryotes. In the bacterial ISC assembly system, the presence of the HscA/

HscB system induces a 700-fold enhancement in the rate of Fe/S cluster transfer from IscU to Grx5 (Shakamuri *et al.*, 2012). Hence, the formation of this the Isu1-Ssq1-Grx5-complex likely provides a kinetic advantage for holo-Grx5 maturation over the accidental collision of Isu1 and Grx5. Finally, the Grx5-bound Fe/S cofactor is crucial for Grx5 function, as mutation of the active-site cysteine of Grx5 impaired both Fe/S cluster binding and its physiological function (Belli *et al.*, 2002) (this work). *In vivo* data presented in this work are consistent with the idea that Grx5 binds the Fe/S cluster only transiently, and further transfers it towards apo-proteins as previously suggested from *in vitro* findings (Bandyopadhyay *et al.*, 2008; Rouhier *et al.*, 2010). However, based on the available data, it cannot be excluded that, after maturation to its holo-form, Grx5 fulfills an enzymatic function or serves as a redox partner within the ISC assembly pathway. The sum of data presented in this study strongly suggests that the monothiol Grx5 is involved in a Fe/S cluster transfer step. It was clearly shown that Grx5 i) receives its own Fe/S cluster from Isu1 during complex formation of both proteins with the Ssq1 chaperone, ii) functions in Fe/S cluster transfer from the site of cluster synthesis on the Isu1 scaffold to target apoproteins, and iii) operates after the Ssq1-Jac1 chaperone-mediated Fe/S cluster release from Isu1. The recent data from the bacterial system strongly suggest that this scheme is likely a general feature of all ISC assembly systems (Bandyopadhyay *et al.*, 2008; Bonomi *et al.*, 2011; Shakamuri *et al.*, 2012).

These findings suggest a detailed model of how Grx5 is integrated into the ISC assembly pathway, in particular into the well-established catalytic cycle of the dedicated Ssq1-Jac1 chaperones (Fig. 4.1). (Vickery and Cupp-Vickery, 2007; Kampinga and Craig, 2010). Unraveling of this Hsp70 cycle has largely benefitted from numerous studies on the role these chaperones in protein folding (Bukau and Horwich, 1998; Mayer and Bukau, 2005; Craig and Marszalek, 2011; Hartl *et al.*, 2011; Schlecht *et al.*, 2011). According to the current model for Hsp70 chaperone function (Vickery and Cupp-Vickery, 2007; Kampinga and Craig, 2010), Ssq1 in its ATP-state binds the holo-form of Isu1 which has been assembled by the cysteine desulfurase complex Nfs1-Isd11 and other early-acting components of the ISC assembly machinery (Lill *et al.*, 2012) (Fig. 4.1, steps 1-2). Complex formation between Ssq1 and holo-Isu1 is facilitated by the J-type co-chaperone Jac1 which recruits Isu1 and targets it to Ssq1 (Fig. 4.1, step 2). ATP hydrolysis, stimulated by both Isu1 and Jac1, induces a conformational change

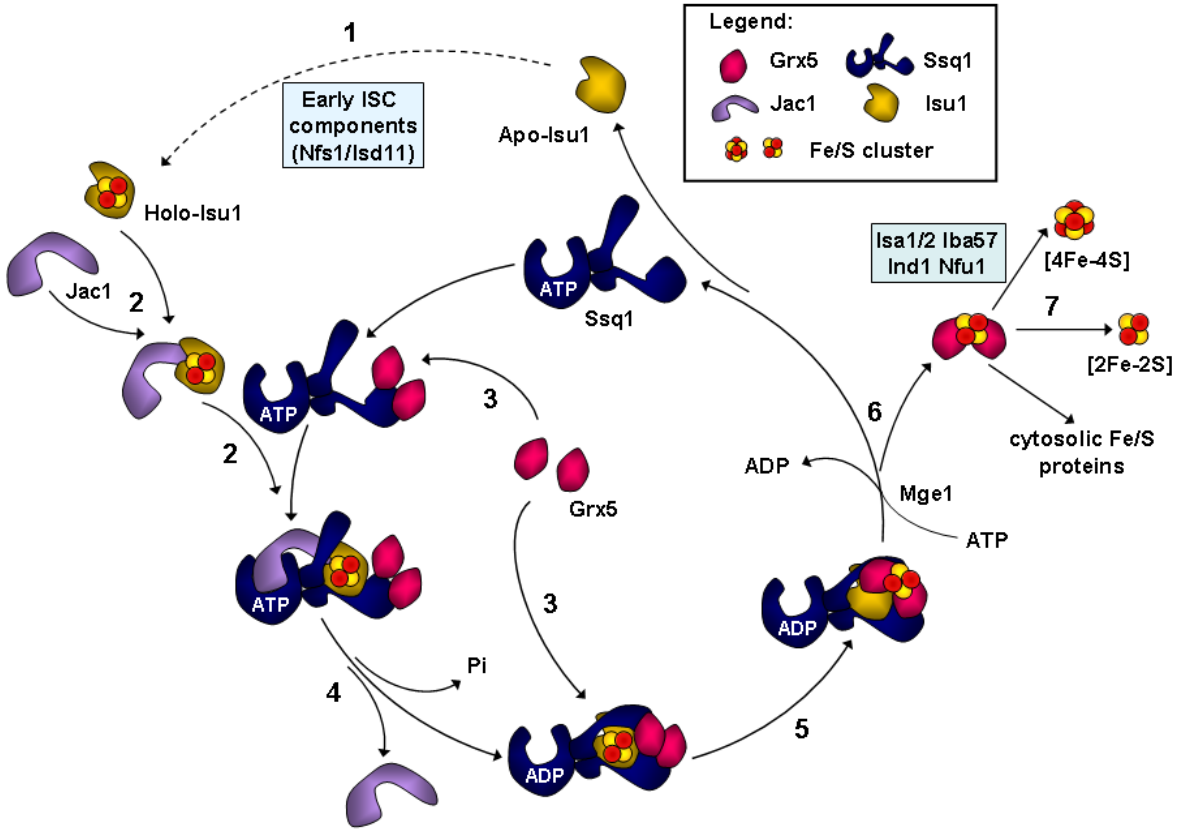

Figure 4.1 Working model for the roles of the mitochondrial chaperones Ssq1-Jac1 and the glutaredoxin Grx5 in Fe/S protein maturation. The model is based on the well-established working cycle of the Hsp70 chaperone system in the ISC assembly pathway (Vickery and Cupp-Vickery, 2007; Kampinga and Craig, 2010) and integrates the findings on Grx5 function made in this work. (**1**) Initially, a Fe/S cluster is synthesized *de novo* on the scaffold protein Isu1 involving the early-acting ISC assembly components such as Nfs1-Isd11 (Lill *et al.*, 2012). (**2**) The co-chaperone Jac1 recruits the Fe/S cluster-loaded Isu1 and targets it to the ATP-bound form of the Hsp70 chaperone Ssq1. (**3**) Grx5 binds to Ssq1 either in its ATP- and ADP-bound state, but has a higher affinity for the ADP-form of Ssq1. Most likely Grx5 binding to Ssq1 precedes that of Isu1, but the presence of Grx5 on Ssq1 is no prerequisite for binding of Isu1 to the chaperone. (**4**) Jac1- and Isu1-induced ATP hydrolysis triggers a conformational change of the peptide binding domain of Ssq1 leading to tight binding of the LPPVK motif of Isu1 and of Grx5. (**5**) The simultaneous presence of these two proteins on Ssq1 facilitates efficient Fe/S cluster transfer from Isu1 to Grx5. (**6**) The nucleotide exchange factor Mge1 mediates the exchange of ADP to ATP on Ssq1. The associated conformational switch leads to less stable binding of Isu1 and Grx5 resulting in the dissociation of the trimeric Ssq1-Isu1-Grx5 complex. (**7**) Finally, Grx5 facilitates Fe/S cluster integration into recipient apo-proteins, a function performed in cooperation with the late-acting ISC targeting factors such as Isa1/2, Iba57, Ind1 and Nfu1. For further details see text and (Lill *et al.*, 2012).

of Ssq1to its closed ADP-state thus stabilizing the interaction between the Ssq1 peptide binding domain and the LPPVK motif of Isu1, while Jac1 leaves the complex (Fig. 4.1, step 4). This induces a conformational change on Isu1 that is, in analogy to the bacterial ISC assembly system (Bonomi *et al.*, 2011; Shakamuri *et al.*, 2012), likely to destabilize Fe/S cluster binding on the Isu1 scaffold protein (Fig. 4.1, step 5; see also below). The nucleotide exchange factor Mge1 then supports the exchange of ADP to ATP which in turn leads to dissociation of Isu1 and the closing of the cycle (Fig. 4.1, step 6). The monothiol Grx5 enters this cycle by associating with Ssq1 at a specific binding site that is independent of that of Isu1, since both proteins can interact simultaneously with Ssq1 (Fig. 4.1, step 3). In keeping with this view, the LPPVK peptide of Isu1 increased rather than interfered with Ssq1-Grx5 association making it unlikely that Grx5 binds to the canonical peptide binding site of Hsp70. This fully explains why Grx5 was unable to stimulate the ATPase activity of Ssq1, unlike Jac1 and Isu1. Even though the ADP state of Ssq1 binds Grx5 most efficiently, the entry of Grx5 may also precede the association of Ssq1 and the Isu1 scaffold. This is evident from the fact that the *in vivo* interaction between Grx5 and Ssq1 was even stronger in the absence of Isu1. While this shows that Grx5-Ssq1 can interact independently of Isu1, the observed increase in binding *in vivo* may be mostly due to low ATP levels prevailing in the absence of functional Isu1 and other ISC assembly machinery members such as Jac1 and Nfs1. *In vitro*, a 2-fold increase in Grx5-Ssq1 affinity was observed upon addition of the LPPVK peptide. The two qualitatively contradictory observations can be understood on the basis that the ADP-bound state of Ssq1 represents the optimal binding partner for Grx5. The tight binding and vicinity of both Isu1 and Grx5 on the ADP-state of Ssq1 may then facilitate Fe/S cluster transfer from Isu1 to Grx5 (Fig. 4.1, step 5). As mentioned above, Fe/S cluster binding to IscU is loosened up by ATP hydrolysis favoring its transfer to Grx5 in the bacterial system (Bonomi *et al.*, 2011; Shakamuri *et al.*, 2012). After dissociation of the trimeric complex Ssq1-Isu1-Grx5 (Fig. 4.1, step 6), holo-Grx5 cooperates with the late-acting targeting factors of the ISC assembly machinery to deliver and assemble Fe/S clusters on target apo-proteins (Fig. 4.1, step 7). Thus, Grx5 functions at the interface of the early phase of Fe/S protein biogenesis leading to the synthesis of the Fe/S cluster and the late phase of cluster integration into apo-proteins.

This raised the interesting question of whether Grx5 belongs to the core ISC assembly machinery involved in the maturation of all Fe/S proteins, or whether it fulfills a more specific function. An important clue towards answering this question came from our finding that Grx5 was required for the maturation of mitochondrial [2Fe-2S] and [4Fe-4S] proteins as well as of cytosolic Fe/S proteins. This behavior is similar to that of Nfs1, Isu1, Jac1 or Ssq1, and clearly defines Grx5 as a member of the core mitochondrial ISC assembly machinery which is needed for maturation of all cellular Fe/S proteins (Lill *et al.*, 2012). We therefore conclude that Grx5 is a late-acting component of the core ISC assembly machinery, yet precedes the function of the more specific ISC targeting factors. These include the Isa1/2 and Iba57 proteins which are involved in the biogenesis of [4Fe-4S] proteins by facilitating the conversion of [2Fe-2S] to [4Fe-4S] clusters (Gelling *et al.*, 2008; Kim *et al.*, 2010; Muhlenhoff *et al.*, 2011; Sheftel *et al.*, 2012) (Fig. 4.1, step 7). The [4Fe-4S] clusters generated by the Isa and Iba57 proteins are then thought to transiently bind to the ISC targeting proteins Ind1 and Nfu1 which specifically deliver them to target apoproteins, such as respiratory complexes I and II or lipoate synthase (this study and (Bych *et al.*, 2008; Sheftel *et al.*, 2009; Cameron *et al.*, 2011; Navarro-Sastre *et al.*, 2011). In support of this sequence of events, this work has documented that maturation of the Fe/S cluster of Nfu1 requires Grx5 function (Fig. 3.29).

Binding of Grx5 was specific for the dedicated chaperone Ssq1. Grx5 only weakly bound to the general mitochondrial Hsp70 chaperone Ssc1 involved in protein folding and import. Moreover, no significant interaction of Ssq1 with canonical Fe/S apoproteins in mitochondrial extracts was observed (Fig. 3.9) suggesting that this protein is not involved in target Fe/S protein folding and/ or stabilization. As mentioned above, the Grx5 interaction does not involve the peptide binding site of Ssq1. This unusual association is reminiscent of the interaction between the chaperone Ssc1 and Tim44 during mitochondrial protein import, where the Ssc1-bound Tim44 is released from Ssc1 upon peptide binding prior to ATP hydrolysis (D'Silva *et al.*, 2004; Chacinska *et al.*, 2009). As a further example, the co-chaperone CHIP has no effect on the basal ATPase activity of Hsp70s and Hsp90s (Stankiewicz *et al.*, 2011). The observation that Grx5 can bind to Ssq1 in the absence of its client protein Isu1 is again reminiscent of the interaction of Ssc1 with Tim44 during mitochondrial protein import. Ssc1 binds to Tim44 independently of the ability of Ssc1 to associate with unfolded proteins *in transit* (D'Silva *et al.*, 2004; Chacinska *et al.*, 2009).

Taken together, this work establishes an unusual interaction between a monothiol glutaredoxin and a specialized mitochondrial Hsp70 chaperone that both play a crucial role in the maturation of all cellular Fe/S proteins. The simultaneous association of both the scaffold protein Isu1 and Grx5 on this dedicated chaperone leads to efficient Fe/S cluster transfer from Isu1 to Grx5. This scenario mechanistically explains the accumulation of Fe/S clusters on Isu1 in cells depleted of either Ssq1, its co-chaperone Jac1 or Grx5 (Muhlenhoff *et al.*, 2003a). Single domain monothiol glutaredoxins are widespread in bacteria and eukaryotes, indicating that their function in ISC assembly is highly conserved (Lillig *et al.*, 2008). Despite severe phenotypic consequences, the deletion of *GRX5* is not lethal in yeast (Rodriguez-Manzaneque *et al.*, 1999; Rodriguez-Manzaneque *et al.*, 2002). This indicates that in this organism its function can be bypassed, likely through a direct yet inefficient transfer of Fe/S clusters from the Isu1 scaffold protein to late ISC assembly factors and/ or target apoproteins. In multicellular organisms, however, mutations in Grx5 are lethal and associated with fatal human disease (Rodriguez-Manzaneque *et al.*, 2002; Wingert *et al.*, 2005; Camaschella *et al.*, 2007; Ye *et al.*, 2010). Notably, humans and most other eukaryotic species do not possess a dedicated Hsp70 chaperone for the mitochondrial ISC assembly pathway and rather utilize the multifunctional Ssc1 (Pukszta *et al.*, 2010), which is the only mitochondrial Hsp70 protein. As Ssc1 is required in many important processes, such as protein import or folding, its involvement in certain pathways as well as its substrate specificity, are defined not by Ssc1 itself but by the co-chaperones and/ or its other interacting partners. As example, Mdj1 is a co-chaperone involved in protein folding, and Pam18 functions in protein import into mitochondria. Ssc1 function in Fe/S cluster biogenesis in organisms lacking Ssq1 is defined by its co-chaperone Jac1 which delivers the Fe/S-loaded Isu1 substrate and stimulates ATPase activity of the chaperone. Currently it is not known whether Grx5 functionally interacts with Ssc1 during Fe/S cluster. If an Hsp70-Grx5 interaction appears under these conditions, Grx5 would be most likely more critical for Fe/S cluster release from the scaffold and delivery to the target apo-proteins, than in case of organisms containing specialized Hsp70 Ssq1. This interaction seems likely as *S. pombe* Grx5 was more prone to bind Ssc1 rather than Ssq1 when expressed in *S. cerevisiae* (data not shown). It would be interesting to see how Grx5 and Hsp70 proteins may have evolved to efficiently cooperate in Fe/S protein assembly.

4.3 Mitochondrial BolA-like proteins and their role in Fe/S cluster maturation.

Although BolA-like proteins are highly conserved in bacteria and eukaryotes, their function is not clear. Conclusions drawn from several studies performed on BolA-like proteins from various organisms vary from a function in oxidative stress protection (Willems *et al.*, 2013), through the coordination of cell cycle progression (Kim *et al.*, 1997), to the involvement in the regulation of cellular iron homeostasis in yeast cells (Kumanovics *et al.*, 2008; Li *et al.*, 2009). The only feature of BolA-like proteins that seems to be maintained throughout the evolution is the association with monothiol glutaredoxins. Very little is known about BolA-like proteins in mitochondria, especially as their deletion in yeast does not cause any obvious phenotype. In this work, the function of the *S. cerevisiae* mitochondrial BolA-like proteins Yal044W (human BOLA1 homolog) and Aim1 (BOLA3 homolog) was investigated.

The potential role of the Aim1 protein is more clear than that of Yal044W due to the discovery of human patients carrying a mutation that introduces a premature stop codon in the *BOLA3* open reading frame (Cameron *et al.*, 2011). Affected individuals came from uncomplicated pregnancies but died 1 month after birth. Biochemical analysis showed a severe combined deficiency of the 2-oxoacid dehydrogenases, associated with a defect in lipoate synthesis and accompanied by defects in complexes I, II, and III of the mitochondrial respiratory chain but with normal aconitase activities. This set of symptoms suggested a role of BOLA3 as a specialized factor in Fe/S cluster biogenesis. Studies performed in this work showed that this function of BOLA3 seems to be conserved throughout the evolution as its *S. cerevisiae* homolog, Aim1, is involved in the maturation of a small subset of [4Fe-4S] proteins including Lip5 and Sdh2. Similar to human patients the observed phenotype was not strong. Except for Lip5 and Sdh2, none of the tested [4Fe-4S] and [2Fe-2S] proteins was affected by the *AIM1* deletion, indicating that Aim1 is indeed a specialized maturation factor. Yeast cells lacking Aim1 protein do not display growth retardation, not even on non-fermentable carbon sources, a phenotype that is in contrast to the human BOLA3 patients who died in the early stages of life. Hence, simple organisms, like *S. cerevisiae*, seem to be able to cope with absence of this helper protein. This differs from the functional impairment of the major maturation factors of [4Fe-4S] proteins, the yeast Isa1/2 and Iba57 proteins, leading to a strong growth defect on non-fermentable carbon sources (Gelling *et al.*, 2008; Muhlenhoff *et al.*, 2011). It is important to emphasize that the maturation of those target proteins that are affected by *AIM1* deletion strongly depends on Isa1/2

and Iba57 (Gelling *et al.*, 2008; Muhlenhoff *et al.*, 2011) as well as on Ind1 (in case of complex I in other fungi and human cells, (Bych *et al.*, 2008; Sheftel *et al.*, 2009)) and to some extend also on Nfu1 (this study and (Navarro-Sastre *et al.*, 2011)). Taken together, Aim1 is a dispensable "helper" maturation factor of a small subset of Fe/S proteins in yeast mitochondria. BOLA3/ Aim1 protein may become more important under certain conditions, such as increased oxidative stress, where they could serve in complex with GLRX5/ Grx5 (see below for details) as a "repair" system for the subset of damaged Fe/S proteins. This scenario would explain why human patients survive the pregnancy time, where they are largely protected from exogenous stress and receive all necessary components from the mother, but die shortly after birth. To validate this point of view, further studies have to be performed in yeast and human cells, where the importance of Aim1/ BOLA3 protein is investigated under different conditions, for example, oxidative stress. In case of Yal044W no effect on mitochondrial Fe/S protein synthesis was observed upon its gene deletion pointing into direction of Yal044W performing another, yet undefined function. However, the fact that it was able to rescue *aim1Δ* cells when overexpressed, suggests that Yal044W and Aim1 proteins may have some overlapping functions in yeast mitochondria.

What could be the precise molecular function of BolA-like proteins in mitochondria? BolA-like proteins were associated with monothiol glutaredoxins by both bioinformatics and experimental approaches (Huynen *et al.*, 2005; Yeung *et al.*, 2011; Li and Outten, 2012; Willems *et al.*, 2013). Yeast cytosolic monothiol glutaredoxins Grx3/4 were shown to form functional complex with BolA-like protein Fra2 (Li *et al.*, 2009). Although, an interaction between Grx5 and both Yal044W and Aim1 via GSH-coordinated [2Fe-2S] bridging cluster was detected *in vitro* (Bo Zhang personal communication), in this work neither the Fe/S cluster binding to BolA-like proteins, nor their interaction with Grx5 could be verified *in vivo* by immunoprecipitation assays. Consistent with interaction idea, Cameron and coworkers suggested that BOLA3 might interact with monothiol glutaredoxin (in this case GLRX5) although also in their study the interaction was not verified. All BolA-like proteins possess a highly conserved histidine residue that together with GSH and the active-site cysteine of monothiol glutaredoxin, can serve as a ligand for a [2Fe-2S] cluster (Li and Outten, 2012). If BOLA3/ Aim1 do interact with GLRX5/ Grx5 via GSH-mediated bridging Fe/S cluster *in vivo*, this couple could be then directly involved in the maturation of, for example, lipoate synthase. Mutations of this histidine residue in Aim1 should then give the same phenotype as complete deletion of *AIM1* gene. However, these

experiments have so far not been carried out. In contrast to the BOLA3, the interaction between BOLA1 and GLRX5 proteins was detected *in vivo* (Willems *et al.*, 2013), but the biochemical role of this complex formation was not investigated. One would expect that also the yeast BOLA1 homolog Yal044W should form a functional complex with Grx5. The role of Yal044W protein in the mitochondria could not yet be determined due to the lack of an obvious phenotype of *YAL044W* deletion strain.

Cytosolic Fe/S cluster assembly, as well as the maintenance of iron homeostasis by Grx3/4, strictly depends on a mitochondria-derived sulfur-containing component ("X"). Grx5 is the terminal component of the core ISC assembly machinery which causes activation of the iron regulon and affects cytosolic Fe/S cluster-containing enzymes upon its gene deletion. This suggests that Grx5 is most likely directly involved in facilitating "X" export from the mitochondria, although additional work is needed to prove this point. One might speculate, that similarly to Fra2 that forms a complex with Grx3/4, mitochondrial BolA-like proteins also could be indirectly involved in maintenance of iron homeostasis via complex formation with Grx5. However, the deletion of mitochondrial BolA-proteins does not cause the activation of iron regulon, thus if Grx5-BolA complexes are involved in "X" export, a Grx5 homodimer is perfectly able to perform this function alone. To further investigate this theory, it would be interesting to explore whether Grx5 levels change upon BolA deletion, and whether there is an increase of iron binding to the Grx5 and BolA proteins in Atm1-depleted cells. The latter is especially interesting as Atm1 is an ABC transporter involved in "X" export from the mitochondria. If Grx5 is also involved in this process, then upon Atm1 depletion one should observe an accumulation of "X" or a Grx5-bound Fe/S cluster. Another possiblility could be, as suggested by Willems and coworkers for the BOLA1 protein (Willems *et al.*, 2013), that Yal044W is simply a reductase working together with Grx5. This idea would extend the function of Grx5, which has normally a low activity to reduce GSH-mixed disulfides, and allow maintaining thiol redox potential of the mitochondria, especially in the oxidizing conditions. This assumption is consistent with the fact that BOLA1 homologs are present only in the aerobic species (Willems *et al.*, 2013) and that *grx5Δ* cells suffer from severe oxidative stress (Rodriguez-Manzaneque *et al.*, 1999). To validate this point of view, the activity of the Grx5-Yal044W complex to reduce GSH-mixed disulfides needs to be determined. Further work should focus on determining the actual function of Yal044W, whether alone or in complex with Grx5 protein.

4.4 Role of Nfu1 protein in Fe/S clusters maturation in mitochondria.

Although Nfu1 protein was indirectly connected to Fe/S cluster biosynthesis from its similarity to the C-terminal part of *A. vinelandii* NifU, its actual role in this process was not clear. Deletion of the *NFU1* gene in yeast did not show any obvious phenotype, but double deletion with *ISU1* allowed to link the Nfu1 protein with the ISC machinery. Studies performed on purified proteins from other organisms suggested a role as an alternative scaffold protein (Touraine *et al.*, 2004; Yabe *et al.*, 2004) or a target-specific carrier protein (Py *et al.*, 2012). Similarly to the BolA-like proteins, the breakthrough in the potential understanding of the protein function came with the discovery of disease-causing *NFU1* mutations which were associated with a fatal mitochondrial disease. In the first study a non-sense mutation was identified that led to alternative mRNA splicing and complete loss of the protein (Cameron *et al.*, 2011), while in the second one, a G→C point mutation led to glycine to the cysteine ($Gly^{208}Cys$) exchange just next to the active-site (CXXC) of NFU1 (Navarro-Sastre *et al.*, 2011). This fatal infantile encephalopathy and/ or pulmonary hypertension was associated with low activities of lipoic acid-containing proteins and complexes I, II, and III of the respiratory chain (Cameron *et al.*, 2011; Navarro-Sastre *et al.*, 2011). In striking similarity to BOLA3 patients, affected individuals came from uncomplicated pregnancies and showed no evident symptoms at birth, but with time they developed severe developmental retardation, brain abnormalities and pulmonary hypertension and eventually died between 3 months (Cameron *et al.*, 2011) and one year (Navarro-Sastre *et al.*, 2011) after birth. *NFU1* depletion in cultured HeLa cells reproduced phenotype observed in patients (Navarro-Sastre *et al.*, 2011), pointing to a role of NFU1 in the assembly of complex Fe/S proteins such as respiratory complexes I and II and lipoate synthase (LAS) that contain eight, three or two Fe/S clusters, respectively (Cameron *et al.*, 2011; Navarro-Sastre *et al.*, 2011). Interestingly, the lipoic acid defects could not be reverted by the addition of lipoic acid to the medium (Oliver Stehling unpublished data), a result consistent with the inability of exogenously provided lipoic acid to rescue a LAS knockout mouse (Yi and Maeda, 2005). Information provided by the patient cells and cell culture studies allowed us to investigate the Nfu1 function in yeast in more detail. In this work, in agreement with the previous yeast studies (Schilke *et al.*, 1999), *NFU1* deletion showed wild-type growth rates, no activation of the yeast iron regulon or iron accumulation in the mitochondria, and only a minor reduction in aconitase activity. When the activities of Sdh2 and lipoate-dependent enzymes (PDH and KGDH) were tested in *S.*

cerevisiae, strong defects were detected similarly to those seen in patients' and HeLa cells. Interestingly, yeast Nfu1 $Gly^{194}Cys$, with mutation corresponding to the glycine to cysteine exchange found in patients was able to partially rescue PDH and KGDH activity when overexpressed. This partial rescue explains why patients with $Gly^{208}Cys$ exchange in the NFU1 survived longer (Navarro-Sastre *et al.*, 2011) than the ones with the mutation leading to the complete loss of the protein (Cameron *et al.*, 2011).

Both Sdh2 and Lip5 contain [4Fe-4S] clusters. Surprisingly, ^{55}Fe radiolabeling and immunoprecipitation experiments revealed that iron binding to lipoate synthase was not affected in *nfu1Δ* cells when compared to the WT. This situation resembles that observed upon Isa1/2 and Iba57 depletion, where the radical SAM proteins Lip5 and Bio2 were shown to be inactive despite wild-type levels of iron binding (Muhlenhoff *et al.*, 2007; Gelling *et al.*, 2008; Muhlenhoff *et al.*, 2011). Similarly to Isa1/2 and Iba57 proteins, Nfu1 seems to be involved in the catalytic activation of Lip5. Taking into the consideration that also Aim1 was shown to be involved in this process, what could be the specific role of Nfu1? Previous studies demonstrated that Nfu-like proteins are able to bind a Fe/S cluster *in vitro* (Leon *et al.*, 2003; Tong *et al.*, 2003), yet *in vivo* data were missing. In this work, ^{55}Fe binding to the wild-type Nfu1 protein was tested. No significant iron binding could be detected, most likely due to the labile nature of the cluster. On the other hand, the Nfu1 $Gly^{194}Cys$ mutant showed significant ^{55}Fe binding. This result indicates that the glycine to cysteine exchange next to the CXXC active-site of Nfu1 in affected patients has a stabilizing effect on Fe/S cluster binding. Additionally iron binding to Nfu1 protein was dependent on several core members of the ISC assembly machinery (Nfs1, Isu1, Ssq1, and Grx5), but not on the late-acting Isa1/2 indicating that yeast Nfu1 is likely a [2Fe-2S] protein, similary to the plant AtNfu2 (Leon *et al.*, 2003). However, human NFU1 is able to assemble a labile [4Fe-4S] cluster coordinated by two hNfu1 monomers *in vitro*, (Tong *et al.*, 2003), thus it is not completely clear what type of cluster is bound to Nfu-like proteins. Since Nfu1 receives its cluster from Isu1, a function as a scaffold protein alternative to Isu1 can be ruled out. More likely, Nfu1 acts as a transfer protein acting at the late stages of Fe/S cluster assembly, explaining why the stabilization of the Fe/S cluster impairs Nfu1 function and why a single amino acid exchange resulted in disease development in humans. Mutated $Gly^{208}Cys$ NFU1 protein was most likely not able to efficiently transfer its Fe/S cluster to the target proteins. Moreover, Nfu1 without active-site cysteines (Nfu1 $Cys^{196}Ser$ $Cys^{199}Ser$) showed the

same phenotype as the deletion mutant in yeast, further suggesting that the Nfu1-bound cluster is necessary for its function. The phenotype observed in *nfu1Δ* cells differs from the one observed in cells lacking Isa1/2 and Iba57, as the latter are essential for the maturation of all [4Fe-4S] proteins (Muhlenhoff *et al.*, 2011), whereas Nfu1 seems to be needed only for the efficient maturation of a small subset of targets. Taken together, Nfu1 protein is most likely, similarly to Aim1, a specific auxiliary maturation factor. Although Nfu1 seems to be dispensable in yeast as *nfu1Δ* cells display a mild phenotype, higher eukaryotes are apparently more dependent on the late-acting components of the ISC assembly machinery as they have many cell types with different functions and needs. Thus, those gene defects in the Fe/S cluster biogenesis that elicit minor defects in a simple unicellular organism as yeast can have a strong impact on complex multicellular organisms.

5 Conclusions and outlook

Mitochondrial Fe/S protein biogenesis is a complex process, essential for cell viability and highly conserved throughout evolution. Although the details on molecular level are missing, the process of *de novo* Fe/S cluster synthesis on the scaffold protein Isu1, as well as the role of chaperone proteins in the Fe/S cluster release from Isu1 is becoming well understood. In contrast, the mechanisms on how preassembled Fe/S clusters are subsequently delivered to a large variety of different target proteins is not yet clear. Although several proteins involved in this process have been identified, their function and the interplay between them are poorly understood. In this work several key findings were made that may contribute to a better understanding of how Fe/S clusters are delivered to target proteins in mitochondria. However, several new questions appeared that need to be answered in the future.

After *de novo* Fe/S cluster synthesis the scaffold protein Isu1 is engaged by the chaperone system comprised of the Hsp70 family member Ssq1, co-chaperone Jac1 and nucleotide exchange factor Mge1. Data obtained within this work show that Grx5 is the last member of the core ISC assembly machinery. Hence, Grx5 connects the early stages of ISC assembly, where Fe/S cluster is assembled *de novo*, to the late phases, where after dissociation of the trimeric complex Ssq1-Isu1-Grx5 (Fig. 4.1 step 6), a Fe/S cluster loaded holo-Grx5 most likely cooperates with late-acting targeting factors to deliver and assemble Fe/S clusters on target apo-proteins.

	Required maturation factors:				
Target proteins:	**Grx5**	**Isa1/2 Iba57**	**Nfu1**	**Aim1**	**Ind1**
[2Fe-2S]	+				
Aconitase-like	+	+			
Radical SAM	+	+	+	+	
Sdh2	+	+	+	+	
Complex I	+	+	+	+	+

Table 5.1 Target proteins and factors involved in their maturation.

Since the Grx5-bound, GSH-coordinated bridging [2Fe-2S] cluster is bound in a labile fashion, Grx5 is potentially a perfect transfer protein that is able to easily donate its cluster to target proteins. As no other factors involved in maturation of [2Fe-2S] cluster-containing proteins have been identified to date, it seems likely that Grx5 is able to perform this function on its own. [4Fe-4S] cluster protein strongly depends on Isa1/2 and Iba57 proteins in addition to Grx5 (Gelling *et al.*, 2008; Muhlenhoff *et al.*, 2011). Moreover, some [4Fe-4S] target proteins require additional maturation factors like Nfu1, Aim1 and Ind1 (see table 5.1). Since [4Fe-4S] clusters are not all the same with respect to their coordination, stability and surrounding environment, they also may require different maturation pathways. The different requirements for the maturation of [4Fe-4S] proteins in mitochondria are summarized in the Table 5.1 and Fig. 5.2. One of the questions which immediately arises is how late factors cooperate with each other in order to mature [4Fe-

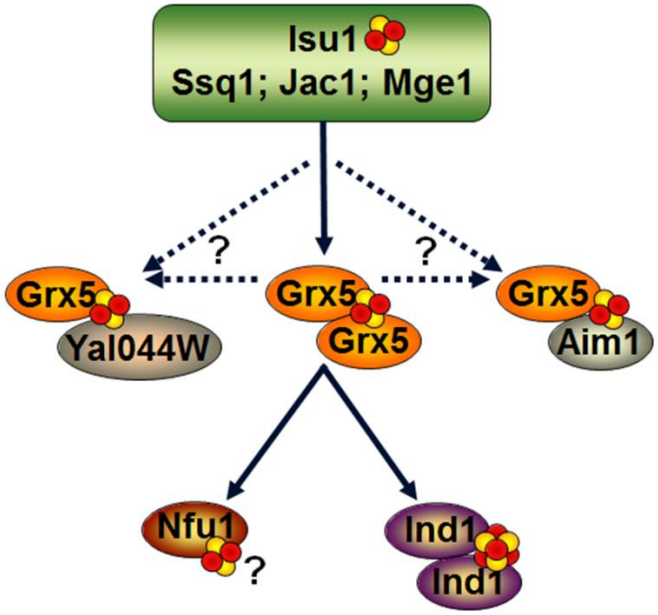

Figure 5.1 Maturation of the late acting ISC targeting factors. After Fe/S cluster assembly on the scaffold protein Isu1, the cluster release is facilitated by the specialized chaperone system comprised of Ssq1, Jac1 and Mge1, and by the monothiol glutaredoxin Grx5. The released Fe/S cluster is then bound to a Grx5-Grx5 homodimer in a GSH-coordinated bridging fashion. It is likely that Fe/S cluster containing species Grx5-Aim1 and Grx5-Yal044W are also formed at this point or through the conversion of Grx5-Grx5 homodimer (dotted lines). Grx5 is needed for maturation of Nfu1 and most likely also Ind1 proteins. Nfu1 binds either a [2Fe-2S] (this work and (Leon *et al.*, 2003)) cluster or a [4Fe-4S] cluster (Tong *et al.*, 2003). Ind1 binds a [4Fe-4S] cluster (Sheftel *et al.*, 2009). The excat role of Isa1-Isa1-Iba57 complex in this pathway is presently unclear and thus it was not included in this figure.

4S] proteins? The process requires the conversion of a Grx5-bound [2Fe-2S] cluster to the final [4Fe-4S] cluster present on the target proteins (Fig. 5.1). It is completely unclear how this conversion is achieved. Grx5 was shown to directly interact with Isa proteins in *S. pombe* (Kim *et al.*, 2010), suggesting that the Fe/S cluster could be transferred from Grx5 to the Isa1/2 proteins. Alternatively, these proteins can work together as a complex to build a [4Fe-4S] cluster and insert it into, for example, aconitase. The latter option seems more likely, as Isa1/2 proteins have been shown to bind iron independently from the scaffold protein Isu1 (Muhlenhoff *et al.*, 2011), although *in vitro* analysis of *S. pombe* Isa1/2 homolog ISA suggests that it is capable of binding [2Fe-2S] cluster (Wu and Cowan, 2003). The next important question concerns the role of Nfu1 and Ind1 proteins that are able to bind [2Fe-2S] (or [4Fe-4S]) and [4Fe-4S] cluster respectively (Fig. 5.1).

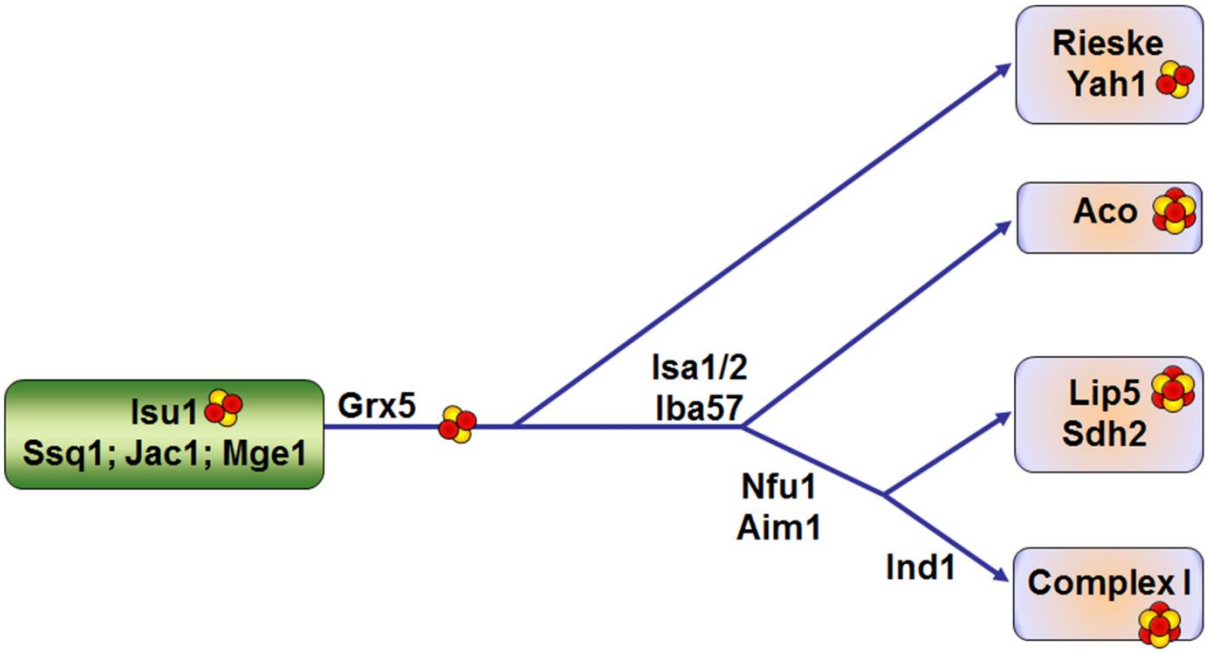

Figure 5.2 Maturation of distinct mitochondrial Fe/S target proteins. The maturation of ISC targeting factors is described in Fig. 5.1. Grx5 is required for maturation of all mitochondrial Fe/S proteins. No additional factors are known to be required for the maturation of [2Fe-2S] proteins (Rieske and Yah1 proteins as examples). Proteins containing [4Fe-4S] clusters need additional targeting factors. A major role in maturation of all [4Fe-4S] proteins is played by Isa1/2 and Iba57 proteins. Isa1/2 and Iba57 are directly involved in maturation of aconitase-type proteins (Aco). Complex Fe/S proteins, that contain more than one Fe/S cluster, require additional maturation factors to receive functional cofactors. Radical-SAM proteins (here Lip5 as example) and complex II subunit Sdh2 depend on Nfu1 and the BolA-like protein Aim1. Complex I with eight Fe/S clusters displays the most complicated maturation scheme where additionally to Grx5, Isa1/2, Iba57, Nfu1, and Aim1 also P-loop NTPase protein Ind1 is needed.

It is possible that Fe/S cluster-loaded Nfu1 is directly or by cooperating with Isa1/2 and Iba57 proteins, involved in the maturation or catalytic activation of its target proteins. The most complex maturation scheme is observed in case of complex I that contains eight Fe/S clusters of which four are of the [4Fe-4S] type. In addition to Grx5, Isa1/2, Iba57, Nfu1 and Aim1/ BOLA3 also role of Ind1 protein was indicated (Fig. 5.2). Like Nfu1, Ind1 may serve as a Fe/S cluster transfer protein which provides one or more Fe/S clusters directly to complex I (Sheftel *et al.*, 2009).

A further novel question that arises from this work concerns the role of the interaction of Grx5 with BolA-like proteins. Since monothiol glutaredoxins have been associated with BolA-like proteins (Huynen *et al.*, 2005; Li and Outten, 2012), it seems likely that the holo-Grx5 homodimer is further converted to Grx5-Aim1 and Grx5-Yal044W heterodimeric species binding a bridging [2Fe-2S] cluster (Fig. 5.1). If this is the case, how do this species integrate into Fe/S protein maturation in mitochondria? Deletion of Aim1 causes mild phenotype in yeast with only few affected target proteins, suggesting that it is not a general maturation factor and/ or can by bypassed. It is not clear whether Aim1 works in parallel to or after Isa1/2 proteins. Another possibility is that Aim1 (or Aim1-Grx5 complex) serves as a Fe/S cluster repair factor. A possible involvement of Yal044W (or Grx5-Yal044W complex) in Fe/S proteins maturation process remains to be elucidated. Careful biochemical analysis of late-acting factors will provide insights into the late steps of ISC assembly machinery on the molecular level.

As mentioned above, Grx5 is the last component of ISC assembly machinery the depletion of which causes activation of iron regulon and loss of activity of cytosolic Fe/S cluster proteins. This suggests that Grx5 is likely involved in a late step of the export of component "X" from mitochondria. If this is the case, how does Grx5 deliver "X" to the Atm1 ABC transporter? Recently, Cowan and coworkers suggested that component "X" could be a [2Fe-2S] cluster coordinated by four GSH molecules (Qi *et al.*, 2012). If this theory is true, the [2Fe-2S] cluster coordinated by two Grx5 molecules and two GSH molecules would be an ideal intermediate. The two Grx5 molecules could be exchanged by two GSH molecules to generate the exported substrate "X".

Taken together, this work contributes to a better description of how Fe/S clusters are handled in mitochondria after *de novo* synthesis on the scaffold protein Isu1. First, the simultanous interaction of Isu1 and Grx5 on the specialized Hsp70 chaperone Ssq1 is important

for efficient Fe/S cluster transfer from Isu1 to Grx5. Second, Grx5 is a crucial factor for maturation of all cellular Fe/S proteins. Third, an auxiliary role of yeast Nfu1 and Aim1 as dedicated maturation factors was established. These findings provide a better insight into how late-acting components of the mitochondrial ISC assembly machinery cooperate with each other to efficiently insert the Fe/S cluster target apo-proteins. As Grx5, Aim1 and Nfu1 are disease relevant, this work leads to better understanding of how their functional loss may contribute to the disease development and progression.

6 References

Adam, A.C., Bornhovd, C., Prokisch, H., Neupert, W., and Hell, K. (2006). The Nfs1 interacting protein Isd11 has an essential role in Fe/S cluster biogenesis in mitochondria. Embo J *25*, 174-183.

Adinolfi, S., Iannuzzi, C., Prischi, F., Pastore, C., Iametti, S., Martin, S.R., Bonomi, F., and Pastore, A. (2009). Bacterial frataxin CyaY is the gatekeeper of iron-sulfur cluster formation catalyzed by IscS. Nature Struct Mol Biol *16*, 390-396.

Aldea, M., Garrido, T., Hernandez-Chico, C., Vicente, M., and Kushner, S.R. (1989). Induction of a growth-phase-dependent promoter triggers transcription of bolA, an Escherichia coli morphogene. Embo J *8*, 3923-3931.

Amutha, B., Gordon, D.M., Gu, Y., Lyver, E.R., Dancis, A., and Pain, D. (2008). GTP is required for iron-sulfur cluster biogenesis in mitochondria. J Biol Chem *283*, 1362-1371.

Andrew, A.J., Dutkiewicz, R., Knieszner, H., Craig, E.A., and Marszalek, J. (2006). Characterization of the interaction between the J-protein Jac1p and the scaffold for Fe-S cluster biogenesis, Isu1p. J Biol Chem *281*, 14580-14587.

Andrew, A.J., Song, J.Y., Schilke, B., and Craig, E.A. (2008). Posttranslational regulation of the scaffold for Fe-S cluster biogenesis, Isu. Mol Biol Cell *19*, 5259-5266.

Angelini, S., Gerez, C., Ollagnier-de Choudens, S., Sanakis, Y., Fontecave, M., Barras, F., and Py, B. (2008). NfuA, a new factor required for maturing Fe/S proteins in Escherichia coli under oxidative stress and iron starvation conditions. J Biol Chem *283*, 14084-14091.

Balk, J., Aguilar Netz, D.J., Tepper, K., Pierik, A.J., and Lill, R. (2005). The essential WD40 protein Cia1 is involved in a late step of cytosolic and nuclear iron-sulfur protein assembly. Mol Cell Biol *25*, 10833-10841.

Balk, J., and Lobreaux, S. (2005). Biogenesis of iron-sulfur proteins in plants. Trends Plant Sci *10*, 324-331.

Balk, J., Pierik, A.J., Netz, D.J., Muhlenhoff, U., and Lill, R. (2004). The hydrogenase-like Nar1p is essential for maturation of cytosolic and nuclear iron-sulphur proteins. Embo J *23*, 2105-2115.

Bandyopadhyay, S., Gama, F., Molina-Navarro, M.M., Gualberto, J.M., Claxton, R., Naik, S.G., Huynh, B.H., Herrero, E., Jacquot, J.P., Johnson, M.K., and Rouhier, N. (2008). Chloroplast monothiol glutaredoxins as scaffold proteins for the assembly and delivery of [2Fe-2S] clusters. Embo J *27*, 1122-1133.

Barras, F., Loiseau, L., and Py, B. (2005). How Escherichia coli and Saccharomyces cerevisiae build Fe/S proteins. Adv Microb Physiol *50*, 41-101.

Barros, M.H., Nobrega, F.G., and Tzagoloff, A. (2002). Mitochondrial ferredoxin is required for heme A synthesis in Saccharomyces cerevisiae. J Biol Chem *277*, 9997-10002.

Beinert, H. (2000). Iron-sulfur proteins: ancient structures, still full of surprises. J Biol Inorg Chem *5*, 2-15.

Beinert, H.S., R. H. . (1960). Studies on Succinic and DPNH Dehydrogenase preparations by Paramagnetic Resonance (EPR) Spectroscopy. Biochem Biophys Res Commun *3*, 41-46.

Bekri, S., Kispal, G., Lange, H., Fitzsimons, E., Tolmie, J., Lill, R., and Bishop, D.F. (2000). Human ABC7 transporter: gene structure and mutation causing X-linked sideroblastic anemia with ataxia with disruption of cytosolic iron-sulfur protein maturation. Blood *96*, 3256-3264.

References

Belli, G., Polaina, J., Tamarit, J., De La Torre, M.A., Rodriguez-Manzaneque, M.T., Ros, J., and Herrero, E. (2002). Structure-function analysis of yeast Grx5 monothiol glutaredoxin defines essential amino acids for the function of the protein. J Biol Chem *277*, 37590-37596.

Bennett, J., and Scott, K.J. (1971). Quantitative staining of fraction I protein in polyacrylamide gels using Coomassie brillant blue. Anal Biochem. *43*, 173-182.

Berndt, C., Lillig, C.H., and Holmgren, A. (2008). Thioredoxins and glutaredoxins as facilitators of protein folding. Biochim Biophys Acta *1783*, 641-650.

Bhan, A., Galas, D.J., and Dewey, T.G. (2002). A duplication growth model of gene expression networks. Bioinformatics *18*, 1486-1493.

Birnboim, H.C., and Doly, J. (1979). A rapid alkaline extraction procedure for screening recombinant plasmid DNA. Nucleic acids research *7*, 1513-1523.

Blaiseau, P.L., Seguin, A., Camadro, J.M., and Lesuisse, E. (2011). Iron Uptake in Yeasts. In: Iron Uptake and Homeostasis in Microorganisms, eds. P. Cornelis and S.C. Andrews, Norfolk, UK: Caister Academic Press, 265-284.

Bonomi, F., Iametti, S., Morleo, A., Ta, D., and Vickery, L.E. (2008). Studies on the mechanism of catalysis of iron-sulfur cluster transfer from IscU[2Fe2S] by HscA/HscB chaperones. Biochemistry *47*, 12795-12801.

Bonomi, F., Iametti, S., Morleo, A., Ta, D., and Vickery, L.E. (2011). Facilitated transfer of IscU-[2Fe2S] clusters by chaperone-mediated ligand exchange. Biochemistry *50*, 9641-9650.

Bradford, M.M. (1976). A rapid and sensitive method for the quantitation of microgram quantities of protein utilizing the principle of protein-dye binding. Anal Biochem *72*, 248-254.

Bridwell-Rabb, J., Iannuzzi, C., Pastore, A., and Barondeau, D.P. (2012). Effector role reversal during evolution: the case of frataxin in Fe-S cluster biosynthesis. Biochemistry *51*, 2506-2514.

Broome-Smith, J.K., and Spratt, B.G. (1982). Deletion of the penicillin-binding protein 6 gene of Escherichia coli. J Bacteriol *152*, 904-906.

Bukau, B., and Horwich, A.L. (1998). The Hsp70 and Hsp60 chaperone machines. Cell *92*, 351-366.

Bushweller, J.H., Aslund, F., Wuthrich, K., and Holmgren, A. (1992). Structural and functional characterization of the mutant Escherichia coli glutaredoxin (C14----S) and its mixed disulfide with glutathione. Biochemistry *31*, 9288-9293.

Butland, G., Babu, M., Diaz-Mejia, J.J., Bohdana, F., Phanse, S., Gold, B., Yang, W., Li, J., Gagarinova, A.G., Pogoutse, O., Mori, H., Wanner, B.L., Lo, H., Wasniewski, J., Christopolous, C., Ali, M., Venn, P., Safavi-Naini, A., Sourour, N., Caron, S., Choi, J.Y., Laigle, L., Nazarians-Armavil, A., Deshpande, A., Joe, S., Datsenko, K.A., Yamamoto, N., Andrews, B.J., Boone, C., Ding, H., Sheikh, B., Moreno-Hagelseib, G., Greenblatt, J.F., and Emili, A. (2008). eSGA: E. coli synthetic genetic array analysis. Nature methods *5*, 789-795.

Bych, K., Kerscher, S., Netz, D.J., Pierik, A.J., Zwicker, K., Huynen, M.A., Lill, R., Brandt, U., and Balk, J. (2008). The iron-sulphur protein Ind1 is required for effective complex I assembly. Embo J *27*, 1736-1746.

Camaschella, C., Campanella, A., De Falco, L., Boschetto, L., Merlini, R., Silvestri, L., Levi, S., and Iolascon, A. (2007). The human counterpart of zebrafish shiraz shows sideroblastic-like microcytic anemia and iron overload. Blood *110*, 1353-1358.

Cameron, J.M., Janer, A., Levandovskiy, V., Mackay, N., Rouault, T.A., Tong, W.H., Ogilvie, I., Shoubridge, E.A., and Robinson, B.H. (2011). Mutations in iron-sulfur cluster scaffold genes NFU1 and BOLA3 cause a fatal deficiency of multiple respiratory chain and 2-oxoacid dehydrogenase enzymes. Am J Hum Genet *89*, 486-495.

Campuzano, V., Montermini, L., Lutz, Y., Cova, L., Hindelang, C., Jiralerspong, S., Trottier, Y., Kish, S.J., Faucheux, B., Trouillas, P., Authier, F.J., Durr, A., Mandel, J.L., Vescovi, A., Pandolfo, M., and Koenig, M. (1997). Frataxin is reduced in Friedreich ataxia patients and is associated with mitochondrial membranes. Hum Mol Genet *6*, 1771-1780.

Chacinska, A., Koehler, C.M., Milenkovic, D., Lithgow, T., and Pfanner, N. (2009). Importing mitochondrial proteins: machineries and mechanisms. Cell *138*, 628-644.

Chan, M.K., Kim, J., and Rees, D.C. (1993). The nitrogenase FeMo-cofactor and P-cluster pair: 2.2 A resolution structures. Science *260*, 792-794.

Chandramouli, K., Unciuleac, M.C., Naik, S., Dean, D.R., Huynh, B.H., and Johnson, M.K. (2007). Formation and Properties of [4Fe-4S] Clusters on the IscU Scaffold Protein. Biochemistry *46*, 6804-6811.

Chen, O.S., Crisp, R.J., Valachovic, M., Bard, M., Winge, D.R., and Kaplan, J. (2004). Transcription of the yeast iron regulon does not respond directly to iron but rather to iron-sulfur cluster biosynthesis. J Biol Chem *279*, 29513-29518.

Ciesielski, S.J., Schilke, B.A., Osipiuk, J., Bigelow, L., Mulligan, R., Majewska, J., Joachimiak, A., Marszalek, J., Craig, E.A., and Dutkiewicz, R. (2012). Interaction of J-protein co-chaperone Jac1 with Fe-S scaffold Isu is indispensable in vivo and conserved in evolution. J Mol Biol *417*, 1-12.

Courel, M., Lallet, S., Camadro, J.M., and Blaiseau, P.L. (2005). Direct activation of genes involved in intracellular iron use by the yeast iron-responsive transcription factor Aft2 without its paralog Aft1. Mol Cell Biol *25*, 6760-6771.

Craig, E.A., and Marszalek, J. (2011). Hsp70 chaperones In: eLS. , Chichester: John Wiley & Sons Ltd, , http://www.els.net [doi: 10.1002/9780470015902.a9780470023188].

D'Silva, P., Liu, Q., Walter, W., and Craig, E.A. (2004). Regulated interactions of mtHsp70 with Tim44 at the translocon in the mitochondrial inner membrane. Nat Struct Mol Biol *11*, 1084-1091.

Dervarti, D.V., Ormejohn, W.H., Hansen, R.E., Beinert, H., Tsai, R.L., Tsibris, J.C.M., Bartholo, R.C., and Gunsalus, I.C. (1967). Identification of sulfur as component of the EPR signal at g equals 1.94 by isotopic substitution. Biochem Biophys Res Commun *26*, 569-576.

Djaman, O., Outten, F.W., and Imlay, J.A. (2004). Repair of oxidized iron-sulfur clusters in Escherichia coli. J Biol Chem *279*, 44590-44599.

Dutkiewicz, R., Marszalek, J., Schilke, B., Craig, E.A., Lill, R., and Muhlenhoff, U. (2006). The hsp70 chaperone ssq1p is dispensable for iron-sulfur cluster formation on the scaffold protein isu1p. J Biol Chem *281*, 7801-7808.

Dutkiewicz, R., Schilke, B., Cheng, S., Knieszner, H., Craig, E.A., and Marszalek, J. (2004). Sequence-specific interaction between mitochondrial Fe-S scaffold protein Isu and Hsp70 Ssq1 is essential for their in vivo function. J Biol Chem *279*, 29167-29174.

Dutkiewicz, R., Schilke, B., Knieszner, H., Walter, W., Craig, E.A., and Marszalek, J. (2003). Ssq1, a mitochondrial Hsp70 involved in iron-sulfur (Fe/S) center biogenesis. Similarities to and differences from its bacterial counterpart. J Biol Chem *278*, 29719-29727.

Fontecave, M., Choudens, S.O., Py, B., and Barras, F. (2005). Mechanisms of iron-sulfur cluster assembly: the SUF machinery. J Biol Inorg Chem *10*, 713-721.

Frazzon, J., and Dean, D.R. (2003). Formation of iron-sulfur clusters in bacteria: an emerging field in bioinorganic chemistry. Curr Opin Chem Biol *7*, 166-173.

Froschauer, E.M., Rietzschel, N., Hassler, M.R., Binder, M., Schweyen, R.J., Lill, R., Muhlenhoff, U., and Wiesenberger, G. (2013). The Mitochondrial Carrier Rim2 Co-Imports Pyrimidine Nucleotides and Iron. Biochem J.

Funk, M., Niedenthal, R., Mumberg, D., Brinkmann, K., Ronicke, V., and Henkel, T. (2002). Vector systems for heterologous expression of proteins in Saccharomyces cerevisiae. Methods Enzymol *350*, 248-257.

Gangon, P. (1998). An Enigma Unmasked: How Hydroxtapatite Works and How to Make it Work For You. In: Validated Biosystems Quarterly Resource Guide for Downstream Processing, http://www.validated.com.

Garg, R.P., Vargo, C.J., Cui, X., and Kurtz, D.M., Jr. (1996). A [2Fe-2S] protein encoded by an open reading frame upstream of the Escherichia coli bacterioferritin gene. Biochemistry *35*, 6297-6301.

Gari, K., Leon Ortiz, A.M., Borel, V., Flynn, H., Skehel, J.M., and Boulton, S.J. (2012). MMS19 links cytoplasmic iron-sulfur cluster assembly to DNA metabolism. Science *337*, 243-245.

Garland, S.A., Hoff, K., Vickery, L.E., and Culotta, V.C. (1999). Saccharomyces cerevisiae ISU1 and ISU2: members of a well-conserved gene family for iron-sulfur cluster assembly. J Mol Biol *294*, 897-907.

Gelling, C., Dawes, I.W., Richhardt, N., Lill, R., and Muhlenhoff, U. (2008). Mitochondrial Iba57p is required for Fe/S cluster formation on aconitase and activation of radical SAM enzymes. Mol Cell Biol *28*, 1851-1861.

Gerber, J., Muhlenhoff, U., and Lill, R. (2003). An interaction between frataxin and Isu1/Nfs1 that is crucial for Fe/S cluster synthesis on Isu1. EMBO Rep *4*, 906-911.

Gerber, J., Neumann, K., Prohl, C., Muhlenhoff, U., and Lill, R. (2004). The yeast scaffold proteins Isu1p and Isu2p are required inside mitochondria for maturation of cytosolic Fe/S proteins. Mol Cell Biol *24*, 4848-4857.

Gladyshev, V.N., Liu, A., Novoselov, S.V., Krysan, K., Sun, Q.A., Kryukov, V.M., Kryukov, G.V., and Lou, M.F. (2001). Identification and characterization of a new mammalian glutaredoxin (thioltransferase), Grx2. J Biol Chem *276*, 30374-30380.

Goldberg, A.V., Molik, S., Tsaousis, A.D., Neumann, K., Kuhnke, G., Delbac, F., Vivares, C.P., Hirt, R.P., Lill, R., and Embley, T.M. (2008). Localization and functionality of microsporidian iron-sulphur cluster assembly proteins. Nature *452*, 624-628.

Gu, M., and Imlay, J.A. (2011). The SoxRS response of Escherichia coli is directly activated by redox-cycling drugs rather than by superoxide. Mol Microbiol *79*, 1136-1150.

Gunshin, H., Allerson, C.R., Polycarpou-Schwarz, M., Rofts, A., Rogers, J.T., Kishi, F., Hentze, M.W., Rouault, T.A., Andrews, N.C., and Hediger, M.A. (2001). Iron-dependent regulation of the divalent metal ion transporter. FEBS Lett *509*, 309-316.

Haack, T.B., Rolinski, B., Haberberger, B., Zimmermann, F., Schum, J., Strecker, V., Graf, E., Athing, U., Hoppen, T., Wittig, I., Sperl, W., Freisinger, P., Mayr, J.A., Strom, T.M., Meitinger, T., and Prokisch, H. (2013). Homozygous missense mutation in BOLA3 causes multiple mitochondrial dysfunctions syndrome in two siblings. J Inherit Metab Dis *36*, 55-62.

Haas, H., Eisendle, M., and Turgeon, B.G. (2008). Siderophores in fungal physiology and virulence. Annu Rev Phytopathol *46*, 149-187.

Hartl, F.U., Bracher, A., and Hayer-Hartl, M. (2011). Molecular chaperones in protein folding and proteostasis. Nature *475*, 324-332.

Hausmann, A., Aguilar Netz, D.J., Balk, J., Pierik, A.J., Muhlenhoff, U., and Lill, R. (2005). The eukaryotic P loop NTPase Nbp35: an essential component of the cytosolic and nuclear iron-sulfur protein assembly machinery. Proc Natl Acad Sci U S A *102*, 3266-3271.

Hausmann, A., Samans, B., Lill, R., and Muhlenhoff, U. (2008). Cellular and Mitochondrial Remodeling upon Defects in Iron-Sulfur Protein Biogenesis. J Biol Chem *283*, 8318-8330.

Herrero, E., and de la Torre-Ruiz, M.A. (2007). Monothiol glutaredoxins: a common domain for multiple functions. Cell Mol Life Sci *64*, 1518-1530.

Hess, D.C., Myers, C.L., Huttenhower, C., Hibbs, M.A., Hayes, A.P., Paw, J., Clore, J.J., Mendoza, R.M., Luis, B.S., Nislow, C., Giaever, G., Costanzo, M., Troyanskaya, O.G., and Caudy, A.A. (2009). Computationally driven, quantitative experiments discover genes required for mitochondrial biogenesis. PLoS genetics *5*, e1000407.

Hiltunen, J.K., Autio, K.J., Schonauer, M.S., Kursu, V.A., Dieckmann, C.L., and Kastaniotis, A.J. (2010). Mitochondrial fatty acid synthesis and respiration. Biochim Biophys Acta *1797*, 1195-1202.

Hjort, K., Goldberg, A.V., Tsaousis, A.D., Hirt, R.P., and Embley, T.M. (2010). Diversity and reductive evolution of mitochondria among microbial eukaryotes. Philos Trans R Soc Lond B Biol Sci *365*, 713-727.

Hoff, K.G., Culler, S.J., Nguyen, P.Q., McGuire, R.M., Silberg, J.J., and Smolke, C.D. (2009). In vivo fluorescent detection of Fe-S clusters coordinated by human GRX2. Chem Biol *16*, 1299-1308.

Hoff, K.G., Cupp-Vickery, J.R., and Vickery, L.E. (2003). Contributions of the LPPVK motif of the iron-sulfur template protein IscU to interactions with the Hsc66-Hsc20 chaperone system. J Biol Chem *278*, 37582-37589.

Hoff, K.G., Silberg, J.J., and Vickery, L.E. (2000). Interaction of the iron-sulfur cluster assembly protein IscU with the Hsc66/Hsc20 molecular chaperone system of Escherichia coli. Proc Natl Acad Sci U S A *97*, 7790-7795.

Hoff, K.G., Ta, D.T., Tapley, T.L., Silberg, J.J., and Vickery, L.E. (2002). Hsc66 substrate specificity is directed toward a discrete region of the iron-sulfur cluster template protein IscU. J Biol Chem *277*, 27353-27359.

Hoffmann, B., Uzarska, M.A., Berndt, C., Godoy, J.R., Haunhorst, P., Lillig, C.H., Lill, R., and Muhlenhoff, U. (2011). The multidomain thioredoxin-monothiol glutaredoxins represent a distinct functional group. Antioxid Redox Signal *15*, 19-30.

Holmgren, A. (1976). Hydrogen donor system for Escherichia coli ribonucleoside-diphosphate reductase dependent upon glutathione. PNAS *73*, 2275-2279.

Huynen, M.A., Spronk, C.A., Gabaldon, T., and Snel, B. (2005). Combining data from genomes, Y2H and 3D structure indicates that BolA is a reductase interacting with a glutaredoxin. FEBS Lett *579*, 591-596.

Iannuzzi, C., Adinolfi, S., Howes, B.D., Garcia-Serres, R., Clemancey, M., Latour, J.M., Smulevich, G., and Pastore, A. (2011). The role of CyaY in iron sulfur cluster assembly on the E. coli IscU scaffold protein. PLoS One *6*, e21992.

Ito, H., Fukuda, Y., Murata, K., and Kimura, A. (1983). Transformation of intact yeast cells treated with alkali cations. J Bacteriol *153*, 163-168.

Ito, T., Tashiro, K., Muta, S., Ozawa, R., Chiba, T., Nishizawa, M., Yamamoto, K., Kuhara, S., and Sakaki, Y. (2000). Toward a protein-protein interaction map of the budding yeast: A comprehensive system to examine two-hybrid interactions in all possible combinations between the yeast proteins. PNAS *97*, 1143-1147.

Iwema, T., Picciocchi, A., Traore, D.A., Ferrer, J.L., Chauvat, F., and Jacquamet, L. (2009). Structural basis for delivery of the intact [Fe2S2] cluster by monothiol glutaredoxin. Biochemistry *48*, 6041-6043.

Jakubowski, W., and Bartosz, G. (1997). Estimation of oxidative stress in Saccharomyces cerevisae with fluorescent probes. Int J Biochem Cell Biol *29*, 1297-1301.

Jensen, L.T., and Culotta, V.C. (2000). Role of Saccharomyces cerevisiae ISA1 and ISA2 in iron homeostasis. Mol Cell Biol *20*, 3918-3927.

Jerabek-Willemsen, M., Wienken, C.J., Braun, D., Baaske, P., and Duhr, S. (2011). Molecular interaction studies using microscale thermophoresis. Assay Drug Dev Technol *9*, 342-353.

Johansson, C., Kavanagh, K.L., Gileadi, O., and Oppermann, U. (2007). Reversible sequestration of active site cysteines in a 2Fe-2S-bridged dimer provides a mechanism for glutaredoxin 2 regulation in human mitochondria. J Biol Chem *282*, 3077-3082.

Johansson, C., Roos, A.K., Montano, S.J., Sengupta, R., Filippakopoulos, P., Guo, K., von Delft, F., Holmgren, A., Oppermann, U., and Kavanagh, K.L. (2011). The crystal structure of human GLRX5: iron-sulfur cluster co-ordination, tetrameric assembly and monomer activity. Biochem J *433*, 303-311.

Kakhlon, O., and Cabantchik, Z.I. (2002). The labile iron pool: characterization, measurement, and participation in cellular processes(1). Free Radic Biol Med *33*, 1037-1046.

Kampinga, H.H., and Craig, E.A. (2010). The HSP70 chaperone machinery: J proteins as drivers of functional specificity. Nat Rev Mol Cell Biol *11*, 579-592.

Kaut, A., Lange, H., Diekert, K., Kispal, G., and Lill, R. (2000). Isa1p is a component of the mitochondrial machinery for maturation of cellular iron-sulfur proteins and requires conserved cysteine residues for function. J Biol Chem *275*, 15955-15961.

Khoroshilova, N., Popescu, C., Munck, E., Beinert, H., and Kiley, P.J. (1997). Iron-sulfur cluster disassembly in the FNR protein of Escherichia coli by O2: [4Fe-4S] to [2Fe-2S] conversion with loss of biological activity. Proc Natl Acad Sci U S A *94*, 6087-6092.

Kim, K.D., Chung, W.H., Kim, H.J., Lee, K.C., and Roe, J.H. (2010). Monothiol glutaredoxin Grx5 interacts with Fe-S scaffold proteins Isa1 and Isa2 and supports Fe-S assembly and DNA integrity in mitochondria of fission yeast. Biochem Biophys Res Commun *392*, 467-472.

Kim, S.H., Kim, M., Lee, J.K., Kim, M.J., Jin, Y.H., Seong, R.H., Hong, S.H., Joe, C.O., and Park, S.D. (1997). Identification and expression of uvi31+, a UV-inducible gene from Schizosaccharomyces pombe. Environ Mol Mutagen *30*, 72-81.

Kispal, G., Csere, P., Guiard, B., and Lill, R. (1997). The ABC transporter Atm1p is required for mitochondrial iron homeostasis. FEBS Lett *418*, 346-350.

Kispal, G., Csere, P., Prohl, C., and Lill, R. (1999). The mitochondrial proteins Atm1p and Nfs1p are essential for biogenesis of cytosolic Fe/S proteins. Embo J *18*, 3981-3989.

Kispal, G., Sipos, K., Lange, H., Fekete, Z., Bedekovics, T., Janaky, T., Bassler, J., Aguilar Netz, D.J., Balk, J., Rotte, C., and Lill, R. (2005). Biogenesis of cytosolic ribosomes requires the essential iron-sulphur protein Rli1p and mitochondria. Embo J *24*, 589-598.

Knieszner, H., Schilke, B., Dutkiewicz, R., D'Silva, P., Cheng, S., Ohlson, M., Craig, E.A., and Marszalek, J. (2005). Compensation for a defective interaction of the hsp70 ssq1 with the mitochondrial Fe-S cluster scaffold isu. J Biol Chem *280*, 28966-28972.

Kosman, D.J. (2003). Molecular mechanisms of iron uptake in fungi. Mol Microbiol *47*, 1185-1197.

Kuhnke, G., Neumann, K., Muhlenhoff, U., and Lill, R. (2006). Stimulation of the ATPase activity of the yeast mitochondrial ABC transporter Atm1p by thiol compounds. Mol Membr Biol *23*, 173-184.

Kumanovics, A., Chen, O.S., Li, L., Bagley, D., Adkins, E.M., Lin, H., Dingra, N.N., Outten, C.E., Keller, G., Winge, D., Ward, D.M., and Kaplan, J. (2008). Identification of FRA1 and FRA2 as genes involved in regulating the yeast iron regulon in response to decreased mitochondrial iron-sulfur cluster synthesis. J Biol Chem *283*, 10276-10286.

Kyhse-Andersen, J. (1984). Electroblotting of multiple gels: a simple apparatus without buffer tank for rapid transfer of proteins from polyacrylamide to nitrocellulose. J Biochem Biophys Methods. *10*, 203-209.

Laemmli, U.K. (1970). Cleavage of structural proteins during the assembly of the head of bacteriophage T4. Nature *227*, 680-685.

Lange, H., Kaut, A., Kispal, G., and Lill, R. (2000). A mitochondrial ferredoxin is essential for biogenesis of cellular iron-sulfur proteins. Proc Natl Acad Sci U S A *97*, 1050-1055.

Leon, S., Touraine, B., Ribot, C., Briat, J.F., and Lobreaux, S. (2003). Iron-sulphur cluster assembly in plants: distinct NFU proteins in mitochondria and plastids from Arabidopsis thaliana. Biochem J *371*, 823-830.

Li, H., Mapolelo, D.T., Dingra, N.N., Naik, S.G., Lees, N.S., Hoffman, B.M., Riggs-Gelasco, P.J., Huynh, B.H., Johnson, M.K., and Outten, C.E. (2009). The yeast iron regulatory proteins Grx3/4 and Fra2 form heterodimeric complexes containing a [2Fe-2S] cluster with cysteinyl and histidyl ligation. Biochemistry *48*, 9569-9581.

Li, H., and Outten, C.E. (2012). Monothiol CGFS glutaredoxins and BolA-like proteins: [2Fe-2S] binding partners in iron homeostasis. Biochemistry *51*, 4377-4389.

Li, J., Saxena, S., Pain, D., and Dancis, A. (2001a). Adrenodoxin reductase homolog (Arh1p) of yeast mitochondria required for iron homeostasis. J Biol Chem *276*, 1503-1509.

Li, L., Chen, O.S., McVey Ward, D., and Kaplan, J. (2001b). CCC1 is a transporter that mediates vacuolar iron storage in yeast. J Biol Chem *276*, 29515-29519.

Lill, R. (2009). Function and biogenesis of iron-sulphur proteins. Nature *460*, 831-838.

Lill, R., Diekert, K., Kaut, A., Lange, H., Pelzer, W., Prohl, C., and Kispal, G. (1999). The essential role of mitochondria in the biogenesis of cellular iron-sulfur proteins. Biol Chem *380*, 1157-1166.

Lill, R., Hoffmann, B., Molik, S., Pierik, A.J., Rietzschel, N., Stehling, O., Uzarska, M.A., Webert, H., Wilbrecht, C., and Muhlenhoff, U. (2012). The role of mitochondria in cellular iron-sulfur protein biogenesis and iron metabolism. Biochim Biophys Acta *1823*, 1491-1508.

Lill, R., and Muhlenhoff, U. (2006). Iron-sulfur protein biogenesis in eukaryotes: components and mechanisms. Annu Rev Cell Dev Biol *22*, 457-486.

Lill, R., and Muhlenhoff, U. (2008). Maturation of iron-sulfur proteins in eukaryotes: mechanisms, connected processes, and diseases. Annu Rev Biochem *77*, 669-700.

Lillig, C.H., Berndt, C., and Holmgren, A. (2008). Glutaredoxin systems. Biochim Biophys Acta *1780*, 1304-1317.

Lillig, C.H., Berndt, C., Vergnolle, O., Lonn, M.E., Hudemann, C., Bill, E., and Holmgren, A. (2005). Characterization of human glutaredoxin 2 as iron-sulfur protein: a possible role as redox sensor. Proc Natl Acad Sci U S A *102*, 8168-8173.

Liu, X.F., Elashvili, I., Gralla, E.B., Valentine, J.S., Lapinskas, P., and Culotta, V.C. (1992). Yeast lacking superoxide dismutase. Isolation of genetic suppressors. J Biol Chem *267*, 18298-18302.

Lotierzo, M., Tse Sum Bui, B., Florentin, D., Escalettes, F., and Marquet, A. (2005). Biotin synthase mechanism: an overview. Biochem Soc Trans *33*, 820-823.

Lundberg, M., Johansson, C., Chandra, J., Enoksson, M., Jacobsson, G., Ljung, J., Johansson, M., and Holmgren, A. (2001). Cloning and expression of a novel human glutaredoxin (Grx2) with mitochondrial and nuclear isoforms. J Biol Chem *276*, 26269-26275.

Malkin, R., and Rabinowitz, J.C. (1966). The reconstitution of clostridial ferredoxin. Biochem Biophys Res Commun *23*, 822-827.

Markiewicz, Z., Broome-Smith, J.K., Schwarz, U., and Spratt, B.G. (1982). Spherical E. coli due to elevated levels of D-alanine carboxypeptidase. Nature *297*, 702-704.

Mayer, M.P., and Bukau, B. (2005). Hsp70 chaperones: cellular functions and molecular mechanism. Cell Mol Life Sci *62*, 670-684.

McDonagh, B., Requejo, R., Fuentes-Almagro, C.A., Ogueta, S., Barcena, J.A., and Padilla, C.A. (2011). Thiol redox proteomics identifies differential targets of cytosolic and mitochondrial glutaredoxin-2 isoforms in Saccharomyces cerevisiae. Reversible S-glutathionylation of DHBP synthase (RIB3). J. Proteomics *74*, 2487-2497.

Mesecke, N., Terziyska, N., Kozany, C., Baumann, F., Neupert, W., Hell, K., and Herrmann, J.M. (2005). A disulfide relay system in the intermembrane space of mitochondria that mediates protein import. Cell *121*, 1059-1069.

Meyer, J. (2008). Iron-sulfur protein folds, iron-sulfur chemistry, and evolution. J Biol Inorg Chem *13*, 157-170.

Meyer, Y., Buchanan, B.B., Vignols, F., and Reichheld, J.P. (2009). Thioredoxins and glutaredoxins: unifying elements in redox biology. Annu. Rev. Genet. *43*, 335-367.

Miao, R., Martinho, M., Morales, J.G., Kim, H., Ellis, E.A., Lill, R., Hendrich, M.P., Munck, E., and Lindahl, P.A. (2008). EPR and Mossbauer spectroscopy of intact mitochondria isolated from Yah1p-depleted Saccharomyces cerevisiae. Biochemistry *47*, 9888-9899.

Mochel, F., Knight, M.A., Tong, W.H., Hernandez, D., Ayyad, K., Taivassalo, T., Andersen, P.M., Singleton, A., Rouault, T.A., Fischbeck, K.H., and Haller, R.G. (2008). Splice mutation in the iron-sulfur cluster scaffold protein ISCU causes myopathy with exercise intolerance. Am J Hum Genet *82*, 652-660.

Molina-Navarro, M.M., Casas, C., Piedrafita, L., Belli, G., and Herrero, E. (2006). Prokaryotic and eukaryotic monothiol glutaredoxins are able to perform the functions of Grx5 in the biogenesis of Fe/S clusters in yeast mitochondria. FEBS Lett *580*, 2273-2280.

Molina, M.M., Belli, G., de la Torre, M.A., Rodriguez-Manzaneque, M.T., and Herrero, E. (2004). Nuclear monothiol glutaredoxins of Saccharomyces cerevisiae can function as mitochondrial glutaredoxins. J Biol Chem *279*, 51923-51930.

Mortenson, L.E.C., J. E.; Valentine, R. C. (1962). An electron transport factor from Clostridium pasteurianum. Biochem Biophys Res Commun *7*, 448-452.

Muhlenhoff, U., Balk, J., Richhardt, N., Kaiser, J.T., Sipos, K., Kispal, G., and Lill, R. (2004). Functional characterization of the eukaryotic cysteine desulfurase Nfs1p from Saccharomyces cerevisiae. J Biol Chem *279*, 36906-36915.

Muhlenhoff, U., Gerber, J., Richhardt, N., and Lill, R. (2003a). Components involved in assembly and dislocation of iron-sulfur clusters on the scaffold protein Isu1p. Embo J *22*, 4815-4825.

Muhlenhoff, U., Gerl, M.J., Flauger, B., Pirner, H.M., Balser, S., Richhardt, N., Lill, R., and Stolz, J. (2007). The ISC proteins Isa1 and Isa2 are required for the function but not for the de novo synthesis of the Fe/S clusters of biotin synthase in Saccharomyces cerevisiae. Eukaryot Cell *6*, 495-504.

Muhlenhoff, U., Molik, S., Godoy, J.R., Uzarska, M.A., Richter, N., Seubert, A., Zhang, Y., Stubbe, J., Pierrel, F., Herrero, E., Lillig, C.H., and Lill, R. (2010). Cytosolic monothiol glutaredoxins function in intracellular iron sensing and trafficking via their bound iron-sulfur cluster. Cell Metab *12*, 373-385.

Muhlenhoff, U., Richter, N., Pines, O., Pierik, A.J., and Lill, R. (2011). Specialized Function of Yeast Isa1 and Isa2 Proteins in the Maturation of Mitochondrial [4Fe-4S] Proteins. J Biol Chem *286*, 41205-41216.

Muhlenhoff, U., Stadler, J.A., Richhardt, N., Seubert, A., Eickhorst, T., Schweyen, R.J., Lill, R., and Wiesenberger, G. (2003b). A specific role of the yeast mitochondrial carriers MRS3/4p in mitochondrial iron acquisition under iron-limiting conditions. J Biol Chem *278*, 40612-40620.

Mullis, K.B., and Faloona, F.A. (1987). Specific synthesis of DNA in vitro via a polymerase-catalyzed chain reaction. Methods in enzymology *155*, 335-350.

Naranuntarat, A., Jensen, L.T., Pazicni, S., Penner-Hahn, J.E., and Culotta, V.C. (2009). The interaction of mitochondrial iron with manganese superoxide dismutase. J Biol Chem *284*, 22633-22640.

Navarro-Sastre, A., Tort, F., Stehling, O., Uzarska, M.A., Arranz, J.A., Del Toro, M., Labayru, M.T., Landa, J., Font, A., Garcia-Villoria, J., Merinero, B., Ugarte, M., Gutierrez-Solana, L.G., Campistol, J., Garcia-Cazorla, A., Vaquerizo, J., Riudor, E., Briones, P., Elpeleg, O., Ribes, A., and Lill, R. (2011). A fatal mitochondrial disease is associated with defective NFU1 function in the maturation of a subset of mitochondrial Fe-S proteins. Am J Hum Genet *89*, 656-667.

Netz, D.J., Pierik, A.J., Stumpfig, M., Bill, E., Sharma, A.K., Pallesen, L.J., Walden, W.E., and Lill, R. (2012a). A bridging [4Fe-4S] cluster and nucleotide binding are essential for function of the Cfd1-Nbp35 complex as a scaffold in iron-sulfur protein maturation. J Biol Chem *287*, 12365-12378.

Netz, D.J., Pierik, A.J., Stumpfig, M., Muhlenhoff, U., and Lill, R. (2007). The Cfd1-Nbp35 complex acts as a scaffold for iron-sulfur protein assembly in the yeast cytosol. Nat Chem Biol *3*, 278-286.

Netz, D.J., Stith, C.M., Stumpfig, M., Kopf, G., Vogel, D., Genau, H.M., Stodola, J.L., Lill, R., Burgers, P.M., and Pierik, A.J. (2012b). Eukaryotic DNA polymerases require an iron-sulfur cluster for the formation of active complexes. Nat Chem Biol *8*, 125-132.

Netz, D.J., Stumpfig, M., Dore, C., Muhlenhoff, U., Pierik, A.J., and Lill, R. (2010). Tah18 transfers electrons to Dre2 in cytosolic iron-sulfur protein biogenesis. Nat Chem Biol *6*, 758-765.

Ojeda, L., Keller, G., Muhlenhoff, U., Rutherford, J.C., Lill, R., and Winge, D.R. (2006). Role of glutaredoxin-3 and glutaredoxin-4 in the iron regulation of the Aft1 transcriptional activator in Saccharomyces cerevisiae. J Biol Chem *281*, 17661-17669.

Olsson, A., Lind, L., Thornell, L.E., and Holmberg, M. (2008). Myopathy with lactic acidosis is linked to chromosome 12q23.3-24.11 and caused by an intron mutation in the ISCU gene resulting in a splicing defect. Hum Mol Genet *17*, 1666-1672.

Onder, O., Yoon, H., Naumann, B., Hippler, M., Dancis, A., and Daldal, F. (2006). Modifications of the lipoamide-containing mitochondrial subproteome in a yeast mutant defective in cysteine desulfurase. Mol Cell Proteomics *5*, 1426-1436.

Outten, F.W., Djaman, O., and Storz, G. (2004). A suf operon requirement for Fe-S cluster assembly during iron starvation in Escherichia coli. Mol Microbiol *52*, 861-872.

Pedrajas, J.R., Porras, P., Martinez-Galisteo, E., Padilla, C.A., Miranda-Vizuete, A., and Barcena, J.A. (2002). Two isoforms of Saccharomyces cerevisiae glutaredoxin 2 are expressed in vivo and localize to different subcellular compartments. Biochem J. *364*, 617-623.

Pedro-Segura, E., Vergara, S.V., Rodriguez-Navarro, S., Parker, R., Thiele, D.J., and Puig, S. (2008). The Cth2 ARE-binding protein recruits the Dhh1 helicase to promote the decay of succinate dehydrogenase SDH4 mRNA in response to iron deficiency. J Biol Chem *283*, 28527-28535.

Pelzer, W., Muhlenhoff, U., Diekert, K., Siegmund, K., Kispal, G., and Lill, R. (2000). Mitochondrial Isa2p plays a crucial role in the maturation of cellular iron-sulfur proteins. FEBS Lett *476*, 134-139.

Picciocchi, A., Saguez, C., Boussac, A., Cassier-Chauvat, C., and Chauvat, F. (2007). CGFS-type monothiol glutaredoxins from the cyanobacterium Synechocystis PCC6803 and other evolutionary distant model organisms possess a glutathione-ligated [2Fe-2S] cluster. Biochemistry *46*, 15018-15026.

Pierik, A.J., Netz, D.J., and Lill, R. (2009). Analysis of iron-sulfur protein maturation in eukaryotes. Nat Protoc *4*, 753-766.

Pierrel, F., Hamelin, O., Douki, T., Kieffer-Jaquinod, S., Muhlenhoff, U., Ozeir, M., Lill, R., and Fontecave, M. (2010). Involvement of mitochondrial ferredoxin and para-aminobenzoic acid in yeast coenzyme Q biosynthesis. Chem Biol *17*, 449-459.

Pomposiello, P.J., and Demple, B. (2001). Redox-operated genetic switches: the SoxR and OxyR transcription factors. Trends Biotechnol *19*, 109-114.

Porras, P., Padilla, C.A., Krayl, M., Voos, W., and Barcena, J.A. (2006). One single in-frame AUG codon is responsible for a diversity of subcellular localizations of glutaredoxin 2 in Saccharomyces cerevisiae. J Biol Chem *281*, 16551-16562.

Portnoy, M.E., Liu, X.F., and Culotta, V.C. (2000). Saccharomyces cerevisiae expresses three functionally distinct homologues of the nramp family of metal transporters. Mol Cell Biol *20*, 7893-7902.

Puig, S., Askeland, E., and Thiele, D.J. (2005). Coordinated remodeling of cellular metabolism during iron deficiency through targeted mRNA degradation. Cell *120*, 99-110.

Puig, S., Vergara, S.V., and Thiele, D.J. (2008). Cooperation of two mRNA-binding proteins drives metabolic adaptation to iron deficiency. Cell Metab *7*, 555-564.

Pujol-Carrion, N., Belli, G., Herrero, E., Nogues, A., and de la Torre-Ruiz, M.A. (2006). Glutaredoxins Grx3 and Grx4 regulate nuclear localisation of Aft1 and the oxidative stress response in Saccharomyces cerevisiae. J Cell Sci *119*, 4554-4564.

Pukszta, S., Schilke, B., Dutkiewicz, R., Kominek, J., Moczulska, K., Stepien, B., Reitenga, K.G., Bujnicki, J.M., Williams, B., Craig, E.A., and Marszalek, J. (2010). Co-evolution-driven switch of J-protein specificity towards an Hsp70 partner. EMBO Rep *11*, 360-365.

Py, B., and Barras, F. (2010). Building Fe-S proteins: bacterial strategies. Nat Rev Microbiol *8*, 436-446.

Py, B., Gerez, C., Angelini, S., Planel, R., Vinella, D., Loiseau, L., Talla, E., Brochier-Armanet, C., Garcia Serres, R., Latour, J.M., Ollagnier-de Choudens, S., Fontecave, M., and Barras, F. (2012). Molecular organization, biochemical function, cellular role and evolution of NfuA, an atypical Fe-S carrier. Mol Microbiol *86*, 155-171.

Qi, W., and Cowan, J.A. (2011). Mechanism of glutaredoxin-ISU [2Fe-2S] cluster exchange. Chem Commun (Camb) *47*, 4989-4991.

Qi, W., Li, J., Chain, C.Y., Pasquevich, G.A., Pasquevich, A.F., and Cowan, J.A. (2012). Glutathione complexed Fe-S centers. Journal of the American Chemical Society *134*, 10745-10748.

Rada, P., Smid, O., Sutak, R., Dolezal, P., Pyrih, J., Zarsky, V., Montagne, J.J., Hrdy, I., Camadro, J.M., and Tachezy, J. (2009). The monothiol single-domain glutaredoxin is conserved in the highly reduced mitochondria of Giardia intestinalis. Eukaryot cell *8*, 1584-1591.

Raguzzi, F., Lesuisse, E., and Crichton, R.R. (1988). Iron storage in Saccharomyces cerevisiae. FEBS Lett *231*, 253-258.

Raulfs, E.C., O'Carroll, I.P., Dos Santos, P.C., Unciuleac, M.C., and Dean, D.R. (2008). In vivo iron-sulfur cluster formation. Proc Natl Acad Sci U S A *105*, 8591-8596.

Rawat, S., and Stemmler, T.L. (2011). Key players and their role during mitochondrial iron-sulfur cluster biosynthesis. Chemistry *17*, 746-753.

Ren, Y., Yang, S., Tan, G., Ye, W., Liu, D., Qian, X., Ding, Z., Zhong, Y., Zhang, J., Jiang, D., Zhao, Y., and Lu, J. (2012). Reduction of mitoferrin results in abnormal development and extended lifespan in Caenorhabditis elegans. PLoS One *7*, e29666.

Rodriguez-Manzaneque, M.T., Ros, J., Cabiscol, E., Sorribas, A., and Herrero, E. (1999). Grx5 glutaredoxin plays a central role in protection against protein oxidative damage in Saccharomyces cerevisiae. Mol Cell Biol *19*, 8180-8190.

Rodriguez-Manzaneque, M.T., Tamarit, J., Belli, G., Ros, J., and Herrero, E. (2002). Grx5 is a mitochondrial glutaredoxin required for the activity of iron/sulfur enzymes. Mol Biol Cell *13*, 1109-1121.

Rouhier, N. (2010). Plant glutaredoxins: pivotal players in redox biology and iron-sulphur centre assembly. New Phytol *186*, 365-372.

Rouhier, N., Couturier, J., Johnson, M.K., and Jacquot, J.P. (2010). Glutaredoxins: roles in iron homeostasis. Trends Biochem Sci *35*, 43-52.

Rouhier, N., Lemaire, S.D., and Jacquot, J.P. (2008). The role of glutathione in photosynthetic organisms: emerging functions for glutaredoxins and glutathionylation. Annu Rev Plant Biol *59*, 143-166.

Rouhier, N., Unno, H., Bandyopadhyay, S., Masip, L., Kim, S.K., Hirasawa, M., Gualberto, J.M., Lattard, V., Kusunoki, M., Knaff, D.B., Georgiou, G., Hase, T., Johnson, M.K., and Jacquot, J.P. (2007). Functional, structural, and spectroscopic characterization of a glutathione-ligated [2Fe-2S] cluster in poplar glutaredoxin C1. Proc Natl Acad Sci U S A *104*, 7379-7384.

Roy, A., Solodovnikova, N., Nicholson, T., Antholine, W., and Walden, W.E. (2003). A novel eukaryotic factor for cytosolic Fe-S cluster assembly. Embo J *22*, 4826-4835.

Rutherford, J.C., and Bird, A.J. (2004). Metal-responsive transcription factors that regulate iron, zinc, and copper homeostasis in eukaryotic cells. Eukaryot Cell *3*, 1-13.

Rutherford, J.C., Ojeda, L., Balk, J., Muhlenhoff, U., Lill, R., and Winge, D.R. (2005). Activation of the iron regulon by the yeast Aft1/Aft2 transcription factors depends on mitochondrial but not cytosolic iron-sulfur protein biogenesis. J Biol Chem *280*, 10135-10140.

Sambrook, J., and Russel, D.W. (2001). Molecular Cloning - A laboratory manual, 3rd edition. CSH Laboratory Press: ColdSpring Harbour, USA.

Schilke, B., Forster, J., Davis, J., James, P., Walter, W., Laloraya, S., Johnson, J., Miao, B., and Craig, E. (1996). The cold sensitivity of a mutant of Saccharomyces cerevisiae lacking a mitochondrial heat shock protein 70 is suppressed by loss of mitochondrial DNA. J Cell Biol *134*, 603-613.

Schilke, B., Voisine, C., Beinert, H., and Craig, E. (1999). Evidence for a conserved system for iron metabolism in the mitochondria of Saccharomyces cerevisiae. Proc Natl Acad Sci U S A *96*, 10206-10211.

Schindelin, H., Kisker, C., Schlessman, J.L., Howard, J.B., and Rees, D.C. (1997). Structure of ADP x AIF4(-)-stabilized nitrogenase complex and its implications for signal transduction. Nature *387*, 370-376.

Schlecht, R., Erbse, A.H., Bukau, B., and Mayer, M.P. (2011). Mechanics of Hsp70 chaperones enables differential interaction with client proteins. Nat Struct Mol Biol *18*, 345-351.

Schonauer, M.S., Kastaniotis, A.J., Kursu, V.A., Hiltunen, J.K., and Dieckmann, C.L. (2009). Lipoic acid synthesis and attachment in yeast mitochondria. J Biol Chem *284*, 23234-23242.

Shakamuri, P., Zhang, B., and Johnson, M.K. (2012). Monothiol glutaredoxins function in storing and transporting [Fe2S2] clusters assembled on IscU scaffold proteins. J Am Chem Soc *134*, 15213-15216.

Shaw, G.C., Cope, J.J., Li, L., Corson, K., Hersey, C., Ackermann, G.E., Gwynn, B., Lambert, A.J., Wingert, R.A., Traver, D., Trede, N.S., Barut, B.A., Zhou, Y., Minet, E., Donovan, A., Brownlie, A., Balzan, R., Weiss, M.J., Peters, L.L., Kaplan, J., Zon, L.I., and Paw, B.H. (2006). Mitoferrin is essential for erythroid iron assimilation. Nature *440*, 96-100.

Sheftel, A.D., Stehling, O., Pierik, A.J., Elsasser, H.P., Muhlenhoff, U., Webert, H., Hobler, A., Hannemann, F., Bernhardt, R., and Lill, R. (2010). Humans possess two mitochondrial ferredoxins, Fdx1 and Fdx2, with distinct roles in steroidogenesis, heme, and Fe/S cluster biosynthesis. Proc Natl Acad Sci U S A *107*, 11775-11780.

Sheftel, A.D., Stehling, O., Pierik, A.J., Netz, D.J., Kerscher, S., Elsasser, H.P., Wittig, I., Balk, J., Brandt, U., and Lill, R. (2009). Human ind1, an iron-sulfur cluster assembly factor for respiratory complex I. Mol Cell Biol *29*, 6059-6073.

Sheftel, A.D., Wilbrecht, C., Stehling, O., Niggemeyer, B., Elsasser, H.P., Muhlenhoff, U., and Lill, R. (2012). The human mitochondrial ISCA1, ISCA2, and IBA57 proteins are required for [4Fe-4S] protein maturation. Mol Biol Cell *23*, 1157-1166.

Shenton, D., Perrone, G., Quinn, K.A., Dawes, I.W., and Grant, C.M. (2002). Regulation of protein S-thiolation by glutaredoxin 5 in the yeast Saccharomyces cerevisiae. J Biol Chem *277*, 16853-16859.

Shethna, Y.I., Dervarta, D.V., and Beinert, H. (1968). Non Heme (Iron-Sulfur) Proteins of Azotobacter Vinelandii. Biochem Biophys Res Commun *31*, 862-868.

Shethna, Y.I.B., H., Hansen, R. E.; Wilson, P. W. (1964). Identification by Isotopic Substitution of EPR Signal at G equals 1.94 in Non-Heme Iron Protein from Azotobacter. Proc Natl Acad Sci U S A *52*, 1263-1271.

Shi, Y., Ghosh, M., Kovtunovych, G., Crooks, D.R., and Rouault, T.A. (2012). Both human ferredoxins 1 and 2 and ferredoxin reductase are important for iron-sulfur cluster biogenesis. Biochim Biophys Acta *1823*, 484-492.

Shiflett, A.M., and Johnson, P.J. (2010). Mitochondrion-related organelles in eukaryotic protists. Annu. Rev. Microbiol. *64*, 409-429.

Silberg, J.J., Tapley, T.L., Hoff, K.G., and Vickery, L.E. (2004). Regulation of the HscA ATPase reaction cycle by the co-chaperone HscB and the iron-sulfur cluster assembly protein IscU. J Biol Chem *279*, 53924-53931.

Sipos, K., Lange, H., Fekete, Z., Ullmann, P., Lill, R., and Kispal, G. (2002). Maturation of cytosolic iron-sulfur proteins requires glutathione. J Biol Chem *277*, 26944-26949.

Spratt, B.G. (1980). Deletion of the penicillin-binding protein 5 gene of Escherichia coli. J Bacteriol *144*, 1190-1192.

Srinivasan, V., Netz, D.J., Webert, H., Mascarenhas, J., Pierik, A.J., Michel, H., and Lill, R. (2007). Structure of the yeast WD40 domain protein Cia1, a component acting late in iron-sulfur protein biogenesis. Structure *15*, 1246-1257.

Stankiewicz, M., Nikolay, R., Rybin, V., and Mayer, M.P. (2011). CHIP participates in protein triage decisions by preferentially ubiquitinating Hsp70-bound substrates. Febs J *277*, 3353-3367.

Stehling, O., Vashisht, A.A., Mascarenhas, J., Jonsson, Z.O., Sharma, T., Netz, D.J., Pierik, A.J., Wohlschlegel, J.A., and Lill, R. (2012). MMS19 assembles iron-sulfur proteins required for DNA metabolism and genomic integrity. Science *337*, 195-199.

Sun, F., Huo, X., Zhai, Y., Wang, A., Xu, J., Su, D., Bartlam, M., and Rao, Z. (2005). Crystal structure of mitochondrial respiratory membrane protein complex II. Cell *121*, 1043-1057.

Takahashi, Y., and Nakamura, M. (1999). Functional assignment of the ORF2-iscS-iscU-iscA-hscB-hscA-fdx-ORF3 gene cluster involved in the assembly of Fe-S clusters in Escherichia coli. J Biochem (Tokyo) *126*, 917-926.

Tamarit, J., Belli, G., Cabiscol, E., Herrero, E., and Ros, J. (2003). Biochemical characterization of yeast mitochondrial Grx5 monothiol glutaredoxin. J Biol Chem *278*, 25745-25751.

Tong, W.H., Jameson, G.N., Huynh, B.H., and Rouault, T.A. (2003). Subcellular compartmentalization of human Nfu, an iron-sulfur cluster scaffold protein, and its ability to assemble a [4Fe-4S] cluster. Proc Natl Acad Sci U S A *100*, 9762-9767.

Touraine, B., Boutin, J.P., Marion-Poll, A., Briat, J.F., Peltier, G., and Lobreaux, S. (2004). Nfu2: a scaffold protein required for [4Fe-4S] and ferredoxin iron-sulphur cluster assembly in Arabidopsis chloroplasts. Plant J *40*, 101-111.

Tovar, J., Leon-Avila, G., Sanchez, L.B., Sutak, R., Tachezy, J., van der Giezen, M., Hernandez, M., Muller, M., and Lucocq, J.M. (2003). Mitochondrial remnant organelles of Giardia function in iron-sulphur protein maturation. Nature *426*, 172-176.

Tsai, C.L., and Barondeau, D.P. (2010). Human frataxin is an allosteric switch that activates the Fe-S cluster biosynthetic complex. Biochemistry *49*, 9132-9139.

Unciuleac, M.C., Chandramouli, K., Naik, S., Mayer, S., Huynh, B.H., Johnson, M.K., and Dean, D.R. (2007). In Vitro Activation of Apo-Aconitase Using a [4Fe-4S] Cluster-Loaded Form of the IscU [Fe-S] Cluster Scaffolding Protein. Biochemistry *46*, 6812-6821.

Urbanowski, J.L., and Piper, R.C. (1999). The iron transporter Fth1p forms a complex with the Fet5 iron oxidase and resides on the vacuolar membrane. J Biol Chem *274*, 38061-38070.

Urzica, E., Pierik, A.J., Muhlenhoff, U., and Lill, R. (2009). Crucial role of conserved cysteine residues in the assembly of two iron-sulfur clusters on the CIA protein Nar1. Biochemistry *48*, 4946-4958.

van der Giezen, M., Tovar, J., and Clark, C.G. (2005). Mitochondrion-derived organelles in protists and fungi. Int Rev Cytol *244*, 175-225.

Vergara, S.V., and Thiele, D.J. (2008). Post-transcriptional regulation of gene expression in response to iron deficiency: co-ordinated metabolic reprogramming by yeast mRNA-binding proteins. Biochem Soc Trans *36*, 1088-1090.

Vickery, L.E., and Cupp-Vickery, J.R. (2007). Molecular chaperones HscA/Ssq1 and HscB/Jac1 and their roles in iron-sulfur protein maturation. Crit Rev Biochem Mol Biol *42*, 95-111.

Viitanen, P.V., Lubben, T.H., Reed, J., Goloubinoff, P., O'Keefe, D.P., and Lorimer, G.H. (1990). Chaperonin-facilitated refolding of ribulosebisphosphate carboxylase and ATP hydrolysis by chaperonin 60 (groEL) are K+ dependent. Biochemistry *29*, 5665-5671.

Vogelstein, B., and Gillespie, D. (1979). Preparative and analytical purification of DNA from agarose. Proc. Natl. Acad. Sci. USA. *76*, 615-619.

Voisine, C., Schilke, B., Ohlson, M., Beinert, H., Marszalek, J., and Craig, E.A. (2000). Role of the mitochondrial Hsp70s, Ssc1 and Ssq1, in the maturation of Yfh1. Mol Cell Biol *20*, 3677-3684.

Wallace, M.A., Liou, L.L., Martins, J., Clement, M.H., Bailey, S., Longo, V.D., Valentine, J.S., and Gralla, E.B. (2004). Superoxide inhibits 4Fe-4S cluster enzymes involved in amino acid biosynthesis. Cross-compartment protection by CuZn-superoxide dismutase. J Biol Chem *279*, 32055-32062.

Wang, T., and Craig, E.A. (2008). Binding of yeast frataxin to the scaffold for Fe-S cluster biogenesis, Isu. J Biol Chem *283*, 12674-12679.

Wiedemann, N., Urzica, E., Guiard, B., Muller, H., Lohaus, C., Meyer, H.E., Ryan, M.T., Meisinger, C., Muhlenhoff, U., Lill, R., and Pfanner, N. (2006). Essential role of Isd11 in mitochondrial iron-sulfur cluster synthesis on Isu scaffold proteins. Embo J *25*, 184-195.

Wienken, C.J., Baaske, P., Rothbauer, U., Braun, D., and Duhr, S. (2010). Protein-binding assays in biological liquids using microscale thermophoresis. Nat Commun *1*, 100.

Willems, P., Wanschers, B.F., Esseling, J., Szklarczyk, R., Kudla, U., Duarte, I., Forkink, M., Nooteboom, M., Swarts, H., Gloerich, J., Nijtmans, L., Koopman, W., and Huynen, M.A. (2013). BOLA1 is an aerobic protein that prevents mitochondrial morphology changes induced by glutathione depletion. Antioxid Redox Signal *18*, 129-138.

Wingert, R.A., Galloway, J.L., Barut, B., Foott, H., Fraenkel, P., Axe, J.L., Weber, G.J., Dooley, K., Davidson, A.J., Schmid, B., Paw, B.H., Shaw, G.C., Kingsley, P., Palis, J., Schubert, H., Chen, O., Kaplan, J., and Zon, L.I. (2005). Deficiency of glutaredoxin 5 reveals Fe-S clusters are required for vertebrate haem synthesis. Nature *436*, 1035-1039.

Wu, H., Lin, L., Giblin, F., Ho, Y.S., and Lou, M.F. (2011). Glutaredoxin 2 knockout increases sensitivity to oxidative stress in mouse lens epithelial cells. Free radical biology & medicine *51*, 2108-2117.

Wu, S.P., and Cowan, J.A. (2003). Iron-sulfur cluster biosynthesis. A comparative kinetic analysis of native and Cys-substituted ISA-mediated [2Fe-2S]2+ cluster transfer to an apoferredoxin target. Biochemistry *42*, 5784-5791.

Xia, T.H., Bushweller, J.H., Sodano, P., Billeter, M., Bjornberg, O., Holmgren, A., and Wuthrich, K. (1992). NMR structure of oxidized Escherichia coli glutaredoxin: comparison with reduced E. coli glutaredoxin and functionally related proteins. Protein science : a publication of the Protein Society *1*, 310-321.

Xu, X.M., and Moller, S.G. (1998). Iron-sulfur cluster biogenesis systems and their crosstalk. Chembiochem *15*, 2355-2362.

Yabe, T., Morimoto, K., Kikuchi, S., Nishio, K., Terashima, I., and Nakai, M. (2004). The Arabidopsis chloroplastic NifU-like protein CnfU, which can act as an iron-sulfur cluster scaffold protein, is required for biogenesis of ferredoxin and photosystem I. Plant Cell *16*, 993-1007.

Yamaguchi-Iwai, Y., Dancis, A., and Klausner, R.D. (1995). AFT1: a mediator of iron regulated transcriptional control in Saccharomyces cerevisiae. Embo J *14*, 1231-1239.

Yamaguchi-Iwai, Y., Stearman, R., Dancis, A., and Klausner, R.D. (1996). Iron-regulated DNA binding by the AFT1 protein controls the iron regulon in yeast. Embo J *15*, 3377-3384.

Yamaguchi-Iwai, Y., Ueta, R., Fukunaka, A., and Sasaki, R. (2002). Subcellular localization of Aft1 transcription factor responds to iron status in Saccharomyces cerevisiae. J Biol Chem *277*, 18914-18918.

Yang, M., Cobine, P.A., Molik, S., Naranuntarat, A., Lill, R., Winge, D.R., and Culotta, V.C. (2006). The effects of mitochondrial iron homeostasis on cofactor specificity of superoxide dismutase 2. Embo J *25*, 1775-1783.

Ye, H., Jeong, S.Y., Ghosh, M.C., Kovtunovych, G., Silvestri, L., Ortillo, D., Uchida, N., Tisdale, J., Camaschella, C., and Rouault, T.A. (2010). Glutaredoxin 5 deficiency causes sideroblastic anemia by specifically impairing heme biosynthesis and depleting cytosolic iron in human erythroblasts. J Clin Invest *120*, 1749-1761.

Yeh, A.P., Chatelet, C., Soltis, S.M., Kuhn, P., Meyer, J., and Rees, D.C. (2000). Structure of a thioredoxin-like [2Fe-2S] ferredoxin from Aquifex aeolicus. J Mol Biol *300*, 587-595.

Yeung, N., Gold, B., Liu, N.L., Prathapam, R., Sterling, H.J., Willams, E.R., and Butland, G. (2011). The E. coli monothiol glutaredoxin GrxD forms homodimeric and heterodimeric FeS cluster containing complexes. Biochemistry *50*, 8957-8969.

Yi, X., and Maeda, N. (2005). Endogenous production of lipoic acid is essential for mouse development. Mol Cell Biol *25*, 8387-8392.

Yoon, H., Golla, R., Lesuisse, E., Pain, J., Donald, J.E., Lyver, E.R., Pain, D., and Dancis, A. (2012). Mutation in the Fe-S scaffold protein Isu bypasses frataxin deletion. Biochem J *441*, 473-480.

Yoon, H., Zhang, Y., Pain, J., Lyver, E.R., Lesuisse, E., Pain, D., and Dancis, A. (2011). Rim2, a pyrimidine nucleotide exchanger, is needed for iron utilization in mitochondria. Biochem J *440*, 137-146.

Zheng, L., Cash, V.L., Flint, D.H., and Dean, D.R. (1998). Assembly of iron-sulfur clusters. Identification of an iscSUA-hscBA-fdx gene cluster from Azotobacter vinelandii. J Biol Chem *273*, 13264-13272.

Zillner, K., Jerabek-Willemsen, M., Duhr, S., Braun, D., Langst, G., and Baaske, P. (2012). Microscale thermophoresis as a sensitive method to quantify protein: nucleic acid interactions in solution. Methods Mol Biol *815*, 241-252.

Curriculum Vitae

This part contains private information and is removed from the open access version.

Acknowledgments

Firstly I would like to thank my advisor Prof. Dr. Roland Lill for giving me the opportunity to conduct my doctoral studies in his laboratory. I really enjoyed the time I have spent working on given projects and I am very grateful for all helpful scientific discussions and suggestions, given support and simply for having faith in me and my abilities.

I would like to thank Prof. Dr. Uwe Maier for serving as the external adviser of this work.

I would like to thank Priv. Doz. Dr. Ulrich Mühlenhoff for given support, helpful scientific discussions and introducing me to many new techniques. I am really grateful for always being there for me and helping me to face any scientific problem that arose while working on my projects.

I would like to thank Dr. Rafał Dutkiewicz for helping me with the ATPase stimulation experiments and Sven-Andreas Freibert for helping with the MST experiments and analyzing of the obtained data.

I would like to thank whole AG Lill for very friendly working atmosphere: Vielen Dank euch allen!

Especially the "Icky-twins" Vicky and Nici for listening, support, giving me a lot of female power in the moments I really needed it, and for a very nice time in and outside the laboratory. Thank You very much Girls!

I also would like to thank few of my friends who I got to know and who were there for me during my doctoral studies. As those: Thank You Lisa and Henrike for making my "German WG experience" a great adventure. Thank You for giving me the courage to start to speak German and for all the patience when I actually tried to do that ;). Thank You Ola for being my Polish person here in Marburg, Deutschland. Thank You Tamara, Marcel and Kathrin for amazing time we had together. Climbing mountains, having a great party or Fledermäuse watching – all is possible with You!

Last but not least, from the bottom of my heart I would like to thank my Parents and my brother Tomek for the love and support that they gave me through my whole life. If not their help I would not be where I am now. Kocham Was!!!